The Type I and Type III Interferon Response in Cystic Fibrosis *Aspergillus fumigatus* Related Lung Disease

By Sarah Louise Laverty

Supervisors:

Dr Peter Kelleher

Dr Anand Shah

Professor Darius Armstrong-James

Imperial College London

Department of Medicine: Infectious Diseases

Centre for Immunology and Vaccinology

Thesis submitted for the degree of Doctor of Philosophy

July 2023

Declaration of Originality

I, Sarah Louise Laverty, declare that all the work presented in this thesis is my own. It has been acknowledged and correctly referenced where any information used is sourced from other published work, unpublished work, or carried out by colleagues.

Sarah Louise Laverty

September 2023

Copyright Declaration

Acknowledgements

I would first like to thank Dr Peter Kelleher for being such a brilliant primary supervisor throughout my PhD. Your support and confidence in my ability allowed the perseverance required of a project that spanned a global pandemic. To my other supervisors, Dr Anand Shah and Professor Darius Armstrong-James, thank you for all the support, expertise and guidance that was essential to the formation of the work in this thesis.

Secondly, I would like to thank the DAJ lab group, specifically Dr Tom Williams, Renad Aljohani, and Dr Luis Gonzales-Hertá for sharing our PhD journeys together. A particular mention to the Brompton crew, Valentina Capizzuto and Louis Hewitt for the understanding, insights, expertise, and empathy provided through the last three years. Valentina, I am grateful for your continued friendship and support, l'amico vero si vede nel momento del bisogno.

I would like to give special mention to the Cystic Fibrosis Trust for providing the funding for this research project and for gifting me this opportunity. An additional special thanks to the one with the lungs that inspired it all, Izzy, someone had to attempt to understand what makes you the way you are…!

Finally, I would like to thank my family. Anna and Rory, I hope to be less annoying now this is over, thank you for putting up with me. Thank you to my Granny, who inspired my love of Biology from a young age through her study of Zoology and love of nature. To Callum, thank you for meeting my worry and stress with your unwavering kindness and imperturbable outlook to life, I couldn't have done it without you. To my parents, I am eternally grateful for the infinite love, support, and encouragement you have provided my whole life and particularly in the last three years, I will get a job now I promise!

Abstract (300 words)

Af is an airborne fungus that healthy human lungs clear daily. *Af* infection in CF leads to more hospitalizations and intravenous antibiotics, contributing to lung function decline. Recent research highlights type I and III IFNs as crucial for fungal immunity. While these IFNs regulate antifungal neutrophil responses in mice, their role in humans remains unexplored, particularly in CF lungs, where IFN levels are downregulated during bacterial and viral infections.

This study investigated *Af* infection response with and without CFTR modulators in CF and CF-corrected human BECs. Cells were infected with the *Af* strain CEA10 as HK conidia or fixed hyphae. Bulk RNA sequencing showed significantly upregulated ISGs in CF-corrected BECs compared to CF BECs post-*Af* infection. GSEA indicated enriched TRAF6-mediated IRF7 activation in *Af*-infected CF-corrected BECs, but not in CF BECs. Monolayer and ALI cultures showed significantly reduced IFNβ and IFNλ1 expression in CF BECs compared to CF corrected BECs post-infection. However, no difference was observed in PBMCs from CF patients and healthy donors post-*Af* infection.

The impact of CFTR modulators (tezacaftor, ivacaftor, and elexacaftor) on the type I and III IFN responses in CF BECs was assessed. Modulator treatment partially restored IFNβ and IFNλ1 expression and significantly upregulated ISGs at 12 hours post-HK conidia infection but not post-hyphae infection. Modulator treatment significantly downregulated NLRC3, a gene inhibiting type I and III IFN signaling through TRAF6, STING and TBK1.

Neutrophils, essential for controlling fungal infections, from healthy donors and CF patients were treated with exogenous IFNβ and IFNλ1. The addition of IFNλ1 (10ng/ml) enhanced the fungicidal capacity of CF neutrophils without increasing NET or ROS.

This study reveals a novel downregulation of type I and III IFN expression in CF BECs after *Af* infection, a defect partially rescued by CFTR modulators. Exogenous IFNλ1 showed promising antifungal and immunoregulatory effects.

Abstract

Aspergillus fumigatus (Af) is a globally distributed, airborne, saprophytic fungus that is inhaled and successfully cleared by the healthy human lung daily. 60% of CF patients worldwide have positive *Af* cultures which is linked to more frequent hospitalisations and need for intravenous antibiotics, ultimately contributing to lung function decline. Increasingly, type I and III interferons (IFN) are described as major contributors to fungal immunity. Recent evidence describes how both type I and III IFN are critical for the regulation of optimal antifungal neutrophil responses in mice, however, this response has not been studied in humans. As downregulation of type I and III IFNs has been observed in response to bacterial and viral challenge in the CF lung, this study aims to address this in *Af* infection.

Healthy, CF and CF corrected human bronchial epithelial cells (BEC) were infected with *Af* strain CEA10 heat killed conidia or fixed hyphae. Bulk RNA sequencing showed significantly more upregulated IFN-stimulated genes (ISGs) following *Af* infection in CF corrected BECs compared to CF. Gene Set Enrichment Analysis (GSEA) revealed that the TRAF6 mediated IRF7 activation was enriched in *Af* infected CF corrected BECs, but not in CF. Expression of IFNβ and IFNλ1 mRNA was significantly reduced in both monolayer and air-liquid interface cultures in CF BECs compared CF corrected BECs ($p \leq 0.01$) post-infection with *Af* conidia and hyphae. Expression of IFNβ and IFNλ1 mRNA was also assessed in PBMCs isolated from patients with CF and healthy donors, however, no difference in expression was observed following *Af* infection.

In 2019, CFTR modulators were introduced on the NHS and have significantly altered treatment courses and improved morbidity and mortality in patients with CF. The impact of

CFTR modulators on type I and III IFN immune responses was assessed following incubation of CF BECs with Tezacaftor, Ivacaftor and Elexacaftor combination therapy at a concentration of 1nM and a 1:1:1 ratio. Modulator treatment partially rescued the expression of IFNβ and IFNλ1 and RNA sequencing confirmed upregulation of significantly more ISGs at 12 hours post conidia infection ($p \leq 0.05$) but not after hyphae infection. Additionally, the expression of NLRC3 was significantly downregulated by modulator treatment. NLRC3 can interact with TRAF6, STING, and TBK1 to reduce their downstream type I and III IFN signalling ability, suggesting a possible mechanism of IFN response rescue.

Neutrophils are professional phagocytes that are essential in the control of fungal infections. To assess the effects of type I and III IFNs on the fungicidal capacity of these cells, neutrophils isolated from healthy donors and patients with CF were treated with exogenous IFNβ and IFNλ1 at 1 and 10ng/ml. NET and ROS production, fungal killing and cell death were measured. Addition of IFNλ1 (10ng/ml) but not IFNβ increased the ability of CF neutrophils to kill *Af* without increasing NET or ROS production or influencing cell cytotoxicity.

In conclusion, this data shows a novel down regulation of type I and III interferon expression in CF BECs, but not PBMCs, after *Af* infection and this defect was partially rescued by CFTR modulators in BECs. Exogenous IFNλ1 exhibited anti-fungal and immunoregulatory activity. Further research into the potential of IFNλ1 immunotherapy in CF *Af* related disease should be considered.

Table of Contents

List of Figures

List of Tables

List of Abbreviations

ABPA	Allergic bronchopulmonary aspergillosis
ALI	Air-liquid interface
Af	*Aspergillus fumigatus*
ANOVA	Analysis of variance
APRIL	A proliferation-inducing ligand
BAFF	B-cell activating factor
BAL	Bronchoalveolar lavage
Bcl10	B-cell lymphoma/leukaemia 10
BEC	Bronchial epithelial cell
BMI	Body mass index
C3a	Complement component 3a
C5a	Complement component 5a
cAMP	Cyclic adenosine monophosphate
CARD9	Caspase recruitment domain-containing protein 9
Cat G	cathepsin G
CCL	C-C motif chemokine ligand
CCR	C-C chemokine receptor
CF	Cystic fibrosis
CFTR	Cystic fibrosis transmembrane conductance regulator
CFU	Colony forming unit
cGAS	Cyclic GMP-AMP synthase
CGD	Chronic granulomatous disease
CLEC6	C-Type Lectin Domain Family 6
CLR	C-type lectin receptor
CPA	Chronic pulmonary aspergillosis
CXCL	C-X-C chemokine ligand
DAMP	Damage-associated molecular patterns
DC	Dendritic cell
DC-SIGN	Dendritic cell-specific intracellular adhesion molecule-3-grabbing non-integrin
DHN	Dihydroxynaphthalene

DNA	Deoxyribonucleic acid
EMA	European Medicines Agency
FcRγ	Fc receptor γ
FDA	Food and Drug Administration
FEV	Forced expiratory volume
FOXI1	Forkhead Box I1
GFP	Green fluorescent protein
GO	Gene Ontology
H_2O_2	Hydrogen peroxide
HIV	Human immunodeficiency virus
HL60	Human Leukaemia 60
HOCl	Hypochlorous acid
IA	Invasive aspergillosis
IFI	Interferon-induced proteins
IFIT	Interferon-induced proteins with tetratricopeptide repeats
IFN	Interferon
IFNAR	Interferon alpha/beta receptor
IFNLR	Interferon lambda receptor
Ig	Immunoglobulin
IKK	IκB kinase
IL	Interleukin
IRF	Interferon regulatory factor
IRT	Immunoreactive trypsinogen test
ISG	Interferon stimulated gene
ISGF	Interferon stimulated gene factor
ITAM	Immunoreceptor tyrosine-based activation motif
JAK	Janus kinase
KEGG	Kyoto Encyclopaedia of Genes and Genomes
KO	Knockout
LAMP1	Lysosome-associated membrane protein 1
LAP	LC3 associated phagocytosis
LDH	Lactate dehydrogenase

LGP2	Laboratory of genetics and physiology 2
MALT1	Mucosa-associated lymphoid tissue lymphoma translocation protein 1
MAPK	Mitogen-activated protein kinase
MBL	Mannan-binding lectin
MDA5	Melanoma differentiation-associated protein 5
MelLec	Melanin-sensing C-type lectin receptor
MHC	Major histocompatibility complex
mo-DC	Monocyte-derived dendritic cells
MPO	Myeloperoxidase
mRNA	Messenger ribonucleic acid
MX	Mx proteins
MyD88	Myeloid differentiation primary response 88
NADPH	Nicotinamide adenine dinucleotide phosphate
NE	Neutrophil elastase
NET	Neutrophil extracellular trap
NFκB	Nuclear factor kappa-light-chain-enhancer of activated B cells
NLR	Nucleotide-binding oligomerization domain-like receptors
NLRC4	NLR family CARD domain-containing protein 4
NLRP3	NLR family pyrin domain containing 3
NOD	Nucleotide-binding oligomerization domain
NOX	Nicotinamide adenine dinucleotide phosphate oxidase II
Nrf2	Nuclear factor erythroid 2-related factor 2
NS	Not significant
OAS	2'-5'-Oligoadenylate Synthetase
P.a.	*Pseudomonas aeruginosa*
PAMP	Pathogen-associated molecular pattern
PBMC	Peripheral blood mononuclear cell
pDC	Plasmacytoid dendritic cell
PPAR	Peroxisome Proliferator-Activated Receptor
PRR	Pattern recognition receptor
PR3	proteinase 3
RelB	Recombination signal sequence-binding protein J kappa enhancer factor B

RIG-1	Retinoic acid-inducible gene I
RLR	Retinoic acid-inducible gene I-like receptor
RNA	Ribonucleic acid
ROS	Reactive oxygen species
SAFS	Severe asthma with fungal sensitisation
SOCS	Suppressor of cytokine signalling
STAT	Signal transducer and activator of transcription
STING	Stimulator of interferon genes
Syk	Spleen tyrosine kinase
TDRD	Tudor domain-containing protein
TGFβ	Transforming growth factor β
Th	T-helper cell
TIR	Toll-interleukin receptor
TLR	Toll-like receptor
TNF	Tumour necrosis factor
TRADD	Tumour necrosis factor receptor type 1-associated DEATH domain protein
TRIF	TIR-domain-containing adapter-inducing interferon-β
TYK	Tyrosine kinase
USP	Ubiquitin-specific protease

Chapter 1: Introduction

1.1 – Cystic Fibrosis

Cystic fibrosis (CF) is an autosomal recessive disease caused by a mutation in the cystic fibrosis transmembrane conductance regulator (*CFTR*) gene which encodes a chloride and bicarbonate ion channel. CF occurs in approximately 1/3500 births, affecting more than 70,000 people globally, and is the most common disease of its kind in the Caucasian population[1, 2]. Clinical manifestations of this disease are thought to be caused by reduced or absent CFTR protein function in epithelial cells in the lung, pancreas, intestines, and reproductive system. CF in the lung is characterised by thick mucus production causing chronic and recurrent infections, contributing to a hyperinflammatory lung environment and, eventually, to lung function decline[3]. CF lungs appear healthy at birth, but patients become symptomatic very quickly, with the first clinical presentations being poor weight gain and recurrent respiratory infections occurring in the first months of life[4]. Thanks to improved understanding, treatments and therapies, the CF lifespan has increased from mid-30s to 44-45 years of age[5].

1.1.1 – *CFTR* and mutations

The *CFTR* gene was discovered and mutations in this gene were determined as the cause of CF in 1989, located on chromosome 7 it is described as consisting of 230kb of DNA spanning over 27 exons[6-8]. The CFTR protein is expressed on cell membranes and phagolysosome membranes of cells across various organs in the body including, but not limited to, the lungs, intestines, pancreas, and liver and is most widely located on the apical surface of epithelial

cells. The function of the transmembrane glycoprotein is to control the movement of chlorine and bicarbonate across membranes, activated by cyclic adenosine monophosphate (cAMP)[9]. This ion movement has an integral role in the homeostasis of the airway surface fluid, so loss or reduction in function of the CFTR protein results in a dehydrated, thickened, and sticky airway mucous layer, reduced muco-ciliary clearance, and a fertile environment for harmful pathogens. Clinical severity of CF is determined by the extent of CFTR function dependent on the type of genetic *CFTR* mutation the individual possesses[10]. The CFTR protein consists of 12 transmembrane domains in two groups each associated with their own nucleotide binding domain and sharing a regulatory domain (Figure 1.1.1).

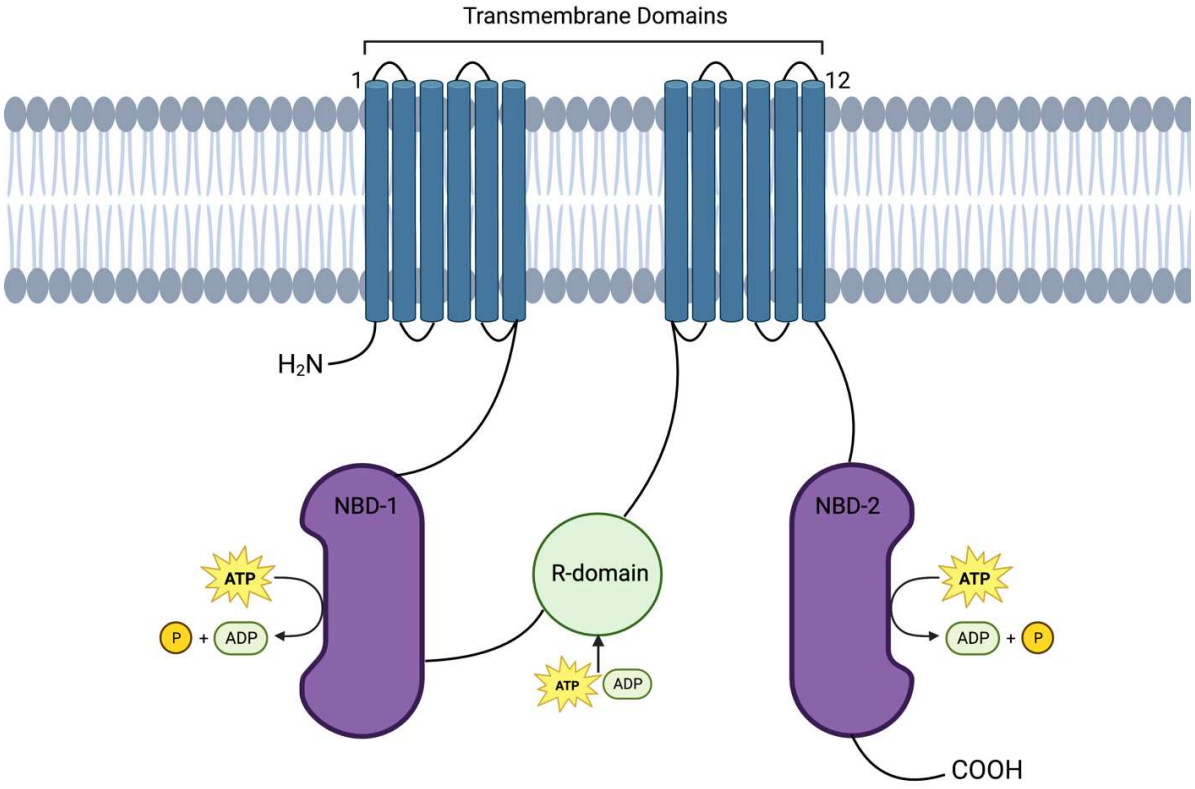

Figure 1.1.1: Cystic fibrosis transmembrane conductance regulator structure. CFTR protein structure. H2N = Amidogan; NBD = nucleotide binding domain; R-domain = regulatory domain; ATP = adenosine triphosphate; ADP = adenosine diphosphate; P = phosphate; COOH = carboxylic acid.

Over 1700 different disease causing *CFTR* mutations have been described, with the most common being a deletion of phenylalanine at codon 508 (F508del) mutation. 80.3% of CF patients in Europe express at least one allele of the F508del mutation, however, this varies depending on geographical region[5, 11]. In 1993, Welsh and Smith defined classes of *CFTR* mutations (class I to V) using *in vitro* cell function and chloride transport assays and based on CFTR protein consequences[12]. This was revised in 1999 and a further class (VI) was added[13]. Class I mutations result in no protein synthesis and therefore complete functional loss. Class II mutations, encompasses the F508del mutation and includes variants resulting in defective protein maturation, processing, or rapid degradation of CFTR, so defective CFTR with some functionality. Both class III and IV mutations allow CFTR protein to be present at the apical membrane but result in defective channel conductance through reduced channel opening and altered conductance through ion selectivity, with class III providing no function but class IV providing some. Class V mutations allow for a reduced amount of functional protein due to abnormal splicing of *CFTR* mRNA. Finally, class VI results in reduced CFTR function because of increased plasma membrane turnover and reduced apical expression through reduction of conformational stability[11]. Increased understanding and matching of mutation to disease pathway have significantly improved patient outcomes.

In 2018, a single-cell RNA sequencing study grouped the cell types of the airway epithelium by gene expression, including known cell types such as goblet, ciliated, and basal cells[14, 15]. This study also revealed a new and rare cell type with very high expression of Forkhead Box I1 (*FOXI1*) and *CFTR* named ionocytes. Despite accounting for less than 1% of the cellular composition of airway epithelium, ionocytes were shown to express 50% of the total *CFTR* mRNA transcripts isolated from the whole epithelium and are thought to be involved in

governing the airway's surface physiology and mucus viscosity[16]. There is no difference in ionocyte abundance between CF and healthy individuals, suggesting the abundance of ionocytes is not affected by functional *CFTR* expression in the airway[16, 17]. Ionocytes have been shown to overcome a limit on NaCl absorption through the CFTR channel by a cation-selective paracellular pathway with basolateral barttin/Cl^- channels[18]. It was predicted that without ionocytes, much of the actively absorbed Na^+ would be refluxed back into the airway surface fluid[18]. Although their contribution to CF pathophysiology is unknown, a better understanding of this cell type could have implications for CF treatment targets.

1.1.2 – Infection and Immunopathology in Cystic Fibrosis

Due to the speed at which CF lungs are colonised and infected with pulmonary pathogens such as *Haemophilus influenzae* and *Staphylococcus aureus* after birth, and later *Pseudomonas aeruginosa* (*P.a.*), human rhinovirus, and *Aspergillus fumigatus* (*Af*) infections, it was assumed the inflammatory airway environment that characterises CF immunopathology arose from chronic and recurrent infections. However, after several studies were conducted to assess the role of lung epithelial and innate immune cells in the acquisition of hyperinflammation including mouse models and CF foetal examination, it soon became clear that inflammation predisposed infection, in turn promoting susceptibility to infection[19-21]. The thick and sticky mucus layer in the CF lung causes hypoxia in the epithelia, which stimulates a 'sterile' inflammatory response through the release of the pro-inflammatory interleukin (IL)-1α and IL-1β[22]. This results in the recruitment of neutrophils, excess reactive oxygen species (ROS) production and further pro-inflammatory cytokine release and promotes susceptibility to infection[23, 24].

The *CFTR* gene has been implemented in the modulation of multiple signalling cascades that are crucial for an effective but regulated immune response. The CFTR protein can directly bind and colocalise the TNFα signalling intermediate, TRADD, and inhibit the production of IL-8, thus regulating activation of nuclear factor kappa-light-chain-enhancer of activated B cells (NF-κB) and reducing immune cell recruitment, however, mutated *CFTR* is unable to do this[25, 26]. Furthermore, *CFTR* mutations reduce cell's ability to produce PPAR, a transcription factor associated with reducing NF-κB activation. Together these result in overactivation of TNFα dependent NF-κB expression[26, 27]. NF-κB overexpression increases pro-inflammatory cytokine production such as TNFα , IL-1, IL-6, and IL-17A, in turn activating oxidant production. Elevated neutrophil influx and the resultant elevated ROS production is a hallmark of CF immunopathology. However, increased neutrophil numbers are not the only source of elevated ROS. Cells with a *CFTR* mutation cannot efflux cysteine, glycine, and glutamic acid, together referred to as the antioxidant glutathione, effectively. Another key ROS and NF-κB regulatory signalling pathway is the Nrf2 pathway and there is evidence of dysfunction in this pathway in cells with mutated *CFTR*[28], therefore, further misbalancing the already exacerbated redox imbalance in the CF lung. Complement effectors affecting neutrophil function of inflammation are heavily involved in disease progression. Studies have shown increased pro-inflammatory C5a and decreased anti-inflammatory C3a in CF, both being linked to a reduction in body mass index (BMI) and forced expiratory volume (FEV) scores[29]. Furthermore, misfolded mutant proteins, such as mutated *CFTR*, cause endoplasmic reticulum stress triggering an unfolded protein response and further inflammation[30].

Between the 1990s and early 2000s, studies have been published that show CF epithelial cells are more susceptible to viral and bacterial infections than healthy cells[31-33]. More recently,

the reason for this increased susceptibility has been centred around the type I and type III interferon (IFN) response. Type I and III IFNs are well known for their antiviral properties, but their importance in bacterial and fungal biology is increasingly being investigated. Type I and III IFNs induce the expression of hundreds of interferon stimulated genes (ISGs) that have powerful effects on cell physiology, including cell proliferation, survival, differentiation, protein translation and differentiation, as well as inhibition of pathogen replication at numerous stages of its lifecycle[34, 35]. Due to their wide range of effects, it is unsurprising that their expression and signalling is tightly regulated. However, many of the elements of the regulatory pathways governing both the signalling pathway and IFN gene expression are themselves regulated by IFN, providing an intricate network of feedback and feedforward regulatory loops[36, 37]. Epithelial cells are potent producers of both type I and type III IFNs, and with many infections in CF beginning at mucosal surfaces, IFNs are predicted to be of major importance. CF bronchial epithelial cells (BECs) were reported to have lower IFNβ, IFNλ1 and IFNλ2/3 expression as well as lower expression of some ISGs and pattern recognition receptors (PRRs) involved in the type I and III IFN response such as TLR3, MDA5, and RIG-I during infection[38]. CF *P.a.* infection shows diminished IFNβ expression and a significant reduction in recruitment and activation of type I IFN-dependent monocyte-derived dendritic cells (mo-DCs)[39]. Interestingly, the type I and III IFN response was reported to be even lower in rhinovirus and *P.a.* co-infection in CF BECs with reduction of many ISGs such as IFIT1, ISG15, 2'-5'-Oligoadenylate Synthetase L (OASL), and IFI44[40]. This year, Gray's group in Edinburgh published data to prove the *CFTR* dependency of dysregulation of the type I IFN signalling in CF macrophages by showing the rescue of this response after treatment with CFTR protein modulators[41]. Mechanistically, there has also been progress with the confirmation of a defective cGAS/STING/IRF3 type I IFN pathway in CF *P.a.* infected human bone marrow derived

macrophages[42]. To my knowledge, there have been no studies published investigating a downregulation in the type I or III IFN response during fungal infection.

As previously mentioned, the immune dysfunction is not limited to mucosal surfaces, but involves innate immune effector cells such as macrophages, basophils, and neutrophils. Airway CF macrophages are present in higher numbers even prior to infection but show impaired pathogen recognition and phagocytosis while displaying hyperinflammatory properties and reduced clearance of apoptotic self-cells, a process referred to as efferocytosis[43-46]. Therefore, they present as poor drivers of defence and present little resolution of inflammation. Eosinophils have not been investigated as thoroughly as other innate immune cells; however, their levels have been shown to be increased in CF and are positively correlated with increased respiratory symptoms and lung function decline[47, 48]. Therefore, it is predicted that they have further mechanistic defects that are contributing to immunopathology in CF.

The increased numbers of neutrophils present in the CF lung drives an aberrant and uncontrolled neutrophilic inflammatory state[49]. Neutrophil dysfunction in CF is like that of macrophages as they have been shown to have reduced pathogen killing ability, while contributing to hyperinflammation. Neutrophils infiltrate the lung in response to cytokines, chemokines and complement factors already described to be released in increased levels in the CF lung, such as IL-8, TNFα, and C5a[49, 50]. When neutrophils enter the lung in response to infection, phagocytosis, generation of ROS and release of cytotoxic peptides occur in a process known as degranulation, and release DNA in the form of a neutrophil extracellular traps (NETs) that can clump microbes also occurs[51]. The damage of excessive ROS production is described

as the perpetuation of the inflammatory response and damage to proteins, lipids, and DNA, leading to cellular dysfunction and injury[52].

Neutrophils express CFTR protein on their cell and phagolysosome membranes, and as CFTR acts as a chloride channel, it is required to supply the phagolysosome with optimal levels of chloride for microbial killing by phagocytosis[53]. Phagocytosis is the process of a cell internalising a microbe, formation of the phagolysosome which is an organelle that encapsulates the microbe that has been internalised. The phagolysosome will then be acidified to degrade the microbe, which starts with the nicotinamide adenine dinucleotide phosphate (NADPH) oxidase II (NOX-2) generating internal ROS[54]. A component of the ROS produced is hydrogen peroxide (H_2O_2), which reacts with chloride ions to produce hypochlorous acid (HOCl), catalysed by the presence of myeloperoxidase (MPO). This reaction allows for the acidification and chlorination of the phagolysosome, which is crucial in the degradation of the microbe, however, due to the CFTR loss of function, it has been shown to be defective in CF neutrophils[55-57]. CFTR dependency of this response has been shown through experiments involving *CFTR* knockdown HL60 cells[58]. Excessive NET production is another characteristic of CF neutrophils. Despite NET production providing a method of capturing and clumping microbes, their protective function is highly debated due to their hyperinflammatory properties and links to increased disease severity in CF and other autoimmune conditions[59]. High levels of DNA, MPO and elastase are detected in the sputum and bronchioalveolar lavage (BAL) of CF patients and positively correlate with increased symptoms and disease severity[60, 61]. Excessive DNA release in the lung increases viscosity of the airway surface liquid and mucus, further hampering the already defective muco-ciliary

clearance. It has also been shown that CF neutrophils suppress apoptosis, leading to increased survival and a lengthening of their inflammatory effects[62, 63].

Finally, proteases, particularly neutrophil-related proteases, have been linked to the immunopathology of CF[64]. Proteases play diverse biological functions across organisms. In the healthy human airway, proteases regulate the airway surface liquid layer, tissue remodelling, and host defence, including inflammation[65-67]. Protease/anti-protease homeostasis prevents inflammation-related tissue damage[68]. In CF, however, excessive neutrophil-driven inflammation disrupts this delicate protease-antiprotease equilibrium, as a result proteases have been associated with increased morbidity and disease progression[69, 70]. Specifically, neutrophil-derived proteases, such as neutrophil elastase (NE), proteinase 3 (PR3) and cathepsin G (Cat G), overwhelm cognate antiproteases, leading to impaired mucus clearance, persistent inflammation, and compromised immune responses and tissue integrity[70, 71]. Notably, the epithelial sodium channel is regulated by proteolytic cleavage and is considered an important component in CF pathogenesis[72].

1.1.3 – Clinical Presentation of Cystic Fibrosis

As previously mentioned, CF is a multisystem disease, primarily affecting the respiratory, digestive, and reproductive systems[73]. The clinical presentation of CF can vary from birth to adulthood, with symptoms and complications becoming more pronounced as individuals age. New-born screening for CF was introduced in the UK in 2007, allowing early diagnosis through an immunoreactive trypsinogen (IRT) test[74]. IRT is produced by the pancreas, and, in healthy individuals, it is then transported to the small intestine and converted to trypsin which aids digestion. In individuals with CF, the transport of IRT is blocked by mucus, forcing its secretion into the bloodstream. New-borns with abnormally raised IRT will then undergo *CFTR* mutation

screening and a sweat test to confirm the diagnosis (chloride levels in sweat >60mmol/l are confirmatory). From birth over 90% of CF infants show symptoms of respiratory problems such as difficulty breathing, coughing, and wheezing due to the inflammation and subsequent respiratory infections leading to pneumonia and bronchitis[75]. Meconium ileus is common in 10-20% of CF infants, where the first stool is abnormally thick and sticky, due to the dehydration of intestinal mucosal surfaces, leading to intestinal blockages[76]. CF is also the cause of poor growth and weight gain from infancy because of the reduced absorption of nutrients through the thick and sticky mucus layer in the digestive system and reduced IRT transportation[77]. As patients with CF progress into childhood and adolescence, the recurrent lung infections and subsequent inflammation starts to become chronic and lung function will begin to decline. Pancreatic insufficiency continues to worsen in 85% of patients, heightening malabsorption of fats and fat-soluble vitamins again contributing to poor weight gain and nutritional deficiencies and starting to cause abdominal pain and other gastrointestinal symptoms[78]. Coming into adulthood, lung disease and function loss continues to persist alongside the pancreatic and digestive complications. CF adults can also face issues with CF-related diabetes due to pancreatic damage, reproductive issues due to thickened cervical mucus in women and congenital absence of the vas deferens in males, liver disease, osteoporosis, and chronic sinus infections[79].

1.1.4 – Treatments for Cystic Fibrosis

Treatment for CF was historically based around managing symptoms and infections. There was a need for fast diagnosis and implementation of a high calorie and high fat diet along with fat-soluble vitamin supplements and pancreatic enzymes to compensate for the intestinal malabsorption and pancreatic insufficiency[80-82]. Compensation and treatment of respiratory

symptoms and infections involves a combination of physical therapies to enhance mucus clearance and inhaled therapies to reduce inflammation and clear infections. Examples of inhaled treatments including DNase to reduce viscosity of the mucus, corticosteroids, and broad-spectrum antibiotics such as azithromycin to reduce bacterial infections and the inflammation associated[83]. In late-stage disease, organ transplantation, especially lung transplantation, are often the only option.

Increased understanding of structure and function of CFTR protein has led to the development of CFTR modulators, which have made a significant impact of those living with CF, improving general health, and reducing treatment burden in up to 90% of patients with CF worldwide. CFTR modulators are small molecules that can improve and even restore the function of the CFTR protein using multiple methods[84]. The small molecules can be separated into five distinct groups determined by their method of function: potentiators, correctors, stabilizers, read-through agents, and amplifiers[85]. Potentiators (e.g., Ivacaftor) can restore the probability of the CFTR channel opening and, therefore, allow ion conductance through the channel. Potentiators can improve CFTR channel function for CF patients with mutations in class III and IV, contributing for about 5% of the CF population. Ivacaftor was approved by the U.S. Food and Drug Administration (FDA) and the European Medicines Agency (EMA) in 2012 and has been on the market for over 10 years[86, 87]. Correctors are small molecules that can rescue folding and increase processing and trafficking of the CFTR protein to the plasma membrane. Correctors can improve CFTR function in class II *CFTR* mutations, which includes the F508del mutation that is the most prevalent CF-causing mutation. Elexacaftor and Tezacaftor are examples of currently used correctors and a combination therapy of Ivacfator, Tezacaftor and Elexacaftor, named Kaftrio was approved by the FDA in 2019 and by the EMA

in 2020, and is now the most common therapy for CF patients aged 12 and above[88-92]. Stabilizers can rescue the channel protein stability while at the plasma membrane, read-through agents can rescue protein synthesis and amplifiers can increase the amount of CFTR protein present.

CFTR modulator treatment has shown to increase FEV scores, reduce pulmonary exacerbations and need for intravenous antibiotics due to lesser detection of microbes such as *P.a.*, increase of BMI, exercise capacity, and general quality of life[93, 94]. There has also been evidence suggesting improved pancreatic and muco-ciliary function, reduction in overall inflammation, and slower deterioration of lung function so reduced need for transplant and better overall survival. As mechanistic studies begin to use CFTR modulator therapies as controls in their experiments, more functional effects are coming to light, such as the rescue of the type I IFN response in macrophages and the increase of Nrf2 ROS regulatory pathway[41, 95, 96] . Hence use of CFTR modulators may have more widespread clinical benefits that just correction of anion channel function[96, 97].

1.2 – *Aspergillus fumigatus*

Aspergillus fumigatus (*Af*) is a ubiquitous saprophytic and filamentous fungus. *Af* is the most commonly occurring *Aspergillus* species that can cause disease in humans, along with *Aspergillus niger, Aspergillus flavus,* and *Aspergillus terreus* to name a few. Despite primarily occurring in air, soil, and decaying vegetation, its ability to survive in a temperature range of 25°C to 38°C and a pH range of 2 to 9, *Af* can be found globally and isolated from many other environments[98].

1.2.1 – *Aspergillus fumigatus* life cycle

Af reproduces through production of asexual spores, termed conidia, from conidial heads on a structure called the conidiospore which is produced when the *Af* reaches starvation[99]. *Af* conidia are more hydrophobic than many other fungal species and extremely small at 2-3μm in diameter allowing them to become buoyant in air and disperse effectively[100]. Because of this, *Af* conidia are consistently the most prevalent fungus in air sampling studies and healthy individuals are expected to inhale and successfully clear 100-1,000 conidia daily[101-103].

Directly after initial release from conidiospores, resting conidia are surrounded by a hydrophobin rodA layer of rodlet and melanin proteins, aiding their protection and dispersal. When conidia encounter an environment with favourable conditions such as sufficient carbon and moisture, they will begin to swell and germinate, breaking and shedding its rodA layer[104, 105]. Eventually, the *Af* will form their vegetative structures called hyphae which can form an extracellular matrix and ultimately, if the environment is stable, they will form a biofilm, where the cycle will start again[106]. At each stage of growth, *Af* possess distinct cell wall compositions[106]. In 2009 there was the first report of *Af* sexual reproduction between an

environmental and a clinical strain under the extremely specific conditions of 3-6 months on poorly aerated oatmeal agar at 30°C[107]. This process has yet to be observed in the environment, however, this cryptic sexual reproductive cycle could account for the increasing levels of diversity and recombination observed in the *Af* strains.

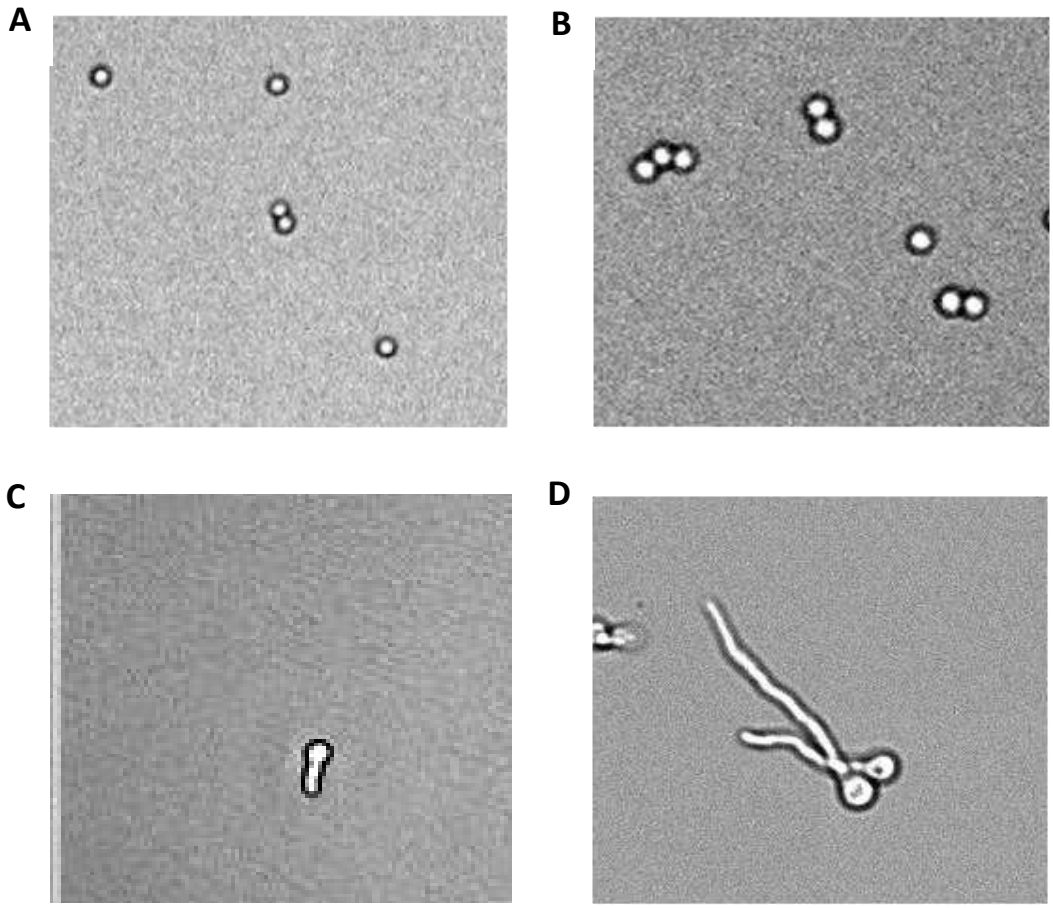

Figure 1.2.1: *Aspergillus fumigatus* Morphological Forms. During starvation a conidial head is formed, and resting conidia (A) are produced and released. Once favourable growing conditions are found by the released conidia, they begin to swell (B) and germinate (C), eventually forming hyphae (D).

1.2.2 – Aspergillosis

Af can cause a range of diseases under the umbrella term Aspergillosis[108]. Risk factors for development of *Aspergillus* related disease include prolonged neutropoenia and monocytopenia, defects in neutrophil function, immunosuppressive therapy post-transplant medication, corticosteroids, structural lung disease, post-viral infection, atopic disorders such as asthma and CF. Aspergillosis can be classified into three broad categories consisting of invasive infection, chronic colonisation or infection, and allergic disease. The type and severity of Aspergillosis depends on the immune status of the host and despite distinct immunopathology across the conditions, symptoms often overlap and converge over time (Figure1.2.2)[109].

Allergic bronchopulmonary aspergillosis (ABPA) is cause by a Type 1 immune hypersensitivity to fungal components and is a complex allergic disorder. Predisposing conditions to ABPA are atopic disorders such as CF and asthma, with estimates of 15% of CF patients and up to 30% of asthma patients struggling with this condition[110, 111]. ABPA can be diagnosed with a combination of microbiological and immunological tests, chest imaging, and symptom assessments, however, it can take years to diagnose due to the non-specific symptoms[109, 112]. *Af* specific and serum total immunoglobulin (Ig)E antibodies are good markers of an allergic response to *Af*, along with positive tests for elevated eosinophil levels, sputum cultures of *Af*, *Af* skin prick tests, and chest radiographs[109]. Symptomatic asthmatic patients who have *Af* sensitisation but do not meet all formal criteria for ABPA are categorised as severe asthma with fungal sensitisation (SAFS)[108]. Clinical features of ABPA include increasing cough, sputum, wheeze, shortness of breath, fatigue, and blood in the sputum. ABPA patients can also be asymptomatic, with a study of 155 asthma patients in 2007 showing a 19% rate of

ABPA positive patients presenting with controlled asthma[113]. In late stages of infection without appropriate treatment, there are signs of pulmonary hypertension and respiratory failure. ABPA exacerbations are common with the previously listed symptoms becoming more severe for a period of time and requiring more extensive treatment. Treatment for APBA is based around reducing the inflammatory immunopathology induced *Af* sensitisation, so it includes inhaled corticosteroids rather than antifungals[114]. However, in some severe cases, the use of itraconazole and voriconazole have been used to reduce the amount of *Af* in the airway, successfully reducing the number of allergens and, therefore, alleviating symptoms[115].

Chronic pulmonary aspergillosis (CPA) encompasses a series of diseases, ranging from aspergilloma (a fungus ball) to chronic non-invasive inflammatory fungal disease[114]. CPA usually proceeds those who have pre-existing lung damage, with 20% of recovered tuberculosis patients developing CPA. Again, CPA has a non-specific list of symptoms such as a cough, wheezing, blood in sputum, weight loss, and fatigue which leads to problems with timely diagnosis[108, 109]. Chest imaging can reveal an aspergilloma, however, not all are apparent, nor do they have a uniform size or shape to confirm diagnosis. Therefore, they need to be combined with a positive *Af* sputum culture, tests for anti-*Af* IgG and IgM antibodies and assessment of clinical symptoms for a successful diagnosis[112]. To treat CPA is challenging as it requires prolonged and intense administration of inhaled and systemic antifungals such as itraconazole and voriconazole. However, it is difficult to monitor progression of recovery and it is common that patients relapse soon after the suspension of treatment[115].

Invasive aspergillosis (IA) is the most severe and aggressive form of aspergillosis and is a major cause of mortality and morbidity in immunosuppressed individuals. Of the >250 species of

Aspergillus, *Af* accounts for 60% of the predicted 300,000 IA cases globally. Symptoms include a cough, fever, chest pain, dyspnoea which is a feeling of running out of air, and coughing up sputum with blood, referred to as haemoptysis[116]. As these symptoms are non-specific, a series of diagnostics are required to confirm IA, which often consist of lung biopsies, sputum cultures, and radiological methods to detect a 'halo sign' characteristic of IA[117, 118]. However, due to the severe immunosuppressed status of many IA patients, other pulmonary infections may be present and chest imaging can be indistinguishable from other conditions. Recipients of hematopoietic stem cell transplants, leukaemia patients, and those with chronic granulomatous disease (CGD) are the most at-risk groups for IA and regularly show mortality rates of 50%[119, 120]. Due to the body hosting the perfect conditions for *Af* growth, hyphenation is aggressive and destructive to surrounding tissue leading to vascular penetration and fungal dissemination as well as damage to the lung tissue resulting in necrosis, intravascular thrombosis, and haemorrhagic pulmonary infarct. Vascular dissemination is found in one third of cases of IA at autopsy and can cause further, more severe complications as hyphae can travel to and infect other organs such as the heart, liver, brain, and kidneys[120]. To prevent such high mortality rates, quick diagnosis and treatment with systemic antifungals is essential, however, this is limited by the difficulty posed with diagnosis[119]. Due to its prevalence and costly, sustained, treatments, IA is the most expensive fungal disease in the US. Potent antifungals called triazoles, such as voriconazole, are the most common treatments for IA and work by inhibiting the activity of an enzyme involved in the synthesis of ergosterol, a crucial component of *Af* cell membranes[121]. However, their effectiveness depends on how complex and persistent the underlying cause of immunosuppression is in the patient, and the speed at which the treatment can be administered[122]. Other treatments include surgical removal of

necrotic tissues and immunomodulatory treatments in selected patients such as IFN in some patients with CGD.

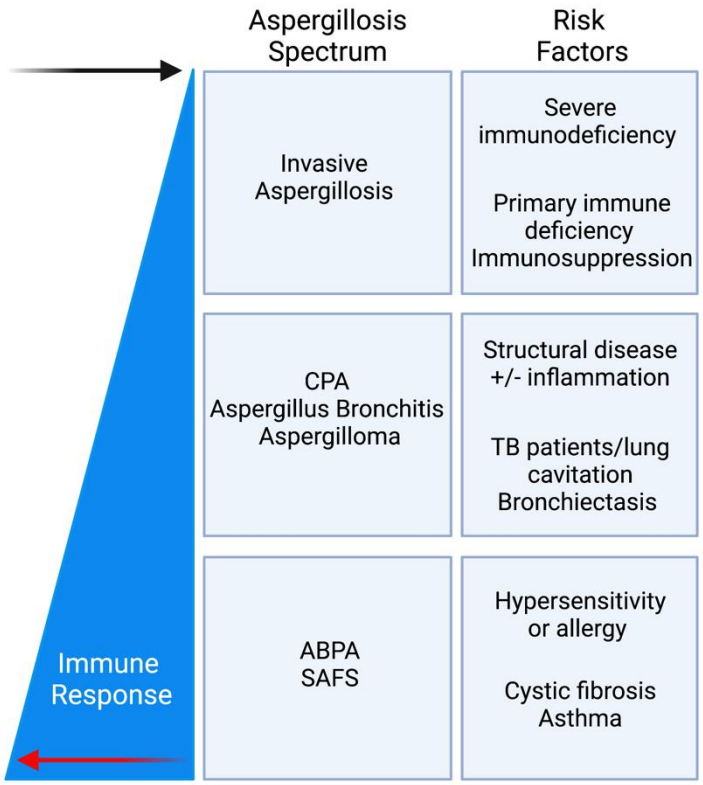

Figure 1.2.2: Clinical Spectrum of Aspergillosis. The clinical presentation of Aspergillosis depends on the immune status of the host. When the host is severely immunosuppressed such as those on immunosuppressants or with a primary immune deficiency they will present with invasive aspergillosis. Patients who present with neither immunosuppression nor hypersensitivity but have risk factors such as lung cavitation or bronchiectasis will present with chronic pulmonary aspergillosis (CPA), *Aspergillus* bronchitis, or aspergilloma. Finally, those who have an exaggerated immune response consisting of hypersensitivity or allergy conditions like cystic fibrosis or asthma will present with allergic bronchopulmonary aspergillosis (ABPA), or severe asthma with fungal sensitisation (SAFS).

Due to increasing azole use in both clinical and environmental environments, there has been a surge of azole-resistance rates[123]. With limited numbers of antifungals, lack of research funding in the area, and heavy reliance on azoles for treatment, this is a growing and pressing concern. *Af* antifungal resistance has reached rates as high as 28% in Europe in a cohort of

CPA patients on long-term azoles[123]. In 2015, a new clinical antifungal called isavuconazole was approved by the FDA that can inhibit the synthesis of ergosterol through a different mechanism to other azoles[124, 125]. However, an environmental antifungal used in agriculture has since been released that uses the same mechanism for fungal killing. With at least 300 species of fungi associated with human diseases, this is not a problem limited to *Af*, revealing the importance of understanding the mechanisms underlying all fungal infections and host responses with the aim to develop new therapeutics[126-128].

1.2.3 – *Aspergillus fumigatus* Immune Recognition

Af has three key attributes that allow it to be a successful disease-causing human pathogen. *Af* replicates efficiently at 37°C, its spore particle size is 2-3μm meaning it is relatively successful at bypassing pulmonary barriers and chemical immune defences, and finally, the hydrophobic rodA and melanin layers previously mentioned that serve to conceal PAMPS such as the β-glucans, galactomannans, and other polysaccharides that make up 90% of the *Af* cell wall at this stage, making them immunologically inert[129, 130]. In healthy individuals, the *Af* conidia will encounter the airway mucosa, including the bronchial and alveolar epithelial lining and the airway surface fluid, mucus, and lung resident immune cells such as alveolar macrophages. The muco-ciliary tract, along with the lung resident immune cells and soluble antimicrobial proteins in the airway surface liquid successfully clear and control the inhaled *Af* in a healthy lung daily[108]. However, in risk factor groups such as immunocompromised individuals, the resting conidia bypass the pulmonary barriers more easily and settle in the alveoli, where they begin to swell. This means the hydrophobic surface layer breaks open to reveal the cell wall, along with the PAMPs it is composed of. The cell wall is >90% polysaccharides and is composed of an alkali-insoluble fibrillar skeleton, which is made of an

outer layer of galactomannan, β(1,5)-galactofuranose residues attached to α-mannan linear chains, and an inner layer of β(1,3);(1,4)-glucans linked to chitin, with both layers bound together by covalent bonds and other polysaccharides such as α(1,3) glucan. When the fungi hyphenate, the cell wall composition changes again, with less β(1,3)-glucans, less, but not loss of melanin, and differing distribution of carbohydrates[131, 132]. At body temperature, the swelling and shedding of the hydrophobin rodA layer takes around 4 hours, with germination starting at 6 hours and hyphae formation between 8-9 hours. It has recently been discovered that *Af* can also alter its cell wall depending on environmental conditions, such as different pH, oxygen levels, and even in the presence of antifungals[106, 133]. All the described cell wall components of *Af* can be recognised by the human innate immune cells such as alveolar macrophages, dendritic cells, and epithelial cells, through multiple membrane bound intra- and extracellular PRRs such as C-type lectin receptor (CLRs), and Toll-like receptors (TLRs). Nucleotide-binding oligomerisation domain (NOD)-like receptors (NLRs) and retinoic acid-inducible gene-I (RIG)-like receptors (RLRs) are involved in intracellular recognition of *Af* as well as soluble scavenger receptors such as lung surfactant proteins and pentraxin3 (Figure1.2.3)[98, 104, 134].

1.2.3.1 – C-type Lectin Receptors

CLRs are arguably the most important PRRs in fungal recognition due to their affinity to β(1,3)-glucans and galactomannan. CLRs are a superfamily of proteins with over 1,000 members and are divided into 17 groups based on their domain organisation and phylogeny[135]. They are named because of their ability to bind carbohydrates in a calcium dependent manner, however, as the superfamily expanded and more CLRs were discovered, it was determined that not every member bind carbohydrate, with some able to bind protein, lipids, and other

inorganic molecules. There are four CLRs that can recognise *Af*, dectin-1, dectin-2, melanin-sensing CLR (MelLec), and dendritic cell-specific intracellular adhesion molecule-3-grabbing non-integrin (DC-SIGN)[136]. Dectin-1 is a group V CLR that recognises β(1,3)-glucan, therefore, it can recognise swelling and germinating *Af* at the cell surface, with some evidence to suggest that it can also play a role in some intracellular interactions when internalised in endosomes[137]. Dectin-1 is expressed primarily on phagocytes, such as macrophages, DCs, neutrophils, and monocytes, as well as bronchial and alveolar epithelial cells, therefore, it is heavily involved in the activation of the innate immune system and expression is upregulated during fungal infection and inflammation[138]. Once bound to β(1,3)-glucan, dectin-1 engages with spleen tyrosine kinase (Syk) through its immunoreceptor tyrosine-based activation (ITAM)-like motif[139]. It can then lead to canonical and non-canonical NF-κB activation. Canonical NF-κB activation occurs through recruitment of caspase recruitment domain-containing protein 9 (CARD-9), formation of a CARD9/ B-cell lymphoma/leukemia 10 (Bcl10)/ mucosa-associated lymphoid tissue lymphoma translocation protein 1 (MALT1) complex that activates IκB kinase (IKK) and subsequently NF-κB. CARD9-independent non-canonical NF-κB pathway relies on the ubiquitination and processing of NF-κB2 precursor protein, p100, to activate the p52/recombination signal sequence-binding protein J kappa enhancer factor B (RelB)/NF-κB complex. Dectin-1 can also activate the type I and III IFN pathways through Syk/IRF5 signalling and the importance of this signalling pathway in candidiasis and aspergillosis has been highlighted in mice studies[140, 141]. The importance of dectin-1 is highlighted through multiple studies showing dectin-1 knock-out (KO) mice, and polymorphisms in humans result in high susceptibility to fungal infection post haemopoietic stem cell transplant[142].

Dectin-2, also known as CLEC6A, is a group II CLR but is expressed on monocytes, plasmacytoid DCs (pDCs), basophils, and Kupffer cells. Dectin-2 has a high affinity to α-mannans; therefore, it can recognise swelling and germinating *Af*[143]. Fungal recognition by dectin-2 also stimulates the activation of NF-κB through the CARD9/Bcl10/MALT1 complex, however, it lacks ITAM-like motifs, so requiring coupling to the Fc receptor gamma chain (FcRγ) to do this[144]. There is no evidence Dectin-2 can recognise or activate *Af* signalling pathways intracellularly. The activation of NF-κB initiates a pro-inflammatory response with the release of cytokines such as IL-1β, TNFα, IL-6, IL-12, and type I and III IFNs, which drive effective phagocytosis, ROS production, and the differentiation of T-helper (Th) cells to a Th1 and Th17 phenotype[145]. This response is crucial for the effective clearance of *Af*[146, 147]. Deficiency in dectin-2 in humans is associated with elevated levels of IA and other fungal infections[148, 149].

Other important CLRs involved in *Af* recognition are MelLec, a group V CLR, and DC-SIGN, a group II CLR[150]. MelLec was discovered in 2014 and can recognise dihydroxynaphthalene (DHN)-melanin which is present on the hydrophobin rodA layer. This makes MelLec essential for early recognition and clearance of resting conidia and it is expressed on innate immune cells such as macrophages, DCs, and neutrophils[150]. Studies in humans and mice have shown the importance of MelLec, with KO mice and humans with a polymorphism both showing increased susceptibility to aspergillosis and fungal dissemination causing IA[151].

1.2.3.2 – Toll-like Receptors

TLRs are a small family of proteins discovered in 1989, of which there have been 10 discovered in humans. They are a crucial set of PRRs for viral, bacterial, and fungal infections and work either alone or in heterodimerisation with other TLRs, and non-TLR receptors[152]. TLRs consist of leucine rich repeats and a cytoplasmic toll-interleukin receptor (TIR) domain. TLR3 and TLR4

can induce IFN related pathways through activation of TIR-domain-containing adaptor-inducing IFNβ (TRIF). All other TLRs, including TLR4, can signal through the myeloid differentiation primary response 88 (MyD88) signalling cascade to signal a pro-inflammatory NF-κB response[153]. In early 2000s, Wang, et al., first described TLR4 as a receptor for *Af* hyphae and since then TLR2, TLR3, TLR7, and TLR9 have been implemented in fungal recognition[154]. Immediately, their importance in fungal immunity became clear when MyD88 deficient mice became highly susceptible to *Af* disease.

TLR4 is expressed on innate immune cells and epithelial cells and can recognise *Af* hyphae to signal for pro-inflammatory cytokines such as type I and III IFNs, IL-1β, and TNFα[154, 155]. Multiple studies have shown defective phagocytosis and neutrophil fungal killing when TLR4 expression is reduced through the use of TLR antagonists or removed entirely in KO cell lines and mouse models[156, 157]. TLR2 can recognise β-glucan and zymosans, is expressed on innate immune cells and epithelial cells and forms a heterodimer with TLR1 and TLR6 when bound to fungal stimulus. It has been shown to be recruited to phagosomes holding engulfed zymosan and its absence results in an altered inflammatory response to fungus characterised by lower TNFα, increased IL-4, and higher mortality rates in IA models[158]. TLR3, TLR7, and TLR9 are endosomal TLRs that can recognise fungal RNA and DNA. Similarly to TLR2, TLR9 has been shown to be actively recruited to phagosomes containing *Af* and signals for NF-κB activation[159]. Polymorphisms of TLR9 in humans has been linked with increased susceptibility to both ABPA and IA, showing its function in *Af* immunity can be complex[160-162]. TLR3 and TLR7 can initiate a type I IFN response signalling through TRIF and again, polymorphisms in these TLRs have shown increased incidences of IA and ABPA[155, 163]. Furthermore, TLR3 deficiency was associated with severe infection in mice, and a *TLR3* SNP resulting in a loss-of-

function phenotype of DCs was associated with increased susceptibility to aspergillosis and concomitant failure to activate antifungal CD8+ T cells in HSCT patients[164].

1.2.3.3 – NOD-like Receptors

NLRs are intracellular PRRs characterised by the presence of a central NOD and typically contain leucine-rich repeats with a variable N-terminus domain. There are 23 known human NLRs which can be split into two classes, the inflammasome forming NLRs and NOD1/2[165]. They are thought to act like scaffolding proteins in the cytosol, providing a coordinated assembly of signalling molecules that can initiate both the NF-κB and mitogen-activated protein kinase (MAPK) signalling and inflammatory pathways. Despite the signalling pathways being under researched, there is mounting evidence that NOD1 and NOD2 are involved in the recognition of *Af*[166-168]. NOD1 can recognise *Af* and is upregulated and recruited to phagosomes during *Af* infection[167]. NOD2 has also been shown to be upregulated during *Af* infection and some NOD2 dependent pathways have been upregulated, however, how either NOD1 or NOD2 recognise or signal this recognition is unclear. NOD1 KO mice and human cells showed a protective phenotype against IA, with more effective fungal killing through optimal ROS production and NOD2 polymorphisms shows reduced risk of IA post stem-cell transplantation[169, 170]. Inflammasomes are multiprotein complexes formed in response to infection or tissue damage which play a crucial role in inflammatory responses by activating and regulating the production of key pro-inflammatory cytokines, IL-18 and IL-1β[171]. Their formation can be initiated through detection of microbes and other sterile stimuli by the intracellular NLRs such as NLR family pyrin domain containing 3 (NLRP3). Mounting evidence suggests internalised *Af* conidia, fungal-induced ROS production, and potassium efflux are recognised by and activate NLRP3 inflammasomes [171, 172].

1.2.3.4 – RIG-I-like Receptors

RLRs are a family of cytoplasmic PRRs that are known to have a key role in the antiviral response and initiation of type I and III IFNs[173]. There are three identified human RLRs, known as retinoic acid-inducible gene I (RIG-I), melanoma differentiation-associated protein 5 (MDA5), and laboratory of genetics and physiology 2 (LGP2) also known as DExH-box helicase 58 (DHX58)[173]. They are known to signal both dependently and independently of each other, often working together to enhance type I IFN signalling. Similarly to NLRs, fungal recognition by RLRs is not well understood, however, recent evidence has suggested MDA5 can recognise *Af* double stranded DNA[174]. MDA5 can signal through MAVS to drive production of type I and III IFN which in turn induces expression of C-X-C motif chemokine ligand (CXCL)9 and CXCL10 which are essential for optimal antifungal neutrophil immunity[174-176]. Furthering this, Wang, et al., published a mouse model showing MAVS expression in alveolar macrophages was essential for *Af* immunity and reported on a human study which showed MAVs polymorphisms increased IA susceptibility in patients that underwent hematopoietic stem cell transplantation[177]. Despite limited information on the role of LGP2 in fungal immunity, it has been shown that it can interact with MDA5 and enhance its double stranded DNA binding ability, in turn increasing the type I and III IFN response generated by MDA5 activation[175]. Therefore, LGP2 could act as a potentiator of *Af* recognition by MDA5[175].

1.2.3.5 – Soluble Receptors

Several soluble cytoplasmic scavenger receptors are thought to have a significant impact on fungal immunity. Lung surfactant proteins A and D, and mannan-binding lectin (MBL) are C-type lectins that can bind carbohydrate domains on the *Af* cell wall in a calcium-dependent manner. They can then opsonise the *Af*, enhancing fungal recognition and phagocytosis by

effector cells such as macrophages and neutrophils[178]. Despite no mechanistic understanding of the ability of MBL to recognise and react to *Af,* a study in an IA mouse model revealed exogenous MBL treatment increased neutrophil ROS production and increased fungal control and survival[179, 180]. A third soluble receptor that has been linked to fungal immunity is pentraxin-3 which is readily produced by monocytes, macrophages, and DCs during *Af* infection[181, 182]. Pentraxin-3 can increase fungal recognition, in turn increasing essential antifungal responses such as pro-inflammatory cytokine release and phagocytosis[183, 184]. A rat model of IA has shown a lack of pentraxin-3 results in ineffective phagocytosis and exogenous treatment of pentraxin-3 can rescue this defect[185].

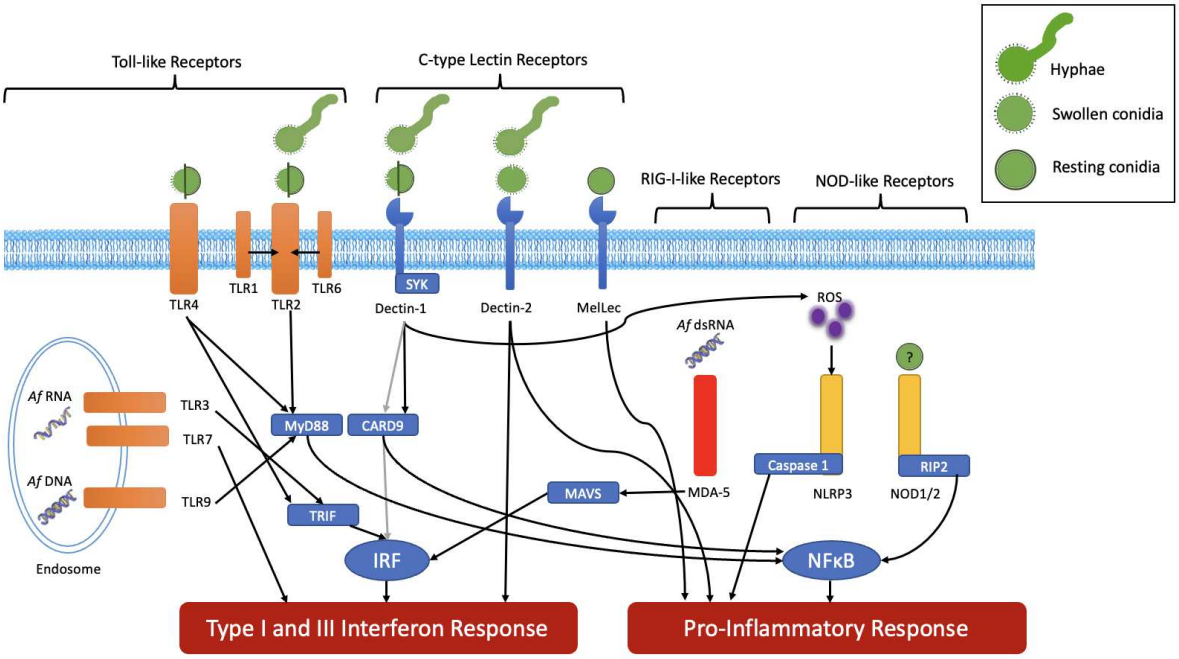

Figure 1.2.3: *Aspergillus fumigatus* recognition and immune activation. Schematic of the pattern recognition receptors (PRRs) and signalling pathways involved in the recognition and initiation of the type I and III interferon response and pro-inflammatory responses to *Aspergillus fumigatus,* including what morphology or element of *Aspergillus* infection initiates the response. Various PRRs initiate these responses and are split into their relevant families; Toll-like receptors (TLRs), C-type lectin receptors (CLRs), RIG-I-like receptors (RLRs) and NOD-like receptors (NLRs). Where the pathway is unknown there is a direct arrow. The signalling pathway showing Dectin-1/Syk/CARD9/IRF signalling is coloured grey as this represents a known interferon response pathway discovered in response to *C. albicans*.

1.2.4 – Innate immune response to *Aspergillus fumigatus*

Due to the ubiquitous nature of *Af* conidia, effective daily clearance of fungus from the lung is required. In healthy individuals this is primarily achieved with the physical barriers such as the muco-ciliary tract, airway surface liquid, and epithelial cells. In some cases, lung resident alveolar macrophages, inflammatory monocytes, and neutrophils are required for optimal control[186]. The crosstalk between the epithelial barrier and lung resident phagocytes is essential for a controlled and coordinated response [187].

Data from murine studies show that RAG2KO/IL2rgKO mice which lack both innate and adaptive lymphocytes, eliminate *Aspergillus* conidia and prevent formation of tissue invasive filamentous hyphae in the respiratory tract[188]. Data indicates that myeloid phagocytes are necessary and sufficient to control *Af* infection. Confirmation of the role of epithelial cells in host immunity to *Af* will require targeting gene deletion studies involving fungal receptors and down-stream signalling pathways in defined subsets linked to infection outcomes in murine models. The importance of myeloid phagocytes in humans is highlighted by the absence of invasive aspergillosis in severe combined deficiencies affecting lymphocyte function[189]. Although lymphocytes are redundant for protection against *Af* in healthy controls, they are important in those with a defect of myeloid function as seen in haematopoietic stem cell transplant recipients[190].

Alveolar macrophages and dendritic cells phagocytose *Af* conidia, which is facilitated by pentraxins opsonised spores[191]. Germinating conidia expose β 1-3 glucans and leads to Dectin-1 mediated release of IL-1α/β by alveolar macrophages and dendritic cells[137]. The IL-1 cytokines activate pulmonary epithelial cells, which lead to secretion of neutrophil chemoattractants CXCL1 and CXCL5[174, 192, 193]. Other inflammatory mediators including

leukotriene B4, C5a, galectin 3 and CXCL2 also promote neutrophil migration into lung airways[194]. Monocyte chemoattractants CCL2, CCL7, CCL12 promote influx of inflammatory CCR2+ monocytes into lung airways, which differentiate into mo-DCs[195]. Neutrophils also play a key role in promoting oxidative killing and elimination of *Af* conidia by mo-DCs. Neutrophils, monocytes, and mo-DC phagocytose conidia and eliminate germinating spores via NAPDH oxidase[196]. Secretion of type I IFNs by monocytes leads to upregulation of type III IFN, which augments fungal killing by myeloid phagocytes[163]. Fungal infection of mo-DC and neutrophils leads to secretion of CXCL9 and CXCL10, via CLR-SYK-CARD-9-SYK and type I IFN pathways respectively, which recruits plasmacytoid DC (pDCs) from the circulation into the lung[188]. Although pDCs do not bind to *Af* conida, they further promote their oxidative killing by neutrophils. Mechanistic basis for pDC augmentation of neutrophil oxidative burst is unknown but may involve type I and III IFNs. In addition, secretion of GM-CSF also upregulates neutrophil oxidative killing, although the source of GM-CSF is not currently known[197].

1.2.4.1 – Epithelial Cells

Despite most the inhaled *Af* conidia being cleared from the lung by the muco-ciliary tract before reaching the epithelial surface, epithelial cells and their fungal recognition are an essential first-line cellular defence in *Af* immunity[187]. Epithelial cells can recognise several fungal cell wall components such as galactosaminogalactan and chitin which initiates an antifungal phenotype capable of orchestrating a response in other innate immune cells, especially macrophages and neutrophils[98]. After fungal recognition, epithelial cells will produce pro-inflammatory cytokines and chemokines through IL-1α/MyD88/NF-κB, p38/ERK1-2, and type I and III IFN signalling to recruit effector cells[163, 198]. Several studies have shown the importance of this recruitment of neutrophils and C-C chemokine receptor

type 2 ($CCR2^+$) macrophages in prevention of fungal colonisation. Epithelial cells themselves also have a fungal phagocytotic ability through actin-dependent internalisation and cathepsin D and lysosome-associated membrane protein 1 (LAMP1) dependent phagolysosome acidification[199, 200]. This epithelial phagocytosis has been shown to be so effective that <3% of internalised *Af* conidia are able to continue growing, germinate, and lyse the cell. Studies have shown that lack of epithelial phagocytotic ability in immunodeficient mice results in increased aspergillosis linked morbidity and mortality[201]. Some particularly virulent strains of *Af* have the unique ability to germinate and cross the epithelial barrier through actin tunnels which avoids epithelial barrier damage, and therefore, detection through recognition of both PAMPs and damage-associated molecular patterns (DAMPs)[98, 202]. Lack of detection and failure to initiate innate immune response unsurprisingly leads to poor prognosis.

1.2.4.2 – Alveolar Macrophages

Alveolar macrophages are a distinct long-lived macrophage phenotype that self-propagate and are resident in the lung, both in the airway surface fluid and in the alveolar spaces[203]. Alveolar macrophages possess nearly all the PRRs that recognise *Af* that have been previously described, making them very effective at recognising swollen and germinating conidia. Fungal recognition results in Syk-dependent signalling which can initiate ROS and NADPH release, ROS-dependent activation of LC3 associated phagocytosis (LAP), activation of the inflammasome, and NF-κB and IRF1/5-dependent pro-inflammatory cytokine and chemokine release[204]. Alveolar macrophages are essential for antigen presentation and immune-cell crosstalk during *Af* infection. Depletion of alveolar macrophage populations in mice models resulted in increased neutrophil recruitment but reduced fungal control[205, 206].

1.2.4.3 – Inflammatory Monocytes, Monocyte-derived Dendritic Cells, and Plasmacytoid Dendritic Cells

After epithelial initiation of inflammation, $CCR2^+$ monocytes and mo-DCs are responsible for transportation of *Af* conidia to lymph nodes in order to activate an adaptive immune response[195, 207, 208]. Inflammatory monocytes rapidly differentiate into mo-DCs in the presence of *Af* infection and lack of this differentiation can result in reduced fungal killing[195]. $CD14^+$ and $CD16^+$ monocytes can control fungal growth through iron restriction and starvation of *Af* conidia and germlings[207]. Further importance of $CCR2^+$ monocytes has recently been reported using a mouse model. Espinosa, et al., showed that type I IFN release from $CCR2^+$ monocytes initiates a coordinated type III IFN release which is required for optimal priming of antifungal neutrophils[163]. Without type III IFN priming, neutrophils release sub-optimal ROS, resulting in reduced fungal killing and increased susceptibility to IA.

pDCs are an essential cellular effector in antifungal immunity, despite constituting for less than 0.1% of the overall cellular composition of the blood[209]. pDCs are not able to directly kill *Af* but inhibit growth of hyphae by an unknown mechanism[210]. They have been observed spreading over the length of the hyphae and releasing apoptosis-inducing gliotoxins during this process[211]. They can recognise *Af* through the CLRs dectin-2 and DC-SIGN and potently produce cytokines such as type I IFNs and TNFα that are key in immune cell recruitment and boosting of the adaptive immune response[141, 149].

1.2.4.4 – Neutrophils

Since excessive neutrophil infiltration and neutropenia are both major pre-disposing features for aspergillosis in humans, neutrophils are undoubtably the most important effector cells in *Af* immunity[212]. Neutrophils are the most abundant immune cell in the body that, after

maturity, will circulate the body[51]. During infection, neutrophils are recruited to the site of infection where they will survey the organ tissue for pathogens and elicit a multi-pronged defence approach. The mechanisms neutrophils deploy are NADPH oxidase-dependent ROS production, phagocytosis, degranulation, cytokine and chemokine release, and NET formation[213]. During *Af* infection, neutrophils are recruited by several chemokines, including CXCL1, CXCL2, CXCL5 and CXCL8. The release of these chemokines are initiated primarily in a MyD88-dependent manner by epithelial cells, subsequently in a CARD-9 dependent manner by other immune cells, and finally lung-infiltrating neutrophils during active infection[214-216]. As neutrophils are granulocytes, immediately after activation and fungal recognition, they will degranulate which is the release of their granules containing antimicrobial proteins such as neutrophil elastase (NE), myeloperoxidase (MPO), and lactoferrin. Many of these proteins have been reported to have several antifungal effects, such as arresting hyphal growth and killing through iron-depletion, contributing to ROS production, and acidification of the phagolysosome[217-219]. Neutrophils can effectively phagocytose *Af* conidia in a Syk-kinase signalling dependent way, however, the mechanisms of fungal recognition and completion of this process is poorly understood.

The NADPH oxidase-dependent ROS production is extremely important in fungal clearance as many mouse models lacking this response have shown increased morbidity and mortality to fungal infection[220]. In humans, CDG is a condition in which immune cells have defective NADPH oxidase and, therefore, lose the ability to generate ROS[221]. Individuals with CDG are highly susceptible to IA with high mortality rates. As previously mentioned, a functional type I and III IFN response is essential to optimal priming of antifungal neutrophils, particularly regarding the generation of an effective ROS response[141, 163, 174]. Despite this response not

being well studied in fungal infection, patients with CF have a downregulated or defective type I and III IFN response during viral and bacterial infections and this could explain their susceptibility to aspergillosis.

Neutrophils also produce NETs in response to *Af* infection, which consist of extracellular traps made up of DNA with antimicrobial molecules, such as MPO and NE, attached[222]. The role of NETs in fungal killing is complicated, it is thought they contribute to an arrest in hyphae growth but are major contributors to damaging hyperinflammation. Neutrophils preferentially form NETs in response to *Af* hyphae rather than conidia and are fungistatic which helps to limit spread of infection[222, 223]. NETs contain chelators of essential ions such as calprotectin which can bind to iron, zinc, and magnesium, immobilising fungal filaments and depleting the fungi of the nutrients needed to grow and replicate[224]. Release of extracellular ROS in NETs by neutrophils in response to large fungal filaments leads to IL-1β secretion, which promotes further neutrophil recruitment to sites of infection. On the other hand, phagocytosis of fungal conidia and generation of intracellular ROS, inhibits the secretion of IL-1β and leads to formation of neutrophil clusters, which have been shown to be more effective at fungal killing[224]. Therefore, although NETs can provide some protection against infection, they also promote inflammatory immune responses and tissue damage, for example, excess NET activity is associated with renal disease in SLE and vascular disease in primary anti-phospholipid syndrome. In cases of CGD, when defective ROS production is unable to control fungal infection, there is an increase in NET production[225]. Due to their lack of protective function along with their hyperinflammatory state, it is thought that NETs are more likely to contribute to damaging chronic inflammation rather than aid in fungal clearance[226].

1.2.4.5 – Eosinophils and Natural Killer Cells

Eosinophils are another granulocyte that contribute to *Af* immunity and whose overrepresentation is a hallmark of ABPA[227]. Eosinophils can directly kill *Af* through production of DNA traps, similar to NETs, however, overstimulation of this response can be damaging and is thought to contribute to the development of ABPA and related symptoms[227-229]. These cells are also important for immunomodulatory functions as they regulate IL-23 and IL-17 production in the lung[230]. Natural killer (NK) cells also have a direct killing effect on *Af* conidia and hyphae and are readily recruited, acting in a compensatory manner during neutropenia. NK cells possess TLR2, TLR4, and TLR9, so it is predicted they detect *Af* through these PRRs, however, this has not been confirmed to date. Fungal cytotoxicity by NK cells is predicted to be related to the release of molecules such as granulysin, granzymes, and perforin, which act as chemoattractants, trigger apoptosis, and aid in the lysis of target cells[231].

1.2.5 – Adaptive immune response to *Aspergillus fumigatus*

In mouse models of acute pulmonary aspergillosis, complete aberration of the adaptive immune response showed no increased susceptibility to fungal infection, suggesting the adaptive immune system is redundant in *Af* immunity[163, 195]. However, in patients who have received hematopoietic stem cell transplantations and those living with HIV, a lack of an adaptive immune system increases susceptibility to fungal infection[189]. Furthermore, *Af* specific $CD4^+$ T-cell transfer in mice has a protective effect in IA disease[232, 233]. Therefore, when there is an immunodeficiency surrounding the innate immune response, the adaptive immune response is an essential back-up for host defence.

1.2.5.1 – T-cells

The T-cell subsets that are involved in *Af* immunity are the $CD4^+$ T-cells, which are known as T-helper cells. Antigen presenting cells will interact with naïve Th cells and initiate their differentiation into a pathogen-specific subset, depending on the antigen and the cytokines released from the antigen presenting cell[234]. The relevant Th cell subsets in fungal immunity are Th1, Th2, and Th17. Th1 is induced by IL-12 and can be neutralised by IL-4[235]. Studies in mouse models show that positive outcomes in IA is positively correlated with high levels of IL-12 and negatively correlated with IL-4, suggesting the importance of Th1 in *Af* immunity[236, 237]. Furthering this, Th1 cells produce high levels of IFNγ which can stimulate antifungal responses from neutrophils and macrophages, whose importance has been discussed previously in detail[236]. In patients with ABPA, a phenotyping of the peripheral blood mononuclear cells reveals a Th2 bias, resulting in reduced fungal control and an allergic inflammatory environment[238]. Th2 differentiation is stimulated by IL-4 release and results in the neutralisation of the Th1 response[239]. A Th2 bias in the Th1/Th2 balance results in the development of *Af* sensitivity as Th2 cells produce IL-4, IL-5, IL-10, and IL-13 which triggers an allergic inflammation consisting of eosinophil influx and ineffective macrophage activation[234]. Unlike Th2, Th17 cells can provide protective functions through their release of IL-17, IL-21, and IL-22 and communication with neutrophils, increasing both their recruitment and antifungal function[240]. Th17 differentiation is triggered by TGFβ, IL-6, and IL-23 and the importance of this response is shown in patients with CGD, who have reduced IL-17 release, showing increased IA susceptibility[241]. However, the balance of the Th17 response is essential as overactive Th17 will result in neutrophilia and the associated pathogenic inflammation[242]. Furthermore, Th17 responses can enhance damage during Th2 bias in ABPA cases, again due to increasing neutrophil recruitment[243].

1.2.5.2 – B-cells

Antibodies are secreted by terminally differentiated B cell (plasma cells). Antibodies have 2 core regions including a variable region which recognize antigens, and a constant region consisting of 5 main isotypes which eliminate antigens in different ways. The 5 main isotypes are IgM, IgD, IgG, IgA and IgE. IgG is essential for protection against pathogens and is the antibody class responsible for the memory response in secondary immunity[244]. IgM enhances phagocytosis and surveys ABO blood group antigens on erythrocytes[245]. IgE is associated with allergy and is thought to be protective against parasites. IgA is a secretory antibody found in mucosal surfaces and contributes to first defence in mucosal immunity, and finally, IgD is associated with homeostasis and antibody production[246]. *Af* infected B-cell deficient mice displayed increased survival and fungal killing with increased and effective Th1 responses, therefore, B-cells are not required for protection against *Af*[245]. However, increased *Af* specific IgE and IgG antibodies are a hallmark characteristic of aspergillosis, and both are used for diagnostic purposes[109]. IgE, as the allergy associated antibody, is detected at high levels in ABPA patients and can interact with basophils and mast cells, causing them to degranulate and release histamine, heparin, and other proteases[247]. Histamine acts to increase mucus secretion and stimulate sensory nerves, furthermore, it activates the Th2 response which leads to an influx of eosinophils, which can release a myriad of toxic proteins[248]. These functions can lead to a hostile host environment for parasites, which IgE is protective against, however, when this response is initiated in the absence of a parasite it is ineffective in pathogen clearance and causes a damaging allergic inflammatory response, such as what is observed during ABPA.

1.2.6 – *Aspergillus fumigatus* and Cystic Fibrosis

Af has been detected in up to 60% of CF sputum cultures globally, with 30% of patients displaying *Af* sensitivity and 8.1% of patients with CF had positive diagnosis for ABPA in the UK in 2021[249]. There are several reasons why CF is a major predisposing factor to aspergillosis. In healthy individuals, over 90% of *Af* conidia are successfully cleared by the muco-ciliary tract, the defectiveness of which is the hallmark characteristic of CF[12, 108]. Epithelial cells are then important in the recognition and phagocytosis of *Af* swollen conidia, in healthy individuals this prevents growth in >97% of conidia, however, defective *CFTR* results in reduced *Af* uptake, killing, and induction of a dysregulated inflammatory signalling that is crucial for the induction of a coordinated and effective immune response[187]. Patients with CF present with an altered epithelial surface through reduction of tight junctions, allowing *Af* to germinate and hyphenate through the epithelial barrier without damaging it more effectively, therefore reducing the release of DAMPs[75, 186]. Essential innate immune cells in *Af* immunity are macrophages and neutrophils and both possess reduced antimicrobial functions in CF[43, 60]. A contributing factor to the reduced antimicrobial activity is a reduction in effective phagocytosis due to a lack in acidification and chlorination of the phagolysosome because of the lack of CFTR protein function on the phagolysosome membrane[250]. Neutrophils express the CFTR protein both on their phagolysosome membranes and cell surface membranes and it is thought to have an important role in supplying the phagolysosomes the chloride ions required for optimal microbe killing. After the phagolysosome encapsulates the microbe, NOX2 activation generates ROS, including H_2O_2. MPO enters the phagolysosomes and catalyses the reaction of chlorine and H_2O_2 to form HOCl, which is the active ingredient in bleach and is essential for the acidification of the phagolysosome and chlorination and

degradation of ingested microbes[60]. Therefore, despite the elevated number, increased survival, and increased ROS production of neutrophils in the CF airway, there is defective control or killing of pathogens and a reduction in the neutrophilic homeostatic ability, contributing to the overall hyperinflammatory state (Figure1.2.6). Abnormal TLR trafficking has also been observed in CF epithelial cells and macrophages, resulting in reduced *Af* recognition by TLR PRRs[251, 252]. Additionally, as evidence emerges to suggest the importance of *Af* activated NLRP3 inflammasomes in the clearance of *Af* it is important to highlight the overactive, but paradoxically, ineffective inflammasome function observed in CF [171, 172]. Defective adaptive immunity is also reported in CF, with overactive Th2 and Th17 responses and reduced Th1 response, contributing to reduced fungal clearance and prolonged allergic inflammation[253-256]. Due to the reduced fungal clearance, there is continued release of fungal allergens and the associated neutrophilic inflammation over time which will eventually cause enough damage to the airway and the development of bronchiectasis[257].

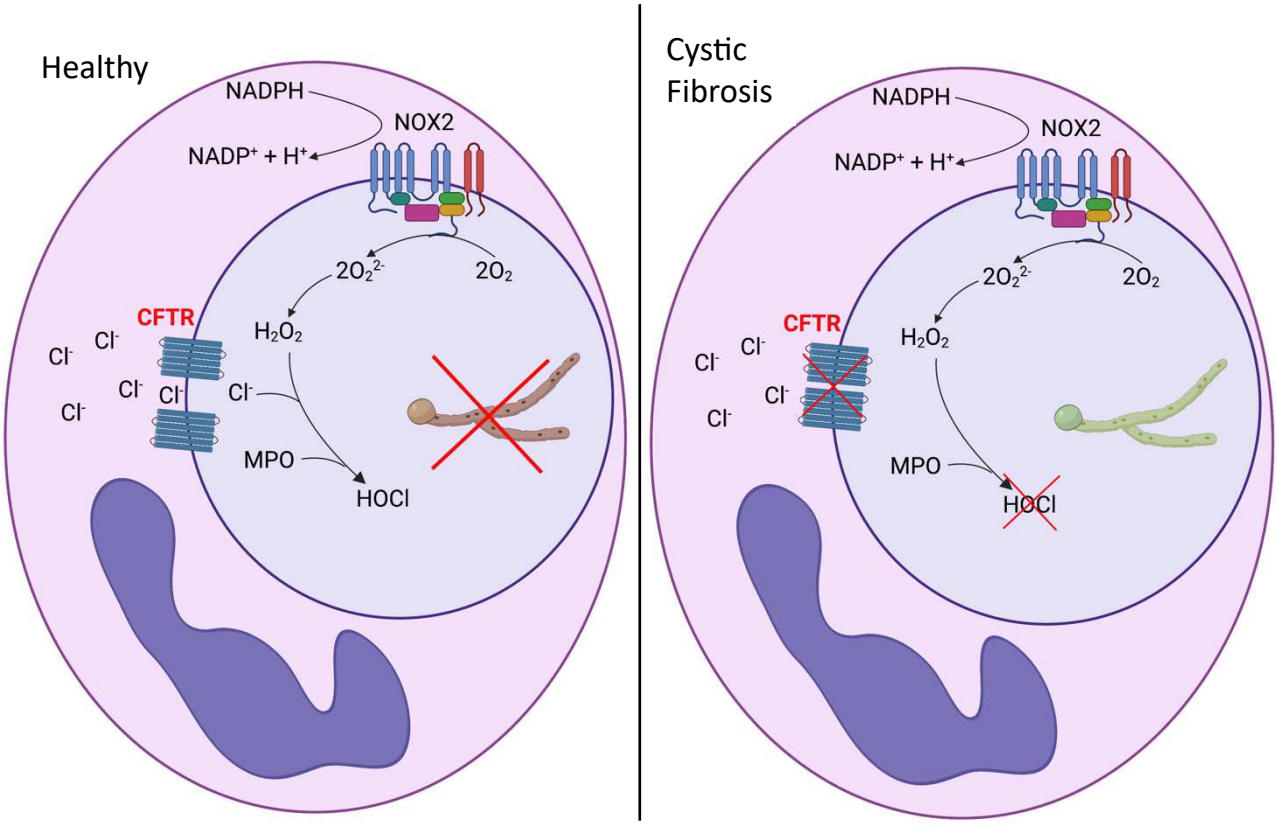

Figure 1.2.6: Acidification of phagolysosome during *Aspergillus fumigatus* killing. Healthy neutrophils engulf *Af* and acidify the phagolysosome through NOX2 forming ROS such as H_2O_2, which then reacts with MPO and Cl^- to form HOCl. With defective CFTR in CF neutrophils, this reaction fails to happen, therefore, failed phagolysosome acidification and reduced fungal killing. NOX2: NADPH oxidase; H_2O_2: hydrogen peroxide; MPO: myeloperoxidase; Cl^-: chloride ions; HOCl: hypochlorous acid; CFTR: cystic fibrosis transmembrane conductance receptor.

1.3 – Type I and III Interferons

There are three families of IFNs based on homology, named type I, type II, and type III IFNs. Type II IFNs have just one member, IFNγ, which is involved in both the induction and regulation of the pro-inflammatory response[258]. The type I IFN family was discovered in the 1957 and consists of 17 subtypes in humans[259, 260]. They were initially described for their antiviral functions and subsequently their importance in immunoregulation and in defence against bacterial and fungal pathogens. Type III IFNs were discovered in 2003 and consist of 4 subtypes in humans[34, 261]. Initially, due to the similarity between type I and type III IFNs, it was thought that type III IFNs were redundant in antiviral protection, however, their importance was highlighted by the discovery that their front-line defence at epithelial surfaces causes significantly less inflammatory damage than the type I IFN response and they have unique effects on innate immune cells[262, 263]. Type I and III IFNs can induce the expression of many ISGs which can have a significant impact on cell physiology and can act directly on pathogens to control the inflammatory response and microbial growth. Due to their breadth of functions, it is unsurprising that their expression and production is tightly regulated by complex feedback and feedforward signalling loops[264-266]. Despite their similarities, type I and III IFNs have distinct spatial and mechanistic functions.

1.3.1 – Interferon Structure and Homology

All three of the IFN subsets are part of the class II cytokine family which encompasses IL-10-related cytokines such as IL-10, IL-20, and IL-22. All class II cytokines possess a conserved structure made up of six α-helices and their receptors form extracellular cytokine binding sites through formation of two extracellular type III fibronectin domains[267]. In humans, type I IFN

genes are located in a cluster on chromosome 9 and are known to have evolved through gene duplication and divergence, meaning there is variation between vertebrate species[268]. The 17 type I IFNs in humans all signal through one receptor, made up of the subunits IFNAR1 and IFNAR2, forming the heterodimeric IFNAR which is ubiquitously expressed in all cell types. When binding, the type I IFNs have a high affinity to IFNAR2 and low affinity to IFNAR1 and when bound together the receptor forms a functioning signalling complex[269]. IFNα has 13 subtypes in humans ranging from IFNα1-13, all consisting of 166 amino acids apart from IFNα2 that possesses a deletion at position 44[267]. IFNβ and IFNω genes exist as a single copy with 166 and 172 amino acids respectively. IFNω has a 75% identity homology with IFNα, whereas IFNβ only has 30% homology with IFNα[37].

Type III IFNs have only four subtypes in humans, IFNλ1, IFNλ2, IFNλ3 (also referred to as IL-29, IL-28A, and IL-28B), and finally IFNλ4. Type III IFNs have a distinct receptor, also consisting of two subunits, namely IL-10Rβ and IFNLR1[270]. Receptor binding occurs in the same way as type I IFNs, as they bind with high affinity to IFNLR1 and then recruit the low-affinity receptor chain IL-10Rβ to allow the complex to be able to begin signalling. In humans, IFNLR is primarily expressed on respiratory, intestinal, and vaginal epithelial cells, hepatocytes, B-cells, neutrophils, pDCs, moDCs, and macrophages[271]. However, due to the differential receptor expression during infection, the number of cells receptive to type III IFN is predicted to grow[272]. Type III IFN genes are located on chromosome 19, all consisting of 189-200 amino acid sequences that possess around 90% homology within the family, and approximately 30% homology with the type I IFNs[273].

1.3.2 – Interferon Production and Signalling

Interferon signalling is induced by detection of PAMPs by both cytosolic and endosomal PRRs (Fig1.3.2). The PRRs that can initiate classical signalling of type I and III IFN expression are TLR3, TLR4, RIG-I, MDA5, and cGAS[270, 272, 274]. The type of IFN that is produced will depend on what PRR is stimulated and where the PRR is located in the cell[272, 275]. There is evidence to suggest that TLR4 stimulation at the plasma membrane initiates type III IFN expression while TLR4 activation in the endosome can result in the expression of type I IFN. Classical signalling to stimulate the expression of type I IFN results in IRF3 activation and IFNβ expression, IFNβ will stimulate the expression of ISGs, including IRF7 which will then result in IFNα subtypes being produced and further ISG stimulation[276, 277]. IRF5 is another interferon regulatory transcription factor that can induce IFNβ expression[176]. IRF3 and IRF7 can induce type III IFN expression, along with some distinct signalling pathways such as IRF1 activation and Kurzer antigen subunit 70 (Ku70) signalling[176, 278, 279]. The main producers of type III IFNs are epithelial cells but also include hepatocytes, dendritic cells, and fibroblasts following infection. Type I IFNs are produced in large amounts by pDCs but can also be produced by macrophages, fibroblasts, epithelial cells, endothelial cells, and B and T-cells. Furthering this, type III IFNs can induce the production of type I IFNs in response to some pathogens. This has only been investigated in a restricted subset of cells including lung and intestinal epithelial cells[280].

After expression, production, and release of type I and III IFNs, they will be detected by their distinct receptors on neighbouring cells and will signal downstream for the expression of ISGs in a very similar way. Once activated, type IFNAR chains will interact with Janus kinase 1 (JAK1) and Tyrosine kinase (TYK2) and activate the interferon-stimulated gene factor 3 (ISGF3) complex, IFNLR also activates ISGF3 but through a TYK2 independent mechanism[281]. ISGF3

consists of signal transducer and activator of transcription (STAT)1 and STAT2 which, when phosphorylated, will recruit and bind IRF9 to form the activated heterotrimeric complex[37]. This complex will translocate to the nucleus and induce the expression of many overlapping ISGs, however, differences in magnitude, kinetics, and intrinsic signalling qualities of the ISG expression induced by type I and III IFNs provide distinct biological outcomes[282]. Type I IFNs can also signal through STAT3 which have been observed to both stimulate a subset of type I ISGs and negatively regulate STAT1-dependent ISG activation to modulate both the type I and III IFN response[283, 284]. Type I and III IFNs can also signal through p38 MAPK signalling[285]. Type I IFN signalling will happen rapidly after pathogen recognition in a systemic manner with a high potency, resulting in a hyper-inflammatory response that will continue in a cyclical fashion[272]. Type III IFN signalling will be induced more slowly after pathogen recognition with a lower potency and restricted mainly to epithelial surfaces, allowing a sustained, less inflammatory protection at epithelial barriers[280].

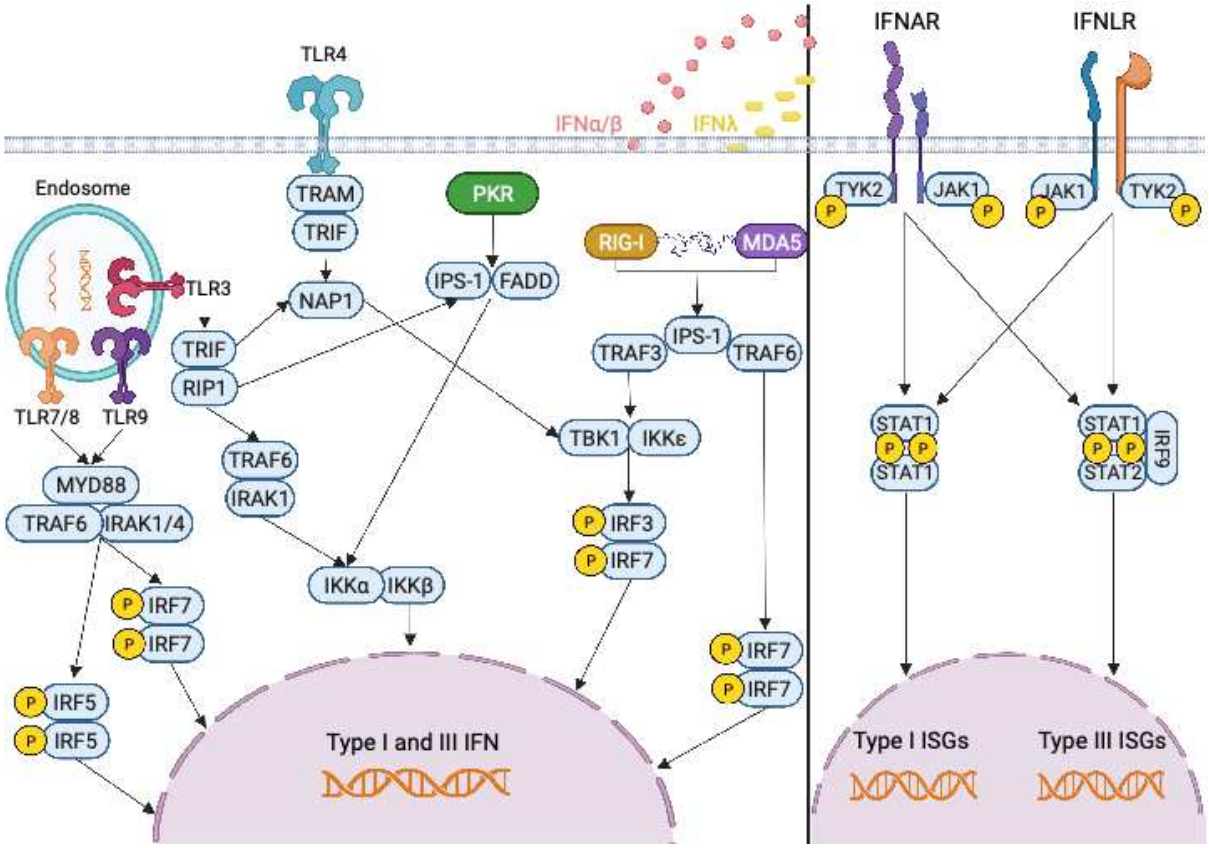

Figure 1.3.2: Schematic of type I and type III Interferon signalling. Type I and III IFN expression is signalled for through various pathways, initiated by recognition of a variety of pathogen stimulus by pattern recognition receptors. Toll-like receptor (TLR) 4 can recognise pathogens extracellularly and signal through TIR-domain-containing adapter-inducing interferon-β (TRIF) and transmembrane adaptor protein (TRAM) to activate an interferon regulatory factor (IRF) 3 and IRF7 heterodimer. TLR3 recognises pathogen double stranded (ds)RNA and signals through TRIF and receptor interacting protein 1 (RIP1) to activate TNF receptor-associated factor 6 (TRAF6) and interleukin-1 receptor-associated kinase 1 (IRAK1) heterodimer that finally activates I-kappa-B kinase alpha (IKKα) and IKKβ to stimulate expression of type I and III IFNs. TLR7/8/9 can recognise pathogen specific DNA or RNA in the endosome and all signal through myeloid differentiation primary response 88 (MYD88), TRAF6, IRAK1/4 complex to activate either an IRF7 or IRF5 homodimer. Protein kinase R (PKR) is an enzyme that can detect dsRNA in the cytoplasm and can signal through interferon-beta promoter stimulator 1 (IPS-1) and fas-associated protein with death domain (FADD) to activate the same IKKα/β heterodimer as TLR3. Finally, retinoic acid-inducible gene I (RIG-I) and melanoma differentiation-associated protein 5 (MDA5) can both recognise RNA and dsRNA respectively in the cytoplasm and activate a heterodimeric complex involving IPS-1 and either TRAF3 or TRAF6. TRAF3 signals through TANK-binding kinase 1 (TBK1)/IKKε to activate IRF3/7 heterodimer and TRAF6 can activate a IRF7 homodimer.

Once produced, type I and III IFNs are transported out of the cell and signal through JAK/STAT signalling to stimulate the expression of interferon stimulated genes that can influence cell physiology such as cell proliferation, survival, differentiation, and protein translation as well as having direct effect on pathogens through inhibition of pathogen replication at numerous life cycle stages.

1.3.3 – Interferon Stimulated Genes and Immunity

Approximately 450 ISGs have been identified to be commonly induced by type I IFNs in humans, however, this is thought to be higher with some studies predicting IFNs control up to 10% of the human genome[286]. There have been 62 core ISGs identified to be expressed across many animal species, including humans and mice, and represent an evolutionarily conserved group shown in Table 1.3.3[286]. Type III IFNs induce expression of a very similar pool of ISGs, including the core 62. A study using vaginal epithelial cells identified few distinct genes such as IFIT3, IFI30, CXCL10, CXCL11, and Tudor domain containing 7 (TDRD7) that were upregulated by IFNλ1 but not IFNβ, encompassing functions including immune cell recruitment, antigen presentation, and inhibition of pathogen protein translation[287]. However, this study was carried out with just one time point, therefore, it is unclear whether varying ISG signatures would have been observed over time. Due to epithelial surfaces coming into continuous contact with environmental microbes, there is significant importance on the body's ability to provide protection while preventing a destructive inflammatory response. The spatial segregation of type I and III IFN receptors suggests type III IFNs are particularly important at maintaining the sustained protective but less inflammatory response at epithelial surfaces including the respiratory tract, gastrointestinal tract, and the cervical and vaginal lining[274, 280]. Only when the anatomical barrier is breached, does a systemic and highly inflammatory type I IFN response provide a protective response. A patient reported with a

IFNAR2 loss of function mutation successfully controlled infections until the administration of a live vaccine which bypassed the type III IFN controlled epithelial barriers and resulted in the patient succumbing to infection at 1 years old, confirming a key role of type III IFN at epithelial barriers[288].

Table 1.3.3: Core ISGs and their functions. The 62 conserved ISGs across all mammalian cells split into functional abilities[286].

PAMP sensing + IFN signalling	**Anti-microbial properties**	**Cell signalling + Apoptosis**	**Ubiquitination + Protein modification**	**Antigen presentation**	**IFN negative regulation**	**Miscellaneous**
AZ12	ADAR	CASP8	DTX3L	B2M	CD274	C2
cGAS	APOL1,2,3, + 4	CD47	HERC6	ERAP1	IFI35	CMPK2
IRF1	C19orf66	IL15RA	N4BP1	HLA	NMI	CMTR1
IRF7	IFIT2	LGALS9	NUB1	NLRC5	PARP14	DNAJA1
IRF9	IFIT3	RICTOR	PARP9	PSMA5	SOCS1	DNAJC13
LGP2 (DHX58)	ISG15	TRAIL (TNFSF10)	RBCK1	PSMB8	TRAFD1	EHD4
MDA5 (IFIH1)	ISG20		RNF19B	PSMB9	TRIM21	FAM46A
MYD88	MORC3		RNF213	PSMB10	USP18	FMR1
RIG-I (DDX58)	MOV10		RNF31	PSME1	USP25	PNPT1
RNF114	MX1		UBA7	PSME2		SERTAD1
STAT1	OAS1		UBE2L6	RFX5		SLC25A28
STAT2	PARP12			TAP1		SP110
TLR3	PKR			TAP2		TDRD7
TRIM25	PML			TAPBP		WARS
	RSAD2			TAPBPL		XAF1
	SAT1					ZCCHC2
	SCOTIN					ZNFX1
	ZAP					

Due to the number of genes induced, the effect ISGs have on both the cell physiology and the pathogen life cycle is vast[289]. Regarding pathogen life cycle, several genes are involved in preventing entry to the cell (e.g., IFITM1-3, CH25H), nuclear import (e.g., MX1, MX2), arresting mRNA (e.g., IFI16, APOBECs) and protein (e.g., IFIT1-5, ZAP) synthesis, replication (e.g., IFI6, Viperin), and promoting degradation (e.g., ISG20, OAS1-3)[35, 289-296]. Many PRRs and IFN regulatory factors are expressed at baseline in cells, however, after IFN signalling many of them are enhanced. These include cGAS, RLRs, NLRs, STAT1/2, and IRF1/3/7/9, promoting both a range of pathogen recognition and further IFN and innate immune signalling[281]. Both type I and III IFN signalling can promote tightening of the cell junctions at epithelial linings and in the central nervous system including the brain, which maintains the integrity of epithelial barriers[297, 298]. In macrophages, type I IFN can promote antimicrobial pro-inflammatory cytokine production, phagocytosis, and antigen presentation[188]. The type III IFN response can also promote an antimicrobial response in macrophages, however, this response involves more regulation of pro-inflammatory cytokine release and includes enhancement of macrophage-mediated tissue remodelling and regeneration processes[163, 188]. A similar effect is observed in dendritic cells, with type I IFNs promoting maturation and activation, antigen presentation, cytokine production, and a type I IFN positive feedback loop during infection, while type III IFNs can also promote microbial protection while also promoting modulation of the magnitude of cytokine production, tissue homeostasis and immune surveillance effects[299]. Neutrophils express ISGs in response to both type I and III IFNs, however, inflammatory cytokines such as TNF and IL6 were induced predominantly by the former, with virus infected mice defective in IFNAR showing higher viral and inflammatory burdens than KO IFNLR mice[300]. KO of IFNLR on neutrophils in mice models has shown reduced control of viral and fungal infection through defective recruitment, suboptimal ROS production,

differential gene expression, and reduced phagocytosis[301]. It is important to note that loss of type III IFN function promotes further upregulation of type I IFN production which can result in overactive recruitment and activation of neutrophils, resulting in a damaging hyperinflammatory state[163]. This emergence of type III IFNs as potent regulators of neutrophil function was unexpected and further work needs to be completed to understand the complexity of this response.

ISGs can have a direct and indirect impact on the adaptive immune response. It is predicted that type I IFN signalling will have more of a direct impact on both B and T-cells and type III IFN signalling will have a direct impact on B-cells and an indirect impact on T-cells, due to receptor expression and spatial differences observed in mice[302, 303]. B-cell responses can be directly impacted by enhancing stimulatory cytokines (e.g., B-cell activating factor [BAFF], a proliferation-inducing ligand [APRIL]) and TLR-mediated IgG and cytokine production[302, 304, 305]. T-cell responses can be enhanced by ISGs through stimulating both class I and class II major histocompatibility complex (MHC) expression, increasing antigen-presentation by stimulating migration through CCR5/7 and lymphocyte function associated antigen 1 (LFA-1), and co-stimulatory molecule expression (e.g., C80, CD86)[303, 306-308]. ISGs can also promote T-cell proliferation and survival through expression of cytokines and chemokines (e.g. CXCL9/10, IL-15), and reduce negative regulators[302, 303, 309, 310].

1.3.4 – Immunoregulatory Effects of Interferons

Due to the potency and variety of effects the type I and III IFN responses can yield, it is unsurprising that they are tightly regulated both intrinsically in the cell and by the ISG expression itself. Cells have been described as entering an IFN-desensitised state that is

capable of lasting several days[311-313]. Defects in this desensitisation can result in autoimmune diseases such as systemic lupus erythematosus[314]. IFN desensitisation includes immediate, early, and sustained methods. Immediate and early methods can be cell intrinsic, including the endocytosis and degradation of IFNAR and IFNLR and phosphatases inhibiting phosphorylation of JAK-STAT signalling[313]. Further JAK-STAT signalling prevention can be ISG mediated through expression of genes such as suppressor of cytokine signalling (SOCS) which are expressed early after IFN production[315]. SOCS proteins can prevent STAT binding and JAK activity by binding to phosphorylated tyrosine residues and recruiting proteins involved in degradation and receptor ubiquitination[316]. ISG mediated sustained IFN desensitisation is achieved through expression of ubiquitin-specific peptidase 18 (USP18) for type I IFN and USP22 for type III IFN which works by removing ISG15 conjugates from target proteins where ISG15 is modulating the stability, localisation, activity, and interactions of these proteins[317-319]. USP18 can also bind the intercellular domain of IFNAR2 and IL-10R2, causing transformational changes to reduce the affinity for type I and III IFNs and preventing the binding of JAK1 and TYK2 respectively and, therefore, mounts a more sustained shutdown of JAK-STAT signalling[320, 321].

1.3.5 – Clinical Applications of Interferons

The therapeutic potential of type I and III IFNs is vast and has only started to be explored. Due to their earlier discovery and better understanding, the therapeutical use of type I IFNs have been explored more thoroughly although with advances in the understanding of type III IFN functions, it is thought they may provide more benefit with reduced inflammatory side effects. To date, no type III IFN drugs have been approved for use in humans but there are several in clinical trials specific for chronic hepatitis B, C, and D infections which are reporting the same

or improved effects with minimal side effects when compared to their currently approved and used IFNα2a equivalent[322, 323]. Of the type I IFNs several have been approved and are commercially used for a variety of conditions, these include IFNα2a, IFNα2a, IFNβ1a, and IFNβ1b[324]. IFNβ has been used to treat multiple sclerosis since 1993 and has been shown to slow the development of brain lesions, reduce relapse rates, and arrest disease progression by 46.8% over a 21-year period[325-328]. Although it is predicted that the protective mechanism of this treatment is through induction of regulatory T-cells, poor disease understanding means this is not well understood. IFNα subtypes have a variety of clinical uses, from cancer treatments to chronic viral infections, with the earliest use documented in 1998 for chronic hepatitis C[329]. Again, the mechanism of efficacy in hepatitis infections is poorly understood, but it predicted to be a combination of the direct antiviral effect many ISGs possess, along with modulating $CD8^+$ T-cell activation[330-333]. Type I IFNs do possess anti-tumour effects and IFNα subtypes are widely used in conjunction with other therapies to treat cancers such as haematological malignancies, melanomas, and solid tumours[334]. They can be protective through increasing recruitment of antigen presenting cells, inducing autoantibody production for self-recognition, and increasing NK and T-cell activation. More recently, during the COVID-19 pandemic inhaled and systemic IFNα, IFNβ, and IFNλ were investigated as treatments[335, 336]. There were many contradictory studies published as differing outcomes were observed depending on the severity of the case. In mild COVID-19 cases there was improved outcomes, however, limited data prevents conclusional statements. A large trial completed recently shows that early treatment with pegylated type III IFN is helpful in preventing progression of COVID-19[337]. In severe and moderate cases there was no association with worsening but no consistent significant improvement on mortality or progression to ventilation yet with many studies treating with differing doses and time points of infection it is difficult to draw

conclusions[336]. Significant toxicity of type I IFN means that efficacy of type III IFN should be assessed in clinical trials to observe the benefit and risk of adjunctive cytokine therapy in fungal infections. Furthermore, with increasing evidence of the protective effects of both type I and III IFN in bacterial and fungal immunity, further work needs to be done to assess their protective roles and therapeutic potential.

1.4 – Aims and Hypothesis

As evidenced above, *Af* can cause serious morbidity and contribute to lung function decline in patients with CF. There is a variety of functional issues in CF immunity which allow *Af* to persist in the lung, several of which are directly or indirectly controlled by type I and III IFN responses (e.g., fungal recognition, phagocytosis, neutrophil ROS production). Type I and III IFNs have been reported to be downregulated in response to bacterial and viral infections in CF, with very recent work being published on the mechanisms of this defect, however, this has yet to be investigated in fungal infections. Moreover, polymorphisms in the MAVS and IFIH genes show increased susceptibility to IA in patients after haemopoietic stem cell transplants[177]. Therefore, it is hypothesised that there is a downregulated type I and type III IFN response during *Af* infection in cells with a *CFTR* mutation and that this defect results in reduced fungal clearance by CF neutrophils. This thesis aims to investigate both the type I and III IFN response in cells with a *CFTR* mutation and the effect of exogenous type I and III IFN on the antifungal capabilities of CF neutrophils.

1. To assess the type I and III IFN response to *Af* in bronchial epithelial cells with functional and defective *CFTR*.
2. To assess the effect of CFTR modulators on the type I and III IFN response to *Af* in bronchial epithelial cells with defective *CFTR*.
3. To assess the type I and III IFN response to *Af* in PBMCs isolated from healthy donors and from patients with a *CFTR* mutation.
4. To assess the effect of exogenous type I and III IFN on the antifungal function of neutrophils isolated from healthy donors and patients with a *CFTR* mutation.

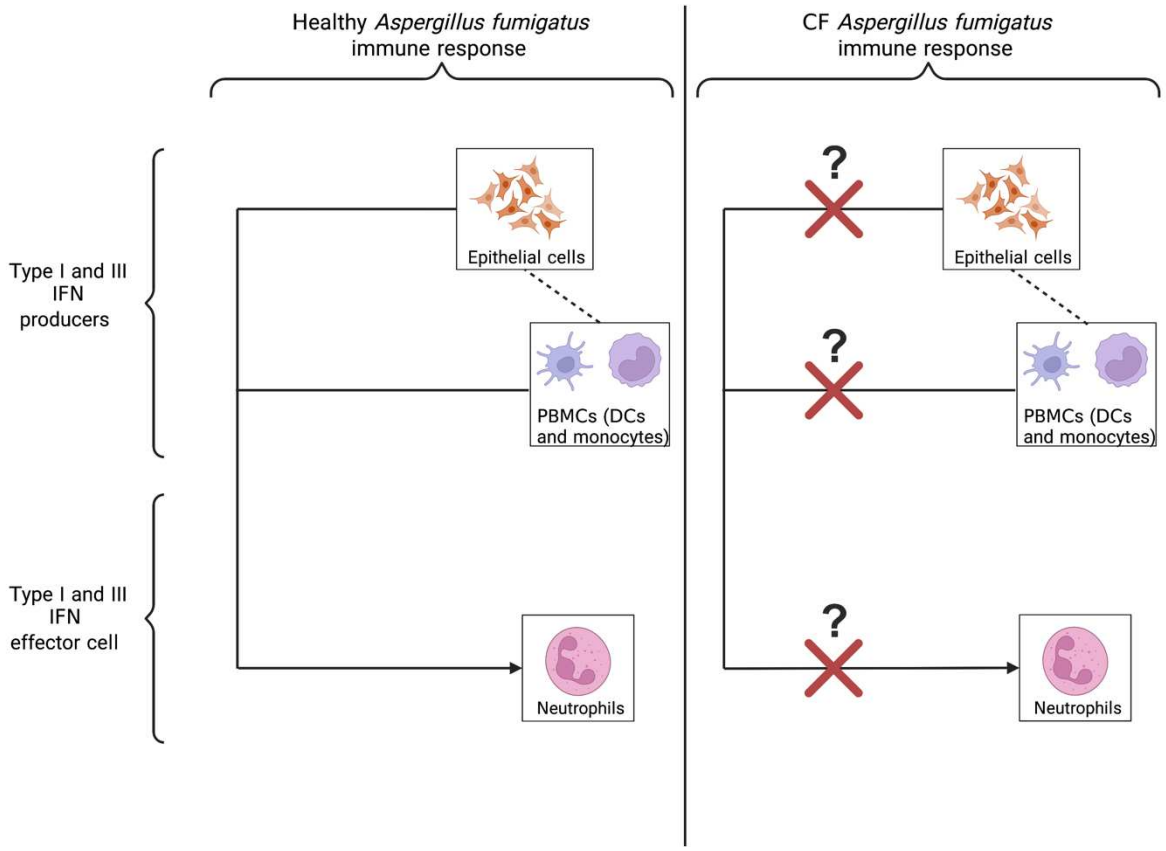

Figure 1.4: Graphical abstract.

Chapter 2: Methods

2.1- Cell culture, isolation, and infection

2.1.1- Epithelial Cell Monolayer Culture

BEAS-2B BECs (ECACC, Sigma), CFBE41o$^-$ Human CF Bronchial Epithelial Cell Line (SCC151, Merck), CFBE41o$^-$ 4.7 WT-CFTR Human CF Bronchial Epithelial Cell Line (SCC158, Merck) were grown at 37°C with 5% CO_2 in Minimum Essential Medium α (MEM α, Gibco) supplemented with 10% (v/v) FBS. Cells were growth to a maximum passage of 15 and the passage was kept consistent between controls cells in experiments wherever possible. No antibiotics or antifungals were used during culture or infection with any cell lines. Cells are referred to as healthy BECs, CF BECs and CF corrected BECs respectively.

2.1.2- Epithelial Cell Air Liquid Interface (ALI) Culture

Healthy bronchial epithelial cells (passage 2 or passage 3) and a primary CF bronchial epithelial cell line isolated from a 32 male with ΔF508 homozygous deletion mutation (CF-AB045202, Epithelix; passage 2 or passage 3) were cultured for 2 days on a glucose-coated (for 30 miniutes) 24-well transwell plate (6.5mm diameter inserts, 0.4um pore size, Corning) with hAEC medium (Epithelix), containing growth factors and supplemented with antibiotics, on the apical and basal surface to ensure cells were at confluency. After 2 days, media was removed from the apical surface and the cells were washed twice with warm PBS. Basal media was then changed every 2 days for a further 20-26 days for complete differentiation of pseudostratified epithelium. Mucus production started at 14 days and required a warm PBS wash once a week on the apical surface of the culture. The differentiated cultures of ALI

contain goblet, basal and ciliated cells and allow for formation of tight junctions which are known to be critical for epithelial barrier integrity. The presence of goblet cells were confirmed with the observation of mucus production and ciliated cells were confirmed through observing the mucus swirls on the apical surface. The presence of basal cells was assumed due to the well characterised nature of this method.

2.1.3- Fungal Culture, Harvest and Preparation

Fungus used during this project was *Af* strain CEA-10 (FGSC A1163) from the Fungal Genetics Stock Centre and Discosoma spp. red fluorescent protein (dsRed) *Af* which was gifted from Georgios Chamios. The CEA-10 and dsRed were grown on sterile potato dextrose agar (PDA; Oxoid, CM0041) in a T25 flask (ThermoFisher) for 4-5 days. Resting conidia were harvested by adding 10ml sterile PBS (Gibco) 0.1% TWEEN (Sigma) to the flask, rocking gently back and forth. Harvested conidia were filtered through Miracloth (Calbiochem, UK). The suspension was then spun down at 3000g for 10 minutes and resuspended in PBS.

To prepare swollen conidia and hyphae the resting conidia were incubated at 37°C with 5% CO_2 for 3 and 9 hours respectively in clear RPMI, collected using PBS 0.1% TWEEN and resuspended in PBS. Resting and swollen conidia and hyphae were fixed in 4% paraformaldehyde (PFA) overnight, neutralised with 0.1% NH_4Cl, washed the indicated number of times and resuspended in PBS. Heat killed conidia were prepared by placing resting conidia in a water bath at 90°C for 1 hour. For NETosis assays, resting dsRed *Af* conidia was used and incubated for 7 hours at experimental conditions in a clear and flat-bottomed, white-walled 96-well plate in clear RPMI before addition of cells. At this stage, they are starting to hyphenate and are referred to as germlings.

2.1.4- Epithelial Cell Fungal Infection and Stimulation

Epithelial cells were seeded at $5x10^5$ cells/ml in 12 well plates for RT-PCR and $5x10^4$ cells/ml in 96 well plates for ELISAs and LDH assays 24 hours prior to infection. After 24 hours, stimulation with fixed resting and swollen conidia, fixed hyphae, and heat killed conidia at a Multiplicity of Infection (MOI) of 2 or 8 or Poly(I:C) at 100μg/ml in MEM without FBS for RT-PCR and ELISA and clear MEM without FBS for LDH assays (Note: FBS was removed from all media during infection or stimulation assays). The cells were placed in the incubator for the indicated time at 37°C with 5% CO_2 before the supernatant and cells were harvested. Uninfected cells were treated with PBS and served as a control.

For BECs at ALI, after 20-26 days of differentiation, fixed hyphae, and heat killed conidia (MOI=8) were placed on top of the apical surface and incubated at 37°C with 5% CO_2 for the indicated time. The cells that were uninfected were treated with PBS as a control. After infection, the apical surface was washed with 200μl cold PBS and collected, and basal media was collected, and cells were harvested for analysis.

2.1.5- Epithelial Cell CFTR Modulator Treatment

CF cells were treated with a combination treatment of Ivacaftor, Tezacaftor, and Elexacaftor at a 1:1:1 ratio at 0.33ng/μl each, therefore an optimised total concentration of 1ng/μl (see section 4.1). Treatment was carried out 24 hours prior to infection by removing media, washing the cells twice with warm PBS and replenishing the media with the appropriate concentration of the combination treatment. This process was repeated 24 hours later directly before infecting with fungus or stimulating.

2.1.6- Study Set-up, Design and Current Participants

The patient groups included in this study are CF with fungal disease, CF without fungal disease, non-CF fungal disease, non-CF chronic lung disease without fungal disease and healthy controls.

Patients were recruited as part of two longitudinal studies. The Fungal Resistance Evolution and Acquisition in Chronic Lung Disease (FREAL) study is an 18-month longitudinal observation study involving patients with CF and other chronic lung diseases such as COPD and asthma. Targeting Immunotherapy in Fungal Infections in Cystic Fibrosis (TrIFIC) is a multi-centre cohort study investigating immunotherapeutic options in individuals with CF *Aspergillus* bronchitis/ABPA and healthy controls.

2.1.7- Ethics Statements

The Study Coordination Centre has obtained approval for FREAL (IRAS ID: 244685; REC reference: 19/LQO/1663) and TrIFIC (IRAS ID: 270828; REC reference: 20/LO/0110) from the Research Ethics Committee (REC) and Health Regulator Authority (HRA). The studies also received confirmation of capacity and capability from each participating NHS Trust before accepting participants into the study or any research activity is carried out. The studies were conducted in accordance with the recommendations for physicians involved in research on human subjects adopted by the 18th World Medical Assembly, Helsinki 1964, and later revisions.

2.1.8- Sample Collection

Each patient gave 20-30ml lithium heparin blood tubes (LH; BD Biosciences), PAXgene DNA blood tube (BD Biosciences), PAXgene RNA blood tube (BD Biosciences), serum separating blood tube (BD Biosciences), a sputum sample and a urine sample. FREAL patients also gave a nasal brush and a SAM strip.

2.1.8.1 - Whole Blood Processing

The LH whole blood tubes were centrifuged at 300g for 10 minutes, plasma was removed and stored at -80°C. The plasma-depleted LH blood was pooled into 50ml falcon tubes (Corning) and diluted 1:1 in phosphate-buffered saline (PBS; Sigma) with 2% fetal bovine serum (FBS; SAFC, Lot No. 19B370) and layered on 15ml histopaque (Sigma) in a Sepmate tube (StemCell Technologies). The layered blood was centrifuged for 10 minutes at 1200g, and the supernatant was poured into a 50ml falcon tube and diluted with PBS 2%FBS to wash. The diluted supernatant was centrifuged at 300g for 10 minutes and the supernatant was discarded. The pellet was resuspended in PBS, and PBMCs were counted and spun again at 300g for 10 minutes. The PBMC pellet was resuspended in freezing media of FBS 10% dimethyl sulfoxide (Sigma-Aldrich), frozen using a Mr Frosty (Thermofisher) at $1x10^7$/ml in -80°C for 24 hours and subsequently transferred to liquid nitrogen. The PAXgene DNA tubes were frozen upright at -20°C for 24 hours and then moved to -80°C. The PAXgene RNA tubes were left upright at room temperature for 2 hours until they were stored at -80°C. The serum separating tube was centrifuged at 1200g for 10 minutes, serum was removed and stored at -80°C.

2.1.9- PBMC Culture and Infections

PBMCs were isolated, frozen, and stored in liquid nitrogen from LH whole blood tubes as previously stated. Cryovials of PBMCs were removed from liquid nitrogen when required, thawed in a water bath warmed to 37°C and slowly added to 15ml RPMI-1640 supplemented with 10% FBS and 50 Units/ml Benzonase (Sigma) referred to as R10 Benz media. The cells were washed twice in 15ml of the same media and subsequently resuspended in 2-5ml of R10 Benz media and placed across two wells of a 6-well plate for 2 hours at 37°C and 5% CO_2. After 2 hours, the cells were harvested and plated in 96 well plates at $5x10^5$/well in RPMI-1640 supplemented with 1% FBS, 5% HEPES, 5% sodium pyruvate and 1% PenStrep. Cells were stimulated with 100ng/ml poly(I:C) or infected with fixed hyphae (MOI=4) for 6 hours, after which the supernatant and cells were collected.

2.1.10- PMN Isolation

Blood for polymorphonuclear (PMN) cell isolation was collected in LH whole blood tubes and processed quickly after collection. 5mls of Polymorphprep (Progen) were added to 15ml tubes and 5ml of whole blood was carefully layered on top. The tubes were spun at 500g for 30 minutes at 20°C with the brakes off. After the spin was complete the PMN and PBMC fractions were collected separately, washed with cold PBS, and spun at 1400rpm for 7 minutes at 4°C. The PBMCs were frozen in freezing media as previously stated. Red blood cell (RBS) lysis buffer was added to the PMNs for a maximum of 10 minutes and the cells were washed twice with cold PBS and used straight after isolation.

2.1.11- Neutrophil Infection and Stimulation

PMNs were isolated as previously described and kept on ice prior to being used. Neutrophils were pre-treated with IFNβ or IFNλ1 at 0.1ng/ml, 1ng/ml or 10ng/ml for 30 minutes. For the NETosis assay, the cells were then plated at $3.75x10^4$ cells/well in a clear and flat-bottomed, white-walled 96-well plate in 100μl of RPMI-1640 supplemented with 10% FBS and 1% PenStrep, stimulated with 20ng/ml PMA (Sigma) or infected with live dsRED germlings (MOI=0.5) and placed in the incubator at 37°C for 3 hours. For the ROS assay, cells were plated at a final concentration of $1x10^5$cells/well in 200μl RPMI without phenol red in a clear and flat-bottomed, white-walled 96-well plate and infected with fixed CEA-10 hyphae at MOI=0.5 or MOI=1. For the CFU, cells were plated at a final concentration of $1x10^5$cells/well in 500μl of RPMI 1% PenStrep in a 24-well plate and infected with MOI=0.5 live resting CEA-10 conidia. Finally, for the LDH assay, cells were plated at $5x10^4$cells/well in 200μl RPMI without phenol red in a clear and flat-bottomed, white-walled 96-well plate and infected with live swollen CEA-10 MOI=0.5 and incubated at 37°C for 18 hours.

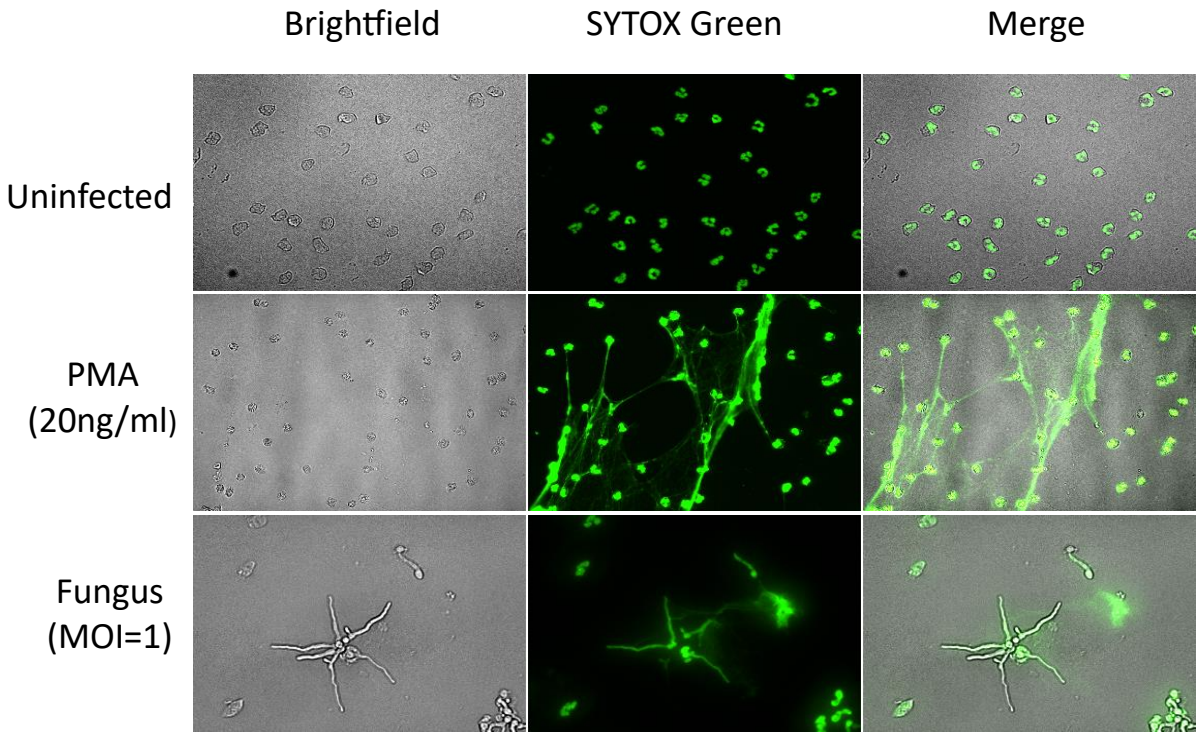

Figure 2.1: Representative figure of neutrophil NETosis. Neutrophils were isolated from healthy donors, plated at $3.75x10^4$ cells/well and stimulated with PMA (20ng/ml) or infected with *Af* (MOI=1) for 3 hours. Cells were fixed and stained with SYTOXgreen and imaged on Cell Discoverer 7.

2.2- RNA Sequencing

2.2.1- RNA Quality Assessment

RNA was extracted from CF and CF corrected BECs (RNeasy kit, Qiagen) with an optional DNase step (RNase-free DNase Set, Qiagen) and QIAshredder columns used for homogenisation (QIAshredder, Qiagen). RNA concentration, OD260/280, and OD260/230 values were quantified using a NanoDrop 8000 UV-Vis Spectroometer (Thermofisher) and some sample quality was confirmed on a 4150 Tapestation System (Agilent). The Nanodrop provided readings for OD 260/280 and OD 260/230 ratios and the Tapestation provided an RNA Integrity Number (RIN) as measurements of RNA quality and quantity. The OD 260/280 provides a ratio that indicates the purity and composition of a sample, a high 260/280 value (>2) can indicate presence of nucleic acids and a low value (<2) can indicate presence of protein, phenol or other contaminants. The OD 260/230 ratio provides a secondary measure of RNA purity and can indicate the presence of phenol or carbohydrates in the RNA samples. An OD 260/280 and 260/230 ratio of 1.8-2.2 is generally considered as “pure” for RNA. The RIN number is a tool to estimate the integrity of RNA samples, the Tapestation considers the entire electrophoretic trace of the sample and can detect the presence of degradation products. Only samples with >200ng of RNA, OD 260/280, and OD 260/230 values of >1.8, and <2.2 and RIN values >8 were sent for RNA sequencing at Novogene, Cambridge.

RNA sample quality control (QC) was also completed by Novogene prior to library preparation. Preliminary QC and sample quantification, integrity and purity were carried out using Agarose Gel Electrophoresis, Bioanalyzer (Agilent 2100), Qubit Fluorometer, and Nanodrop. All 51 samples passed QC with RIN between 9.7-10.

2.2.2- Library Construction and Sequencing

Novogene's Eukaryotic mRNA sequencing was carried out to measure the mRNA transcripts in each sample, using the Illumina Novoseq6000 platform with paired end 150bp, 20 million raw reads per sample. Messenger RNA (mRNA) was purified from total RNA using poly-T oligo-attached magnetic beads. After fragmentation, the first strand cDNA was synthesised using random hexamer primers and followed by second strand cDNA synthesis. After size selection and PCR enrichment, the RNA library was ready for sequencing. All the parameters for size distribution and RNA quality and quantity, measured with Qubit, rtPCR and Bioanalyser, were passed and sequencing was carried out.

2.2.3- Computational Processing of Sequencing Data

2.2.3.1 - Data QC

FastQC was used to assess the quality of the sequencing reads after they were returned from Novogene[338]. A report was created for both reads from each sample, therefore, 102 reports in total. Included in each report is data on per base sequence quality, per tile sequence quality, per sequence quality scores, per base sequence content, per sequence GC content, per base N content, sequence length distribution, sequence duplication levels, overrepresented sequences, and adapter content. All samples passed each level of QC apart from per base sequence content and sequence duplication levels. Per base sequence content fails for RNA sequencing due to the random hexamer binding described in the library construction and will only be considered for DNA sequencing. Sequencing duplication levels always fail for paired-end reads as FastQC is designed for single-end reads and, therefore, this was not considered. Figure 2.1 is an example of the FastQC report for one of the reads (R10_1). As all samples passed QC, no trimming was necessary to proceed to alignment.

A

Measure	Value
Filename	R10_1.fq.gz
File type	Conventional base calls
Encoding	Sanger / Illumina 1.9
Total Sequences	26609888
Sequences flagged as poor quality	0
Sequence length	150
%GC	50

B

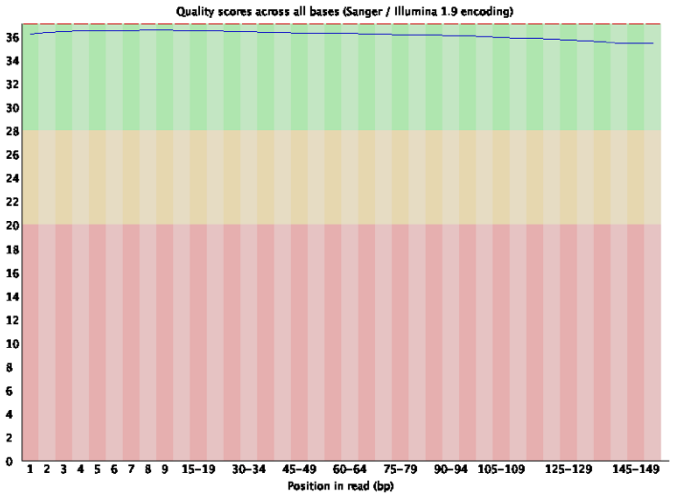

C

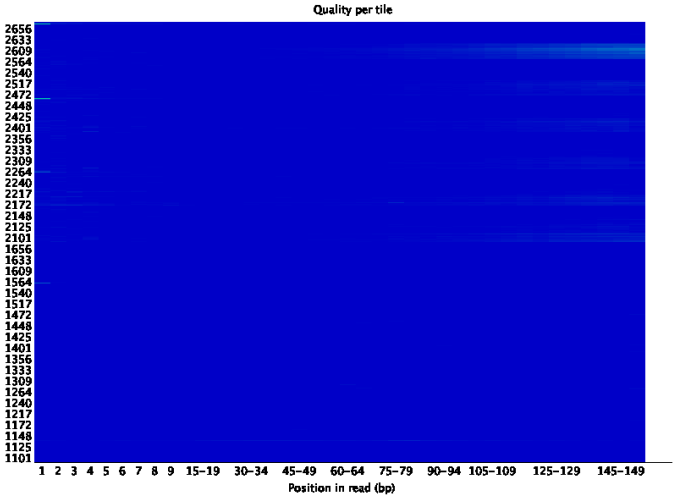

D

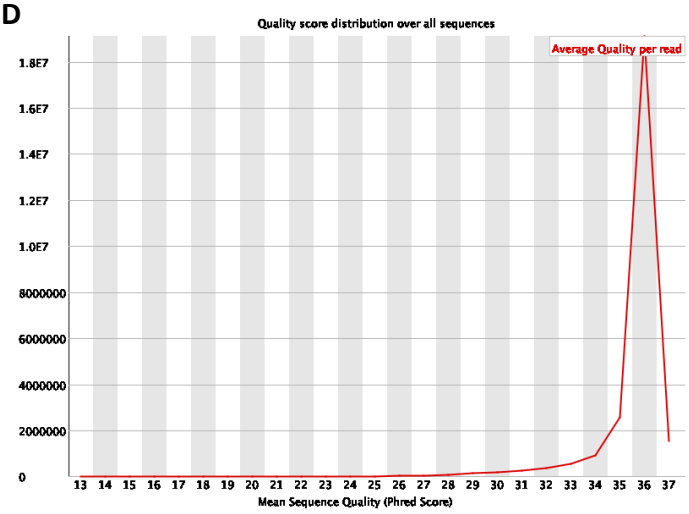

E

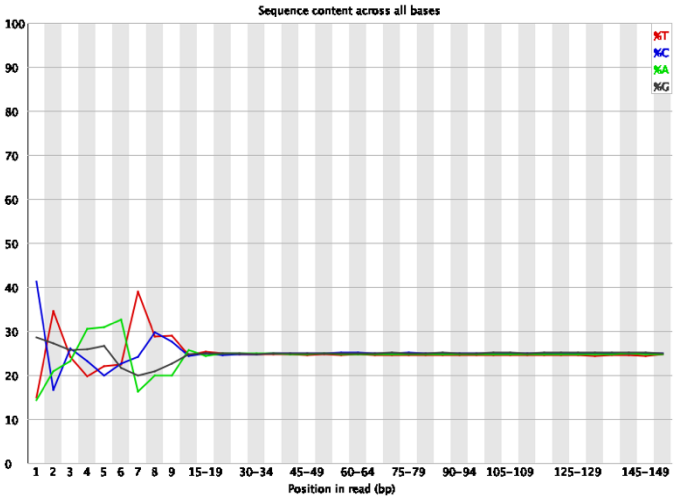

F

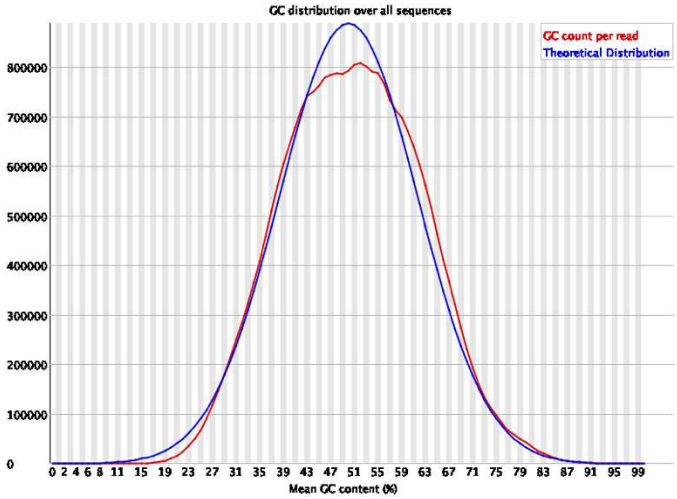

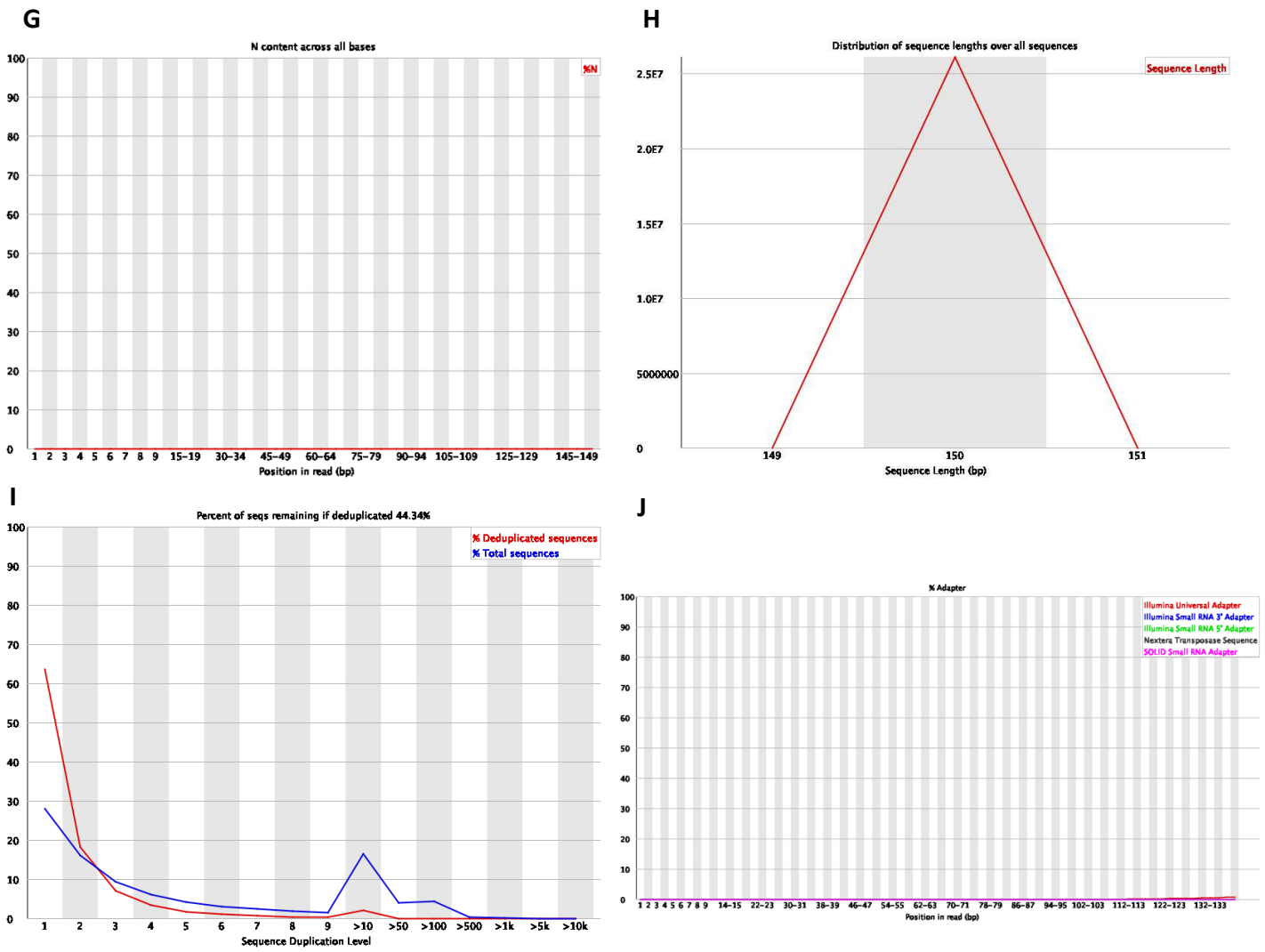

Figure 2.2: An example of the graphical FastQC output for sample R10_1. The report consists of a table for basic statistics (A), graphs for per base sequence quality (B), per tile sequence quality (C), per sequence quality scores (D), per base sequence content (E), per sequence GC content (F), per base N content (G), sequence length distribution (H), sequence duplication levels (I), overrepresented sequences (J) and adaptor content (K). All quality control measures were passed apart from per base sequence content (D) and duplication levels (I). FastQC was designed for DNA sequencing and due to this, it does not account for the random hexamer binding during RNA library preparation, this means the per base sequence content for all RNA sequencing fails FastQC tests for this parameter. Therefore, this was not considered when assessing quality of these RNA sequences. All reads passed initial quality control.

2.2.3.2 - Alignment

HISAT2 v2.2.1 is a sensitive and fast alignment program for mapping next-generation RNA sequencing reads to a reference genome and was used for alignment for all RNA sequencing reads in this project. HISAT2 uses a large graph FM index that represents a population of human genomes and a large set of small graph FM indexes that collectively cover the whole genome. The small indexes in addition to several alignment strategies allow for the quick and accurate alignment method that is referred to as Hierarchical Graph FM index (HGFM) and is unique to HISAT2[339]. The human reference genome used for alignment was Homo_sapiens.GRCh38.dna_sm.toplevel.fa.qz (2022-01-26) from Ensembl[340]. Alignment scores exceeded 85% for all samples, this is considered excellent alignment.

2.2.3.3 - Count matrix and normalisation

After alignment using HISAT2, the output of each paired end read was in a combined ".SAM" file. All files needed to be converted to a ".BAM" file for the count matrix to be created which required SAMtools v1.16.1[341]. Once ".BAM" files were created of the aligned reads, a count matrix was made using the Subread v2.0.3 package feature, named "featureCounts"[342]. Once the count matrix was formed, data was ready for normalisation and analysis.

2.2.3.4 - Qlucore Omics Explorer

The count matrix was uploaded to Qlucore Omics Explorer v3.8 (Qlucore, Lund, Sweden) and data was normalised using the Fragments Per Kilobase of exon per Million fragments aligned (FPKM) method. This method allows for computing expression levels of genes based on the number of fragments mapping to each gene. The inferred expression level for a gene is proportional to the number of features mapping to that gene, and inversely proportional to the transcript length and total number of fragments mapping to features in the sample,

therefore normalising for different baseline expression and lengths of genes. It also considers paired end reads, making it different to Reads Per Kilobase Million (RPKM) normalisation. RPKM has the same principles but was made for single-end RNA-sequencing, in which every read corresponds to a single fragment and not multiple reads to one fragment like paired-end reads. Once normalisation was complete, differential gene expression (DEG) analysis could be completed.

2.2.3.5 – Differentially Expressed Gene (DEG) analysis

Heatmaps of the stated number of DEGs were created using a multiple comparison (one-way ANOVA) of fold change of genes, the number of DEGs in these heatmaps represent any difference between any two conditions stated on the heatmap. These heatmaps were cross referenced with a list of 486 ISGs downloaded from two gene sets from the Molecular Signatures Database (Human MSigDB v2022.1.Hs updated August 2022) called "Blanco Melo Beta Interferon Treated Bronchial Epithelial Cells"[343] and "GOBP Response to Type III Interferon" (Human_NCBI_Gene_ID; GOC:add, ISBN:0126896631, PMID:15546383, PMID:16734557). This allowed for visualisation of the significantly differentially expressed type I and III interferon stimulated genes. The samples were ordered by their name and clustered using hierarchical clustering based on average linkage. The Benjamini-Hochberg test was applied to all heatmaps to correct p-values. Genes were coloured coded on a blue to yellow scale representing downregulated genes to upregulated genes and the extent of the fold change.

Volcano plots were constructed by plotting the negative log10 of the p-value against the log fold change ($p<0.05$) after conducting a two-group comparison (unpaired t-test). Upregulated genes were coloured red and downregulated genes were coloured blue.

Venn diagrams were created to illustrate the relationships and possible overlaps of 2-5 variable lists. Variable lists were created using two group comparisons (unpaired t-test) between the treated and untreated conditions stated and consist of differentially expressed genes with corrected p values of <0.01. Each variable list will be individually coloured and labelled.

2.2.3.6 - Gene Set Enrichment Analysis (GSEA)

GSEA is a computational method that determines where a defined list of genes shows statistically significant, concordant differences between two biological states, the algorithm for which is explained by Subramanian et al., 2005[344]. Hallmark gene sets (H) and the ImmuneSigDB subset of the immunologic signature gene sets (C7) from the Molecular Signatures Database were used for all GSEA analysis[345, 346]. All GSEA was conducted as a comparison between two conditions and gene sets with a corrected p value of <0.1 were regarded significant.

2.2.3.7 - Cytoscape

Cytoscape is a network data integration, analysis and visualisation tool that was used to visualise protein-protein interaction networks (Cytoscape v3.9.1)[347]. StringApp v2.0.0 was installed on Cytoscape and used to provide the protein query function that allowed the formation of protein-to-protein interaction networks from a list of gene names from the variable lists created on Qlucore explained previously. Additionally, stringApp allows retrieval of functional enrichment for Gene Ontology terms, KEGG, Reactome and Wiki Pathways with significance thresholds set at corrected p-value (padj) of <0.1[348]. Visualisation of enrichment results on networks through colour coding is explained where necessary. The enchancedGraphics v1.5.5 app was required for chart visualisation of the functional

enrichment terms[349]. All networks are formed of upregulated genes (padj<0.05) with a minimum fold change of 2. Across all networks, all genes related to ribosomal function and cell growth were removed in order to focus the analysis to the immune response.

2.3- Analysis Techniques

2.3.1- Time-lapse Microscopy of Fungal Growth

Time-lapse microscopy imaging of *Af* growth was conducted by plating CEA-10 at $2.5x10^4$ in 200μl RPMI without phenol red in a clear and flat-bottomed white-walled 96-well plate (Corning) and spun down at 800g for 1 minute. *Af* growth was visualised over 12 hours, in 15-minute intervals, at 37°C with 5% CO_2, (Zeiss Celldiscoverer7) and images were analysed using ImageJ software.

2.3.2- RNA extraction, cDNA synthesis and quantitative PCR

RNA was extracted from submerged culture of BEAS-2Bs, CF BECs and CF corrected BECs, ALI culture of CF BECs, CF corrected BECs, primary CF BECs, and PBMCs after stimulation and infection (RNeasy kit, Qiagen). The optional DNase step (RNase-free DNase Set, Qiagen) was performed and QIAshredder columns were used for homogenisation (QIAshredder, Qiagen). 1μg RNA was used for cDNA synthesis (Omniscript RT kit, Qiagen). Quantitative PCR (qPCR) was performed on (QuantStudio 3, Applied Biosciences) at 95°C for 15 minutes to activate and 45 cycles of 15 seconds at 94°C and 60 seconds at 60°C. Each reaction was performed using 25μl 2x QuantiTect Probe PCR Master Mix, 0.4uM of forward and reverse primer (Sigma-Aldrich; Table 3), 0.2uM of probe (Sigma-Aldrich; Table 3), 200ng template cDNA and made up to 50μl with RNase-free water (QuantiTect Probe PCR kit, Qiagen). The reactions and results

were analysed using the Thermofisher cloud. Each gene was normalised against 18S RNA and data was converted into fold change of mRNA expression of each target gene by calculating $2^{-(\Delta\Delta Ct)}$. ΔCt was calculated by subtracting the Ct value of the housekeeping gene from the Ct value of the gene of interest, ΔΔCt was then calculated by subtracting the ΔCt of the uninfected control average from the ΔCt of the sample and, finally, the fold change was calculated using the formula $2^{-(\Delta\Delta Ct)}$.

Table 2.1: Primer and probe sequences used in qPCR.

Target gene	**Sequence (5' – 3')**	**Length**	**GC%**	**Tm (°C)**
IFNβ	Forward: **CGCCGCATTGACCATCTA**	18	55.5	65.9
	Reverse: **TTAGCCAGGAGGTTCTCAACAATAGTCTCA**	30	43.3	70.6
	Probe: **FAM-TCAGACAAGATTCATCTAGCACTGGCTGGA-TAMRA**	30	46.6	74.3
IFNλ1	Forward: **GGACGCCTTGGAAGAGTCACT**	21	57.1	66.8
	Reverse: **AGAAGCCTCAGGTCCCAATTC**	21	52.3	65.5
	Probe: **FAM-AGTTGCAGCTCTCCTGTCTTCCCCG-TAMRA**	25	60	74.9
IL-8	Forward: **CTGGCCGTGGCTCTCTTG**	18	66.6	67.4
	Reverse: **CCTTGGCAAAACTGCACCTT**	20	50	66.2
	Probe: **FAM-CAGCCTTCCTGATTTCTGCAGCTCTGTGT-TAMRA**	29	39	75.7
18S RNA	Forward: **CGCCGCTAGAGGTGAAATTCT**	21	52.3	66.4
	Reverse: **CATTCTTGGCAAATGCTTTCG**	21	42.8	66.4
	Probe: **FAM-ACCGGCGCAAGACGGACCAGA-TAMRA**	21	47	77.1
TNFα	Forward: **CTTCTCCTTCCTGATCGTGG**	19	54.6	65.9

	Reverse: **GCTGGTTATCTCTCAGCTCCA** Probe: **FAM-CAGGCAGTCAGATCATCTTCTCGAAC-TAMRA**	23 21	59.3 45	66.3 75.4

2.3.3 – ELISA

BEAS-2B cells, CFBE41o- Human CF Bronchial Epithelial Cell Line (CF BECs) or CFBE41o- WT-CFTR Human CF Bronchial Epithelial Cell Line (CF corrected BECs) were seeded 24 hours before infection at $5x10^4$ cells/well and were infected with a variety of *Af* stimulation at stated MOIs. The cells were incubated further for the indicated time at 37°C with 5% CO_2 and the supernatant was harvested. IFNλ1 production was assessed using Human Duoset ELISA Kits (R&D Systems). 100µl of capture antibody was added to 96-well plates and incubated at room temperature overnight. The next day, wells were aspirated and washed three times with 400µl of wash buffer. ELISA plates were then blocked with 300µl of reagent diluent for at least 1 hour at room temperature. After blocking, plates were then ready to carry out the ELISA assay. A seven-point IFNλ1 standard was prepared for each plate performing a 2-fold serial dilution of IFNλ1 standard in reagent diluent, creating a detection range from 4000pg/ml to 62.5pg/ml. 100µl of sample or standards well added per well, the plate was covered and incubated for 2 hours at room temperature. Three more washes with 400µl wash buffer were carried out and 100µl of Streptavidin-HRP was added to each well. The plate was covered and incubated at room temperature, for 20 minutes in the dark. Again, three washes were completed with 400µl of wash buffer and 100µl of substrate solution with another 20-minute incubation at room temperature in the dark. After the final 20 minutes, 50µl of stop solution was added to each well and the plate was ready for absorbance to be measured. Absorbance was measured

immediately using an absorbance plate reader at 450nm with wavelength corrections set at 540nm and the values subtracted. Concentrations were calculated from the standard curve.

Supernatant from PBMC infections were used to assess TNFα production using a Human Duoset ELISA Kit (R&D Systems). The same method as previously described was followed and a seven-point TNFα standard was prepared for each plate performing a 2-fold serial dilution of in reagent diluent, creating a detection range from 1000pg/ml to 15.6pg/ml.

2.3.4- Lactate Dehydrogenase (LDH) Activity Assay

BEAS-2B cells were seeded at $5x10^4$ cells/well in 200µl RPMI without phenol red with 1% FBS for 24 hours before infection with fixed resting CEA-10 conidia in a 96-well plate, after 0-4 washes PBS post-fixation with 4% PFA, at a MOI=8. The cells were incubated for a further 18 hours at 37°C with 5% CO_2 and the supernatant was harvested.

CF BECs were seeded at $2.5x10^5$ cells/well in 1ml MEM without phenol red with 1% FBS treated for 24 hours before treatment with a combination of Ivacaftor, Tezacaftor, and Elexacaftor at a 1:1:1 ratio at 0.33ng/µl each, therefore, a total concentration of 1ng/µl. A second treatment was carried out at 24 hours and cells were incubated for a further 24 hours at 37°C with 5% CO_2 and the supernatant was harvested.

Freshly isolated neutrophils were seeded at $1x10^5$ cells/well in 200µl RPMI with 1% PenStrep. Cells were pre-treated with IFNβ or IFNλ1 at appropriate concentrations for 30 minutes and infected with live CEA-10 resting conidia at MOI=1 or stimulated with PMA (20ng/ml) for 3 hours at 37°C with 5% CO_2 and the supernatant was harvested.

LDH levels in the supernatant from BEAS-2B cells, CF BECs, and neutrophils were measured, using a commercial kit, CytoTox 96 Non-Radioactive Cytotoxicity Assay (Promega). 45 minutes prior to the end of previously described experiments, 10μl of 10X Lysis solution per 100μl of media was added to wells of untreated cells to determine the maximum LDH release control. Once experiments were completed, 50μl of supernatant was removed and immediately placed in a 96-well plate flat-bottomed plate (Corning). 50μl of reconstituted Cytox96 Reagent assay buffer was then added to each sample aliquot and plate was incubated for 30 minutes at room temperature in the dark. After 30 minutes, 50μl of Stop Solution was added to each well, any bubbles present were popped, and absorbance was recorded at 492nm straight away.

2.3.5- Flow Cytometry

Neutrophils were isolated with Polymorphprep as previously described, $1x10^6$ neutrophils were stained with the following antibodies: FITC CD3 (BD#555332), FITC CD19 (BD#555415), FITC CD14 (BD#561712), FITC CD16 (BD#556618), FITC CD56 (BD#562784), FITC CD123 (BD#564197), PerCP-Cy5.5 CD11b (BD#562513), APC CD66b (BD#305117). This panel was designed to show the purity of the neutrophil isolation (LSRII) and analysis was completed on FlowJo.

2.3.6- NET formation and Fluorescence Microscopy

$3.75x10^4$ dsRed *Af* conidia were swollen in a black-walled and clear-bottomed 96-well plate for 6 hours in clear RPMI in the incubator at 37°C. Freshly isolated neutrophils were pre-treated with IFNβ or IFNλ1 at appropriate concentrations for 30 minutes and $3.75x10^4$ were placed in each well, some on top of fungus, and incubated at 37°C in 200μl RPMI with

1%PenStrep for 3 hours. After 3 hours, the plates were gently centrifuged for 3 minutes, and the media was removed and stored at -80. The cells and fungus were fixed with 2% PFA for 10 minutes at 4°C and stained with 0.1% SytoxGreen nucleic acid stain (Thermofisher) for 20 minutes in the dark at room temperature. The cells were then imaged using a Cell Discoverer 7 (Zeiss) and images were analysed using the ImageJ Fiji software.

2.3.7- Reactive Oxygen Species (ROS) Activity Assay

The DCFDA cellular ROS assay kit (Abcam) was used to assess ROS production in neutrophils. Freshly isolated neutrophils were pre-treated with IFNβ or IFNλ1 at appropriate concentrations for 30 minutes at 37°C. Cells were stained with 10uM DCFDA solution for a further 30 minutes at 37°C in the dark. Cells were then placed in a black-walled and clear-bottomed 96-well plate at a final concentration of $5x10^4$ with RPMI 1%PenStrep without phenol red and infected with fixed swollen conidia at an MOI=1. The plate was measured immediately on an Infinite F200 Florescence Microplate reader (Tecan) at Ex/Em=485/535nm for 4 hours.

2.3.8- Colony Forming Units (CFU)

Neutrophils were plated at a final concentration of $1x10^5$cells/well in 500μl of RPMI 1% PenStrep in a 24-well plate. Cells were pre-treated with IFNβ or IFNλ1 at appropriate concentrations for 30 minutes and infected with live CEA-10 resting conidia at MOI=1 for 3 hours. After 3 hours the cells were lysed using 0.05% PBS-TWEEN and the lysates moved into 1.5ml lo-bind Eppendorf tubes. Dilutions were then carried out using DPBS to create 1;10, 1:100, and 1:1000 dilutions. Triplicates of 100μl of neat lysate and each dilution were pipetted and spread onto Sabouraud agar on 90mm Petri dishes. The plates were then incubated at

37°C for 24 hours. After 20 hours, colonies were visible but were not overlapping. Colonies were counted manually.

2.3.9- Statistical Analysis

All *in vitro* experiments were completed three times and statistical significance was assessed with Student t-test for 2-group comparison or one-way ANOVA for 3 or more experimental groups. P-values are indicated where appropriate in figure legends, significance was determined when $p<0.05$ and, throughout all figures, significance was represented as *$p<0.05$, **$p<0.01$, ***$p<0.001$, ****$p<0.000$. For all multiple comparisons, significance was determined using adjusted p-values of <0.05 which implies that <5% of significant values will result in false positives, differing from a p value in which implies a <5% of all values will result in false positives. All statistical analysis, apart from transcriptomics, was carried out using GraphPad Prism version 9 and all transcriptomics statistical analysis was completed using Qlucore Omics Explorer version 3.8.

Chapter 3: Effect of *Aspergillus fumigatus* infection on healthy and cystic fibrosis bronchial epithelial cells

3.1 – Optimisation of *Aspergillus fumigatus* infection model in BEAS-2B bronchial epithelial cells

As described in the introduction, type I and III IFNs are emerging as an essential component of the immune response against fungal infections[155, 163]. Both the type I and III IFN response has been previously reported to be downregulated in the CF lung in response to both bacterial and viral pathogens including *Pseudomonas aeruginosa,* and rhinoviruses[38-40]. This downregulation is thought to contribute to increased susceptibility and infection rates in the CF population compared to healthy individuals[31]. Whether there is a downregulation of type I and III IFNs in CF human BECs in response to *Af* has yet to be reported and, therefore, it was aimed to address this question in this project. It was hypothesised that there is a downregulated type I and III IFN response in CF BECs in response to *Af* infection and this was addressed through establishment of a BEC *Af* infection model, RNA sequencing analysis, and confirmation of findings in a BEC air-liquid interface (ALI) *Af* infection model.

To first establish if there is a type I and III IFN response in human BECs after *Af* infection, an infection model using healthy BEAS-2B BECs was established. *Af* morphology changes and size increases over time, explained in the introduction (section 3.1.1) and represented in Fig3.1.1, with swelling starting at 3 hours and germination occurring between 6 and 7 hours. Resting conidia refers to freshly harvested conidia with an intact outer RodA layer. By 3 hours of swelling, the conidia have increased in size and the RodA layer has been disturbed to expose

PAMPs. By 9 hours, *Af* has germinated and grown hyphae, without becoming a biofilm that cannot be quantified.

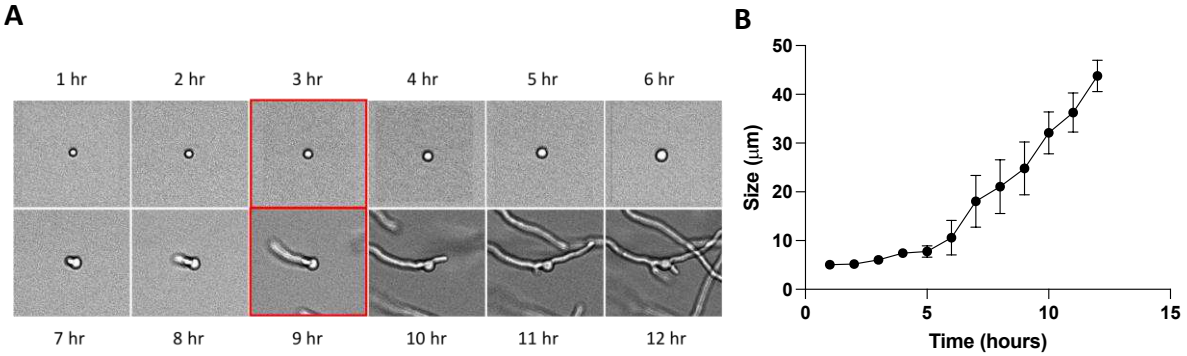

Figure 3.1.1: CEA10 growth over time. *Af* (CEA10) was grown and imaged over 12 hours at 37°C with 5% CO_2 in clear RPMI. (A) Hourly representative growth images of a single *Af* conidia. (B) Size in μm measured hourly over 12 hours (n=3).

Due to the complex nature of the *Af* life cycle, fixation was opted for to arrest the *Af* at the previously stated time points, 0 hour, 3 hours and 9 hours of swelling, referred to as resting conidia, swollen conidia and hyphae. Fixation methods used were heat killing at 90°C for 1 hour and resuspending in 4% PFA overnight at 4°C. PFA fixation and heat killing prevented further growth of *Af* but didn't change the morphology at any time point (Fig3.1.2 A, Fig3.1.2 B). Due to the cytotoxic properties of PFA, the fixed *Af* had to be thoroughly washed after fixation. However, a significant amount of fungus is lost in the supernatant after each wash (Fig3.1.2 C). When the fixed resting conidia was used to infected BEAS-2B BECs (MOI=8), cytotoxicity, TNFα release and conidia loss was limited after 2 washes and, therefore, this fixation method was opted for.

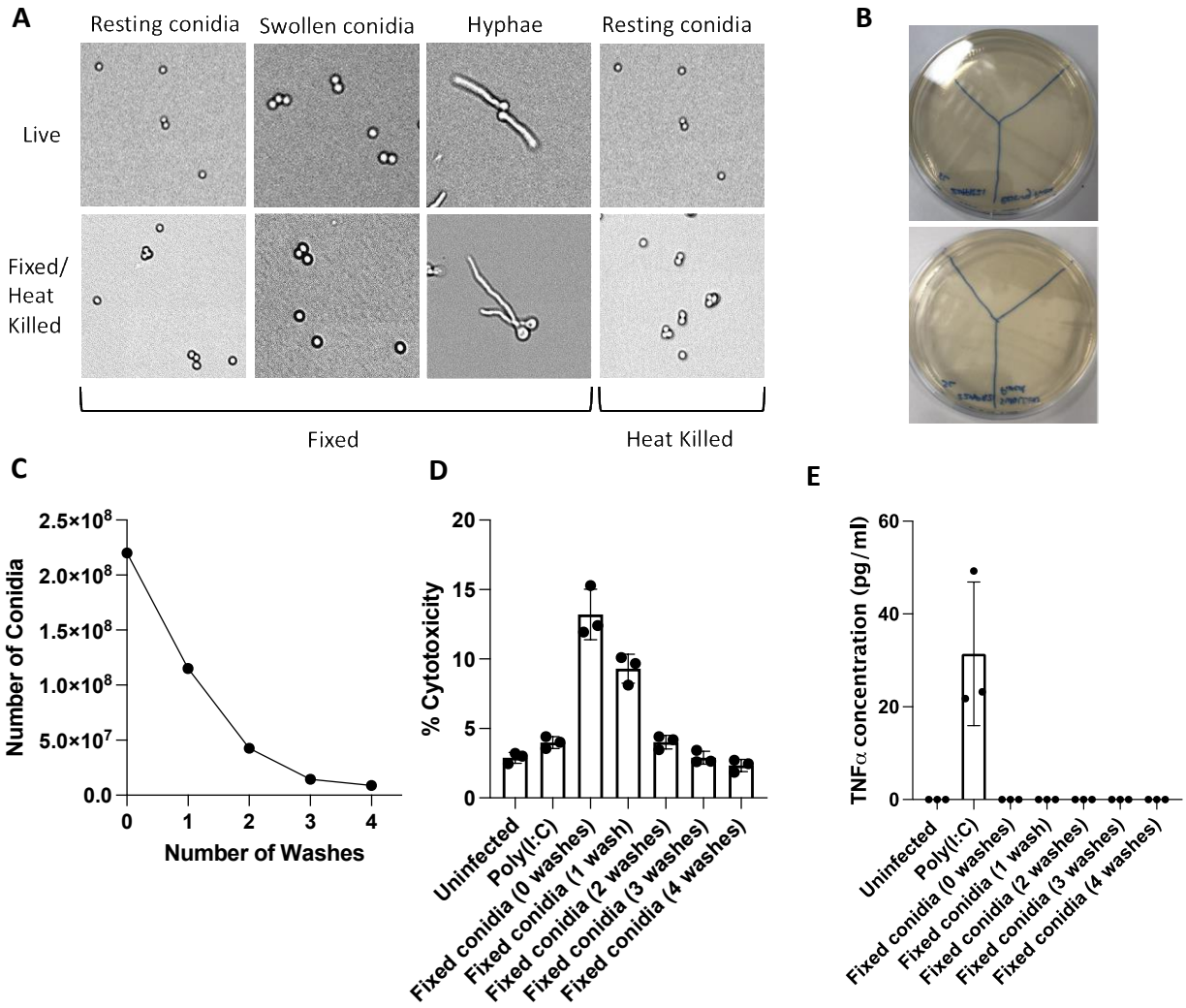

Figure 3.1.2: CEA10 heat killing and fixation optimisation. CEA10 resting conidia, swollen conidia and hyphae were fixed with 4% PFA overnight and resting conidia was heat killed at 90°C for 1 hour. (A) Representative images of CEA10 taken before and after fixation or heat killing at indicated growth stages. Directly after fixation, fixed resting conidia was washed 0-4 times with PBS and used to infect BEAS-2B bronchial epithelial cells at MOI=8 for 24 hours. (B) Images of agar plates without fungal growth after fixed resting conidia, swollen conidia, hyphae and heat killed conidia were plated overnight at 37°C. (C) Count of total fixed resting conidia after each wash with PBS (n=1). (D) LDH levels representing cytotoxicity of BEAS-2B cells after infection with fixed resting conidia at MOI=8 for 24 hours and poly(I:C) at 10ug/ml (n=3). (E) TNFα production by BEAS-2B BECs after 24 hours of infection with fixed resting conidia (n=3) assessed by ELISA. Data are mean ± SD (C) or technical repeats (D).

Fixed resting and swollen conidia, hyphae and heat killed conidia at MOI 2 and 8 were used to infect BEAS-2B BECs in order to induce a type I and III IFN response for 24 hours. IFNβ and IFNλ1 were chosen as representatives of type I and III IFNs as they were detectable after fungal infection. Hyphae and heat killed conidia at an MOI of 8 induced significant IFNβ expression after 24 hours when compared to fixed resting conidia infection (Fig3.1.3 A). Fixed resting and swollen conidia stimulated little IFNβ expression and IFNλ1 production at both MOI of 2 and 8. IL-8 was used as a proinflammatory control due to its relevance in the pathogenesis of CF as its overproduction in the CF lung is associated with increased infections and exacerbations. IL-8 is a potent pro-inflammatory cytokine that is involved in neutrophil chemotaxis and the establishment of the sustained inflammatory response. All forms of fixed and heat killed fungus stimulated some IL-8 expression, with hyphae at MOI=2 and swollen conidia at MOI=8 expressing significantly more IL-8 than fixed resting conidia at 24 hours post infection (Fig3.1.3 B). Hyphae and heat killed conidia at an MOI of 8 induced significant IFNλ1 production after 24 hours when compared to fixed resting conidia infection (Fig3.1.3 C). Heat killed conidia at an MOI of 2 also induced significantly more IFNλ1 production compared to fixed resting conidia infection (Fig3.1.3 C). Due to these data, fixed hyphae and heat killed conidia were chosen as the best stimuli to assess the type I and III IFN response in BEAS-2B BECs.

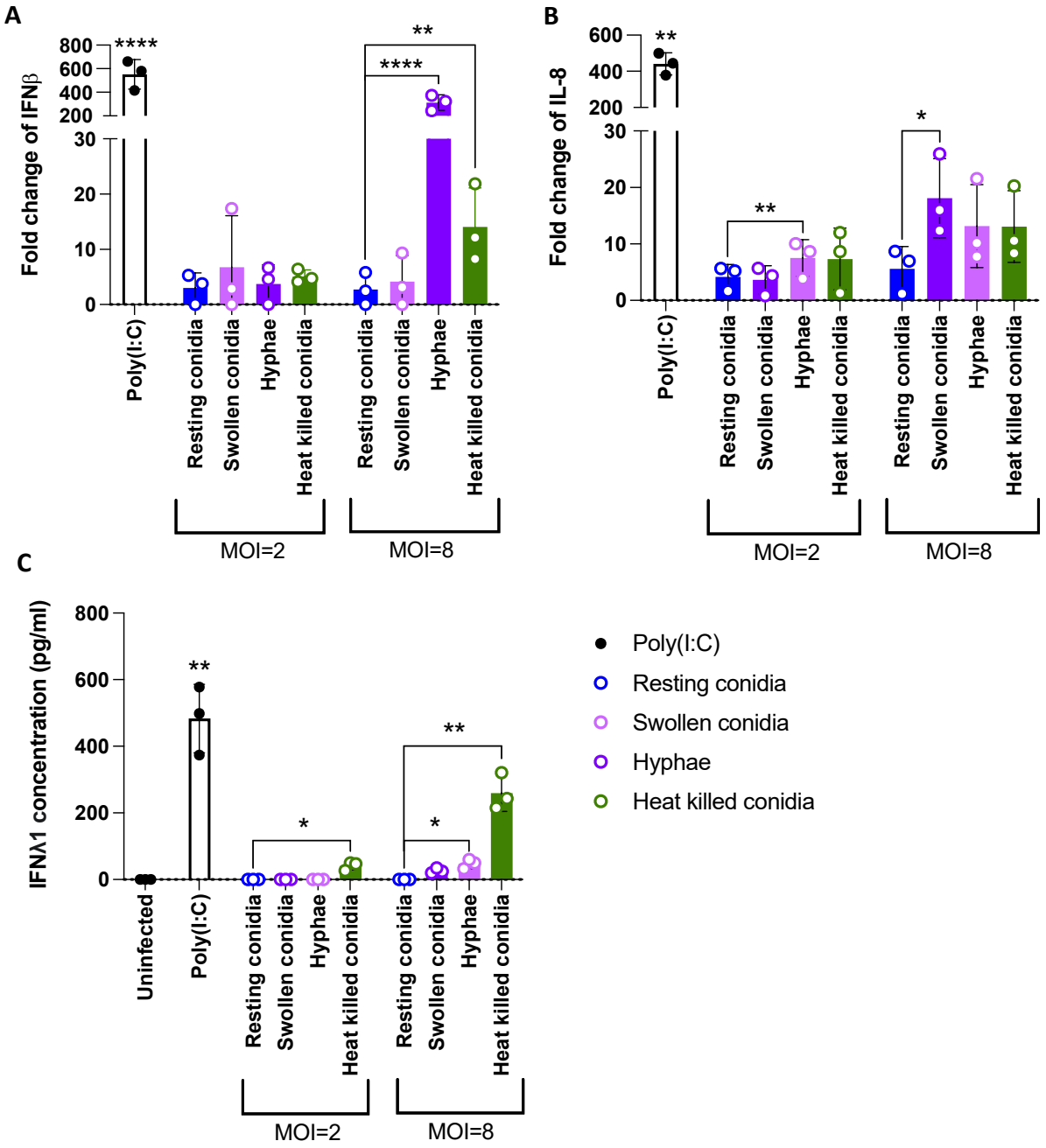

Figure 3.1.3: IFNβ and IFN*λ*1 expression and production by BEAS-2B BECs after fixed and heat killed *Af* infection. BEAS-2B BECs were infected with fixed resting conidia, fixed swollen conidia, fixed hyphae and heat killed conidia at an MOI=2 and MOI=8 for 24 hours. RT-PCR was used to assess (A) IFNβ expression and (B) IL-8 expression after fixed and heat killed fungal stimuli and poly(I:C) stimulation (100ug/ml). All data was normalised to 18S RNA and fold change was calculated using the $\Delta\Delta C_T$ method. (C) IFN*λ*1 concentration (pg/ml) was determined by ELISA after fixed and heat killed fungal infection and poly(I:C) stimulation (10ug/ml). Data from three independent experiments. Data are mean ± SD, *p<0.05, **p<0.01, ***p<0.001, ****p<0.0001.

Fixed hyphae and heat killed conidia at an MOI of 8 were used to infect BEAS-2B BECs at 3, 6, 12 and 24 hours to assess the best time point to assess IFNβ expression and IFNλ1 production. IFNβ expression was significantly increased at 3 and 24 hours after fixed hyphae infection and 12 hours after heat killed conidia infection (Fig3.1.4 A). The poly(I:C) control stimulated an IFNβ expression pattern the same as fixed hyphae (Fig3.1.4 B). IL-8 is significantly expressed by fixed hyphae at all time points and heat killed conidia at 6, 12 and 24 hours (Fig3.1.4 C). Poly(I:C) stimulated IL-8 production across all time points, peaking at 12 hours and reducing at 24 hours. IFNλ1 production was significantly increased by fixed hyphae infection at 3, 6 and 12 hours and heat killed conidia infection at all 4 time points, peaking at 12 hours (Fig3.1.4 E). From this data, it was decided that CF and CF corrected cells infected with fixed hyphae and heat killed conidia at 12 and 24 hours with a MOI=8 should be sent for bulk RNA sequencing.

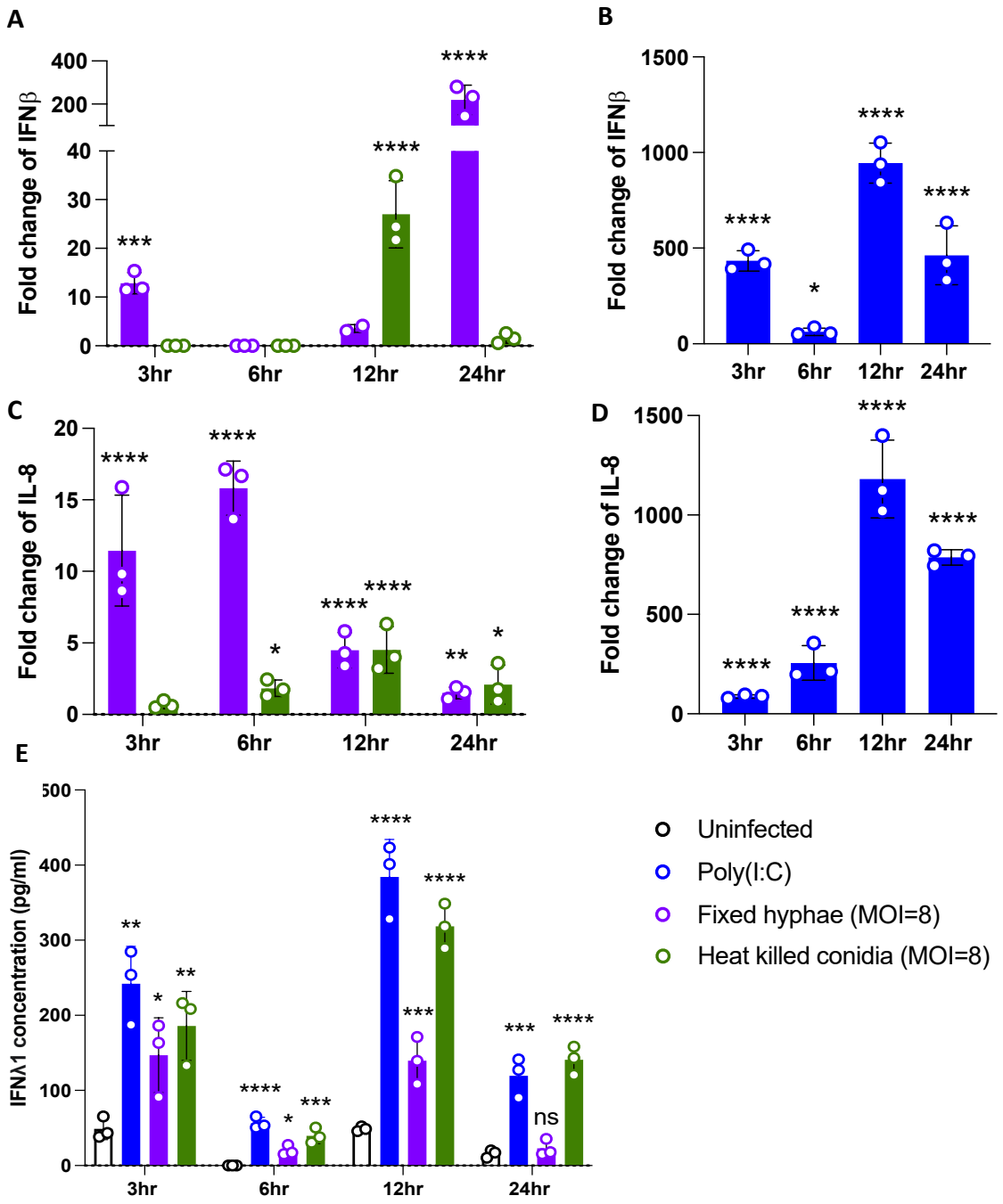

Figure 3.1.4: IFNβ and IFN**λ**1 expression and production by BEAS-2B epithelial cells after *Af* infection. BEAS-2B bronchial epithelial cells were infected with fixed hyphae and heat killed conidia at an MOI=8 for 3, 6, 12 and 24 hours. RT-PCR was used to assess (A-B) IFNβ expression and (C-D) IL-8 expression after *Af* fixed hyphae and heat killed conidia infection and poly(I:C) stimulation (100ug/ml). All data was normalised to 18S RNA and fold change was calculated using the $\Delta\Delta C_T$ method. (E) IFN**λ**1 concentration (pg/ml) after the *Af* fixed hyphae and heat killed conidia infection and poly(I:C) stimulation (10ug/ml) assessed by ELISA, all conditions were compared to uninfected protein levels to test for significance. Data from three independent experiments. Data are mean ± SD, *p<0.05, **p<0.01, ***p<0.001, ****p<0.0001.

3.2 – Transcriptomic characterisation of *Aspergillus fumigatus* infection in CF and CF corrected bronchial epithelial cells

Having observed the increase in IFNβ expression and IFN*λ*1 production in healthy BECs after *Af* infection, the transcriptomic characterisation of the immune response to *Af* in CF and CF corrected BECs was next to be investigated. This was achieved by bulk RNA sequencing of RNA isolated from CF and CF corrected BECs after fixed hyphae and heat killed conidia infection after 12 and 24 hours.

RNA was isolated directly after infection and RNA quality and quantity was assessed using a Nanodrop and a Tapestation. Only samples with >200ng of RNA, OD260/280 values of >1.8, OD260/230 values of >1.8 and RIN values of >8.5 were sent for RNA sequencing at Novogene, Cambridge. Fig3.2.1 A and Table3.2.1 shows a summary of the Tapestation results from 15 RNA samples, 14 of which were sent for RNA sequencing; however, one sample had a RIN value of 7.4 and so was not sent for sequencing. Fig3.2.1 B and Table3.2.2 is an example of an electropherogram from sample B1 and shows good RNA integrity. Fig3.2.1 C and Table3.2.3 is an electropherogram from sample E1, which had a RIN value of 7.4 and showed some degradation. The ribosomal 28S:18S ribosomal RNA ratio is used as a measure of degradation. A ratio of 2.1:1 is considered intact RNA; this ratio reduces and the background for both markers increases as degradation occurs. The lower marker is used to align the sample to the RNA ladder used in the analysis.

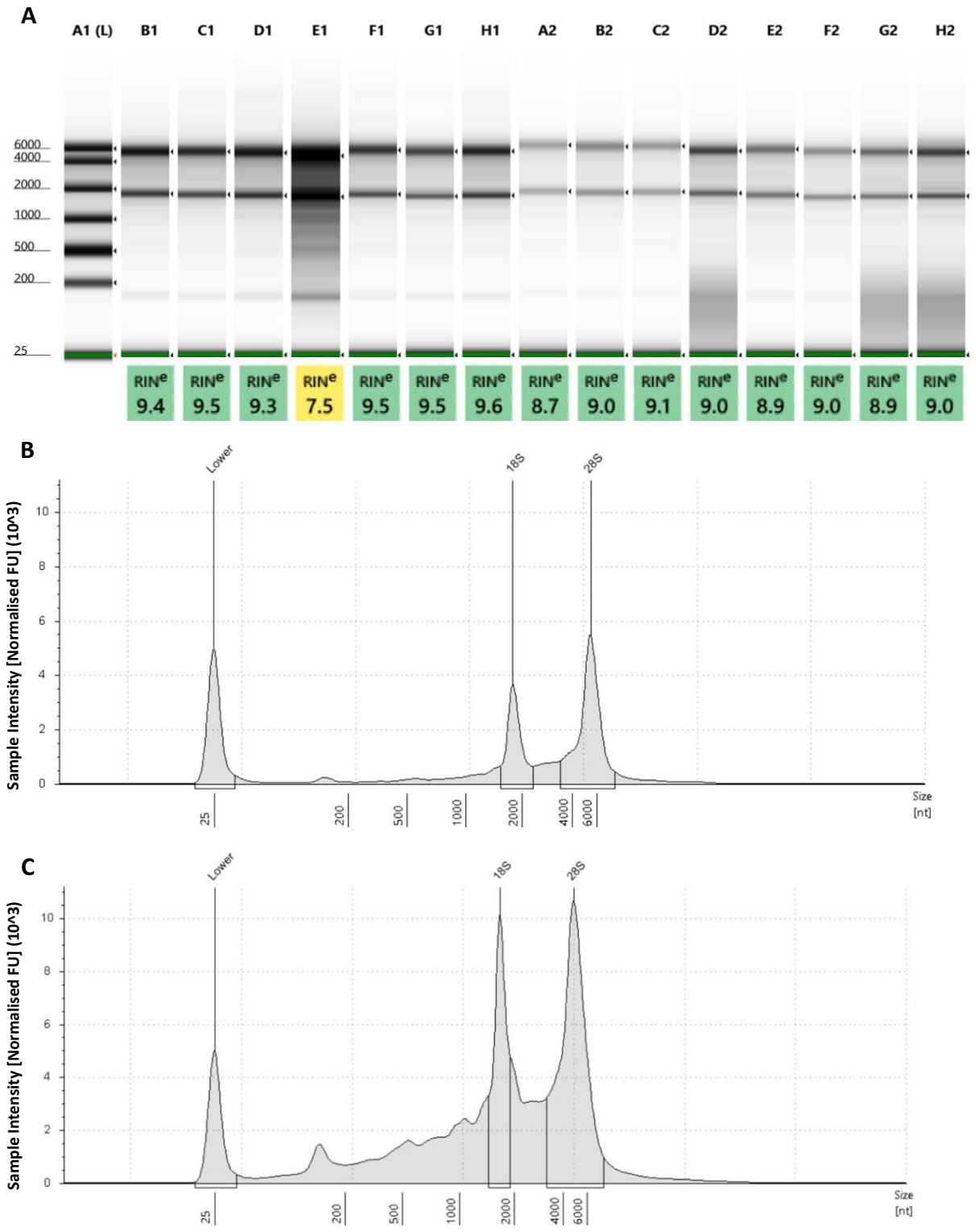

Figure 3.2.1: Aqilent 4200 TapeStation RNA and high sensitivity RNA ScreenTape Assay results report example. (A) A gel image of 15 RNA samples and the ladder from one run on an Agilent TapeStation with respective RIN scores. RIN values are scored from 1 to 10, with a low value showing 'strongly degraded' RNA and a high value indicating 'highly intact' RNA. (B) An example electropherogram of sample B1 (RIN no. 9.4) showing three peaks at 25nt, 1795nt and 5472nt. (C) An example electropherogram, of sample E1 with a RIN no. 7.5, showing more degradation than sample B1.

Table 3.2.1: Sample information related to Fig3.2.1 A.

Well	RINe	28S/18S (Area)	Conc. [ng/ul]	Sample Description	Alert	Ladder
A1	-	-	172	Ladder		Ladder
B1	9.4	2.0	74.8			
C1	9.5	2.0	63.5			
D1	9.3	1.7	82.6			
E1	7.5	2.1	248			
F1	9.5	1.9	54.9			
G1	9.5	1.9	43.5			
H1	9.6	1.7	60.1			
A2	8.7	1.3	27.3			
B2	9.0	1.7	31.0			
C2	9.1	1.4	26.0			
D2	9.0	1.6	79.4			
E2	8.9	1.3	39.7			
F2	9.0	1.5	29.4			
G2	8.9	1.4	57.6			
H2	9.0	2.4	74.7			

Table 3.2.2: B1 sample information from electropherogram in Fig3.2.1 B.

Size [nt]	Calibrated Conc. [ng/ul]	Assigned Conc. [ng/ul]	Peak Molarity [nmol/l]	% Integrated Area	Peak Comment	Observations
25	36.0	36.0	4240	-		Lower Marker
1795	17.2	-	28.3	32.83		18S
5472	35.3	-	19.0	67.17		28S

Table 3.2.3: E1 sample information from electropherogram in Fig3.2.1 C.

Size [nt]	Calibrated Conc. [ng/ul]	Assigned Conc. [ng/ul]	Peak Molarity [nmol/l]	% Integrated Area	Peak Comment	Observations
25	36.0	36.0	4240	-		Lower Marker
1795	40.7	-	72.0	32.19		18S
5472	85.7	-	52.7	67.81		28S

3.2.1 – Transcriptomic characterisation of Poly(I:C) stimulation in CF and CF corrected bronchial epithelial cells

After sequencing, Novogene retuned the raw reads which were then quality checked, trimmed, aligned, normalised, and analysed in house. Poly(I:C) stimulation was used as a control throughout this project as it is a TLR3 agonist and can stimulate a strong type I and III IFN response. To begin analysing the difference in the interferon response in CF and CF corrected cells, the transcriptomic signatures of the cell line's response to poly(I:C) was assessed. In total, there were 7793 differentially expressed genes between the two cell lines, stimulus, and time points (padj=0.01). Fig3.2.1.1 summarises the overall expression matrix of the top 2000 genes differentially expressed after poly(I:C) stimulation for 12 and 24 hours in CF and CF corrected cell lines, done in triplicate, analysed by ANOVA and clustered using hierarchical clustering based on average. Distinct gene signatures between the two cell lines are evident, despite the only difference between the cell lines being that the CF corrected cells were genetically corrected for the F508del mutation in the CFTR gene. The effect of the poly(I:C) is evident in both cell lines, and there is variation between the 12- and 24-hour time point. 98 ISGs are present in the top 2000 differentially expressed genes, highlighted by pink in the panel on the heatmap and these cluster at the top and in the middle of the heatmap, where most of the variation due to poly(I:C) stimulation is observed.

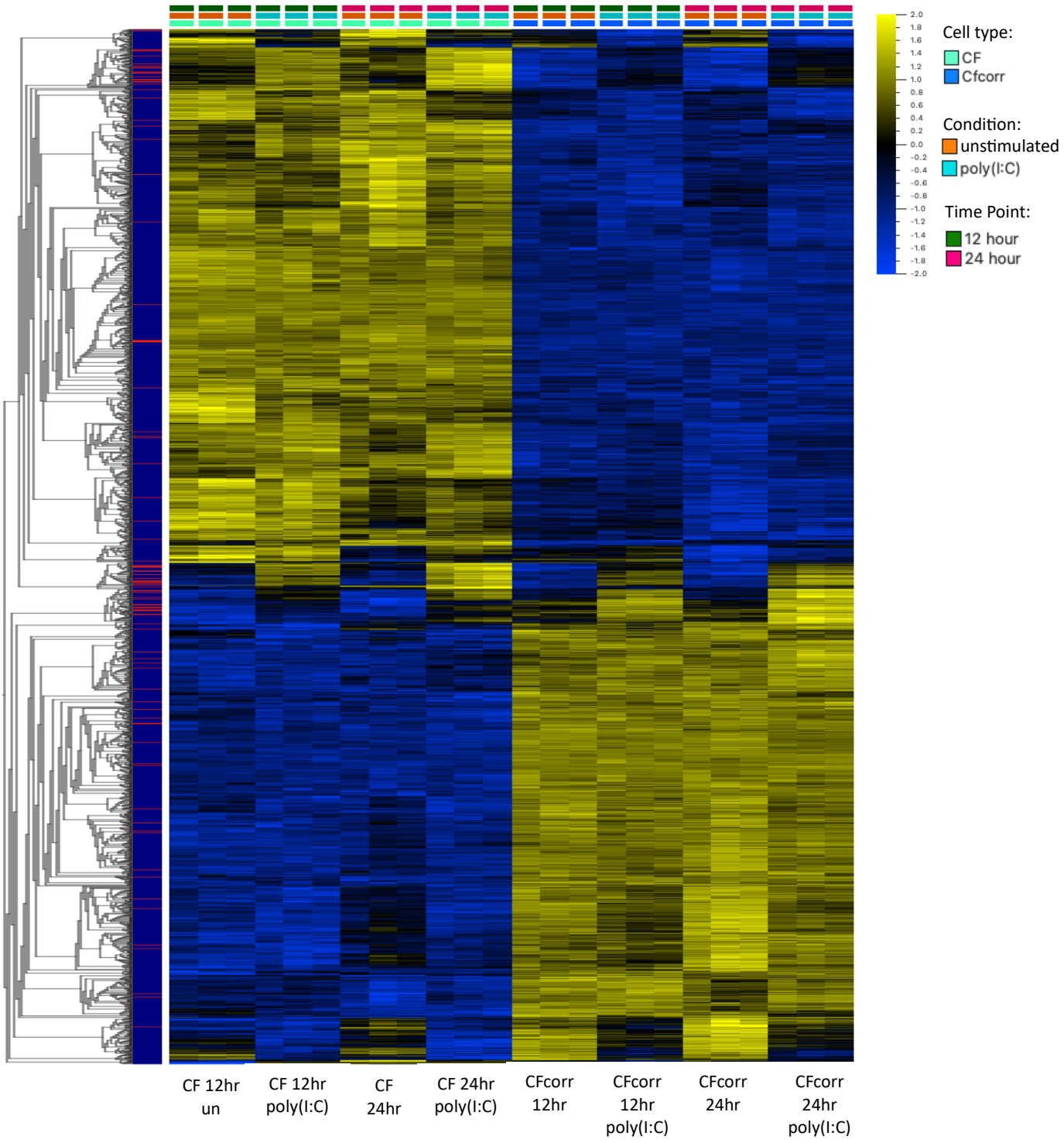

Figure 3.2.1.1: Gene expression heatmap of top 2000 genes differentially expressed after poly(I:C) stimulation. CF and CF corrected BECs were stimulated with poly(I:C) (100μg/ml) for 12 and 24 hours, RNA was isolated and sent for bulk RNA sequencing. Data were compared to unstimulated controls and between the two cell lines using ANOVA to test for significance and Benjamini-Hochberg test to correct p-value. The heatmap was organised by hierarchical clustering based on mean gene expression. Each column represents a sample (n=3), and each row represents a gene (padj<0.01). ISGs are highlighted in pink on the left-hand panel.

3.2.1.1 – DEG analysis of 12-hour Poly(I:C) stimulated CF and CF corrected bronchial epithelial cells

To further investigate the ISG signature of the cell lines, a list of 486 type I and III ISGs was created using a collation of multiple gene sets from the Molecular Signatures Database as detailed in section 2.2.3.5. The significant differentially expressed genes after the ANOVA (Fig3.2.1.1) were then cross referenced with the collated ISG set and the overall expression matrix of the type I and III IFN response is shown in Fig3.2.1.2 A. Overall, after 12 hours of poly(I:C) stimulation in the two cell lines there were 314 significantly differentially expressed ISGs (padj=0.05). Interestingly, it is clear from the heatmap that the CF and CF corrected cells have distinct ISG signatures after stimulation. Differentially expressed ISGs for each individual condition were identified when compared to their appropriate uninfected control using a student's t-test (padj=0.05). This revealed that there were 139 and 140 significant differentially expressed ISGs for CF corrected and CF BECs respectively. 107 of these ISGs were distinct between the two cell lines with 86 overlapping (Fig3.2.1.2 B). When this data had a further filter applied (fold change >2) there were 21 and 12 upregulated ISGs in the CF corrected and CF BECs (Fig3.2.2.2 C, D).

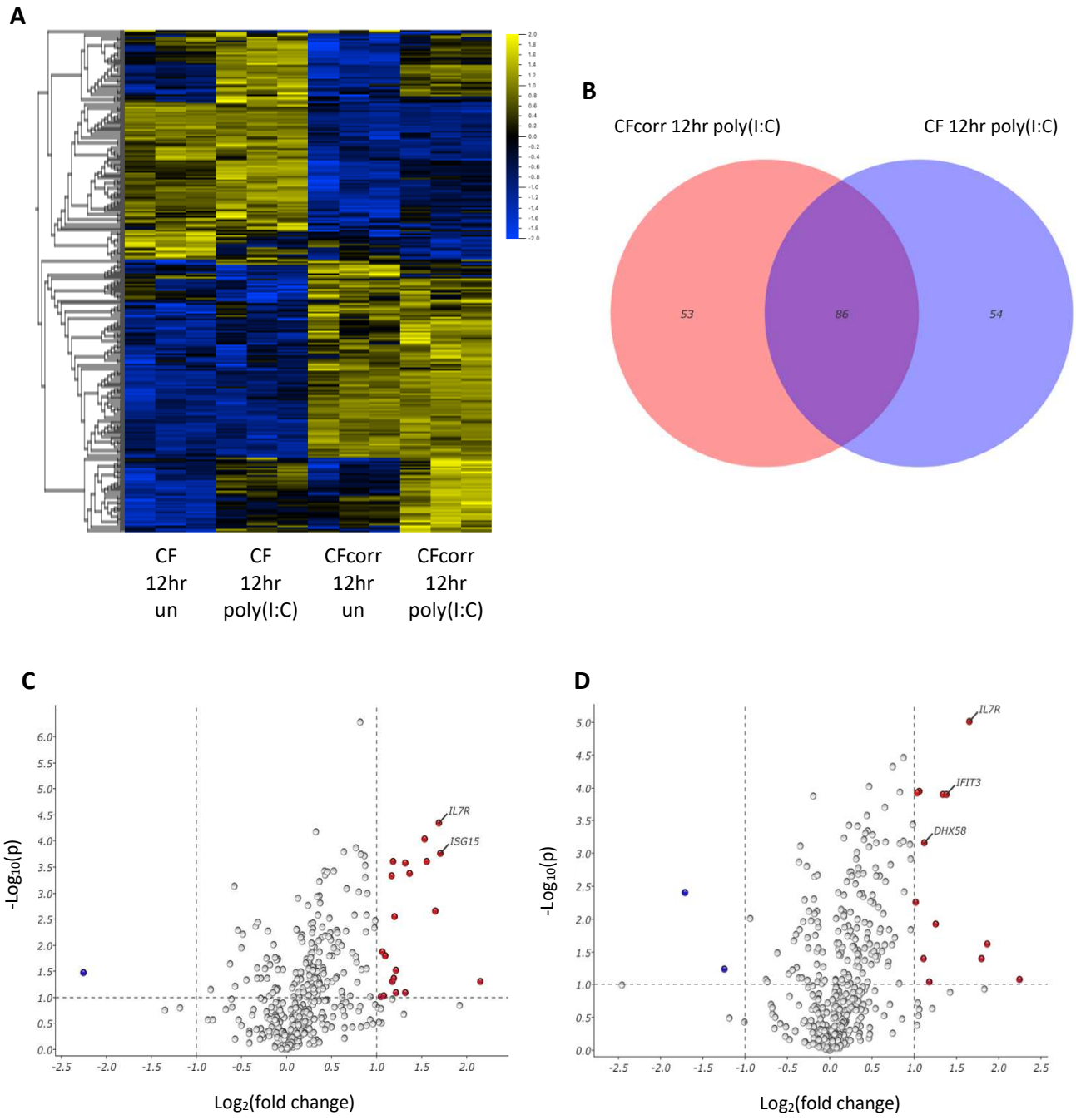

Figure 3.2.1.2: Differentially expressed ISGs of poly(I:C) stimulated CF and CF corrected BECs after 12 hours. CF and CF corrected BECs were stimulated with poly(I:C) (100μg/ml) for 12 hours, RNA was isolated and sent for bulk RNA sequencing. (A) Heatmap was organised by hierarchical clustering based on mean gene expression and only includes genes from a list of 486 ISGs. Each column represents a sample (n=3), and each row represents a gene (padj<0.05). Significance was calculated using ANOVA and Benjamini-Hochberg test to correct p-value. (B) Venn diagram of differentially expressed ISGs compared to unstimulated control of named condition representing overlap of ISG signature in CF and CF corrected BECs. Volcano plots representing differentially expressed ISGs for (C) CF corrected and (D)

CF cells stimulated by poly(I:C) for 12 hours, determined by student's t-test padj<0.05 and fold change >2.

Of the 27 differently expressed genes with a fold change >2, only 6 were overlapping which are highlighted in yellow in Table3.2.2.1. The ISGs expressed by the CF corrected cells had higher fold changes than the CF cells, B4GALNT2 had the highest fold change in the CF corrected cells (8.05) and FGF5 had the highest fold change in the CF cells (4.75). The CF corrected cells also expressed the overlapping ISGs more strongly than the CF cells, for example, IL7R has a fold change of 6.06 compared to 3.15 respectively. There were 2 ISGs downregulated by the CF cells and one downregulated in the CF corrected cells. Importantly, the CF corrected cells showed significantly increased expression of IFNλ1 and IFNλ3 at a fold change of 3.27 and 2.83 respectively. The CF cells did not significantly upregulate either IFNλ1 or IFNλ3 after poly(I:C) stimulation. Overall, 9 more ISGs were upregulated by the CF corrected cells compared to the CF cells after poly(I:C) stimulation for 12 hours and all the ISGs were expressed to a greater extent in the CF corrected cells.

Table 3.2.1.1: All differentially expressed ISGs in CF and CF corrected BECs after poly(I:C) stimulation for 12 hours. Overlapping genes are highlighted in yellow, upregulated genes are in red cells and downregulated in blue (padj<0.05; fold change >2).

CF corrected BECs			CF BECs		
Gene Symbol	**P(adj)**	**Fold Change**	**Gene Symbol**	**P(adj)**	**Fold Change**
B4GALNT2	0.017	8.05	FGF5	0.025	4.75
ISG15	0.010	6.52	GBP5	0.011	3.65
IL7R	0.010	6.06	HCAR3	0.014	3.48
SAMD9L	0.034	5.55	IL7R	0.005	3.15
IFIT3	0.011	4.56	IFIT3	0.006	2.60
VEGFC	0.010	4.20	SAMD9L	0.072	2.39
DHX58	0.011	4.18	SERPINB9	0.026	2.26
CXCL2	0.023	3.85	DHX58	0.014	2.17
PMAIP1	0.011	3.68	C1S	0.014	2.16
OAS2	0.012	3.67	PMAIP1	0.006	2.09
IFNL1	0.023	3.27	IFIH1	0.006	2.05
IFIT1	0.038	3.11	IFIT1	0.045	2.02
CXCL8	0.016	3.10	PLD5	0.038	-3.27
SAMD9	0.011	2.94	IDO1	0.019	-2.37
AIM2	0.017	2.92			
IFIH1	0.011	2.89			
CSF2	0.095	2.84			
IFNL3	0.026	2.83			
OAS1	0.086	2.81			
EXOC3L1	0.026	2.76			
B4GALNT2	0.017	2.65			
PLD5	0.014	-4.78			

3.2.1.2 – GSEA analysis of 12-hour Poly(I:C) stimulated CF and CF corrected bronchial epithelial cells

GSEA was completed on CF and CF corrected cells compared to their uninfected controls using a student's t-test. This revealed that a number of type I interferon gene sets were significantly enriched in CF corrected BECs after 12 hours of poly(I:C) stimulation; 'Hecker IFNB1 Targets' (padj=0.01; normalised enrichment score (NES) = 2.15; 95 genes) (Fig3.2.1.3), 'Der IFN Alpha Response Up' (padj=0.01; NES=1.73; 74 genes) and the general interferon gene set 'Browne Interferon Response Genes' (padj=0.03; NES=1.76; 67 genes). None of these gene sets were significantly enriched by CF BECs. Other gene sets enriched in the CF BECs were type II IFN immune responses 'Der IFN Gamma Response Up' (padj=0.01; NES=1.55); a gene set of 450 genes upregulated by bacterial infection 'Zhou Inflammatory Response Live Up' (padj=0.01; NES=1.73); and the 200 genes defining the inflammatory response in humans 'Hallmark Inflammatory Response' (padj=0.01; NES=1.66), showing a bias towards a more general inflammatory response.

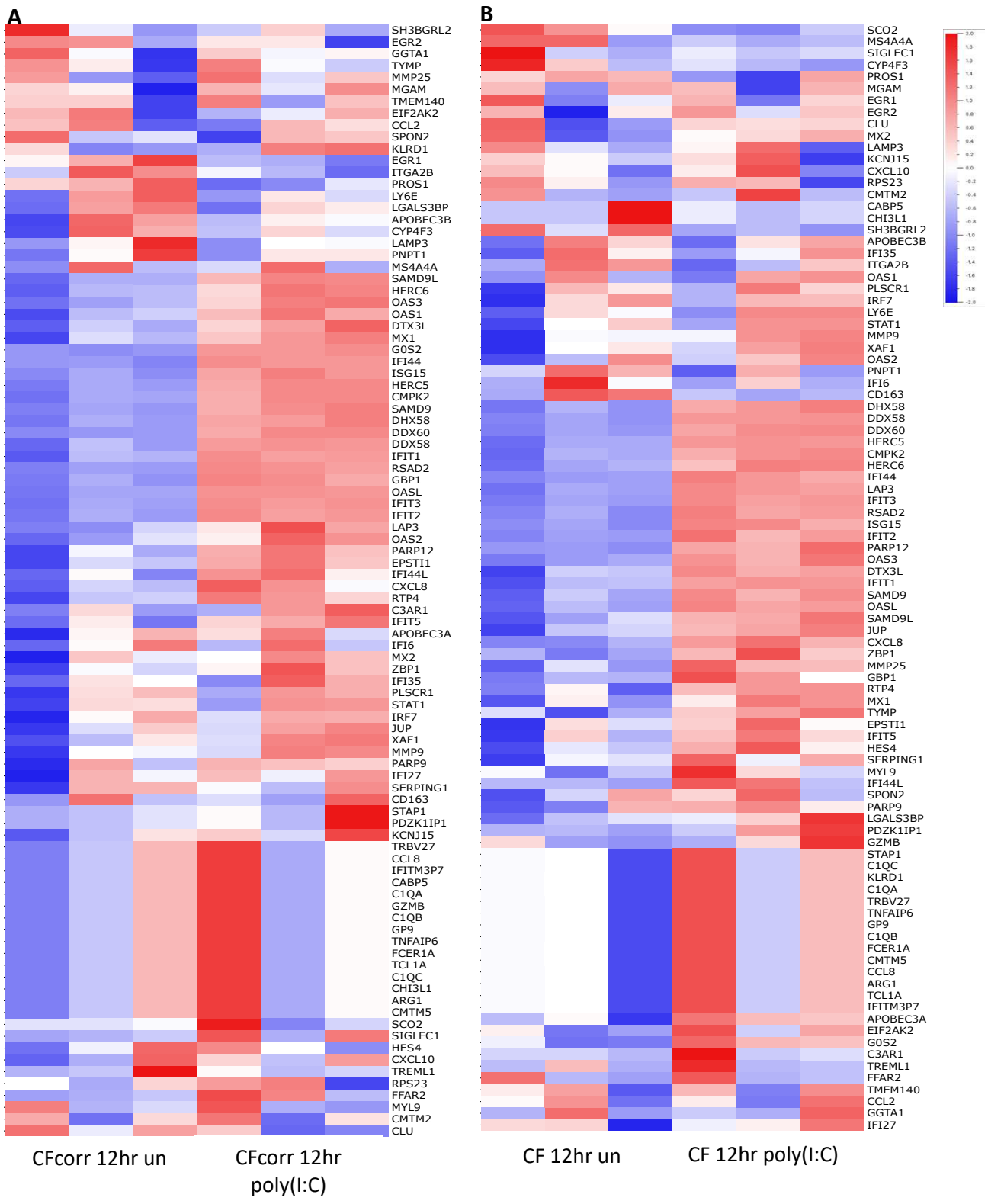

Figure 3.2.1.3: Representative visualisation of GSEA of CF and CF corrected BECs stimulation with poly(I:C) for 12 hours. (A) CF corrected BECs stimulated with 100μg/ml poly(I:C) for 12 hours showed enrichment of 'Hecker IFNB1 Targets' gene set (padj=0.01). (B) CF cells did not show enrichment of this gene set (padj=0.4). Significance calculated using Student's T-test and Benjamini-Hochberg test to correct p-value. Gene set consists of 96 genes. Data is from 3 independent experiments.

3.2.1.3 – Protein-protein interaction network analysis of 12-hour Poly(I:C) stimulated CF and CF corrected bronchial epithelial cells

To further elucidate the response of the CF and CF corrected BECs after 12 hours of poly(I:C) stimulation, protein-protein network analysis was completed using the stringApp on Cytoscape on all differentially expressed genes in stimulated cells compared to uninfected controls. Functional enrichment of the networks revealed there were more genes related to the type I IFN response, highlighted in blue, in the CF corrected network (Fig3.2.1.4 A) compared to the CF network (Fig3.2.1.4 B), with 18 and 14 ISGs respectively. The ISGs in the CF corrected network were also more strongly upregulated than in the CF network, so confirming results observed in previous figures.

A

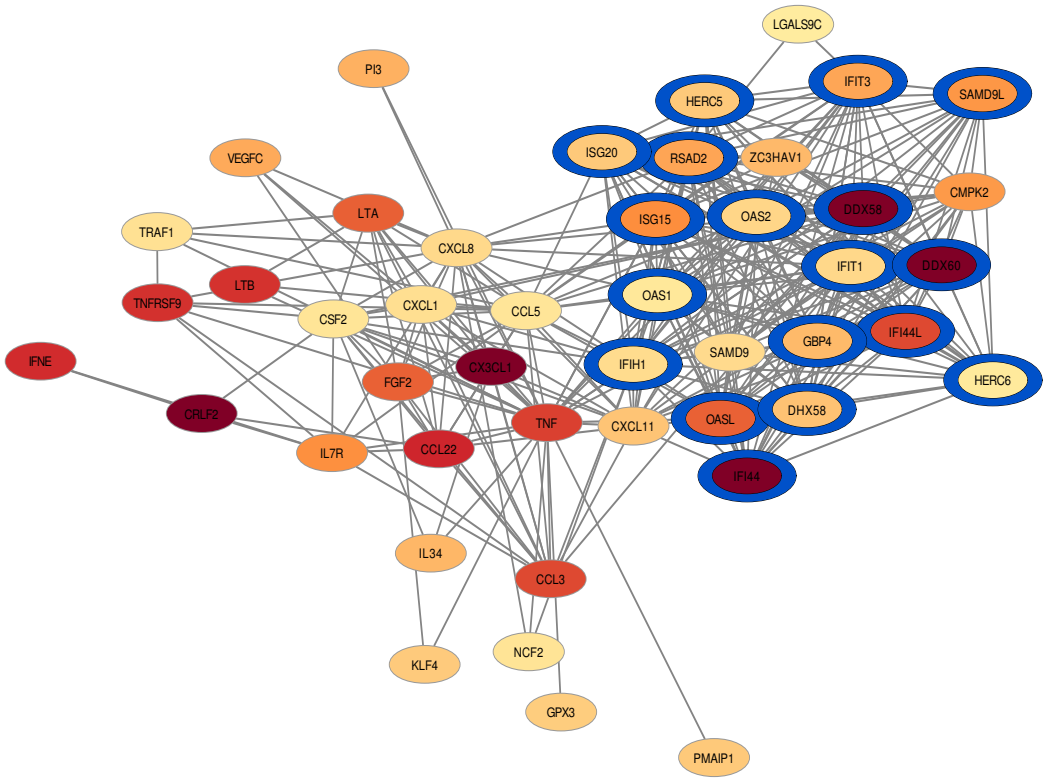

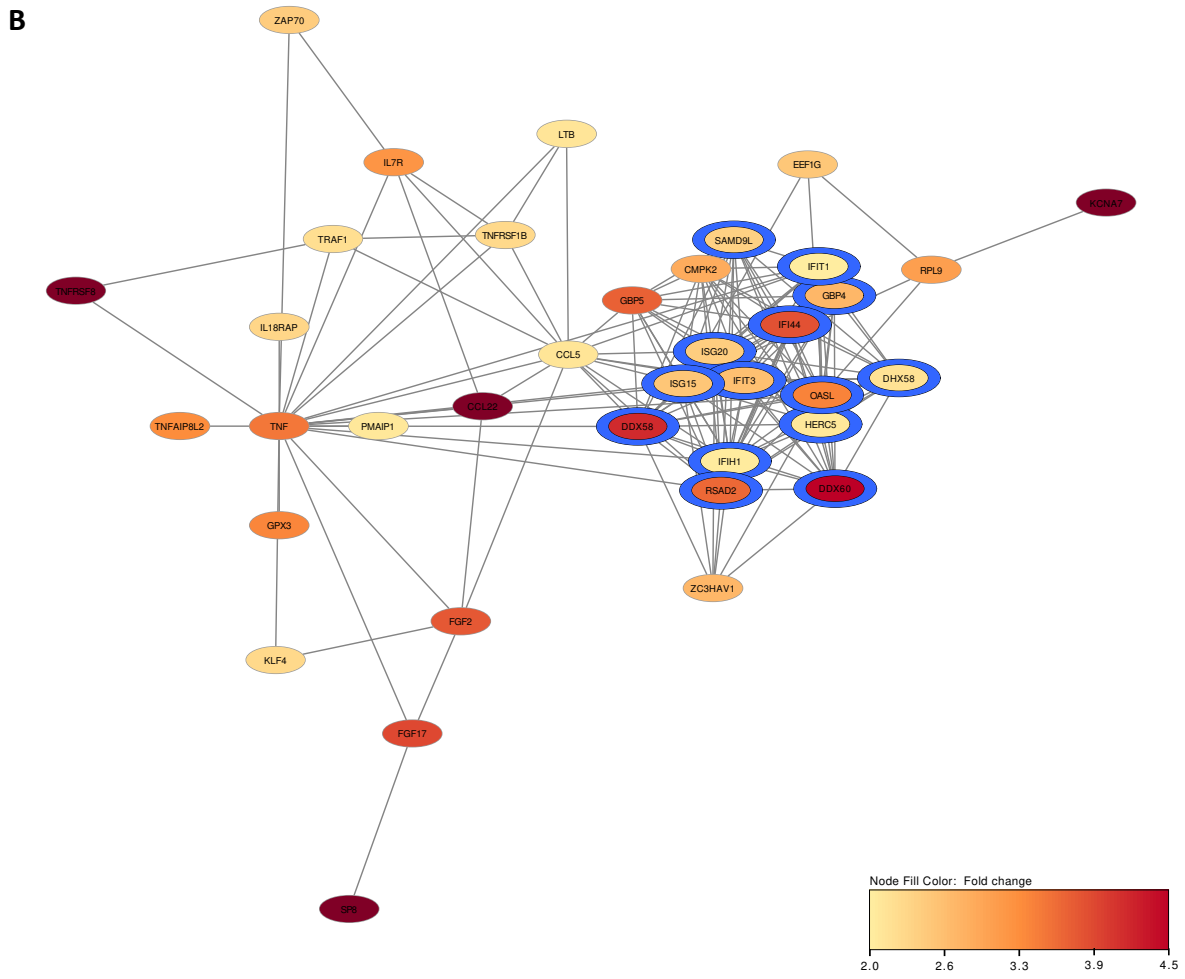

Figure 3.2.1.4: Network analysis of poly(I:C) stimulated CF and CF corrected BECs after 12 hours. Network visualisation of significant immunity-associated proteins (padj<0.05 and fold change >2), after 12 hours of poly(I:C) stimulation in (A) CF corrected BECs and (B) CF BECs. The nodes indicate genes, and the colour represents fold change. Functional enrichment analysis highlights the nodes involved in the type I IFN response (blue) (Cytoscape, stringApp).

3.2.1.4 – DEG analysis of 24-hour Poly(I:C) stimulated CF and CF corrected bronchial epithelial cells

After 24 hours of poly(I:C) stimulation there was a total of 329 differentially expressed ISGs (padj=0.05) (Fig3.2.1.5 A), for both CF corrected BECs (189) and CF BECs (195). Both cell lines expressed more ISGs at 24 hours compared with 12 hours but still had distinct ISG signatures post stimulation (Fig3.2.1.5 A) with only 121 ISGs overlapping (Fig3.2.1.5 B).

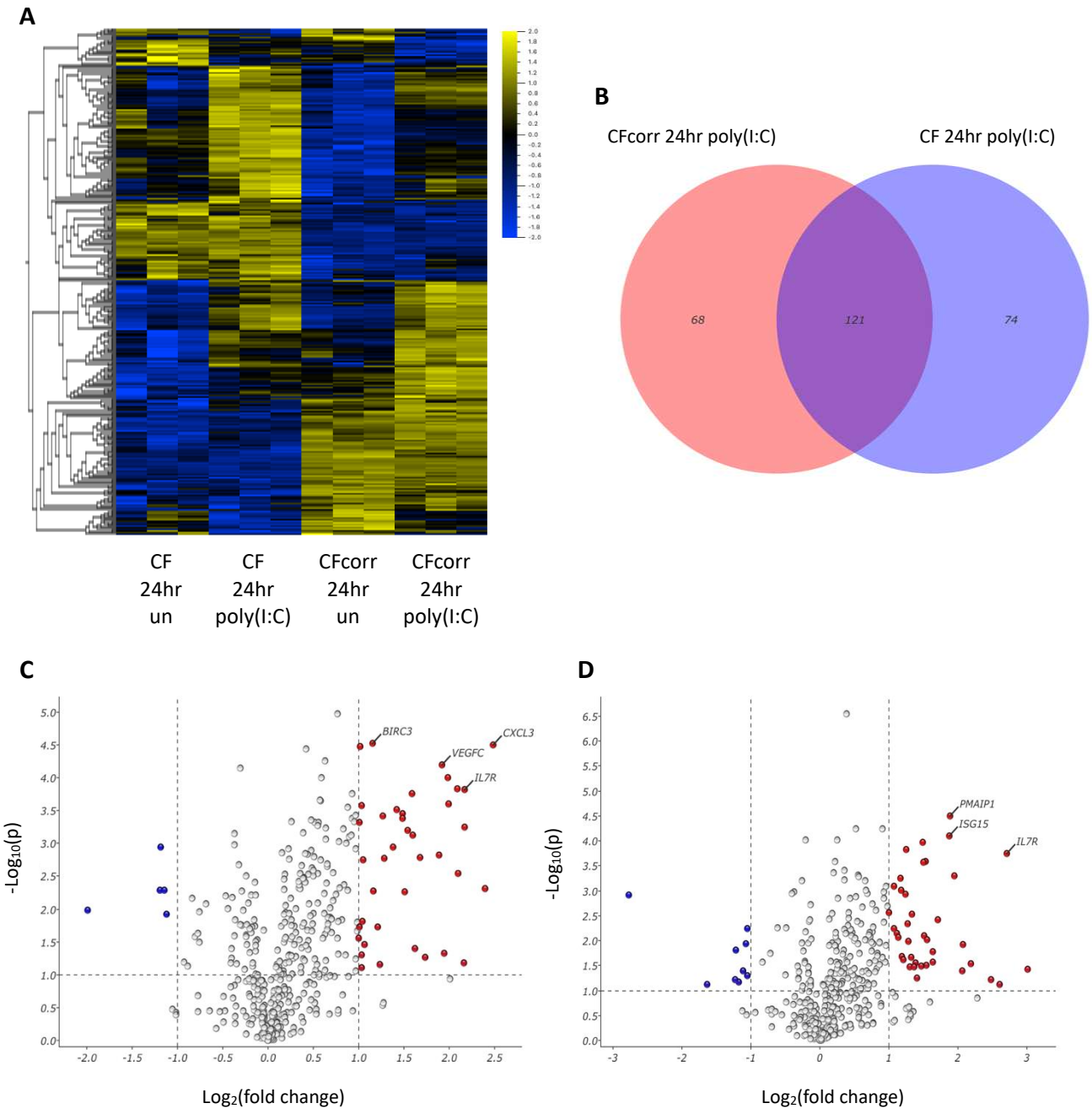

Figure 3.2.1.5: Differentially expressed ISGs of poly(I:C) stimulated CF and CF corrected BECs after 24 hours. CF and CF corrected BECs were stimulated with poly(I:C) (100μg/ml) for 24 hours, RNA was isolated and sent for bulk RNA sequencing. (A) Heatmap was organised by hierarchical clustering based on mean gene expression and only includes genes from a list of 486 ISGs. Each column represents a sample (n=3), and each row represents a gene (padj<0.05). Significance was calculated using ANOVA and Benjamini-Hochberg test to correct p-value. (B) Venn diagram of differentially expressed ISGs compared to unstimulated control of named condition representing overlap of ISG signature in CF and CF corrected BECs. Volcano plots representing differentially expressed ISGs for (C) CF corrected and (D)

CF cells stimulated by poly(I:C) for 24 hours, determined by student's t-test padj<0.05 and fold change >2.

When filtering the genes that were differentially expressed by over 2-fold change (Fig3.2.1.5 C, D), it revealed that both CF and CF corrected BECs expressed 39 upregulated ISGs with 28 of these overlapping (Table3.2.1.2). However, the expression pattern of the responses differed regarding the shared ISGs, for example, guanylate binding protein 5 (GBP5) had the highest expression in the CF BECs with a fold change of 8.05, but this was only upregulated by a fold change of 3.07 in the CF corrected BECs. Notably, IFNλ1 was significantly upregulated by the CF corrected BECs, but not the CF BECs. The CF BECs expressed more downregulated ISGs than the CF corrected BECs.

Table 3.2.1.2: All differentially expressed ISGs in CF and CF corrected BECs after poly(I:C) stimulation for 24 hours. Overlapping genes are highlighted in yellow, upregulated genes are in red cells and downregulated in blue (padj<0.05; fold change >2).

CF corrected BECs			CF BECs		
Gene Symbol	P(adj)	Fold Change	Gene Symbol	P(adj)	Fold Change
CXCL3	0.004	5.59	GBP5	0.011	8.05
APOBEC3G	0.028	5.25	IL7R	0.009	6.52
IL7R	0.006	4.50	ESM1	0.016	6.06
CSF2	0.008	4.49	IL1A	0.014	5.55
HCAR3	0.015	4.47	SHC4	0.011	4.56
SAMD9L	0.020	4.27	IL24	0.041	4.20
PMAIP1	0.006	4.24	ANGPTL4	0.011	4.18
ISG15	0.007	3.98	IFIT3	0.014	3.85
IFIT3	0.005	3.95	PMAIP1	0.007	3.68
LMO2	0.012	3.85	ISG15	0.007	3.67
VEGFC	0.004	3.77	ACE2	0.038	3.27
CXCL8	0.014	3.69	SAMD9L	0.010	3.11
ESM1	0.013	3.33	TNFAIP3	0.048	3.10
SAMD9	0.014	3.19	CSF2	0.058	2.94
GBP5	0.010	3.07	HCAR3	0.011	2.92
TNFAIP3	0.009	3.02	HSD11B1	0.010	2.89
IL23A	0.006	3.00	IFIT1	0.044	2.84
DHX58	0.009	2.90	VEGFC	0.010	2.83
G0S2	0.028	2.84	BIRC3	0.007	2.81
IL6	0.008	2.79	ANTXR2	0.011	2.76
IFIH1	0.008	2.79	BATF2	0.013	2.65
PLAUR	0.007	2.67	G0S2	0.010	2.61
IFIT1	0.012	2.60	SAMD9	0.011	2.57
PLCG2	0.014	2.43	IFIH1	0.032	2.52
IFIT2	0.008	2.40	APOBEC3G	0.042	2.49
FYB1	0.015	2.35	CXCL8	0.011	2.46
IL24	0.062	2.31	PLCG2	0.040	2.42
ANTXR2	0.028	2.23	DHX58	0.042	2.41
BIRC3	0.004	2.23	IFIT2	0.008	2.38
TRPV3	0.045	2.09	DDX60L	0.018	2.36
CTSS	0.014	2.07	OAS2	0.010	2.31
USP18	0.048	2.06	IL23A	0.042	2.28
NFE2L3	0.007	2.05	PDZD2	0.018	2.25
IFNL1	0.012	2.05	PLAUR	0.014	2.24
NAV3	0.017	2.04	IL6	0.049	2.19
DAPP1	0.004	2.03	CTSS	0.050	2.16
RELB	0.008	2.01	NMNAT2	0.047	2.10
RTP4	0.062	2.01	FERMT1	0.017	2.09
ACE2	0.050	2.00	PDCD1LG2	0.031	2.00
PTPN22	0.018	-3.98	PLD5	0.018	-6.84
EDIL3	0.016	-2.29	APOD	0.016	-3.10
PDK4	0.014	-2.28	SERPINB9	0.014	-2.34
IGFBP3	0.045	-2.22	SYT12	0.045	-2.33
IRF8	0.015	-2.17	GALM	0.015	-2.27
			IRF8	0.011	-2.17
			IGFBP3	0.041	-2.11
			PDK4	0.047	-2.08
			B4GALNT2	0.012	-2.08

3.2.1.5 – GSEA analysis of 24-hour Poly(I:C) stimulated CF and CF corrected bronchial epithelial cells

At 24 hours post stimulation, again the CF corrected cells did show significant enrichment of all three of the interferon response gene sets that were previously mentioned (Fig3.2.1.6). The GSEA also showed that CF BECs did show enrichment in the 'Hecker IFNb1 Targets' (padj=0.06; NES=1.57), 'Der IFN Alpha Response Up' (padj=0.07; NES=1.55), but not the 'Browne Interferon Response Genes' (padj=0.12; NES=1.45) gene sets. There was still a bias toward a general inflammatory response with the 'Zhou Inflammatory Response Live Up' (padj=0.03; NES=1.73) and 'Hallmark Inflammatory Response' (padj=0.06; NES=1.82) gene sets being significantly enriched.

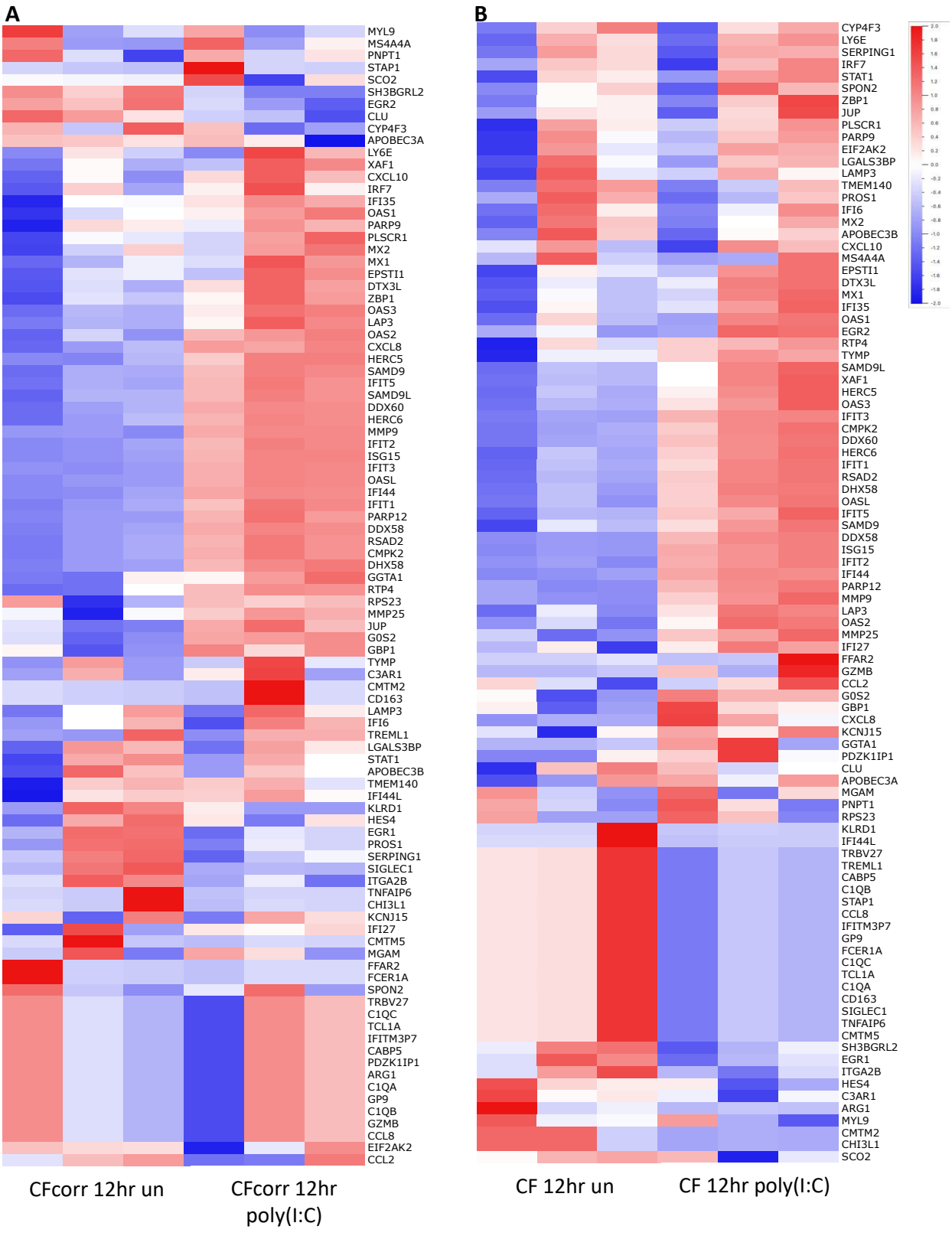

Figure 3.2.1.6: Representative visualisation of GSEA of CF and CF corrected BECs stimulated with poly(I:C) for 24 hours. (A) CF corrected BECs stimulated with 100μg/ml poly(I:C) for 24 hours showed enrichment of 'Hecker IFNB1 Targets' gene set (padj=0.01). (B) CF cells also showed enrichment of this gene set (padj=0.06). Significance calculated using Student's T-test and Benjamini-Hochberg test to correct p-value. Gene set consists of 96 genes.

3.2.1.6 – Protein-protein interaction network analysis of 24-hour Poly(I:C) stimulated CF and CF corrected bronchial epithelial cells

The protein-protein network analysis on all differentially expressed genes with function enrichment revealed a network with 20 genes involved in the type I ISG response in the CF corrected network (Fig3.2.1.7 A), and 15 in the CF network (Fig3.2.1.7 B). This confirms more ISGs were upregulated at 24 hours compared to 12 hours in both cell lines, and that the CF corrected cells elicited a stronger type I and III IFN response at both time points after poly(I:C) stimulation.

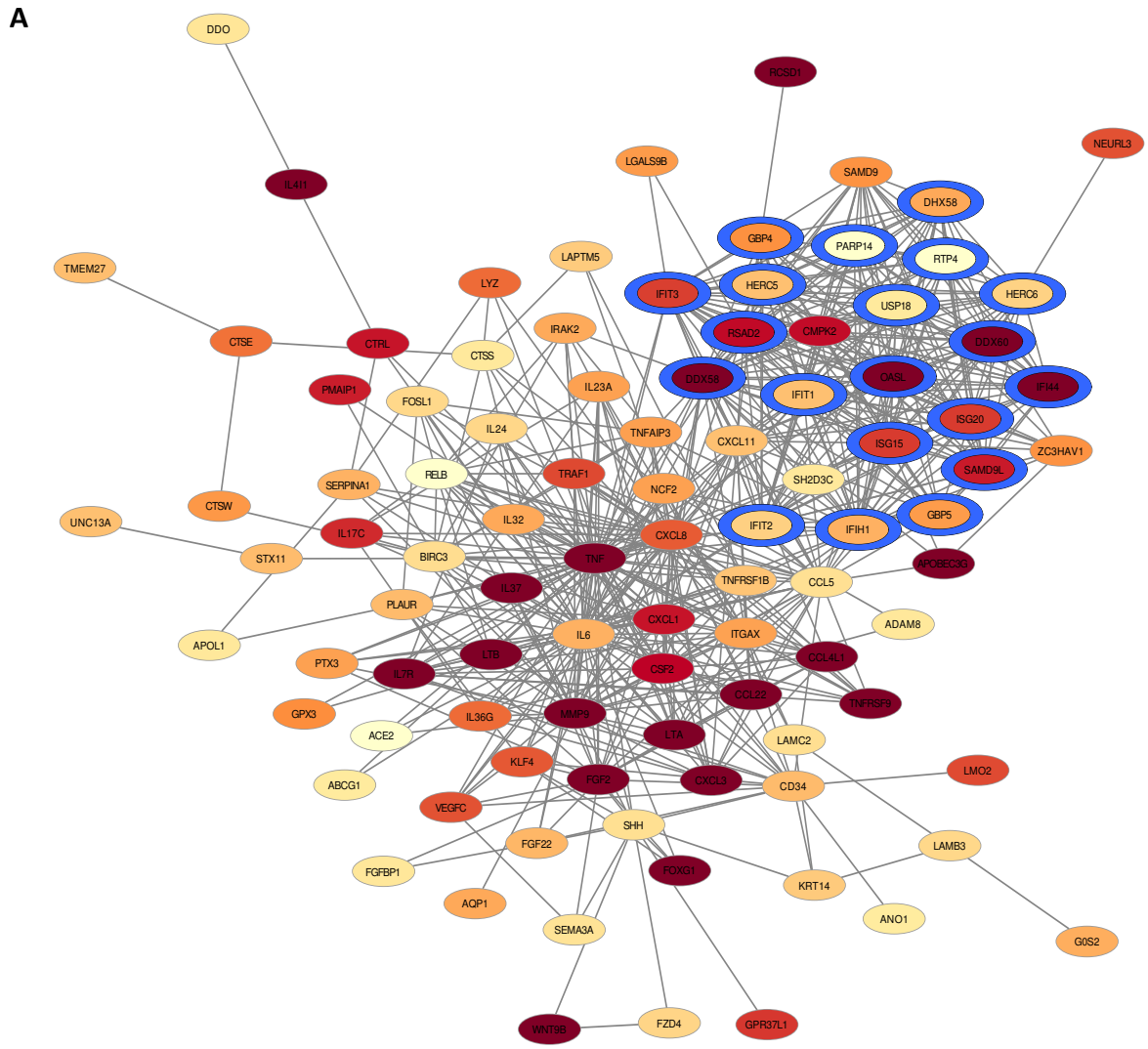

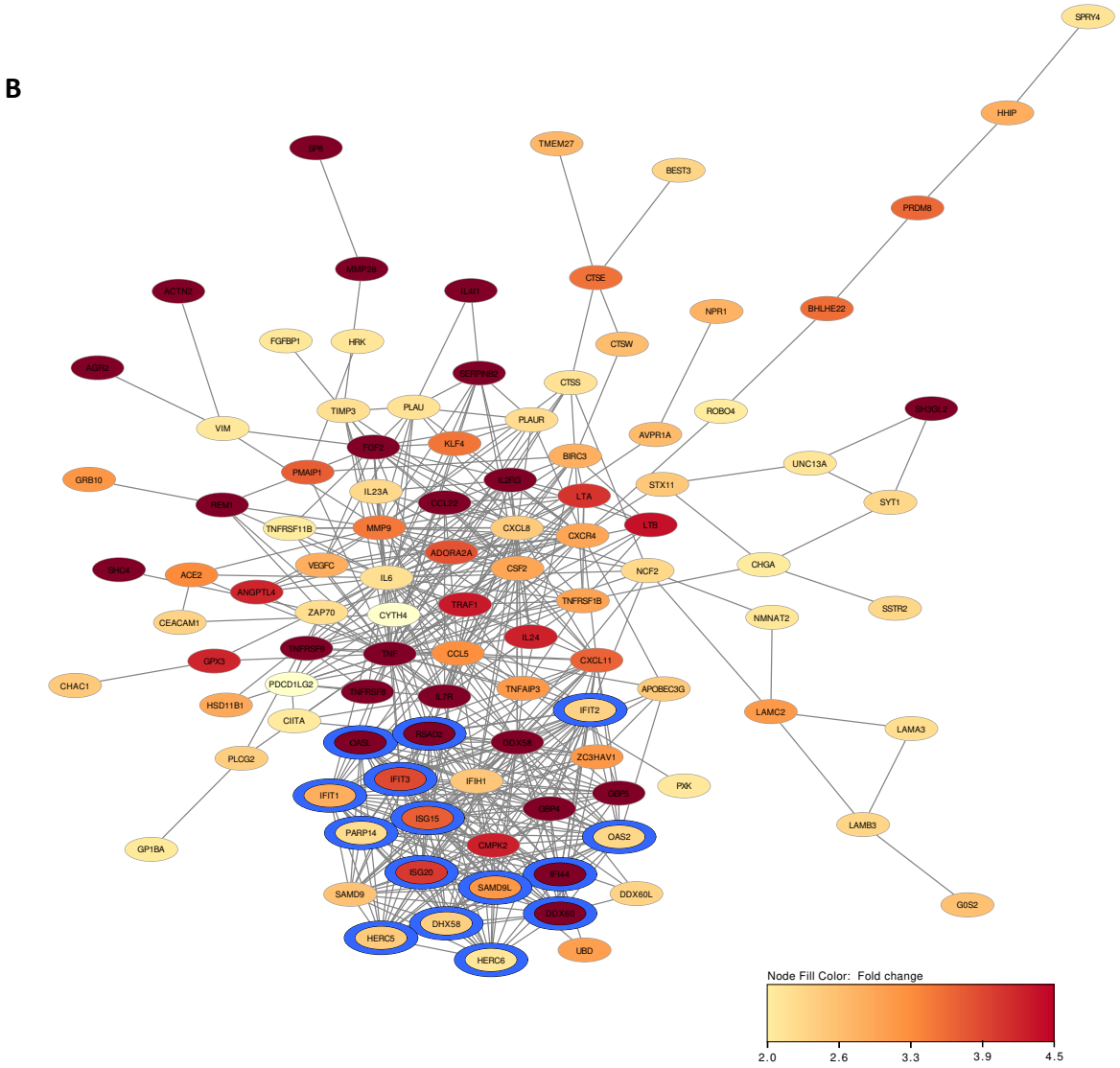

Figure 3.2.1.7: Network analysis of poly(I:C) stimulated CF and CF corrected BECs after 24 hours. Network visualisation of significant immunity-associated proteins (padj<0.05 and fold change >2), after 24 hours of poly(I:C) stimulation in (A) CF corrected BECs and (B) CF BECs. The nodes indicate genes, and the colour represents fold change. Functional enrichment analysis highlights the nodes involved in the type I IFN response (blue) (Cytoscape, stringApp).

3.2.2 – Transcriptomic characterisation of *Aspergillus fumigatus* fixed hyphae infection in CF and CF corrected bronchial epithelial cells

Once a defect in the type I and III IFN response was identified in the CF BECs in response to poly(I:C) it was investigated if this defect was also present in response to *Af* fixed hyphae infection. ANOVA analysis revealed 10572 differentially expressed genes between the two cell lines, infection, and time points. Cluster analysis of the top 2000 differentially expressed genes in the CF and CF corrected cells at 12- and 24-hours post infection done in triplicate and analysed by multigroup comparison showed the distinct gene signatures post infection at both time points (Fig3.2.2.1). The genes that are upregulated after infection are more strongly expressed at 24 hours compared to 12 hours and there is a difference in expression patterns after infection between the two cell lines. The top 2000 differentially expressed genes in Fig3.2.2.1 contains 82 ISGs across both time points.

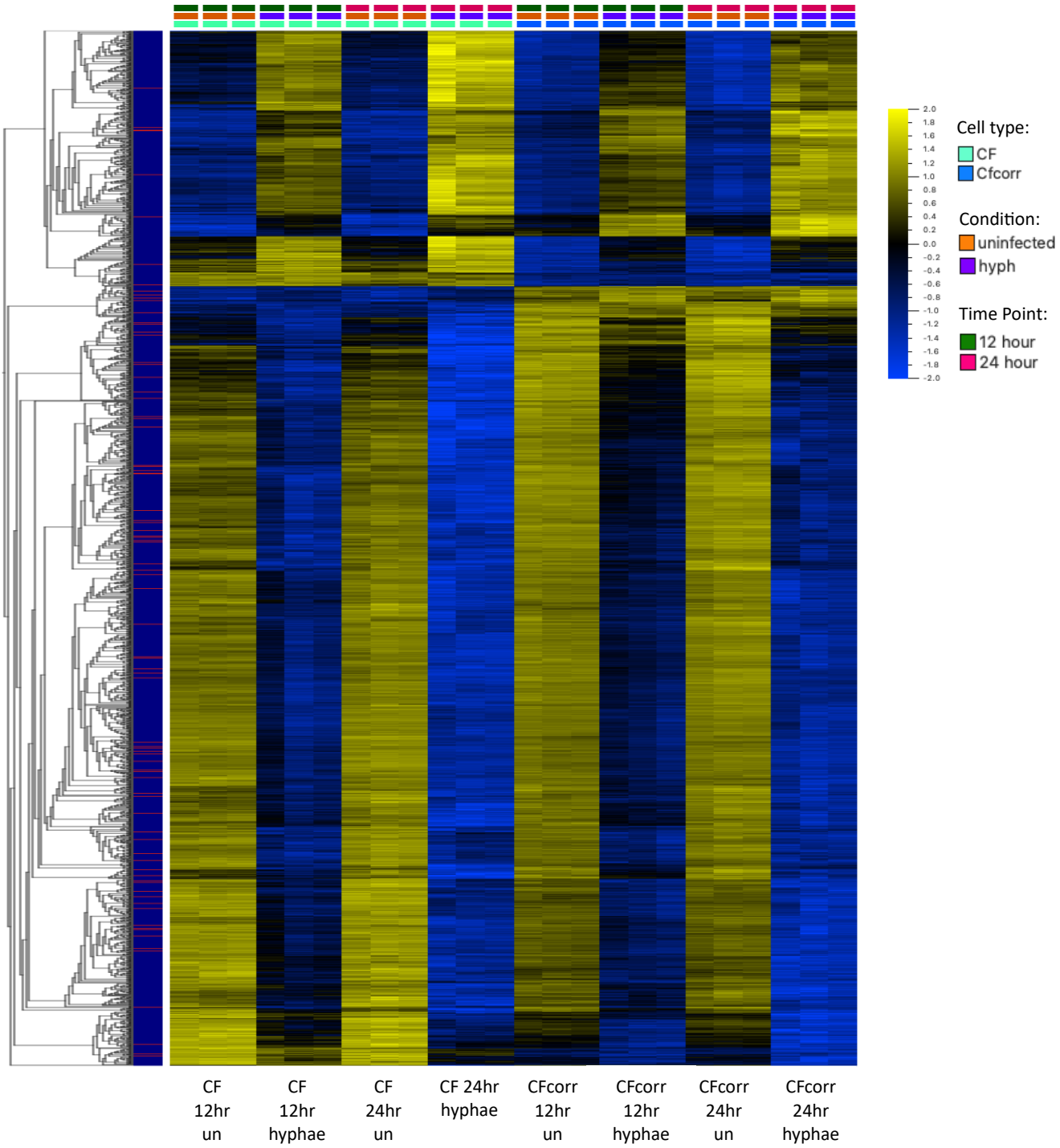

Figure 3.2.2.1: Gene expression heatmap of top 2000 genes differentially expressed after fixed hyphae infection. CF and CF corrected BECs were infected with *Af* hyphae (MOI=8) for 12 and 24 hours, RNA was isolated and sent for bulk RNA sequencing. Data were compared to uninfected controls and between the cell lines and time points using ANOVA to test for significance and Benjamini-Hochberg test to correct p-value. Heatmap was organised by hierarchical clustering based on mean gene expression. Each column represents a sample (n=3), and each row represents a gene (padj=<0.01). ISGs are highlighted in pink on the left-hand panel.

3.2.2.1 – DEG analysis of 12-hour Af fixed hyphae infected CF and CF corrected bronchial epithelial cells

To investigate further the ISG gene list was cross referenced with the differentially expressed genes. A heatmap and ANOVA analysis of these genes clearly shows there are differences in the expression patterns post infection between the two cell lines (Fig3.2.2.2 A) with a total of 361 differentially expressed genes (padj=0.05). When the infected cells were compared to their relevant uninfected controls, a student's t-test revealed there were 268 and 253 differentially expressed ISGs in the CF corrected and CF cells after hyphae infection respectively, 225 were shared between the two cell lines and 43 were distinct to the CF corrected cells (Fig3.2.2.2 B). Volcano plots applying a further filter on the data of a fold change >2 show that although many ISGs are upregulated by the hyphae infection, there are more ISGs downregulated than upregulated in both cell lines (Fig3.2.2.2 C, D) and that the genes upregulated by the two cell lines differ.

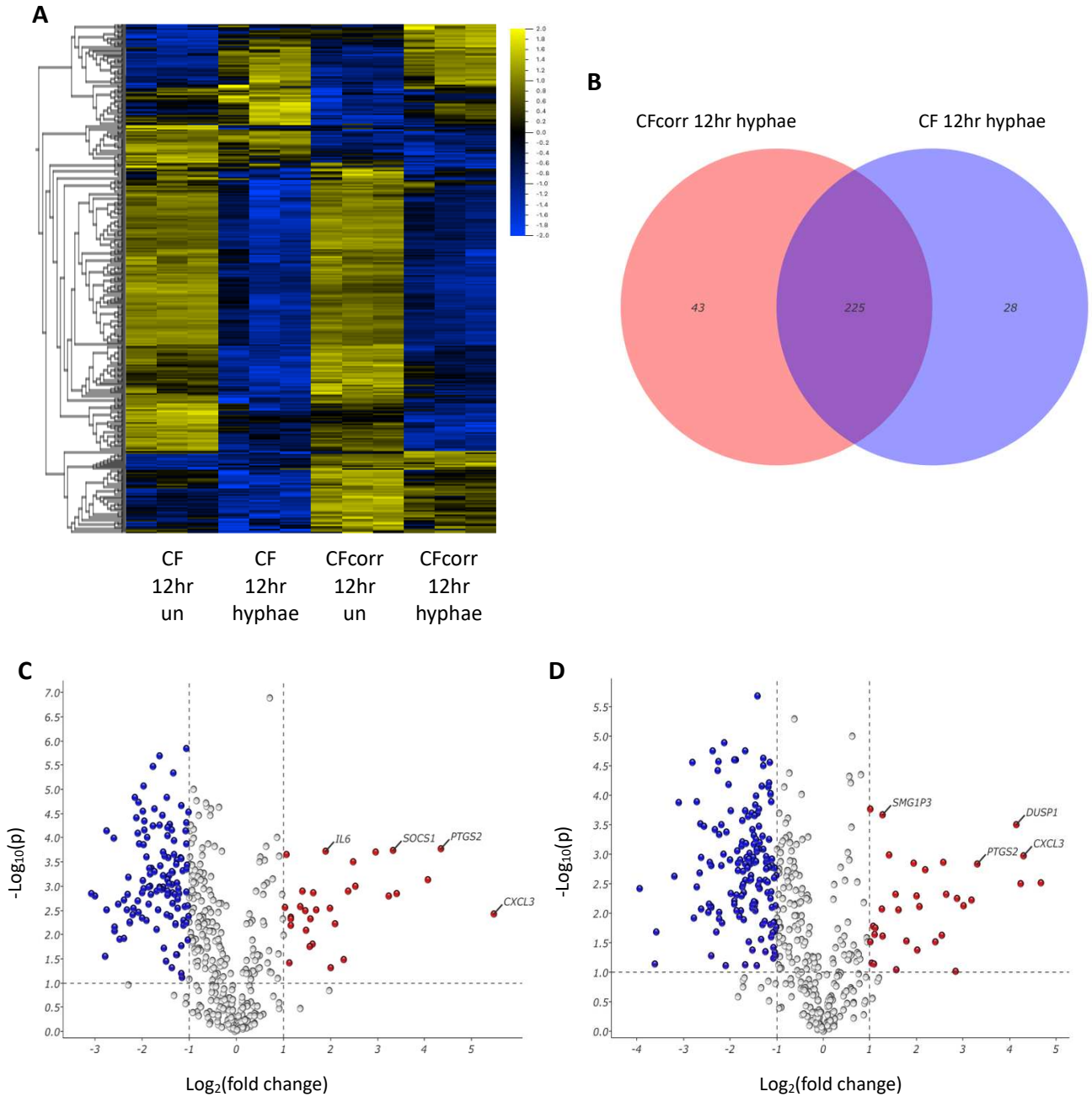

Figure 3.2.2.2: Differentially expressed ISGs of 12 hour fixed hyphae infected CF and CF corrected BECs. CF and CF corrected BECs were infected with *Af* hyphae (MOI=8) for 12 hours, RNA was isolated and sent for bulk RNA sequencing. (A) Heatmap was organised by hierarchical clustering based on mean gene expression and includes genes from a list of 486 ISGs. Each column represents a sample (n=3), and each row represents a gene (padj<0.05). Significance was calculated using ANOVA and Benjamini-Hochberg test to correct p-value. (B) Venn diagram of differentially expressed ISGs compared to unstimulated control of named condition represents overlap of ISG signature in CF and CF corrected BECs. Volcano plots represents differentially expressed ISGs for (C) CF corrected and (D) CF cells infected by *Af* hyphae for 12 hours, determined by student's t-test padj<0.05 and fold change >2.

Of the top 25 upregulated ISGs with the further filter of fold change >2, only 5 are upregulated by both cell lines (Table3.2.2.1). IFIT1 and IFIT3 were significantly upregulated by a fold change of 2.23 and 5.62 respectively in the CF corrected cells but were significantly downregulated by the CF cells by a fold change of -5.48 and -5.89 respectively. IFIT1 is one of the most abundantly expressed ISGs during the antiviral response, but its role in antifungal immunity has not been investigated. Its downregulation in response to fungal infection in CF cells suggests a possible explanation to the reduced fungal killing capacity of CF cells. Interestingly, the gene that is expressed with the highest fold change in the CF BECs is CXCL2 (fold change = 25.55), a strong neutrophil chemoattractant which is not significantly upregulated by CF corrected cells. Other monocyte and neutrophil chemoattractants CXCL3 and CXCL8 are upregulated by both CF and CF corrected cells. CXCL3 is upregulated by a fold change of 44.45 in CF corrected cells compared to 19.72 in CF, whereas the strongest neutrophil chemoattractant CXCL8 is upregulated by a fold change of 3.97 in CF corrected cells and 18.87 in CF cells post infection. Other notable downregulated genes are IFIT5 in both cell lines and IFNλ2 in CF cells, which is not significantly downregulated by the CF corrected cells after hyphae exposure.

Table 3.2.2.1: The top 25 upregulated and top 25 downregulated ISGs in CF and CF corrected BECs after fixed hyphae infection for 12 hours. Overlapping genes are highlighted in yellow, upregulated genes are in red cells and downregulated in blue (padj<0.05; fold change >2).

CF corrected BECs			CF BECs		
Gene Symbol	**P(adj)**	**Fold Change**	**Gene Symbol**	**P(adj)**	**Fold Change**

CXCL3	0.010	44.45	CXCL2	0.010	25.55
APOBEC3G	0.002	20.31	CXCL3	0.006	19.72
IL7R	0.004	16.79	CXCL8	0.010	18.87
CSF2	0.005	10.62	DUSP1	0.003	17.68
HCAR3	0.002	10.11	PTGS2	0.006	9.89
SAMD9L	0.005	9.46	NFKBIZ	0.016	9.03
PMAIP1	0.002	7.81	PDK4	0.019	8.10
ISG15	0.004	5.79	SOCS1	0.015	7.36
IFIT3	0.002	5.62	CREB5	0.014	6.24
LMO2	0.005	5.17	IL6	0.006	5.99
VEGFC	0.014	4.28	ANGPTL4	0.046	5.83
CXCL8	0.008	3.97	CCNA1	0.007	4.54
ESM1	0.002	3.71	IL23A	0.019	4.19
SAMD9	0.009	3.26	PMAIP1	0.014	3.99
GBP5	0.005	3.10	TENT5A	0.006	3.83
TNFAIP3	0.031	3.09	SNORD17	0.020	3.05
IL23A	0.012	2.96	IRF7	0.014	2.95
DHX58	0.035	2.94	SMG1P1	0.006	2.68
G0S2	0.018	2.80	LINC-PINT	0.047	2.41
IL6	0.009	2.77	SMG1P3	0.003	2.41
IFIH1	0.005	2.64	WFDC2	0.020	2.40
PLAUR	0.008	2.56	APOBEC3A	0.037	2.16
IFIT1	0.011	2.23	MAFF	0.045	2.14
PLCG2	0.015	2.23	IL1A	0.035	2.11
IFIT2	0.012	2.22	GAPDH	0.003	2.02
SLC2A12	0.005	-8.46	TMEM229B	0.012	-15.40
TMEM229B	0.005	-8.02	RTP4	0.042	-11.95
CEMIP2	0.001	-6.75	SPSB1	0.008	-9.16
SPSB1	0.009	-6.74	SLC2A12	0.002	-8.63
ABCA1	0.001	-6.06	GCNT4	0.001	-7.05
ZBED6	0.015	-6.02	APOL6	0.027	-6.89
APOL6	0.018	-6.00	CEMIP2	0.002	-6.58
PTAFR	0.007	-5.69	PDCD1LG2	0.011	-6.55
PLD5	0.026	-5.57	SGMS2	0.008	-6.26
DTX4	0.006	-5.23	PTAFR	0.003	-6.24
HCAR3	0.025	-5.21	TBK1	0.006	-6.19
PDCD1LG2	0.009	-5.03	N4BP1	0.020	-6.13
TMEM217	0.005	-4.96	IFIT3	0.003	-5.89
TNFSF15	0.003	-4.89	IRF2	0.022	-5.56
GCNT4	0.013	-4.80	IFIT1	0.018	-5.48
B3GNT7	0.014	-4.78	TNFSF15	0.006	-5.39
AIDA	0.010	-4.59	DTX4	0.019	-5.35
TRANK1	0.008	-4.57	IFIT5	0.007	-5.30
LNPEP	0.001	-4.45	ZBED6	0.019	-5.30
LRRC3	0.001	-4.34	POLR3B	0.019	-5.28
IFIT5	0.006	-4.28	ITGA2	0.001	-5.17
ANKRD12	0.001	-4.25	ANKRD12	0.004	-5.03
N4BP1	0.009	-4.22	IFNL2	0.042	-4.92

3.2.2.2 – GSEA analysis of 12-hour Af fixed hyphae infected CF and CF corrected bronchial epithelial cells

GSEA also revealed enrichment in 'KEGG JAK STAT1/2 Signalling' (padj=0.09; NES=1.77) and 'Reactome TRAF6 Mediated IRF7 Activation' (padj=0.05; NES=1.76) gene sets in the CF corrected cells, as well as the interferon related sets 'Hecker IFNB1 Targets' (padj=0.01; NES=1.54), 'Der IFN Alpha Response Up' (padj=0.09; NES=1.61) and 'Browne Interferon Response Genes' (padj=0.1; NES=1.57). None of these gene sets were significantly enriched in the CF cells and the 'Reactome TRAF6 Mediated IRF7 Activation' (padj=0.1; NES=-1.43) and 'Hecker IFNb1 Targets' (padj=0.1; NES=-1.45) gene sets were significantly downregulated (Fig3.2.2.3).

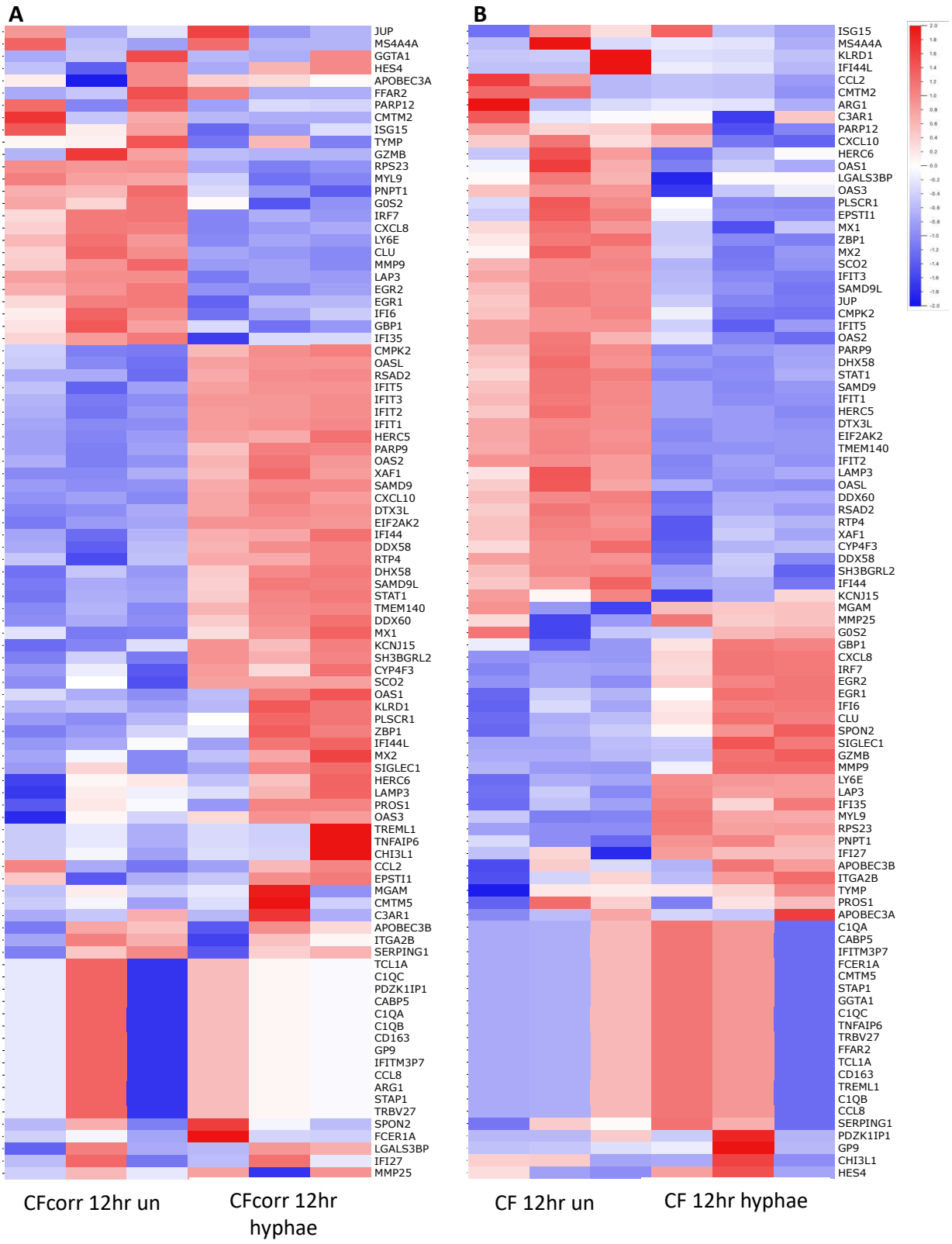

Figure 3.2.2.3: Representative visualisation of GSEA of CF and CF corrected BECs infected with *Af* fixed hyphae for 12 hours. (A) CF corrected BECs infected with *Af* hyphae (MOI=8) for 12 hours showed enrichment of 'Hecker IFNB1 Targets' gene set (padj=0.01). (B) CF cells did not show enrichment of this gene set (padj=0.7). Significance calculated using Student's T-test and Benjamini-Hochberg test to correct p-value. Gene set consists of 96 genes.

3.2.2.3 – Protein-protein interaction network analysis of 12-hour Af fixed hyphae infected CF and CF corrected bronchial epithelial cells

Functional enrichment of the protein-protein network analysis of the differentially expressed genes at 12 hours post hyphae infection showed that there were 6 and 5 genes related to the type I IFN response in the CF corrected and CF cells respectively. Despite there being little difference in the type I ISG expression in the network, the ISGs had higher fold changes in the CF corrected network compared to CF. Further functional enrichment showed the importance of the TRAF6-mediated IRF7 activation (red) and JAK-STAT1/2 signalling (green) in the CF corrected cells (Fig3.2.2.4 A). There was no evidence of genes related to these processes in

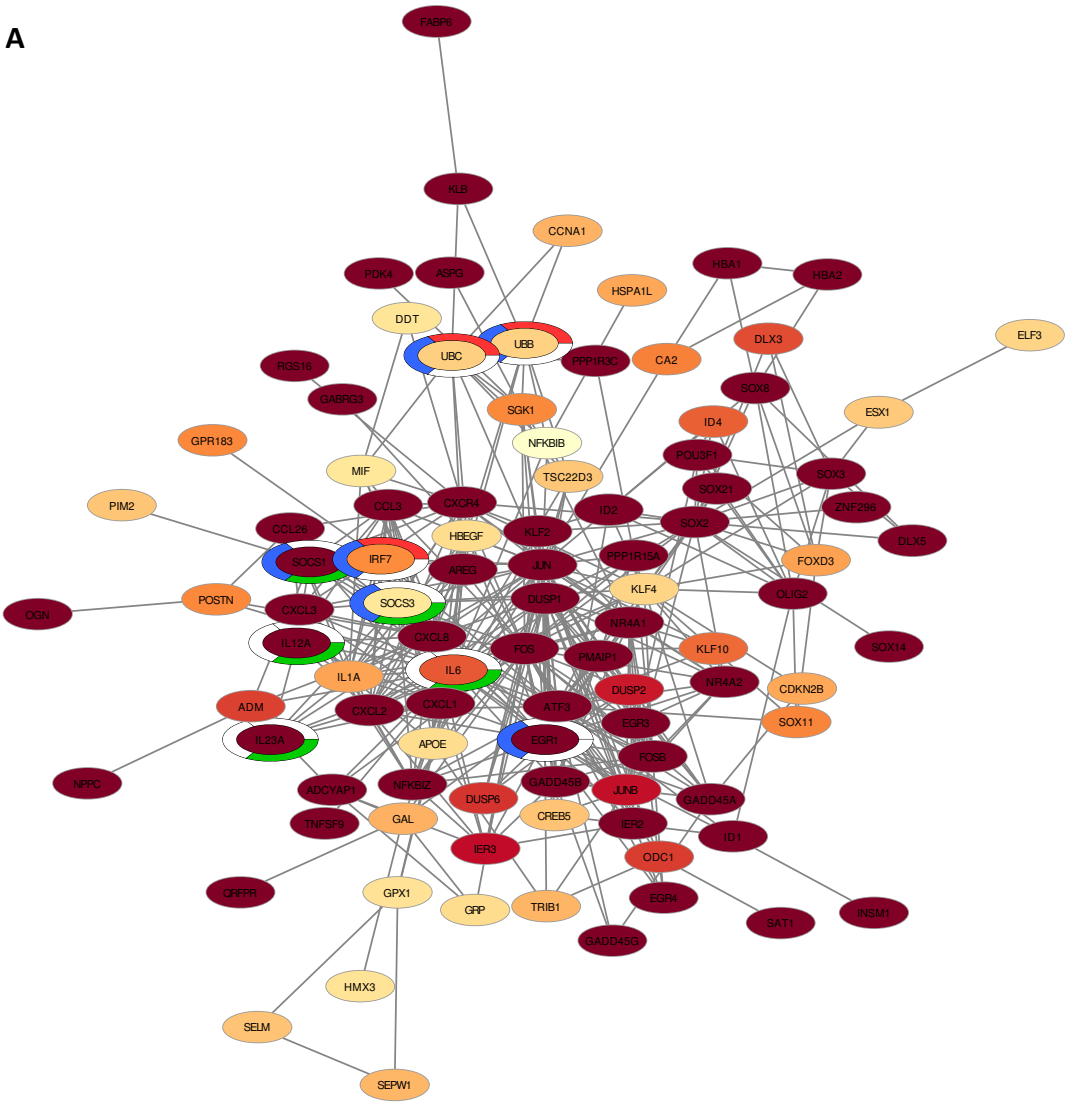

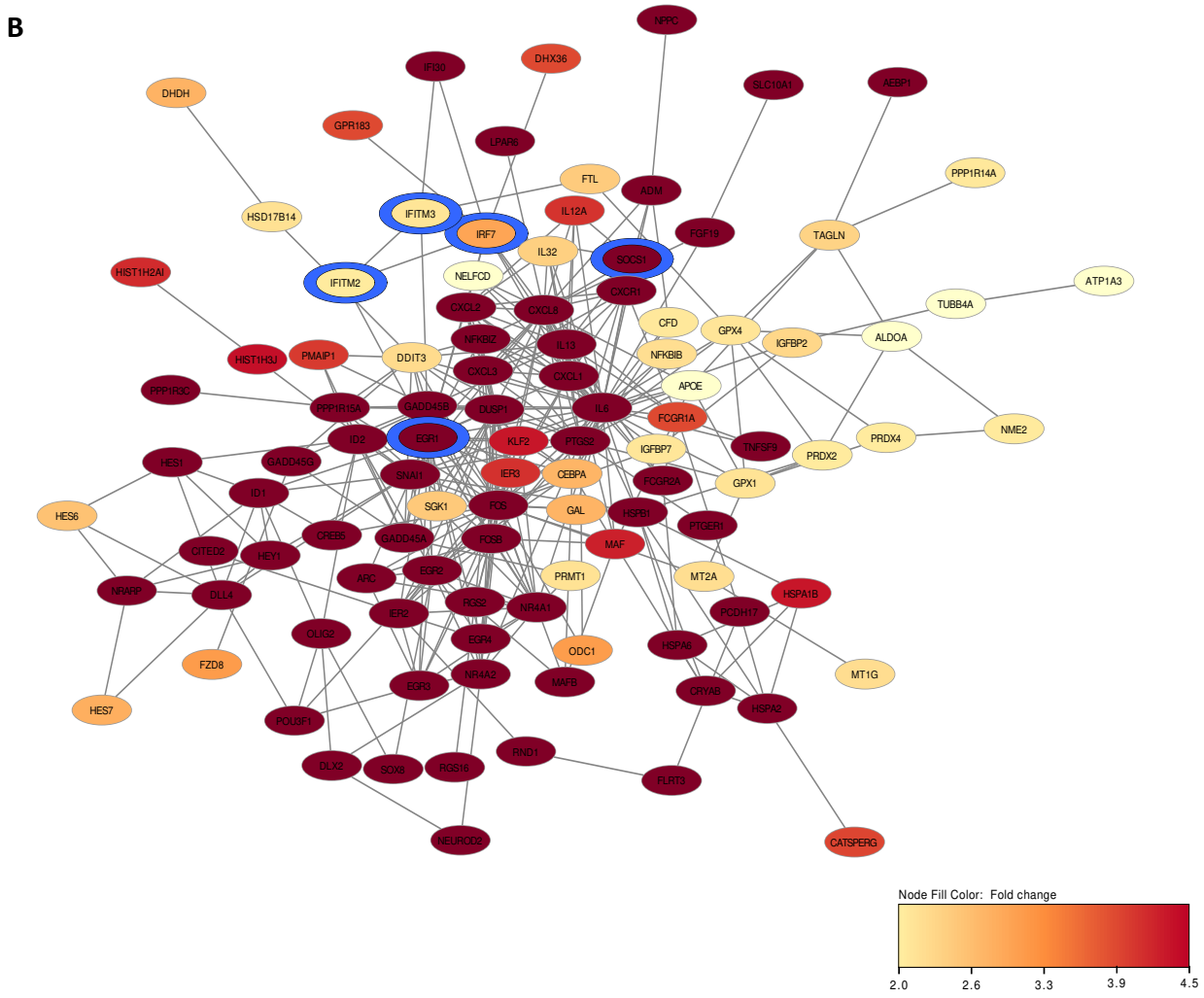

Figure 3.2.2.4: Network analysis of *Af* fixed hyphae infected CF and CF corrected BECs after 12 hours. Network visualisation of significant immunity-associated proteins (padj<0.05 and fold change >2), after 12 hours of fixed hyphae infection in (A) CF corrected BECs and (B) CF BECs. The nodes indicate genes, and the colour represents fold change. Functional enrichment analysis highlights the nodes involved in the type I IFN response (blue), TRAF6 mediated IRF7 activation (red) and JAK-STAT1/2 signalling (green) (Cytoscape, stringApp).

3.2.2.4 – DEG analysis of 24-hour Af fixed hyphae infected CF and CF corrected bronchial epithelial cells

After 24 hours of fixed hyphae exposure, cluster analysis and ANOVA revealed there were 363 differentially expressed ISGs (padj=0.05) between the two cell lines and the infections but that there was a more similar ISG expression pattern after 24 hours of hyphae exposure (Fig3.2.2.5 A) compared to 12 hours (Fig3.2.2.2 A). When compared to their appropriate uninfected controls, CF and CF corrected cells expressed 285 and 275 ISGs respectively. There were 243 ISGs differentially expressed by both cell lines, with only 32 being distinct to the CF corrected cells (Fig3.2.2.5 B). Similarly to the ISG expression at 12 hours post infection, there were more ISGs significantly downregulated than upregulated in both cell lines (Fig 3.2.2.5 C, D).

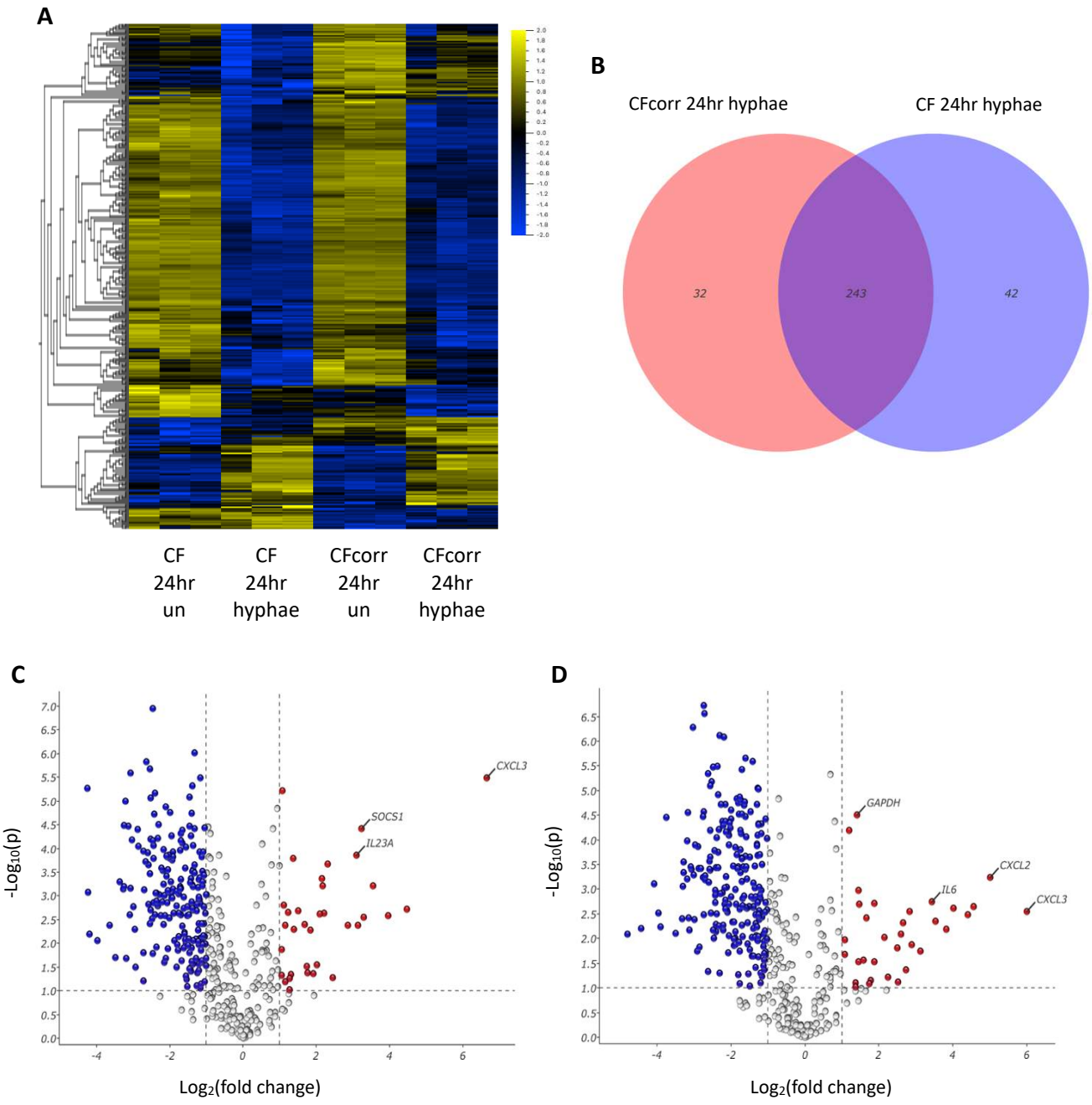

Figure 3.2.2.5: Differentially expressed ISGs in 24 hour fixed hyphae infected CF and CF corrected BECs. CF and CF corrected BECs were infected with *Af* hyphae (MOI=8) for 24 hours, RNA was isolated and sent for bulk RNA sequencing. (A) Heatmap was organised by hierarchical clustering based on mean gene expression and only includes genes from a list of 486 ISGs. Each column represents a sample (n=3), and each row represents a gene (padj<0.05). Significance was calculated using ANOVA and Benjamini-Hochberg test to correct p-value. (B) Venn diagram of differentially expressed ISGs compared to unstimulated control of named condition representing overlap of ISG signature in CF and CF corrected BECs. Volcano plots representing differentially expressed ISGs for (C) CF corrected and (D)

CF cells infected by *Af* hyphae for 24 hours, determined by student's t-test padj<0.05 and fold change >2.

Of the top 25 upregulated ISGs in the two cell lines, there were 18 shared at 24-hour post exposure, compared to just 5 at 12 hours. There were differences in expression patterns between the two cell lines. CF corrected cells showed preference to monocyte recruitment with upregulation of CXCL3 at a fold change of 100.79, compared to 64.55 in CF cells. The CF cells expressed CXCL2 at more than double the strength than the CF corrected cells with fold changes of 32.23 and 11.73 respectively, again highlighting the neutrophil recruitment bias in the CF cell response. IRF7 is upregulated by both cell lines and is a key transcriptional regulator of second phase IFNβ and IFNα genes and can induce further expression of type I ISGs. At 12 hours post infection, the TRAF6 mediated IRF7 activation was downregulated in the CF cells, suggesting the IRF7 expression in the CF cells could be activated by TRIF, MyD88 or IRAK1/4 signalling cascades. As IRF7 is essential to the second wave of type I IFN expression, this could suggest the defect in the CF IFN response results in a delayed reaction by the cells.

Table 3.2.2.2: The top 25 upregulated and top 25 downregulated ISGs in CF and CF corrected BECs after fixed hyphae infection for 24 hours. Overlapping genes are highlighted in yellow, upregulated genes are in red cells and downregulated in blue (padj<0.05; fold change >2).

CF corrected BECs			CF BECs		
Gene Symbol	P(adj)	Fold Change	Gene Symbol	P(adj)	Fold Change
CXCL3	0.001	100.79	CXCL3	0.008	64.55
PTGS2	0.006	22.33	CXCL2	0.003	32.23
CXCL8	0.007	15.56	CXCL8	0.007	23.75
CXCL2	0.003	11.73	ANGPTL4	0.009	21.27
CSF2	0.008	9.80	DUSP1	0.007	16.32
SOCS1	0.001	9.43	PTGS2	0.015	14.10
NFKBIZ	0.011	8.74	NFKBIZ	0.011	11.56
IL23A	0.001	8.55	IL6	0.006	10.76
PMAIP1	0.011	7.26	CREB5	0.033	8.68
IL6	0.002	4.98	CSF2	0.025	7.42
IL1A	0.007	4.64	IL23A	0.008	7.17
TAGAP	0.003	4.52	SOCS1	0.012	6.32
DUSP1	0.002	4.43	PMAIP1	0.018	6.06
LINC-PINT	0.007	4.29	IL24	0.029	5.67
HBEGF	0.040	3.77	CCNA1	0.020	4.43
IL24	0.013	3.58	LINC-PINT	0.006	3.69
IRF7	0.011	3.19	STARD5	0.050	3.68
TGM2	0.006	2.84	IRF7	0.010	3.15
SPOCD1	0.012	2.62	PDK4	0.047	2.99
NMB	0.001	2.59	WFDC2	0.006	2.77
WFDC2	0.007	2.33	DUSP2	0.004	2.73
CREB5	0.011	2.21	GAPDH	0.000	2.66
ARL14	0.005	2.16	KRT8	0.001	2.30
GAPDH	0.001	2.11	TGM2	0.021	2.11
ADRB2	0.028	2.08	IL1R2	0.038	2.10
ABCA1	0.001	-19.07	TMEM229B	0.017	-28.04
TRANK1	0.004	-18.90	RTP4	0.014	-21.76
TMEM229B	0.015	-18.29	SLC2A12	0.003	-16.95
RTP4	0.020	-15.75	TLR3	0.008	-15.69
PTAFR	0.011	-12.52	TNFSF10	0.013	-15.02
MUC16	0.038	-11.15	DTX4	0.000	-13.40
APOL6	0.003	-10.27	SPSB1	0.017	-11.32
DTX4	0.003	-9.65	IRF2	0.010	-10.08
TLR2	0.003	-9.56	SAMD9	0.004	-9.89
CEMIP2	0.001	-9.46	GCNT4	0.002	-9.71
SLC2A12	0.001	-9.26	APOL6	0.002	-9.71
IRF2	0.039	-9.10	PTAFR	0.003	-9.16
ANKRD12	0.001	-8.80	B3GNT7	0.001	-9.07
TNFSF10	0.007	-8.49	SAMD8	0.001	-9.01
THEMIS2	0.003	-8.39	THEMIS2	0.010	-8.83
SAMD8	0.001	-8.35	LRRC3	0.015	-8.73
SAMD9	0.001	-8.15	TNFSF15	0.002	-8.47
B3GNT7	0.005	-7.91	SYT12	0.002	-8.39
TLR3	0.012	-7.74	ANKRD12	0.000	-8.19
IFIT1	0.001	-7.36	N4BP1	0.002	-8.04
LRRC3	0.001	-7.23	TBK1	0.010	-8.01
SLFN11	0.001	-6.61	ABCA1	0.001	-7.84
IDO1	0.031	-6.56	TRANK1	0.033	-7.52

3.2.1.5 – Protein-protein interaction network analysis of 24-hour Poly(I:C) stimulated CF and CF corrected bronchial epithelial cells

Functional enrichment of the protein-protein network analysis of the differentially expressed genes at 24 hours post hyphae infection showed that there were 5 and 2 genes related to the type I IFN response in the CF corrected and CF cells respectively. The CF network (Fig3.2.2.6 B) contained one gene related to the TRAF6-mediated IRF7 activation compared to 5 genes in the CF corrected network (Fig3.2.2.6 A), again highlighting the defect in this signalling cascade. Two genes involved in JAK-STAT1/2 signalling we highlighted in the CF corrected network and no evidence of genes related to this signalling pathway in the CF network.

A

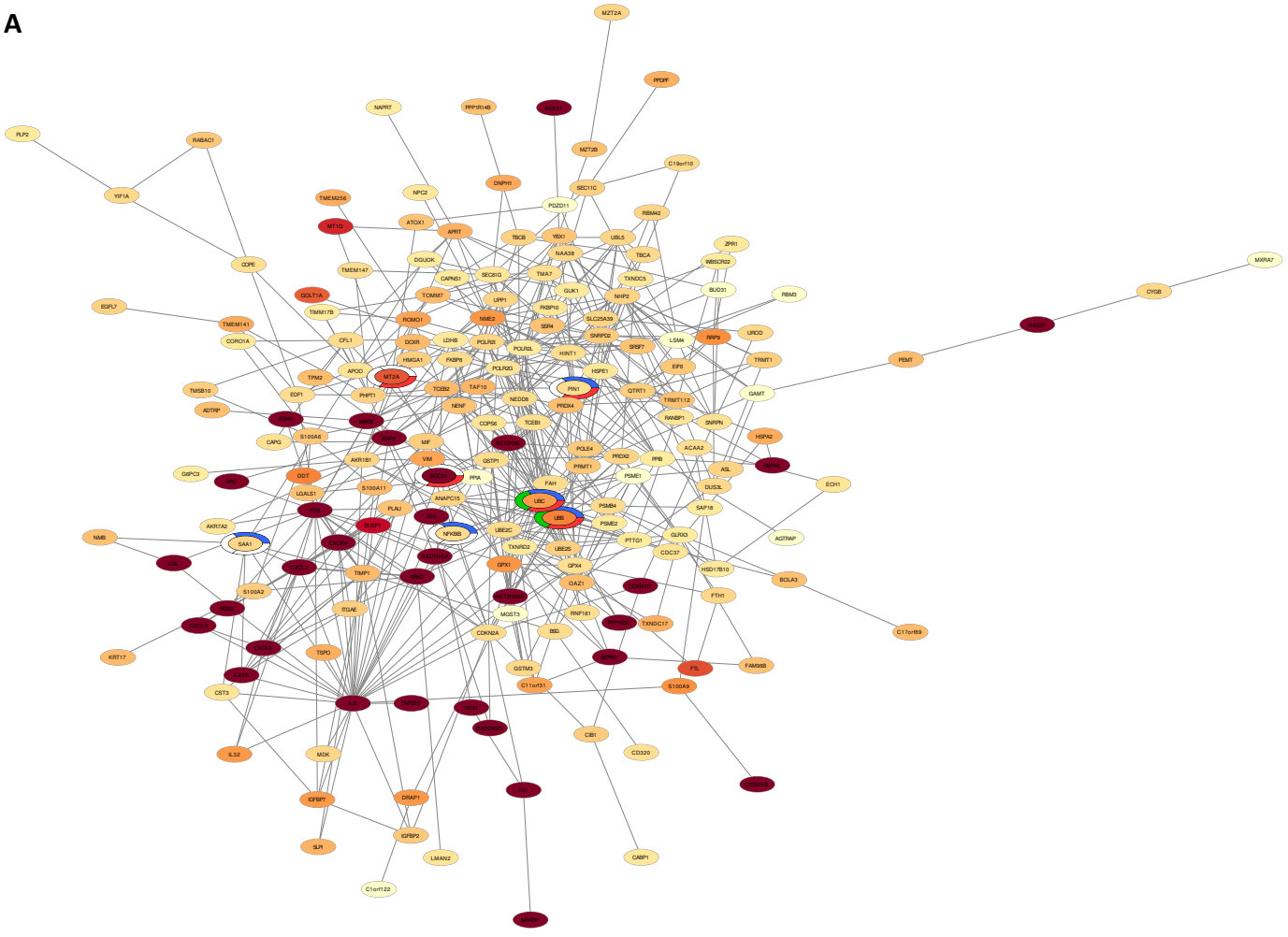

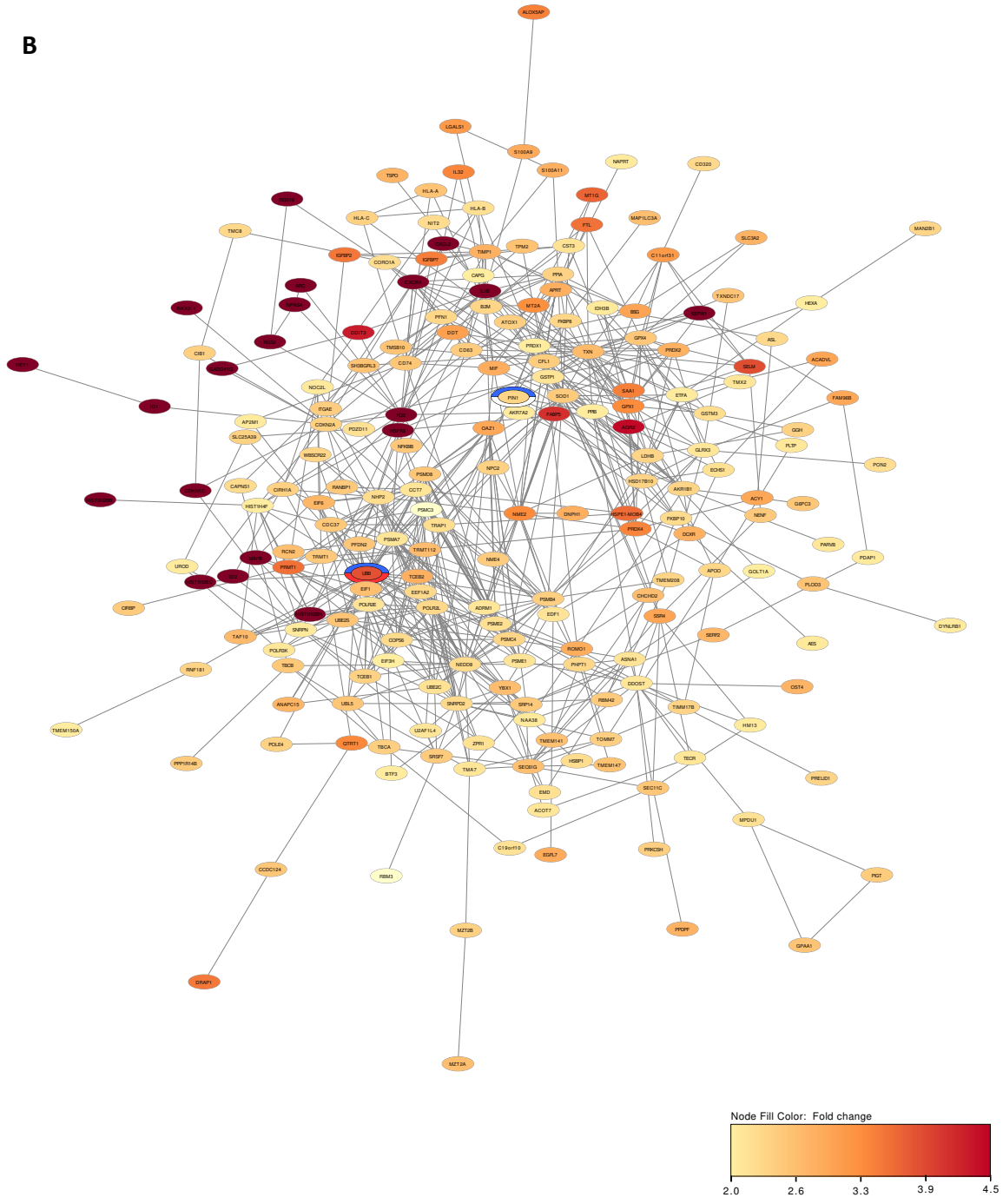

Figure 3.2.2.6: Network analysis of *Af* fixed hyphae infected CF and CF corrected BECs after 24 hours. Network visualisation of significant immunity-associated proteins (padj<0.05 and fold change >2), after 24 hours of fixed hyphae infection in (A) CF corrected BECs and (B) CF BECs. The nodes indicate genes, and the colour represents fold change. Functional enrichment analysis highlights the nodes involved in the type I IFN response (blue), TRAF6 mediated IRF7 activation (red), and JAK-STAT1/2 signalling (green) (Cytoscape, stringApp).

3.2.3 – Transcriptomic characterisation of *Aspergillus fumigatus* heat killed conidia infection in CF and CF corrected bronchial epithelial cells

3.2.3.1 – DEG analysis of 12-hour Af heat killed conidia infected CF and CF corrected bronchial epithelial cells

As type I and III IFN expression was also observed after heat killed conidia infection, RNA isolated from cells infected with heat killed conidia for 12 hours were also sent for bulk RNA sequencing. ANOVA analysis shows 4507 differentially expressed genes between the two cell lines and with infection. Clustering analysis of top 2000 differentially expressed genes in three repeats based on a multigroup comparison shows very distinct gene expression between the two cell lines, and some variation post infection (Fig3.2.3.1). There were 76 ISGs included in this cluster analysis, highlighted in pink on the left-hand panel.

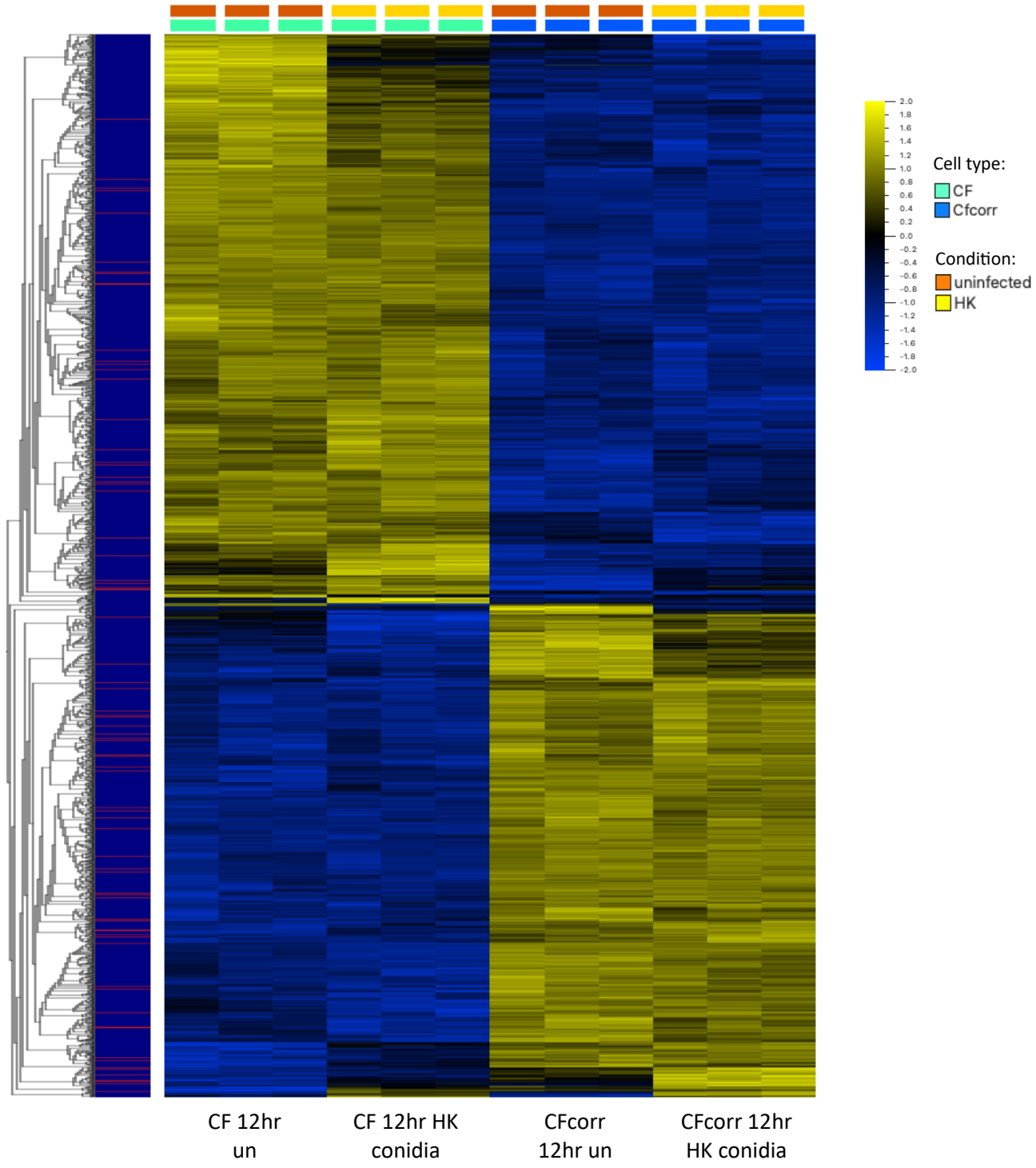

Figure 3.2.3.1: Gene expression heatmap of top 2000 genes differentially expressed after heat killed conidia infection. CF and CF corrected BECs were infected with *Af* heat killed conidia (MOI=8) for 12 hours, RNA was isolated and sent for bulk RNA sequencing. Data were compared to uninfected controls and between the cell lines using ANOVA to test for significance and Benjamini-Hochberg test to correct p-value. Heatmap was organised by hierarchical clustering based on mean gene expression. Each column represents a sample (n=3), and each row represents a gene (padj<0.01). ISGs are highlighted in pink on the left-hand panel.

Again, these differentially expressed genes were cross referenced with the collated list of type I and III ISGs. From Fig3.2.3.2 A it is clear the two cell lines have very different ISG expression patterns, with 285 differentially expressed ISGs revealed by ANOVA analysis. When compared to their individual uninfected controls, student's t-test revealed CF corrected cells differentially expressed 88 ISGs after heat killed conidia infection while CF cells differentially expressed 78. Of the 138 total ISGs expressed between the CF and CF corrected cells post infection, only 28 ISGs were differentially expressed by both with 60 ISGs being distinct for CF corrected cells and 50 for CF cells (Fig3.2.3.2 B). From the volcano plots it is clear to see the CF corrected cells (Fig3.2.3.2 C) upregulated more ISGs than the CF cells (Fig3.2.3.2 D) by a fold change of more than 2.

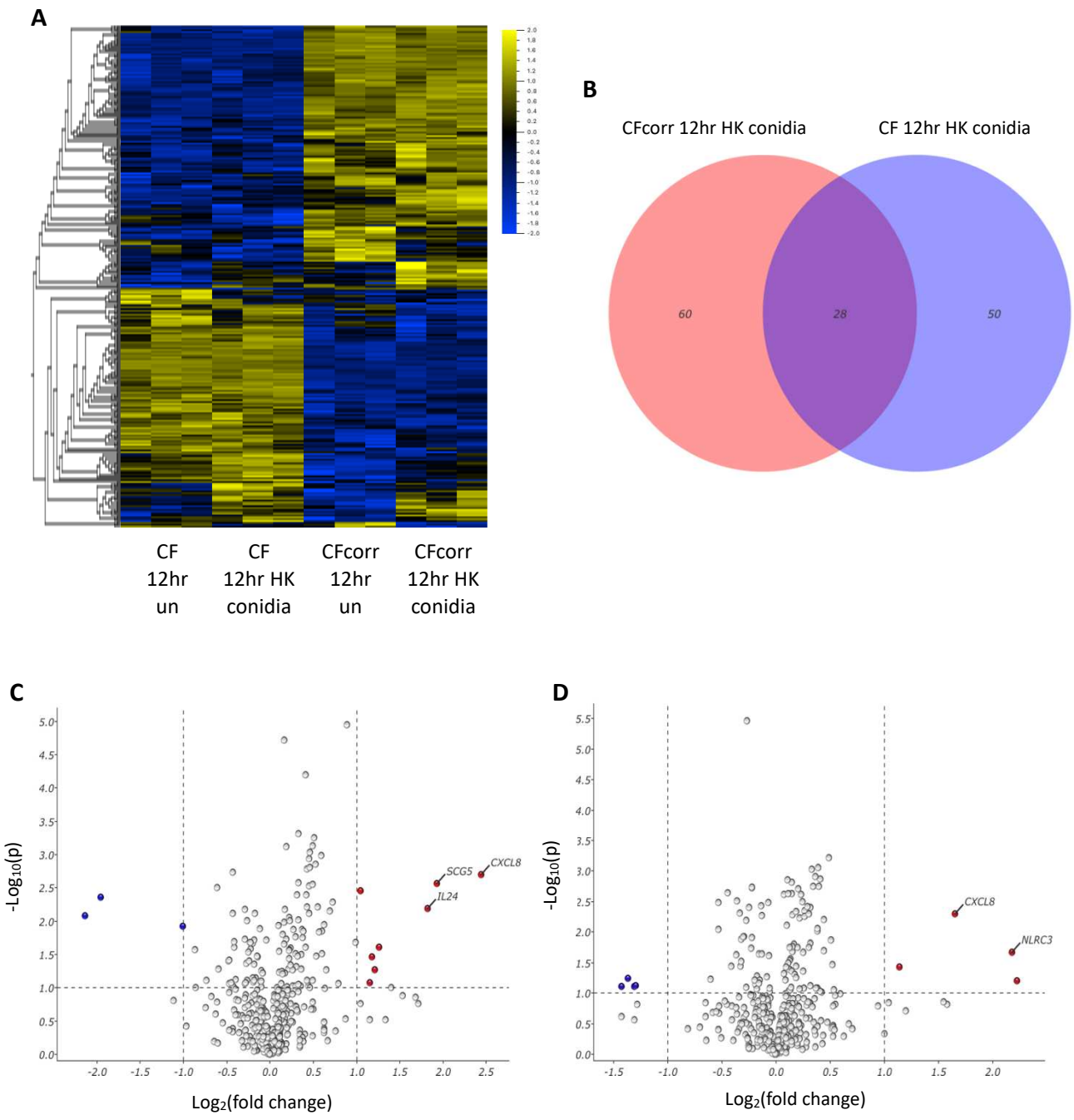

Figure 3.2.3.2: Differentially expressed ISGs of heat killed conidia infected CF and CF corrected BECs after 12 hours. CF and CF corrected BECs were infected with *Af* heat killed conidia (MOI=8) for 12 hours, RNA was isolated and sent for bulk RNA sequencing. (A) Heatmap was organised by hierarchical clustering based on mean gene expression and includes genes from a list of 486 ISGs. Each column represents a sample (n=3), and each row represents a gene (padj<0.05), significance calculated by ANOVA and Benjamini-Hochberg test to correct p-value. (B) Venn diagram of differentially expressed ISGs compared to unstimulated control of named condition representing overlap of ISG signature in CF and CF corrected BECs. Volcano plots representing differentially expressed ISGs for (C) CF corrected

and (D) CF cells infected by *Af* heat killed conidia for 12 hours, determined by student's t-test padj<0.05 and fold change >2.

To assess this in more detail, the significant ISGs that were differentially expressed by more than a fold change of 2, only CXCL8 was expressed by both cell lines (Table3.2.3.1), showing the importance of immune cell recruitment in this response from both cells. Interestingly, the CF cells upregulated NLRC3 by a fold change of 4.51. This gene codes for a protein that interacts directly with and prevents trafficking of STING to prevent STING-dependent activation of the immune response. It is also thought to affect TLR4 activation by the ubiquitination of TRAF6, providing a link to the data observed in previous GSEA showing TRAF6-mediated IRF7 activation defect in the fixed hyphae infected cells. Notably, IFNλ3 is downregulated by the CF cells after heat killed conidia infection, but not by the CF corrected cells.

Table 3.2.3.1: All differentially expressed ISGs in CF and CF corrected BECs after fixed hyphae infection for 24 hours. Overlapping genes are highlighted in yellow, upregulated genes are in red cells and downregulated in blue (padj<0.05; fold change >2).

CF corrected BECs			CF BECs		
Gene Symbol	**P(adj)**	**Fold Change**	**Gene Symbol**	**P(adj)**	**Fold Change**
CXCL8	0.002	5.43	FGF5	0.043	4.67
SCG5	0.003	3.81	NLRC3	0.021	4.51
IL24	0.007	3.54	CXCL8	0.005	3.13
PTGS2	0.025	2.39	SNORD17	0.037	2.20
ANGPTL4	0.049	2.31	IFNL3	0.039	-2.69
CSF2	0.035	2.26	IDO1	0.047	-2.58
MMP3	0.048	2.23	PLD5	0.048	-2.47
KRT34	0.003	2.06	CADPS2	0.046	-2.46
NCALD	0.008	-4.41			
TNFSF10	0.004	-3.89			
SYT12	0.012	-2.01			

3.2.3.2 – GSEA analysis of 12-hour Af heat killed conidia infected CF and CF corrected bronchial epithelial cells

GSEA of the differentially expressed genes in the CF cells infected by heat killed conidia compared to uninfected controls showed enrichment of inflammatory gene sets but no interferon related gene sets (Fig3.2.3.3). Whereas CF corrected cells infected with heat killed conidia showed significant enrichment of 'Hecker IFNb1 Targets' (padj=0.07;NES=1.73) as well as 'Hallmark Inflammatory Response' (padj=0.01;NES=1.67).

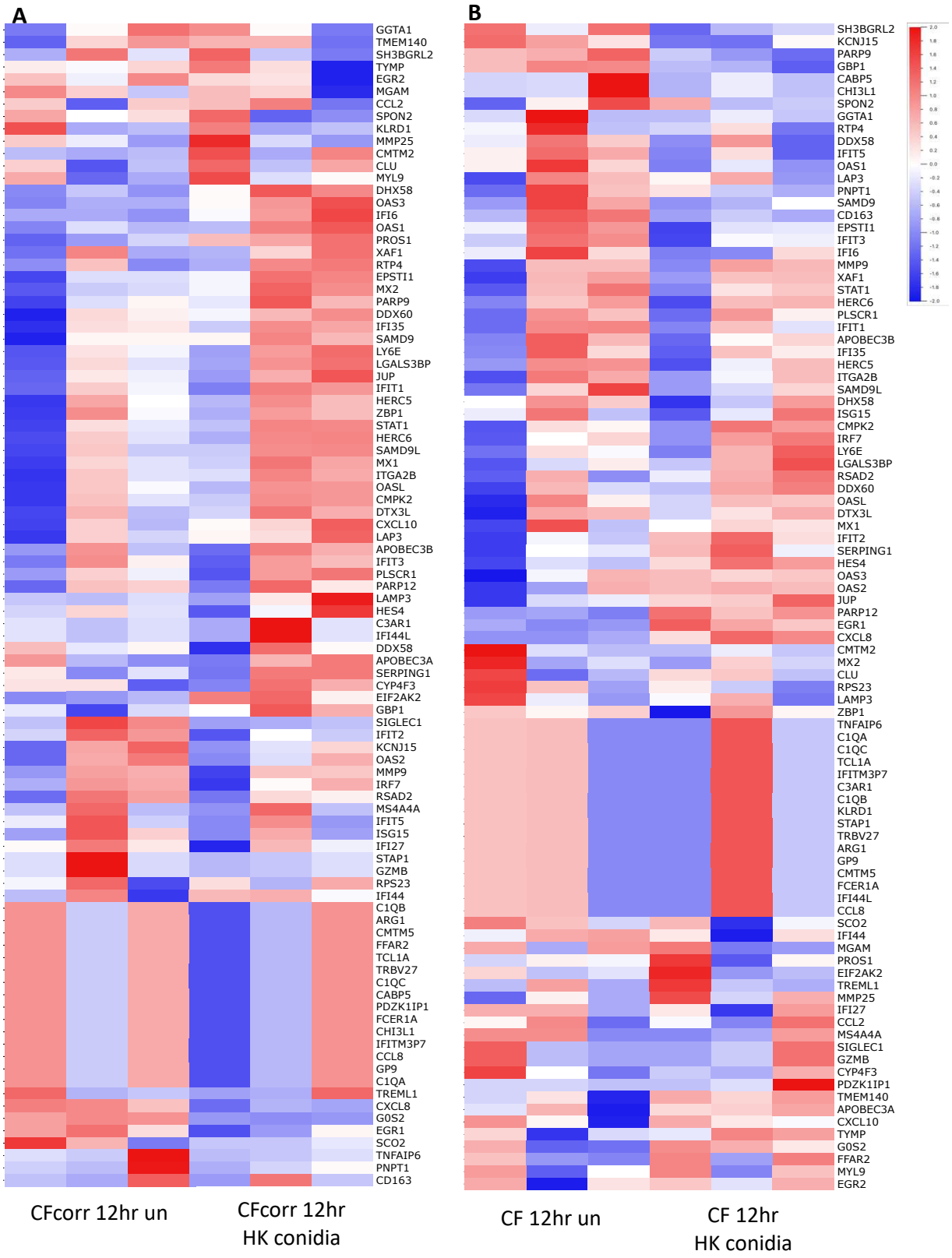

Figure 3.2.3.3: Representative visualisation of GSEA of CF and CF corrected BECs infected with *Af* heat killed conidia for 12 hours. (A) CF corrected BECs infected with *Af* heat killed conidia (MOI=8) for 12 hours showed enrichment of 'Hecker IFNB1 Targets' gene set (padj=0.07). (B) CF cells did not show enrichment of this gene set (padj=0.8). Significance calculated using Student's T-test and Benjamini-Hochberg test to correct p-value. Gene set consists of 96 genes.

3.2.3.3 – Protein-protein interaction network analysis of 12-hour Af heat killed conidia infected CF and CF corrected bronchial epithelial cells

Functional enrichment of the protein-protein network analysis on the upregulated genes expressed by CF and CF corrected BECs after 12 hours of heat killed conidia infection again highlighted the difference in the type I IFN response related genes, with 3 genes out of 16 being related to the interferon response in the CF corrected network and no genes in the CF network falling into this category.

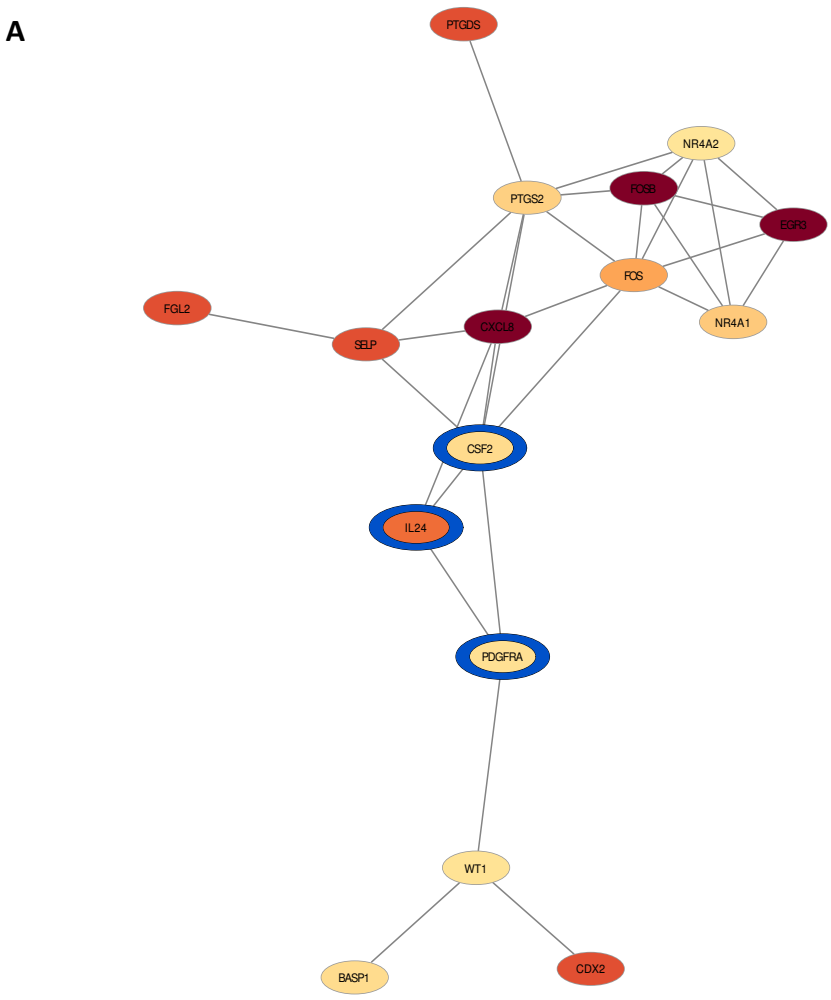

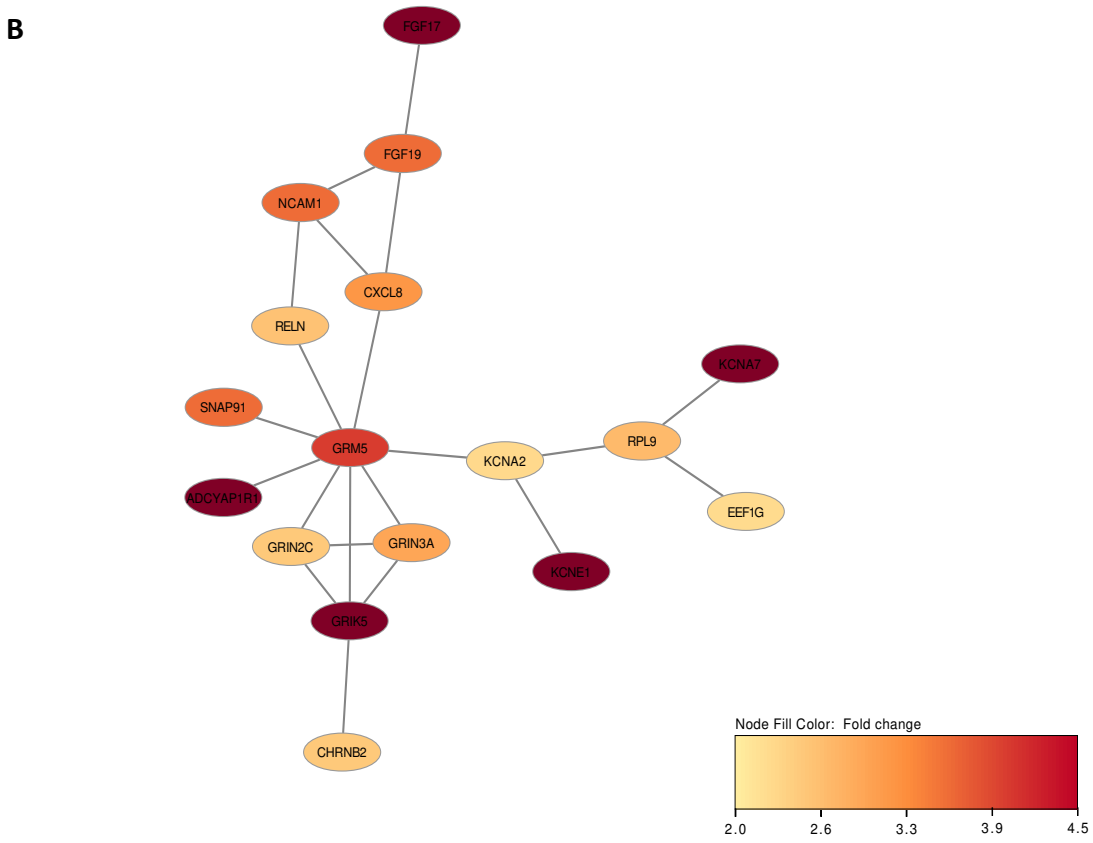

Figure 3.2.3.4: Network analysis of *Af* heat killed conidia infected CF and CF corrected BECs after 12 hours. Network visualisation of significant immunity-associated proteins (padj<0.05 and fold change >2), after 12 hours of heat killed conidia infection in (A) CF corrected BECs and (B) CF BECs. The nodes indicate genes, and the colour represents fold change. Functional enrichment analysis highlights the nodes involved in the type I IFN response (blue) (Cytoscape, stringApp).

3.3 – Confirmation of IFNβ and IFNλ1 response in CF and CF corrected bronchial epithelial cells after *Aspergillus fumigatus* infection

To determine if the defect in the type I and III IFN response observed in the transcriptomics was due to a downregulation in the expression of IFNβ and IFNλ1 in CF cells, as observed in bacterial and viral infections, RT-PCR of infected CF and CF corrected cells was carried out to assess the expression of these genes directly. IFNβ and IFNλ1 expression was significantly increased in CF corrected BECs compared to CF BECs across all time points and stimuli (Fig3.3.1 A and B). Fixed hyphae induced IFNλ1 expression peaked at 3 and 24 hours and IFNβ expression peaked at 24 hours in CF corrected cells. Heat killed conidia induced IFNλ1 expression was consistent across 3 and 12 hours and dropped off at 24 hours, while IFNβ expression peaked at 12 hours. IL-8 was expressed consistently across all stimuli and time points, with CF cells expressing significantly more IL-8 after 12 hours of poly(I:C) stimulation.

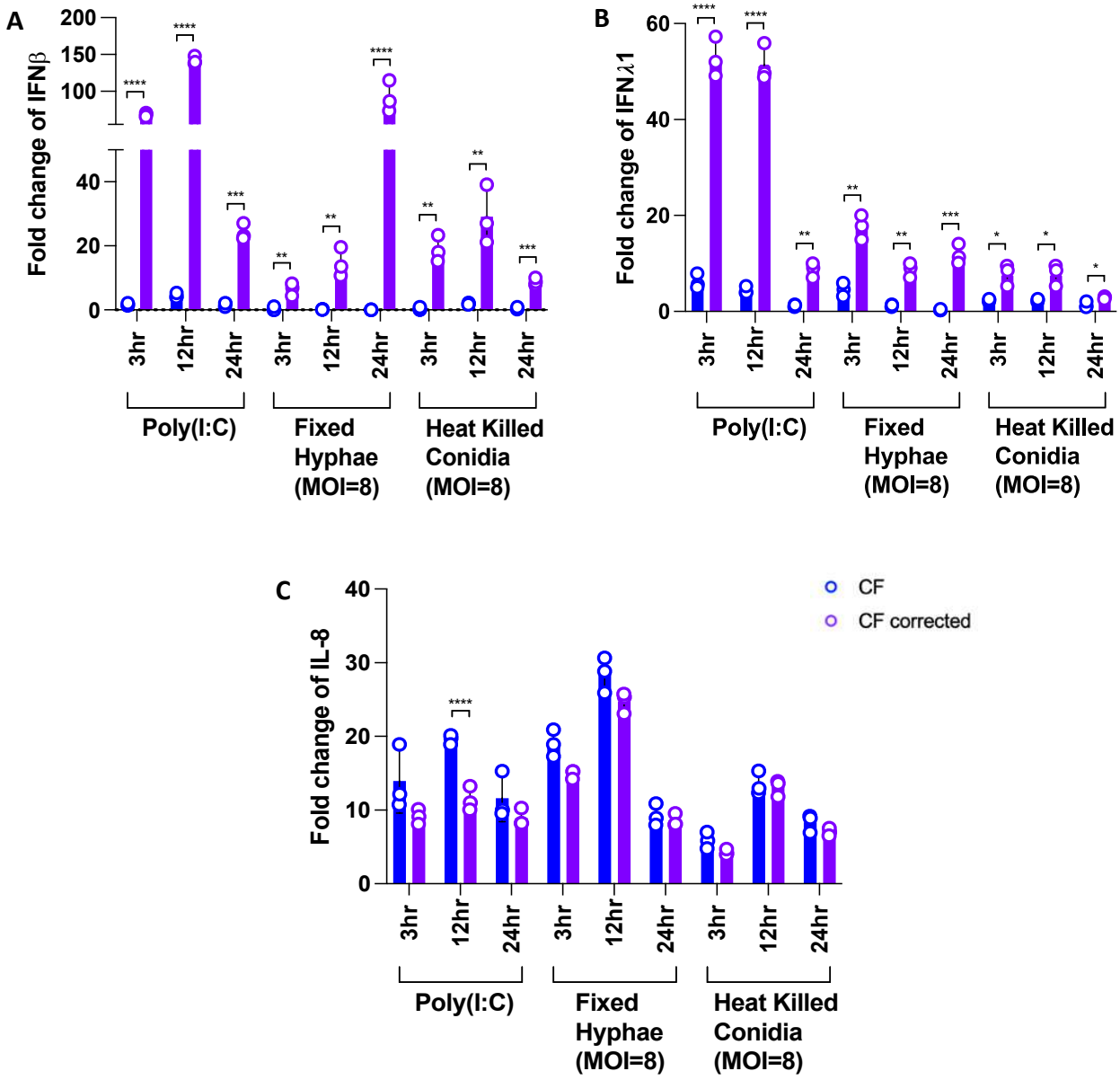

Figure 3.3.1: IFNβ and IFN**λ**1 expression by CF and CF corrected BECs after infection with *Af* fixed hyphae and heat killed conidia. CF and CF corrected BECs were stimulated with poly(I:C) (100ug/ml) and infected with fixed *Af* hyphae (MOI=8) and heat killed *Af* conidia (MOI=8) for 3, 12 and 24 hours. RNA was isolated from washed cells an RT-PCR was carried out to assess expression of (A) IFNβ, (B) IFNλ and (C) IL-8.

As all experiments previously discussed were carried out using one CF cell line and its genetically corrected control, a second CF primary cell line with the F508del mutation was also infected with *Af* to rule out the possibility of a cell line specific defect. This cell line, along with a healthy BEAS-2B cells, were grown to air-liquid interface (ALI), meaning cell cultures consisted of pseudostratified epithelium including mucus producing goblet, ciliated, and basal cells and the formation of tight junctions. The interactions of the differentiated cells make ALI a more accurate model of the CF airway than a monolayer culture.

The CF ALI culture followed a similar IFNβ and IFNλ1 expression pattern to the CF cells grown as a monolayer. Both IFNβ and IFNλ1 expression in the CF cells (Fig3.3.2 B, C) was much lower than that in the healthy cells (Fig3.3.2 A, C) after poly(I:C) stimulus and *Af* fixed hyphae and heat killed conidia infection at both 12 and 24 hours. Fixed hyphae stimulated IFNβ and IFNλ1 expression in BEAS-2Bs, with more expression at 24 hours than 12, whereas poly(I:C) and heat killed conidia infection stimulated more IFNβ and IFNλ1 at 12 hours compared to 24 hours. In the CF cells, there was more IFNβ and IFNλ1 expressed at 12 hours compared to 24 hours in response to both fixed hyphae and heat killed conidia infection but at a much lower level than the healthy cells (fixed hyphae induced IFNβ relative expression was 290 compared to 6 in CF corrected and CF BECs respectively at 24 hours).

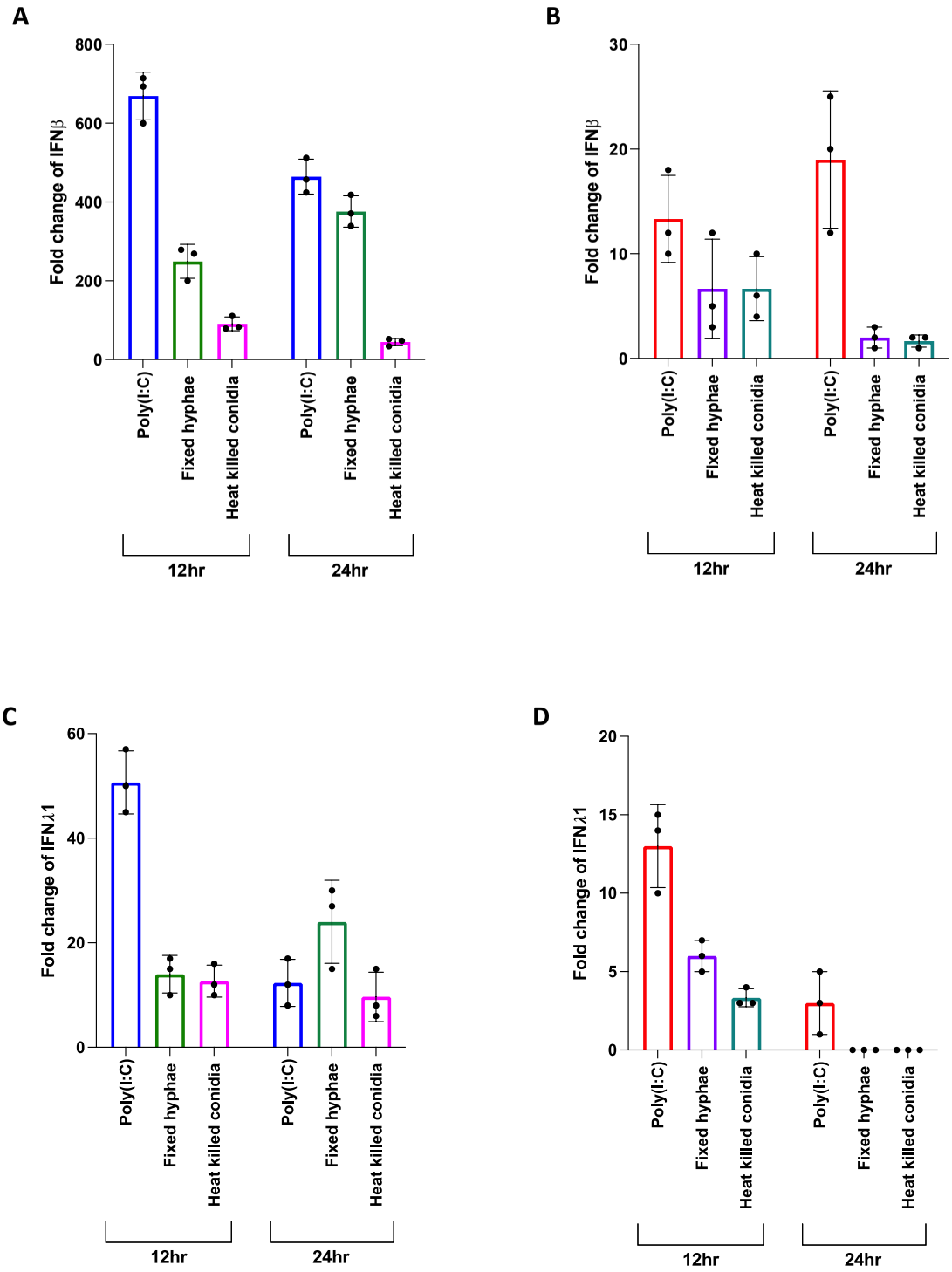
A
Fold change of IFNβ
800
600
400
200
0
Poly(I:C)
Fixed hyphae
Heat killed conidia
Poly(I:C)
Fixed hyphae
Heat killed conidia
12hr
24hr
B
Fold change of IFNβ
30
20
10
0
Poly(I:C)
Fixed hyphae
Heat killed conidia
Poly(I:C)
Fixed hyphae
Heat killed conidia
12hr
24hr
C
Fold change of IFNλ1
60
40
20
0
Poly(I:C)
Fixed hyphae
Heat killed conidia
Poly(I:C)
Fixed hyphae
Heat killed conidia
12hr
24hr
D
Fold change of IFNλ1
20
15
10
5
0
Poly(I:C)
Fixed hyphae
Heat killed conidia
Poly(I:C)
Fixed hyphae
Heat killed conidia
12hr
24hr

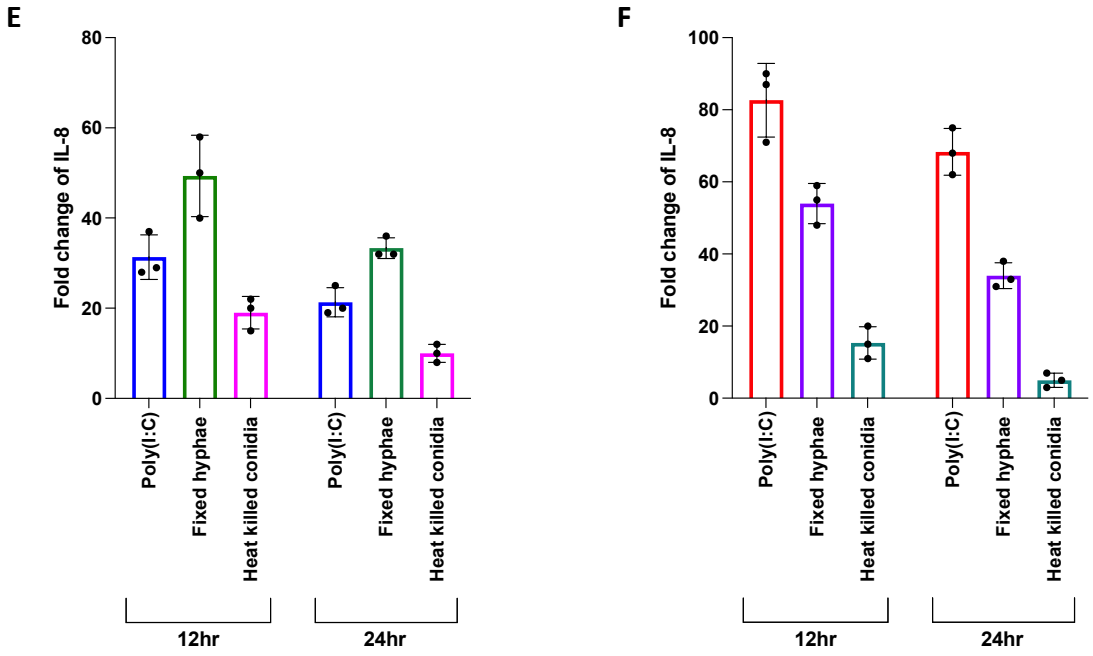

Figure 3.3.2: IFNβ and IFN**λ**1 expression in BEAS-2B cells and a primary CF epithelial cell line at ALI after *Af* fixed hyphae and heat killed conidia infection. Healthy (A, C, E) and CF BECs (B, D, E) were grown to ALI and were stimulated with poly(I:C) (100ug/ml) and infected with fixed *Af* hyphae (MOI=8) and heat killed *Af* conidia (MOI=8) for 12 and 24 hours. RNA was isolated from washed cells and RT-PCR was carried out to assess expression of IFNβ (A, B), IFNλ (C, D), and IL-8 (E, F). Data from three technical repeats.

3.4 – Discussion

In this chapter the data has shown that exposure of healthy control BEAS-2B cells to *Af* heat killed conidia and fixed hyphae upregulates mRNA expression of IFNβ and IL-8 as well as secretion of IFNλ1. 12 hours of poly(I:C) stimulation revealed differential gene expression between CF and CF corrected BECs and distinctive ISG profiles. GSEA of the poly(I:C) stimulated cells showed type I ISG pathways were more prominent in CF corrected cells, whereas type II IFN and pro-inflammatory pathways were more prominent in CF cells. Protein-protein network analysis confirmed upregulation of type I ISGs in CF corrected cells compared to CF cells. After 24 hours of poly(I:C) stimulation there was a greater number of changes in expression of type I and III ISGs in both CF and CF corrected cells and a greater overlap in expression patterns than 12 hours. GSEA 24 hours post poly(I:C) stimulation showed upregulation of type I IFN pathways in CF corrected cells as demonstrated at 12 hours post stimulation. The CF cells generated less of a bias towards the pro-inflammatory gene sets and showed a trend towards an increase in the type I IFN response gene sets. After 12 hours of fixed hyphae infection there were many ISGs differentially expressed with more genes being downregulated, however, the upregulated genes were more strongly upregulated. Important differences in ISGs include downregulation of IFIT1, IFIT3 and IFNλ2 in CF cells compared to all three genes being upregulated in CF corrected cells. CF corrected cells expressed the monocyte chemoattractant, CXCL3, at a higher level than the CF cells, a fold change of 44.45 compared to 19.72 respectively. CF cells expressed the neutrophil chemoattractant CXCL8 at a higher level than CF corrected cells with fold changes of 18.87 and 3.97 respectively, and CXCL2, another powerful neutrophil chemoattractant, was expressed by CF cells at a fold change of 25.55 but not expressed by CF corrected cells. GSEA revealed upregulation of

TRAF6-mediated IRF7 activation, JAK-STAT1/2 signalling and type I ISG related gene sets in CF corrected cells, with none of these gene sets being upregulated in CF cells. Protein to protein interaction network analysis revealed more type I ISGs, TRAF6-mediated IRF7 activation pathway genes and JAK-STAT1/2 signalling genes in the CF corrected network compared to the CF network. At 24 hours post hyphae infection there was more overlap in the ISG signature between the CF and CF corrected cell lines compared to 12 hours. However, in the protein-protein interaction network analysis the type I IFN, TRAF6-mediated IRF7 activation pathway genes and JAK-STAT1/2 signalling genes were more prominent in the CF corrected cells than CF. During heat killed conidia infection at 12 hours there was little overlap of ISGs between the two cell lines compared to hyphae infection and the CF corrected cells expressed more ISGs than CF. Notably, the only overlapping ISG was the neutrophil chemoattractant CXCL8 and the CF cells significantly downregulated IFNλ3 by a fold change of 2.69. There was enrichment of inflammatory gene sets in both cell lines when analysed using GSEA and a trend towards type I IFN gene sets in the CF corrected cell line but not the CF. Again, protein-protein interaction network analysis showed a type I ISG profile in the CF corrected cells but not in the CF cells. RT-PCR confirmation of the downregulated type I and III IFN response observed in the RNA sequencing analysis was completed at both monolayer and ALI in two different CF BEC lines and showed CF BECs expressed significantly less IFNβ and IFNλ than their respective non-CF controls at 3, 12 and 24 hours post poly(I:C) stimulation and *Af* infection in the form of fixed hyphae and heat killed conidia.

Data in this chapter confirms that *Af* infection stimulates a type I and III IFN response and that, in cells with a CFTR mutation, there is a reduction in this response. The reduction in the IFN response in cells with a CFTR mutation was first confirmed using a poly(I:C) stimulus at 12 and

24 hours. At 12 hours post stimulation, there was significantly fewer ISGs significantly expressed in cells with a CFTR mutation and of the 14 that were expressed by the CF cells, only 7 overlapped with the 22 ISGs significantly expressed by the CF corrected cells. Those that overlapped did include some key ISGs such as IFIH1, IFIT1, and IL7R, however, the CF cells did not express OAS1, IFNλ1, and IFNλ3 while the CF corrected cells did. Network and GSEA analysis confirmed these findings, with type I and III IFN related pathways significantly enriched by the CF corrected cells, but not the CF cells. At 24 hours post poly(I:C) stimulation there were 4 more ISGs significantly downregulated by the CF cells compared to the CF corrected cells and the same amount of upregulated ISGs. 31 of the total 48 differentially expressed ISGs in the CF cells were overlapping with the CF corrected cells, suggesting less of a discrepancy of IFN response at 24 hours compared to 12 hours which had an overlap of 7 out of 14. However, again IFNλ1 was upregulated by the CF corrected BECs and not the CF BECs. This was further confirmed by GSEA showing enrichment in two of the type I IFN response pathways by the CF cells. This could suggest that there is a delayed type I IFN response and an aberration of the type III IFN response in cells with a CFTR mutation, however, further work including time course infections would be required to confirm this finding.

To then investigate this in response to *Af* infection the CF and CF corrected BECs were exposed to fixed *Af* hyphae for 12 and 24 hours. *Af* hyphae stimulated a strong ISG response, however, despite this there were more downregulated ISGs than upregulated at both time points. CF cells upregulated 25 ISGs while CF corrected cells upregulated 27 at 12 hours post stimulation, although little difference in the number of ISGs upregulated, CF corrected cells upregulated these genes in a stronger fashion. For example, CXCL3 was upregulated by a fold change of 44.45 in CF corrected cells and 19.72 in CF cells. Of the top 25 upregulated ISGs only 5 genes

were overlapping which were CXCL3, CXCL8, IL6, IL23A and PMAIP1. Several key ISGs were upregulated by CF corrected cells and not CF cells, such as ISG15, IFIH1, and IFIT2. Furthermore, IFNλ2 was significantly downregulated by a fold change of 4.92 in CF cells. The reduction in activation of the IFN response in CF cells compared to CF corrected was further confirmed with GSEA which revealed CF corrected cells showed upregulation of 3 IFN related gene sets as well as the TRAF6 mediated IRF7 activation gene set involving 30 genes. The CF cells, however, showed downregulation of Hecker IFNB1 targets and TRAF6 mediated IRF7 activation gene sets. This highlights a potential pathway that is dysregulated in cells with a CFTR mutation and was also observed in network analysis of all the upregulated genes after infection. Similarly to poly(I:C) stimulation, the CF IFN response at 24 hours more closely mirrored that of the CF corrected cells, providing further information to suggest a delayed response rather than dysfunctional. Functional enrichment of the network analysis at 24 hours did reveal a discrepancy in the TRAF6 mediated IRF7 activation between the CF and CF corrected cells with 5 genes in the CF corrected network and only 1 in the CF network. Despite the IFN response at 24 hours to both poly(I:C) and *Af* fixed hyphae still containing some differences between the two cell lines, there was a pattern towards the CF cells have a more similar ISG signature with the CF corrected cells and more of a discrepancy at 12 hours than 24 hours. The relevance of timing and strength of the IFN response in pathogen protection has been highlighted in the recent SARS-CoV-2 pandemic in which impaired IFN production related to poor viral clearance and overexpression of type I IFN contributed to the cytokine storm observed in severe cases[336, 343]. Mouse models have shown type I IFN treatment to be effective at early stages of infection, but treatments at later-stage infection exacerbated the immune response and resulted in poor outcomes[335]. Furthermore, some clinical studies have

shown the importance of timing of exogenous type I and III IFN treatment in the clinical outcomes of COVID-19 patients[335, 337].

CF and CF corrected cells were also infected with *Af* heat killed conidia for 12 hours to assess the response to different forms of *Af* morphology. The heat killed conidia stimulated less of an IFN response than both poly(I:C) and *Af* fixed hyphae. When the resting conidia is heat killed at 90°C the hydrophobic rodA layer and the cell wall is disrupted, allowing exposure of the fungal cell wall components and DNA. *Af* hyphae has no protective RodA layer and a distinct cell wall composition to swollen conidia, therefore, it reveals many other fungal cell wall components such as glycans and lipids, giving rise to different IFN responses between the heat killed conidia and fixed hyphae infections[98, 132]. Interestingly, of the differentially expressed ISGs after heat killed conidia infection, only one gene overlapped between the two cell lines. CXCL8 was the overlapping gene, upregulated by a fold change of 5.43 in CF corrected cells and 3.13 in CF cells. CXCL8 is heavily involved in neutrophil activation and chemotaxis which have been discussed as important effector cells in the clearance of fungal infection[350]. Interestingly, IFNλ3 was significantly downregulated by a fold change of 2.69 in CF cells in response to heat killed conidia and, with a downregulation of IFNλ2 in response to fixed hyphae, this provides evidence of a downregulated type III IFN response in CF cells during fungal infection. NLRC3 was upregulated by the CF cells by a fold change of 4.51 after heat killed conidia infection which has been defined as a negative regulator of the immune response, including downregulating IFN signalling. NLRC3 is a member of the NLR family, first discovered in 2005 it is found only in the cytoplasm of cells both in the presence and absence of infection[351]. When overexpressed, NLRC3 can interact with TRAF6 to both inhibit its activation and promote its degradation through the proteasome, possibly determining a

mechanism by which the TRAF6 mediated IRF7 activation is downregulated in CF cells[352]. Furthermore, NLRC3 has been shown to directly interact with both STING and TBK1, preventing STING/TBK1 dimerization and signalling, as well as blocking the trafficking and translocation of STING to the nucleus, which is essential or activating the production of type I and III IFN[353]. In the presence of overexpressed NLRC3, both STING and TLR9 have been shown to reduce activation of the IFN response and instead over activate the NF-κB response, which can amplify the inflammatory response both during and after infection, leading to exacerbation of chronic inflammation which is already observed in CF. This gene was not upregulated in CF corrected cells[354, 355]. Work concerning this protein will be further discussed in the final discussion chapter (Chapter 7).

Multiple studies have shown a downregulated or delayed type I IFN response in cells with a CFTR mutation in response to viral and bacterial infections. As discussed in section 1.1.2, cells with a CFTR mutation have shown both lower expression of IFNs, their related ISGs, and PRRs related to their signalling such as TLR3, RIG-I, and MDA5 in response to rhinovirus and poly(I:C)[31]. *P.a.* infected CF BECs also showed reduced IFNβ expression, and in rhinovirus and *P.a.* co-infection both the type I and III IFN response was shown to be even lower[39]. In 2018, the first paper was published highlighting the importance of both the type I and III IFN response in *Af* infection (Section 1.2.4.2), and further work on this has highlighted MDA5/MAVs signalling to be key in this response[163, 174]. Despite the growing evidence importance of the type I and III IFN in fungal infection and the dysfunction of this response in CF, this is the first piece of work to show there is a downregulated or delayed type I and III IFN response to *Af* in cells with a CFTR mutation.

The downregulation of the type I and III IFN response in the CF BECs was confirmed using both monolayer and ALI cultures and RT-PCR of IFNβ and IFNλ1. Due to time restraints, only one experiment using the ALI culture was completed so despite technical repeats, there was only one experimental repeat. Another casualty of the time constraint was the lack of barrier integrity measurements for the ALI and inability to confirm the differentiation of the ALI with anything other than a visual aid. Other limitations of this work include being unable to use live fungal stimulus. As described in section 1.2.1, *Af* transitions through multiple morphologies during its life cycle, and due to BECs alone being unable to effectively control *Af* infection, heat killed or fixed fungus had to be used[98]. Optimisation assays revealed that heat killed conidia and fixed hyphae initiated the largest IFN response and provides two different morphological forms of *Af* to mirror the natural progression of invasive infection. To address this in the future, an ALI BEC/neutrophil co-culture could be used alongside live fungal infection at an MOI of 0.1-0.5 as this would be better controlled. Although heat killed conidia provided a strong IFN response in the healthy cells during optimisation, there was less of a response observed in the CF corrected and CF BECs. If repeating this experiment, a higher MOI would be used to provide more of a response and allow for more differentially expressed genes and larger networks. Furthermore, when completing network analysis, filtering was required to reduce the size of the networks and focus the analysis on the immune response. To do this, all ribosomal genes were removed, alongside genes related to protein translation and cell growth. Although some of these genes could be involved in the immune system, it was decided to remove them for the purpose of this study. Similarly to this, the STRING database was used for functional enrichment analysis on the networks, however, this function is limited to known pathways and gene sets and did not include a gene set for type III IFNs so providing a limitation on this work. As there was evidence suggesting a delayed IFN response rather than a dysregulated

one in both fixed hyphae and poly(I:C) infection and stimulation, time course infection studies should be carried out to confirm this. Finally, more extensive protein work should be carried out to confirm some of the findings, for example, the assessment of other type I and III IFNs such as IFNα and IFNλ2/3, as well as other signalling associated genes such as NLRC3, TRAF6, IRF7, cGAS, JAK and STAT1/2.

In conclusion, this chapter shows evidence for a reduced type I IFN response at 12 hours post infection and stimulation, and a more similar type I ISG signature at 24 hours as well as a downregulated type III IFN response at both time points in CF BECs compared to CF corrected BECs during *Af* infection. This provides the foundation for the possibility of type I and III IFN to be used as an immunotherapeutic agent during fungal infection in CF and shows evidence suggesting NLRC3 overexpression and TRAF6 mediated IRF7 activation are possible mechanisms for this dysfunction.

Chapter 4: Effect of CFTR modulator combination therapy on the cystic fibrosis bronchial epithelial cell immune response to *Aspergillus fumigatus*

4.1 – Optimisation of CFTR modulator combination therapy in CF bronchial epithelial cells

17 years since the discovery of the first CFTR modulator, ivacaftor (VX-770), and 4 years since their introduction onto the NHS, CFTR modulators have had a profound impact on the clinical treatment and presentation of CF. Phase 3 trials of Kaftrio, the commercial name for elexacaftor/tezacfator/ivacaftor combination therapy, showed a 14.3% increase in FEV, a measure of lung function, and a 63% reduction in the rates of pulmonary exacerbations requiring hospitalisation and intravenous antibiotics[356]. While their effect on the chloride and bicarbonate channel is well documented, how these small molecule correctors influence the CF immune system is yet to be reported (discussed in section 1.1.4). Therefore, the impact of CFTR modulator combination therapy on the CF type I and III response to *Af* was investigated. Due to the CFTR dependent type I and III IFN defect identified in the previous chapter, it was hypothesised that CFTR modulator combination therapy would positively impact type I and III IFN response in CF BECs after *Af* infection. This hypothesis was assessed through establishment of a BEC *Af* infection model with addition of CFTR modulators, RNA sequencing analysis of this infection and treatment model, and confirmation of RNA sequencing findings.

Little data has been published regarding the cellular and plasma concentrations of CFTR modulators in patients receiving treatment. The limited data available reports huge variation between patients, sample type, and modulator type with cellular concentrations ranging from

0.01ng/ml to 1.65x10^{5}ng/ml[356-358]. Clinically, for ivacaftor monotherapy the goal plasma concentration to maintain is 250ng/ml[357]. Due to the variation of cellular and plasma concentrations reported on CFTR modulators during active treatment, concentration optimisation was carried out to determine the concentration the CF modulators that could be used to treat CF BECs without causing cytotoxicity or an inflammatory response. CF cells were treated with a range of concentrations of a combination of CFTR modulators, including tezacaftor, ivacaftor and elexacaftor at a 1:1:1 ratio. LDH results show that cytotoxicity begins to increase from 5ng/ml and continues to increase up to 80% at 20ng/ml. TNFα ELISA data also shows there is TNFα production from 5ng/ml and this increases as CFTR modulator concentration increases. Therefore, it was determined that a concentration of 0.33ng/ml of each individual CFTR modulator would be used, with a combined concentration of 1ng/ml.

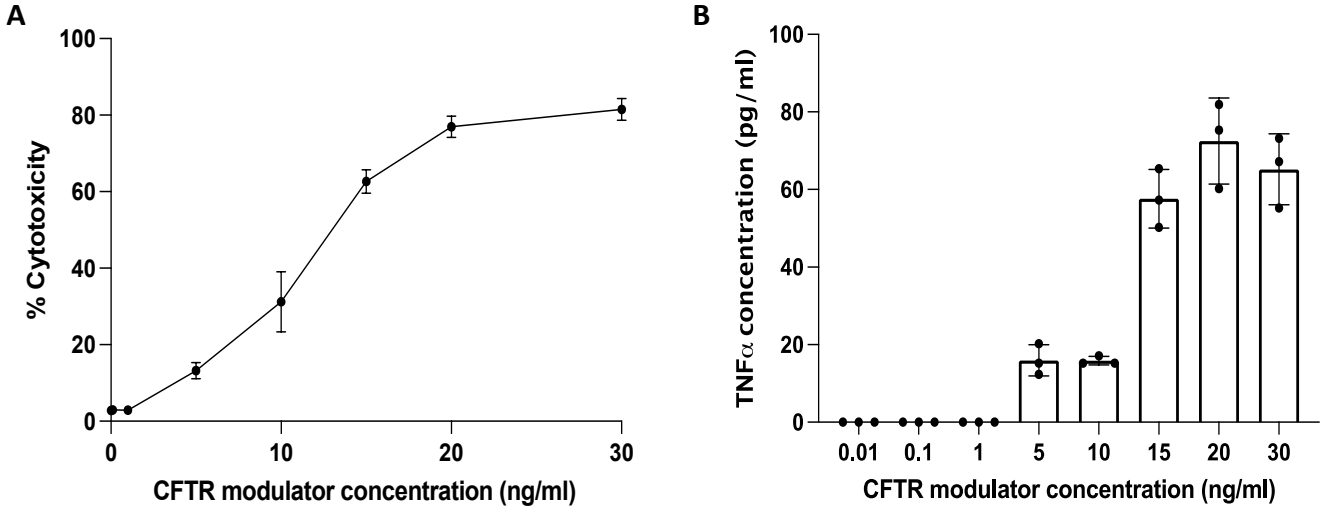

Figure 4.1.1: Cytotoxicity and proinflammatory cytokine release in CF bronchial epithelial cells after CFTR combination therapy. CF BECs were treated with a range of CFTR modulator combination therapy, including ivacaftor, tezacaftor and elexacaftor at a 1:1:1 ratio for 24 hours. (A) Cytotoxicity of this treatment was assessed using a LDH assay and (B) TNFα release was assessed by ELISA. Data shown is from three technical replicates (n=1) as this is a confirmation of previous work from Louis Thewitt, a technician in the lab.

4.2 – Transcriptomic characterisation of the effects of CFTR modulator combination therapy on bronchial epithelial cells

4.2.1 – Transcriptomic characterisation of the effect of CFTR modulator combination treatment on CF bronchial epithelial cells

To begin the investigation on the effect of the CFTR modulator treatment on the CF BECs, the effect of the modulators without *Af* infection was assessed. All CF cells were treated twice with CFTR modulators at a combined concentration of 1ng/ml, once for 24 hours, and a second treatment for a further 12 hours. The double treatment was carried out because stimulated or infected cells were pre-treated with modulator therapy 24 hours prior to and at the time of stimulation/infection and, therefore, the control cells with just modulator treatment required the same double treatment. RNA was isolated and sent for bulk RNA sequencing. Between untreated CF BECs and the modulator treated CF BECs there were 1192 differentially expressed genes (padj=0.01). Due to fewer differentially expressed genes than previous comparisons, Fig4.2.1.1 summaries the top 1000 differentially expressed genes after CFTR modulator treatment for 36 hours including all 29 ISGs from the curated list, highlighted in pink in the panel to the left. It is clear from the heatmap that the treatment significantly alters the gene signature of the CF cells, with several ISGs effected.

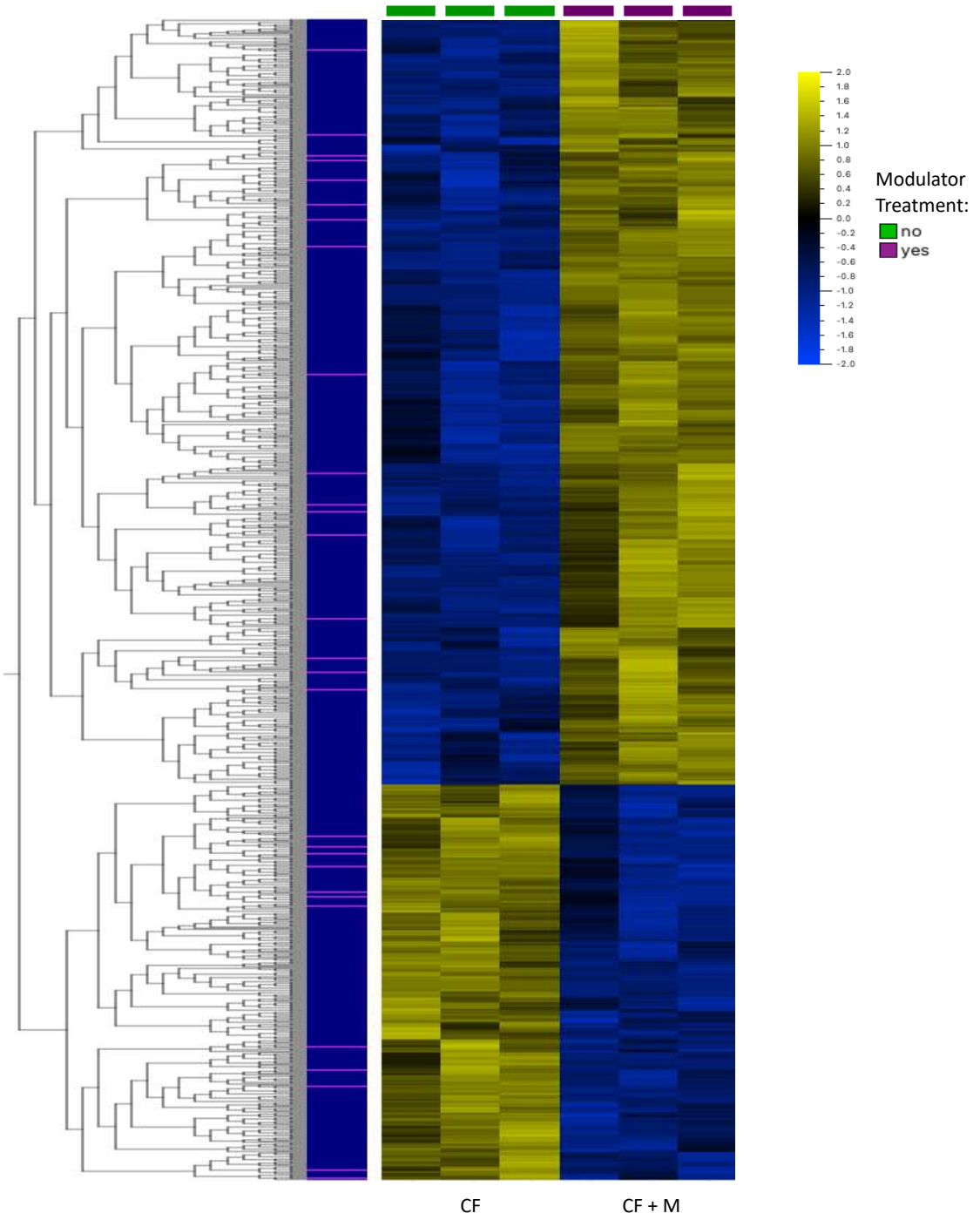

Figure 4.2.1.1: Gene expression heatmap of top 1000 genes differentially expressed after 36 hours of CFTR modulator combination therapy. CF BECs were treated with 1ng/ml of tezacaftor/ivacaftor/elexacaftor combination therapy for 36 hours and RNA isolated and sent for bulk RNA sequencing. Data were compared with unstimulated and untreated CF BECs cultured for 36 hours and significance was calculated using a student's T-test. Heatmap was organised by hierarchical clustering based on mean gene expression. Each column represents a sample (n=3), and each row represents a gene (padj<0.01). ISGs are highlighted in pink on the left-hand panel.

To further assess the effect of the modulators directly on the ISG response, the differentially expressed genes were again cross referenced with the list of ISGs created using the Molecular Signatures Database explained in the methods (section 2.2.3.5). There were 93 significant differentially expressed ISGs (padj=0.05) from the list of 486 and Fig4.1.1.2 A shows the overall ISG expression 36 hours post modulator treatment, revealing a polar shift in the gene signature. To create a two-step filtration on the differentially expressed genes, the volcano plot shows the significantly differentially expressed genes that are upregulated or downregulated by a fold change >2. The volcano plot in Fig4.1.1.2 B shows that modulator treatment results in direct upregulation of IFNλ3 and IL24, the latter of which has direct effect on STAT1 and STAT3 signalling and control of cell survival and proliferation. Interestingly, there is direct downregulation of NLRC3 (Table4.2.1.1), a gene referred to in the previous chapter as being able to have direct effect on the ubiquitination of TRAF6 and STING trafficking and was upregulated by CF cells post *Af* infection.

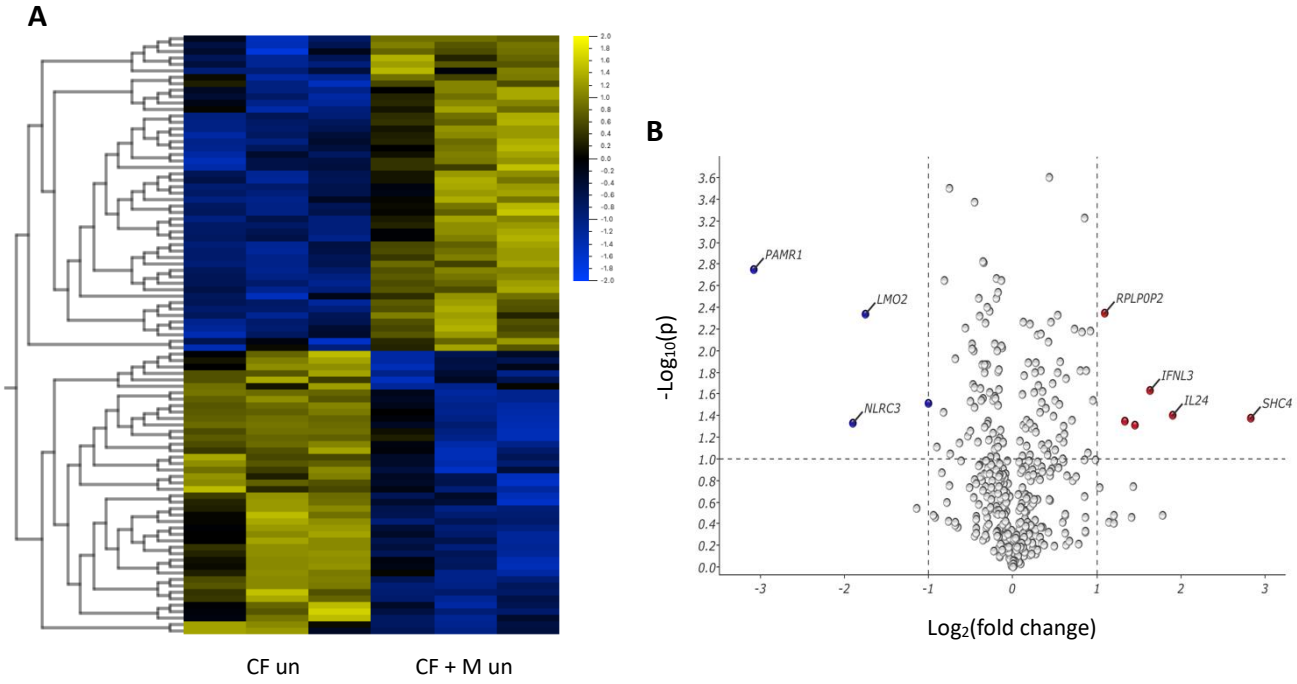

Figure 4.2.1.2: Differentially expressed ISGs of poly(I:C) stimulated CF and CF corrected BECs after 12 hours. CF BECs were treated with combination modulator treatment consisting of 1ng/ml of tezacaftor/ivacaftor/elexacaftor (1:1:1 ratio) for 36 hours. RNA was isolated and sent for bulk RNA sequencing. (A) Heatmap was organised by hierarchical clustering based on mean gene expressed and includes only significantly differentially expressed genes from a curated list of 486 ISGs using ANOVA. Each column represents a sample (n=3), and each row represents a gene. (B) Volcano plot representing differentially expressed genes from the same list of 486 ISGs, determined using a student's t-test (padj<0.05) and fold-change >2, represented as Log_2(fold change).

Table 4.2.1.1: Differentially expressed ISGs in CF BECs after CFTR modulator combination therapy for 36 hours. Upregulated genes are in red cells and downregulated in blue (padj<0.05; fold change >2).

CF BECs		
Gene Symbol	**Padj**	**Fold Change**
SHC4	0.042	7.13
IL24	0.039	3.75
IFNL3	0.023	3.11
IDO1	0.049	2.74
TRIML2	0.045	2.51
RPLP0P2	0.005	2.14
PAMR1	0.002	-8.47
NLRC3	0.047	-3.73
LMO2	0.005	-3.38
SYT12	0.031	-2.00

4.2.2 – Transcriptomic characterisation of the effect of CFTR modulator combination treatment on the response to Poly(I:C) in CF bronchial epithelial cells

4.2.2.1 – DEG analysis of the effect of CFTR modulator treatment on 12-hour Poly(I:C) stimulated CF and CF corrected bronchial epithelial cells

To assess the effect of the modulator treatment on the CF immune response, CF cells were treated with modulators for 24 hours and subsequently stimulated with poly(I:C) for 12 hours. ANOVA analysis revealed 2332 differentially expressed genes (padj=0.01). Clustering analysis of the top 2000 differentially expressed genes reveals the significant impact the CFTR modulators have on the CF BEC gene signature post poly(I:C) stimulation. Of the 2000 differentially expressed genes, there are 95 ISGs included in this expression panel, with many clustered around areas of differing expression.

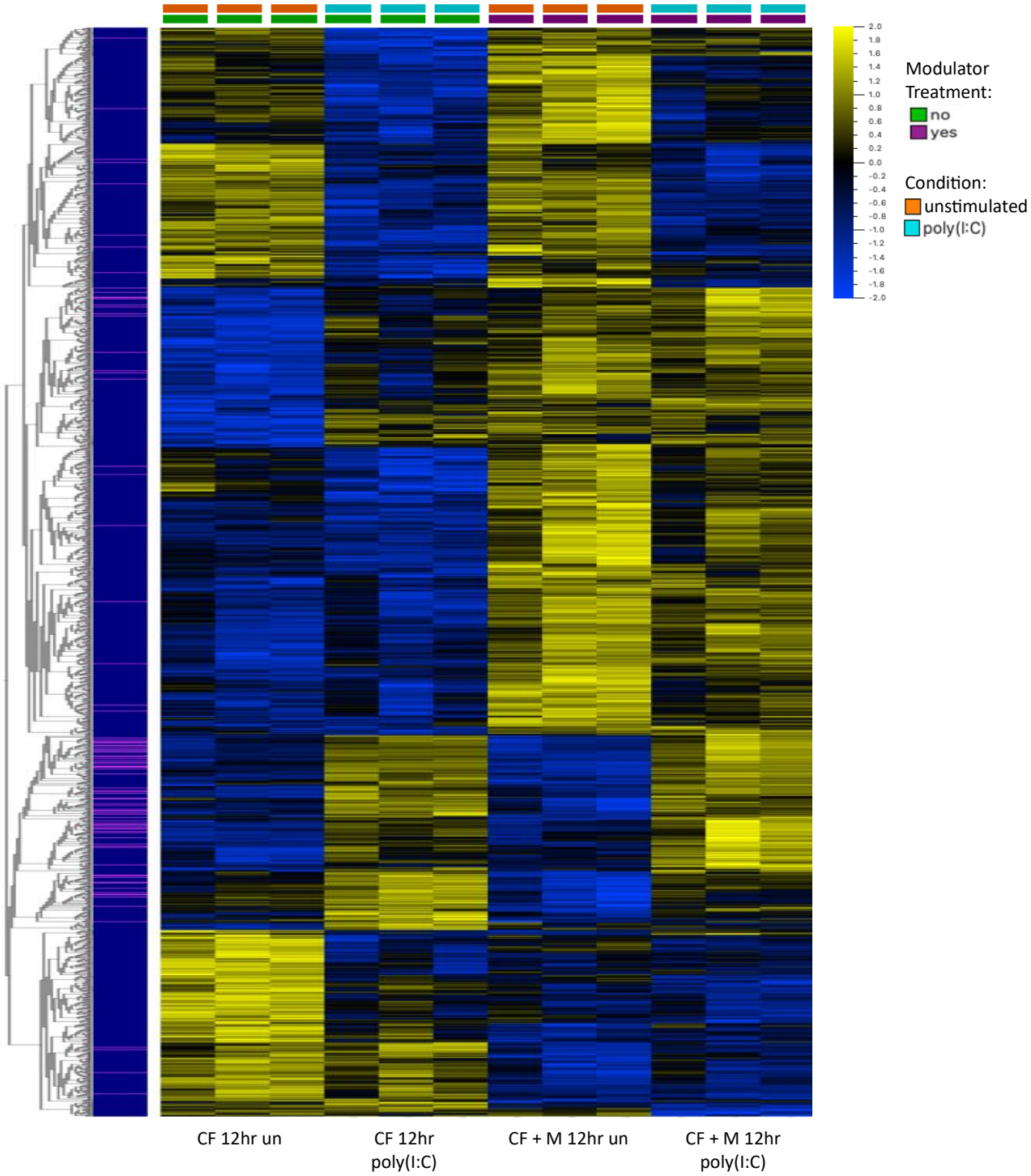

Figure 4.2.2.1: Gene expression heatmap of top 2000 genes differentially expressed after CFTR modulator treatment and poly(I:C) stimulation for 12 hours. CF BECs were treated with combination modulator treatment consisting of 1ng/ml of tezacaftor/ivacaftor/elexacaftor (1:1:1 ratio) for 24 hours prior to, and again alongside poly(I:C) stimulation (100μg/ml) for 12 hours. Heatmap was organised by hierarchical clustering based on mean gene expression. Each column represents a sample (n=3), and each row represents a gene (padj<0.01). ISGs are highlighted in pink on the left-hand panel. Significance was calculated using ANOVA.

After cross-referencing these differentially expressed genes with the list of ISGs, the shift in the ISG signature post modulator treatment became clear (Fig4.2.2.2 A). Of the 486 ISGs, 216 were differentially expressed calculated by ANOVA (padj=0.05) between the modulator treatment and stimulation. 54 ISGs were differentially expressed following poly(I:C) stimulation with modulator treatment and 53 ISGs without, 87 were differentially expressed both with and without modulator treatment (Fig4.2.2.2 B) when data was compared to respective unstimulated and untreated controls. When filtering according to the Log_2(fold change) >2 it became clear that there were more ISGs expressed after poly(I:C) stimulation with modulator treatment compared to without. 12 ISGs were upregulated after poly(I:C) stimulation by the CF cells without modulator and 2 were downregulated, and 25 after modulator treatment with 5 downregulated.

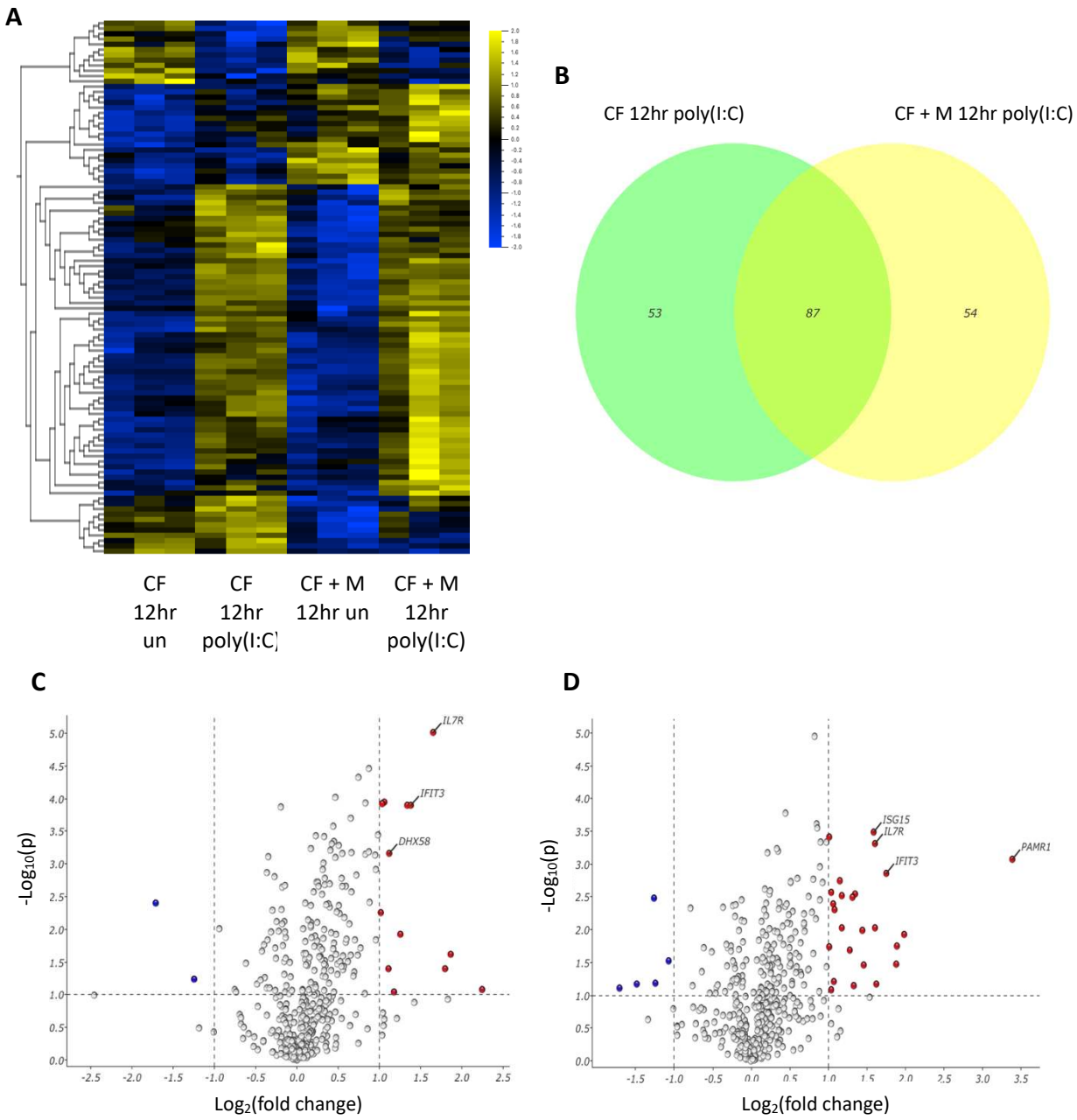

Figure 4.2.2.2: Differentially expressed ISGs after CFTR modulator treatment and poly(I:C) stimulation for 12 hours. CF BECs were treated with combination modulator treatment consisting of 1ng/ml of tezacaftor/ivacaftor/elexacaftor (1:1:1 ratio) for 24 hours prior to, and again alongside poly(I:C) stimulation (100μg/ml) for 12 hours. (A) Heatmap was organised by hierarchical clustering based on mean gene expression and only includes genes from a list of 486 ISGs. Each column represents a sample (n=3), and each row represents a gene (padj<0.05). Significance was calculated using ANOVA. (B) Venn diagram of differentially expressed ISGs compared to uninfected control of named condition representing overlap of ISG signature in CF BECs with and without modulator treatment. Volcano plots representing differentially expressed genes from the same list of 486 ISGs for poly(I:C) stimulated CF

cells (D) with modulator treatment and (C) without modulator treatment, determined by student's t-test padj<0.05 and fold change >2.

Importantly, IFNβ1 was upregulated by a fold change of 2.75 after modulator treatment, but not upregulated at all without. Some key ISGs were also only upregulated after treatment, namely ISG15 and IFIT2. C1S was upregulated by CF cells post poly(I:C) stimulation without modulator treatment, but not with. C1S is a key constituent of the complement subcomponent C1 which activates pro-inflammatory peptide C5a which has been shown to be upregulated in CF soluble fractions[29]. C5a has been related to increased inflammation and a reduced BMI in children with CF. IL-24 was downregulated after poly(I:C) stimulation with modulator treatment, despite it being upregulated by modulator treatment alone (Table4.2.1.1). Over expression of IL-24 is associated with hyper inflammatory states, auto-immune diseases and tissue damage caused by immune cell infiltration.

Table 4.2.2.1: All differentially expressed ISGs in poly(I:C) stimulated CF cells with and without CFTR modulator treatment. Overlapping genes are highlighted in yellow, upregulated genes are in red cells and downregulated in blue (padj<0.05; fold change >2).

CF BECs			CF BECs + Modulators		
Gene Symbol	**P(adj)**	**Fold Change**	**Gene Symbol**	**P(adj)**	**Fold Change**
FGF5	0.025	4.75	PAMR1	0.001	10.48
GBP5	0.011	3.65	GBP5	0.012	3.95
HCAR3	0.014	3.48	SAMD9L	0.018	3.70
IL7R	0.005	3.15	HCAR3	0.033	3.69
IFIT3	0.006	2.60	IFIT3	0.001	3.37
SAMD9L	0.042	2.39	LMO2	0.047	3.08
SERPINB9	0.026	2.26	IFIT1	0.009	3.04
DHX58	0.014	2.17	IL7R	0.000	3.04
C1S	0.014	2.16	ISG15	0.000	3.00
PMAIP1	0.006	2.09	IFNB1	0.035	2.75
IFIH1	0.006	2.05	PLCG2	0.010	2.72
IFIT1	0.045	2.02	DHX58	0.003	2.54
PLD5	0.038	-3.27	TRANK1	0.031	2.51
IDO1	0.019	-2.37	IFIH1	0.003	2.48
			SAMD9	0.021	2.42
			APOBEC3F	0.009	2.26
			ZNFX1	0.003	2.26
			ACE2	0.002	2.22
			IFIT2	0.005	2.12
			APOBEC3A	0.042	2.10
			NMNAT2	0.004	2.09
			PLEKHA4	0.042	2.05
			IRF1-AS1	0.003	2.05
			IL16	0.019	2.02
			PMAIP1	0.000	2.01
			SHC4	0.038	3.27
			PLD5	0.038	2.81
			ADAMTS6	0.003	2.39
			IL24	0.035	2.37
			RPLP0P2	0.030	2.10

4.2.2.2 – GSEA analysis of the effect of CFTR modulator treatment on 12-hour Poly(I:C) stimulated CF and CF corrected bronchial epithelial cells

GSEA analysis further confirmed this as 'Hecker IFNB1 Targets' gene set was the only significantly enriched interferon related in CF BECs stimulated with poly(I:C) after modulator treatment (q=0.10; NES=1.45) but not without (q=0.4; NES=0.38) (Fig4.2.2.3). The ISG signature of the CF cells post modulator treatment with poly(I:C) stimulation doesn't mirror that of the CF corrected BECs but seems to partially correct it. For example, ISG15 is not upregulated in the CF BECs, but it is in the modulator treated CF BECs by a fold change of 3, and by the CF corrected BECs by a fold change of 6.52 (Table 3.2.1.1).

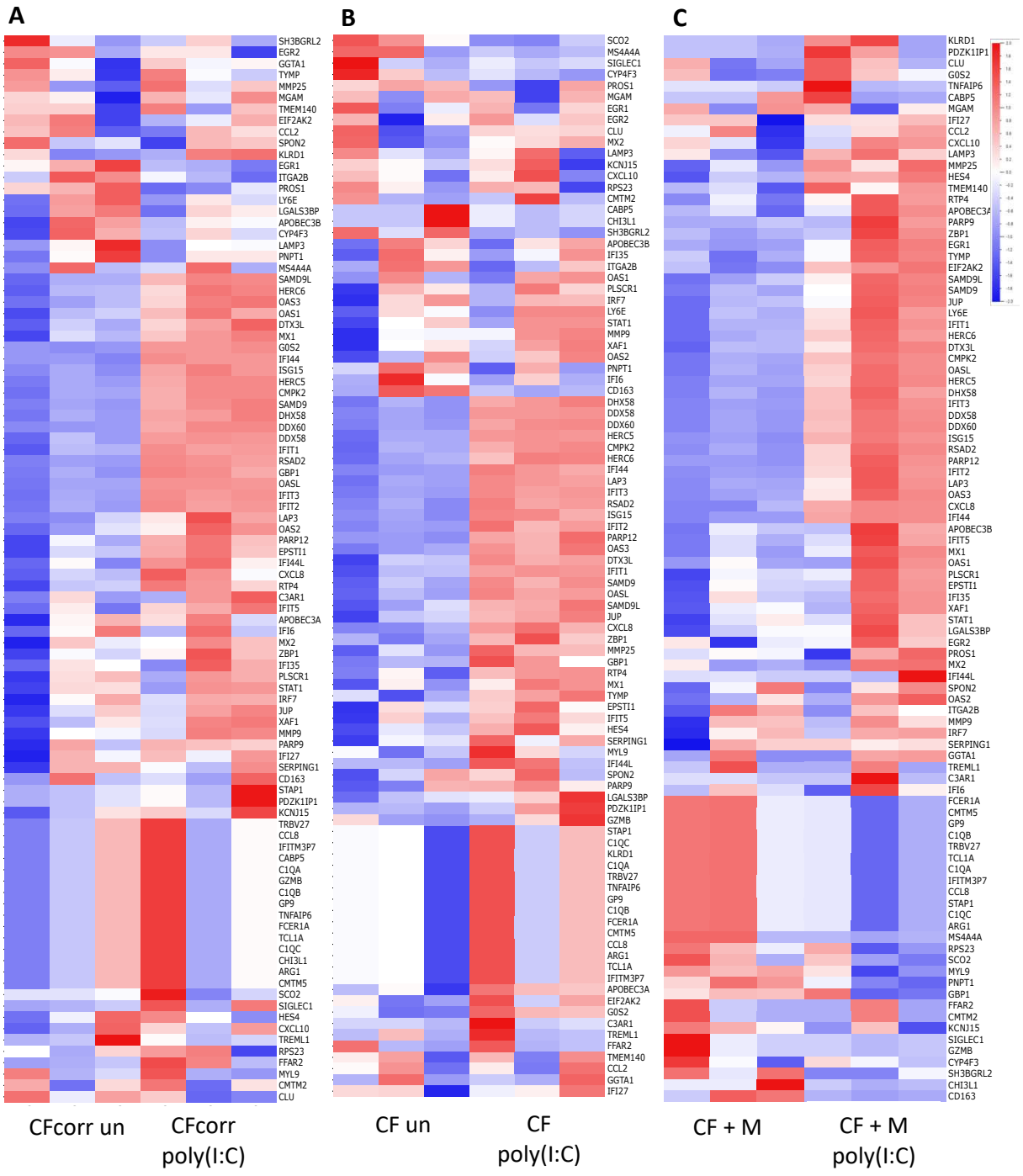

Figure 4.2.2.3: Representative visualisation of GSEA of CF and CF corrected BECs stimulated with poly(I:C) for 12 hours with and without modulator treatment. (A) CF corrected BECs stimulated with 100μg/ml poly(I:C) for 12 hours showed enrichment of 'Hecker IFNB1 Targets' gene set (padj=0.01). (B) CF cells did not show enrichment of this gene set (padj=0.4). (C) CF BECs treated with combination modulator treatment consisting of 1ng/ml of tezacaftor/ivacaftor/elexacaftor (1:1:1 ratio) for 24 hours prior to, and again alongside poly(I:C) stimulation for 12 hours showed significant enrichment of this gene set (padj=0.1). Significance calculated using Student's T-test. Gene set consists of 96 genes.

4.2.2.3 – Protein-protein interaction network analysis of the effect of CFTR modulator treatment on 12-hour Poly(I:C) stimulated CF and CF corrected bronchial epithelial cells

Protein-protein network analysis on all upregulated genes after poly(I:C) stimulation with and without modulator treatment further confirmed the previous findings that more ISGs are upregulated post modulator treatment, with 17 ISGs compared to 14. Functional enrichment of these networks shows the ISGs that are upregulated without modulator treatment are expressed with a higher fold increase after modulator treatment, including OASL, ISG20, DDX58, DDX60 and IFI55 (Fig4.2.2.4).

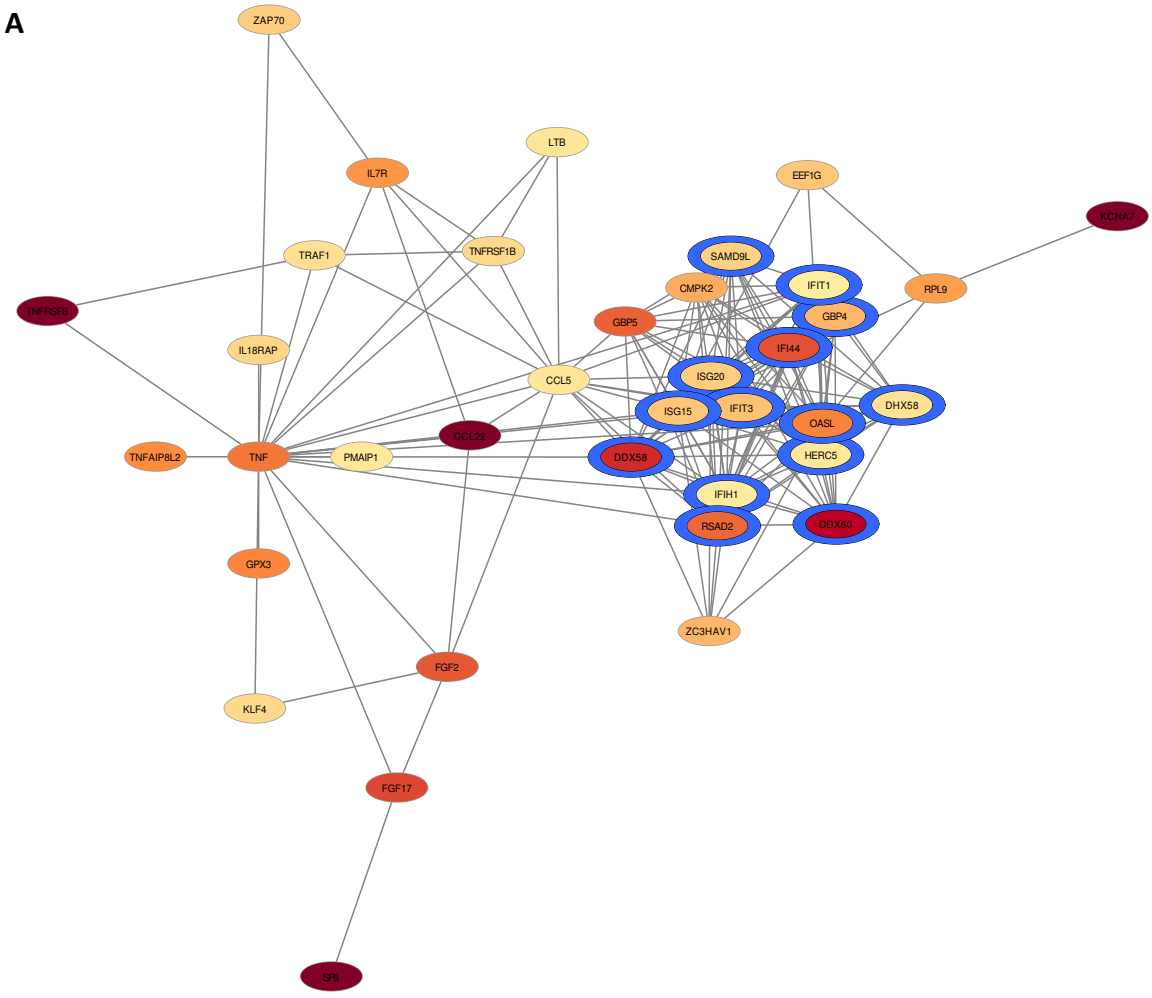

B

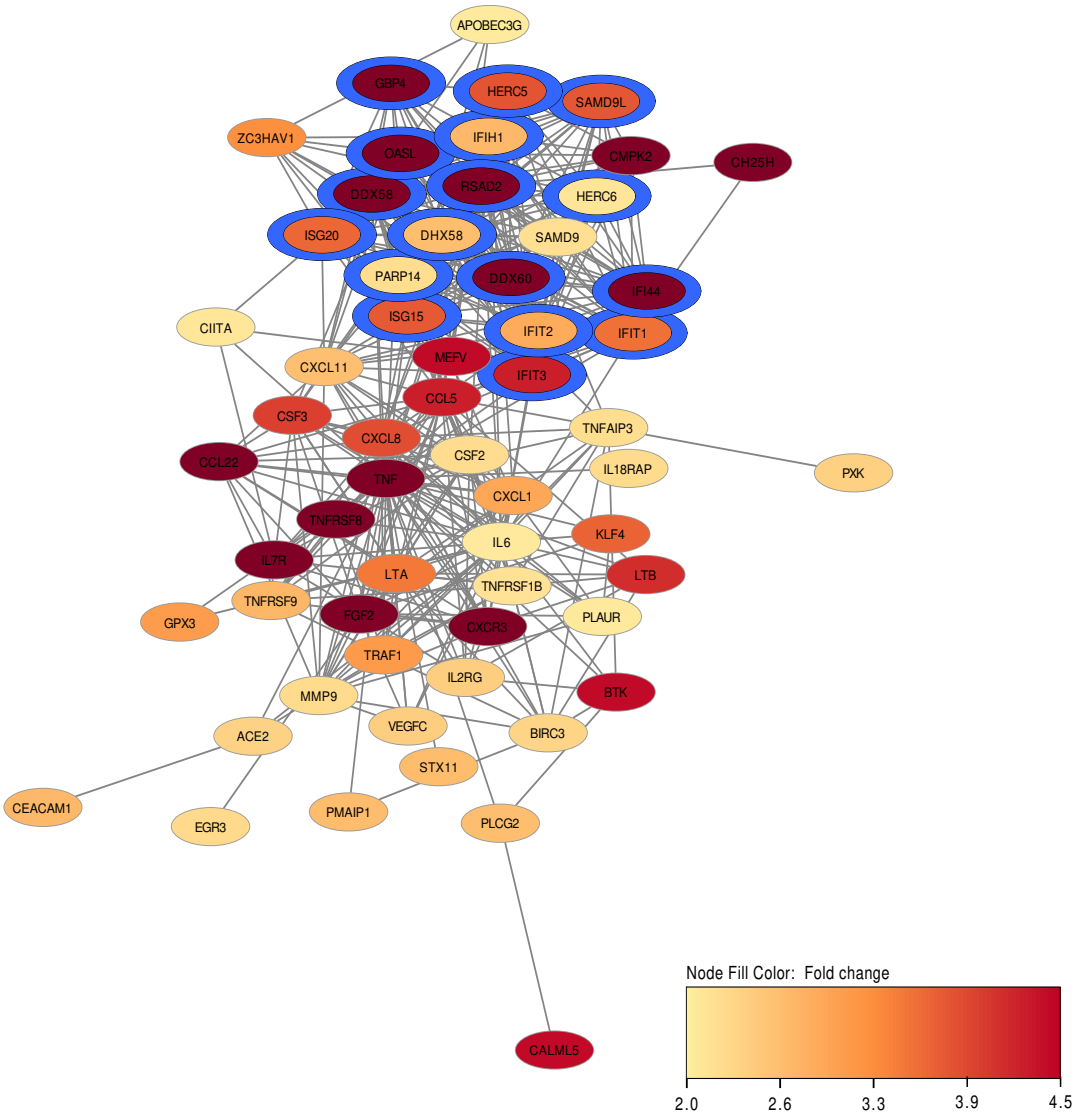

Figure 4.2.2.4: Network analysis of 12 hours of poly(I:C) stimulation in CF BECs with and without modulator treatment. Network visualisation of significant immunity-associated proteins (padj<0.05 and fold change >2), after 12 hours of poly(I:C) stimulation in (A) CF BECs and (B) CF BECs treated with combination modulator therapy. The nodes indicate genes, and the colour represents fold change. Functional enrichment analysis highlights the nodes involved in the type I IFN response (blue) (Cytoscape, stringApp).

4.2.3 – Transcriptomic characterisation of the effect of CFTR modulator combination treatment on the response to heat killed *Af* conidia infection CF bronchial epithelial cells

4.2.3.1 – DEG analysis of the effect of CFTR modulator treatment on 12-hour heat killed conidia infected CF and CF corrected bronchial epithelial cells

The effect of the modulator treatment on the immune response to fungal exposure was assessed by infecting modulator treated CF cells with heat killed conidia for 12 hours. ANOVA analysis revealed 2070 differentially expressed genes (padj=0.01). Clustering analysis of the top 2000 differentially expressed genes in the three repeats based on multigroup comparison shows distinct gene expression between modulator treated and untreated cells and between heat killed conidia infected cells with and without modulator treatment. 61 ISGs are highlighted in the left-hand panel of the heatmap (Fig4.2.3.1).

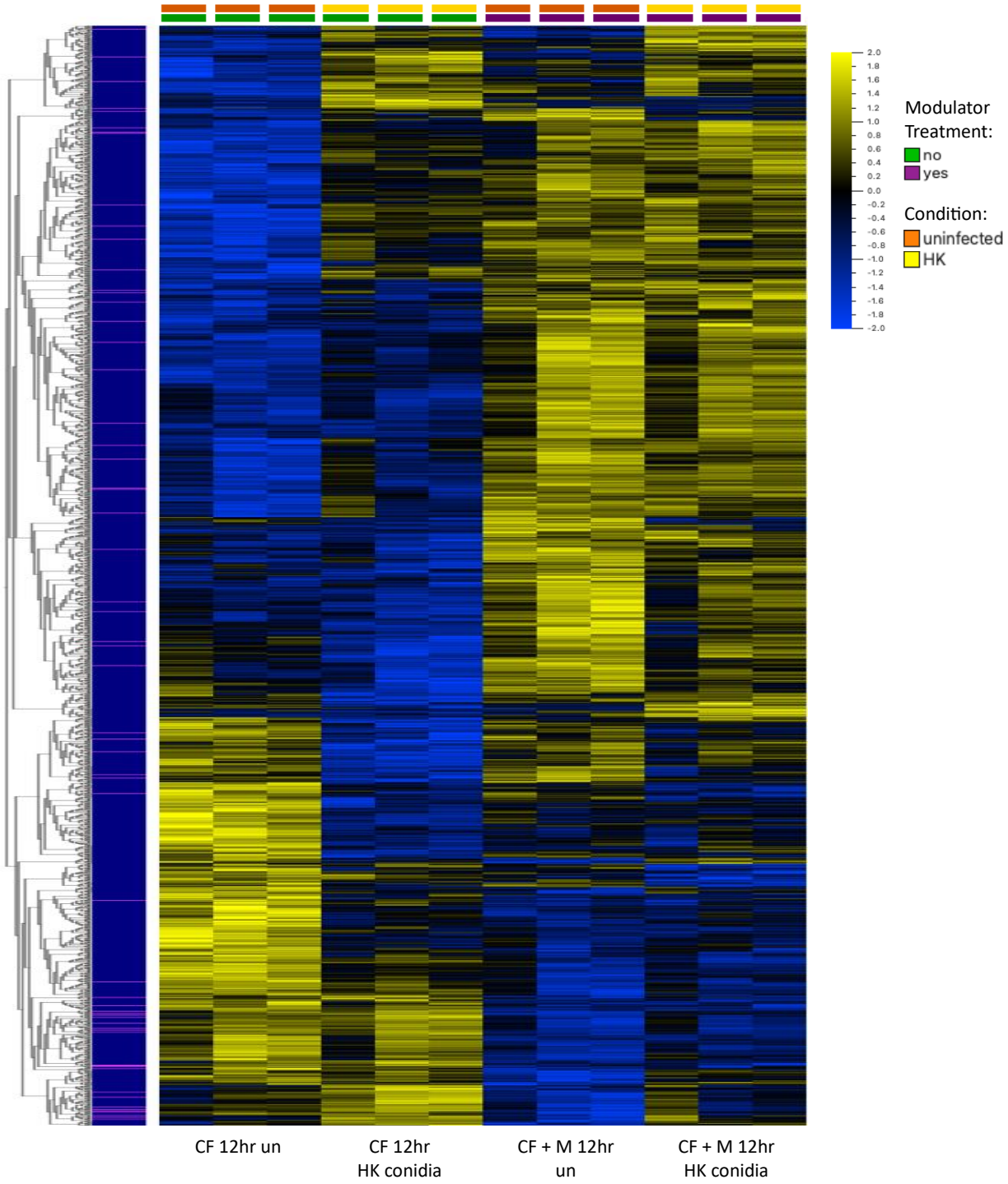

Figure 4.2.3.1: Gene expression heatmap of top 2000 genes differentially expressed after 12 hours of heat killed conidia infection and CFTR modulator treatment. CF BECs were treated with combination modulator treatment consisting of 1ng/ml of tezacaftor/ivacaftor/elexacaftor (1:1:1 ratio) for 24 hours prior to, and again alongside *Af* heat killed conidia infection (MOI=8) for 12 hours. Heatmap was organised by hierarchical clustering based on mean gene expression. Each column represents a sample (n=3), and each row represents a gene (padj<0.01). ISGs are highlighted in pink on the left-hand panel. Significance was calculated using ANOVA.

Investigating further into effect the CFTR modulator treatment has on the type I and III IFN response to heat killed conidia infection, a list of 486 ISGs was cross referenced with the differentially expressed genes previously discussed. Fig4.2.3.2 A shows differences in the ISG signature post modulator treatment with some variation after heat killed conidia exposure and ANOVA analysis reveals a total of 125 differentially expressed ISGs (padj=0.05). With 134 total differentially expressed ISGs (padj=0.05) after heat killed conidia exposure both with and without modulator treatment when data was compared to respective uninfected and untreated controls, only 26 overlapped with 54 being distinct after modulator treatment (Fig4.2.3.2 B).

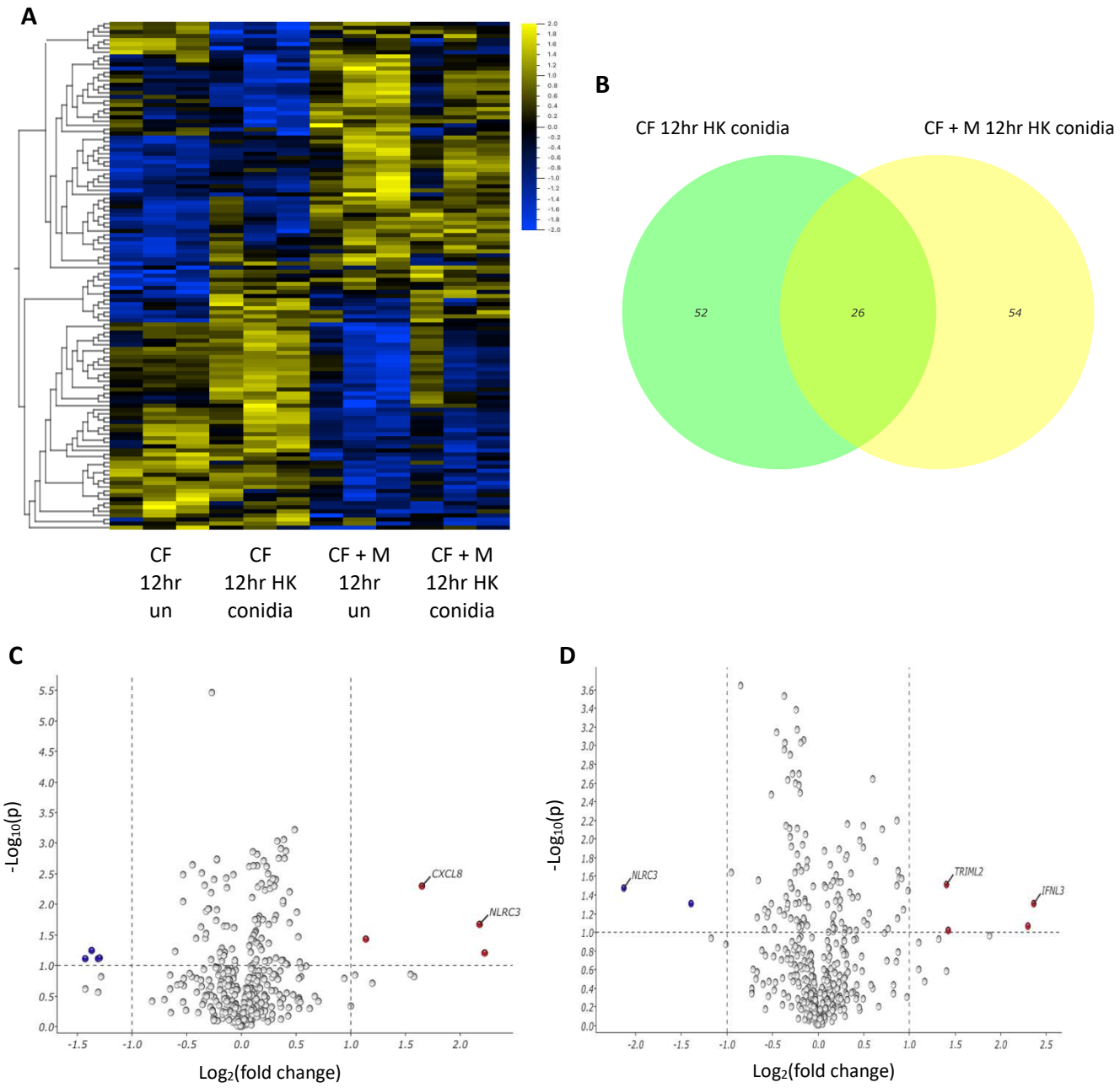

Figure 4.2.3.2: Differentially expressed ISGs of heat killed conidia infected CF BECs for 12 hours with and without modulator treatment. CF BECs were treated with combination modulator treatment consisting of 1ng/ml of tezacaftor/ivacaftor/elexacaftor (1:1:1 ratio) for 24 hours prior to, and again alongside *Af* heat killed conidia infection (MOI=8) for 12 hours. (A) Heatmap was organised by hierarchical clustering based on mean gene expression and only includes genes from a curated list of 486 ISGs. Each column represents a sample (n=3), and each row represents a gene (padj<0.05). Significance was calculated using ANOVA. (B) Venn diagram of differentially expressed ISGs compared to uninfected control of named condition representing overlap of ISG signature in CF BECs with and without modulator treatment. Volcano plots representing differentially expressed genes from the same list of

486 ISGs for *Af* infected CF cells (D) with modulator treatment and (C) without modulator treatment, determined by student's t-test padj<0.05 and fold change >2.

With a further filter of a fold change of >2, there is no difference in the number of upregulated ISGs with modulator treatment, with the only variation in number of genes being that 4 are downregulated without and only 2 with modulator treatment. However, the ISGs that are differentially expressed vary drastically. Firstly, IFNλ3 is downregulated by the CF cells after heat killed conidia infection, however, with modulator treatment, IFNλ3 was upregulated by a fold change of 5.15. CXCL8 was significantly upregulated by CF BECs with heat killed conidia exposure, however, with added modulator treatment, CXCL8 was not upregulated. CXCL8 is a key neutrophil chemoattractant and as a key immunopathogenic feature of CF, reducing the influx of neutrophils to the CF airway could reduce the overall chronic inflammatory cycle. Finally, the downregulation of NLRC3 after heat killed conidia infection and modulator treatment prevents the ubiquitination of TRAF6 and allows normal trafficking of STING, therefore, could explain the mechanism by which the ISG signature is altered post combination modulator treatment.

Table 4.2.3.1: All differentially expressed ISGs in CF and CF corrected BECs after heat killed conidia infection for 12 hours with and without CFTR modulator treatment. Overlapping genes are highlighted in yellow, upregulated genes are in red cells and downregulated in blue (padj<0.05; fold change >2).

CF BECs			CF BECs + Modulator		
Gene Symbol	**P(adj)**	**Fold Change**	**Gene Symbol**	**P(adj)**	**Fold Change**
FGF5	0.043	4.67	IFNL3	0.048	5.15
NLRC3	0.021	4.51	ESM1	0.035	4.93
CXCL8	0.005	3.13	CADPS2	0.046	2.68
SNORD17	0.037	2.20	TRIML2	0.031	2.65
IFNL3	0.049	-2.69	NLRC3	0.033	-4.38
IDO1	0.047	-2.58	MAN1A1	0.049	-2.62
PLD5	0.048	-2.47			
CADPS2	0.046	-2.46			

4.2.3.2 – GSEA analysis of the effect of CFTR modulator treatment on 12-hour Poly(I:C) stimulated CF and CF corrected bronchial epithelial cells

As explained in section 3.2.3, GSEA of the differentially expressed genes in the CF cells infected with heat killed conidia compared to uninfected controls showed enrichment of no IFN related gene sets. With modulator treatment there was still no interferon related gene sets that were significantly enriched, however, the 'Hecker IFNB1 Targets' gene set had padj value that was lower (padj=0.2) than before modulator treatment (padj=0.4).

4.2.3.3 – Protein-protein interaction network analysis of the effect of CFTR modulator treatment on 12-hour Poly(I:C) stimulated CF and CF corrected bronchial epithelial cells

Functional enrichment of the network analysis on all significantly upregulated genes after heat killed conidia infection in CF BECs shows that without modulator treatment there are no type I ISGs out of the 17 genes in the network. After modulator treatment, despite there only being 5 genes in the protein-protein network, 3 were type I ISGs.

A

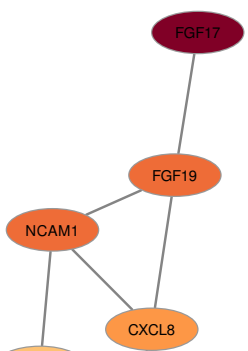

B

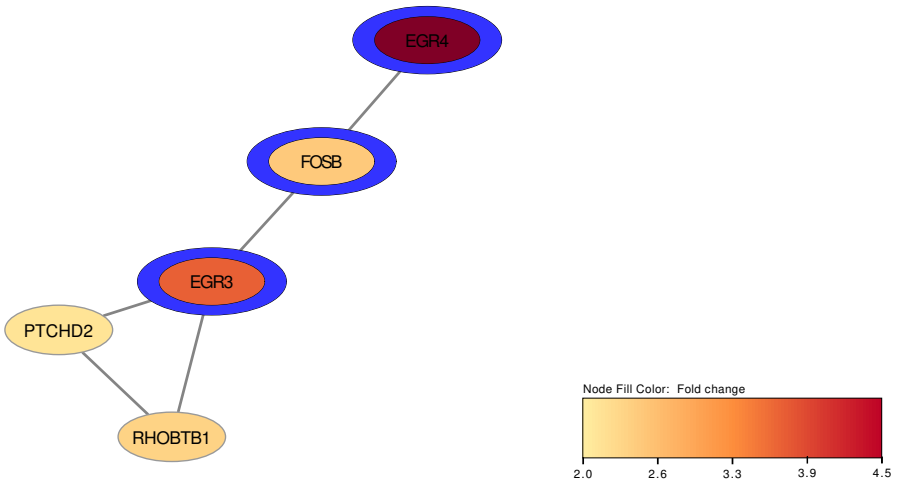

Figure 4.2.3.3: Network analysis of *Af* heat killed conidia infected CF BECs after 12 hours with and without CFTR modulator treatment. Network visualisation of significant immunity-associated proteins (padj<0.05 and fold change >2), after 12 hours of heat killed conidia infection in (A) CF BECs and (B) CF BECs with CFTR modulator treatment. The nodes indicate genes, and the colour represents fold change. Functional enrichment analysis highlights the nodes involved in the type I IFN response (blue) (Cytoscape, stringApp).

4.3 – Confirmation of IFNβ and IFNλ1 response in modulator treated CF bronchial epithelial cells after *Aspergillus fumigatus* infection

To determine if the rescue of the type I and III response due to the CFTR modulator treatment observed in the transcriptomics was due to increased expression of IFNβ and IFNλ1 expression in CF cells directly, RT-PCR of infected and modulator treated cells was carried out. Significantly higher IFNβ and IFNλ1 expression was observed after modulator treatment in poly(I:C) stimulated and heat killed conidia infected cells but not after fixed hyphae infection (Fig4.3.1). However, when compared to the IFNβ and IFNλ1 expression in the CF corrected BECs with the same stimulation (Fig3.3.1), the levels of expression after modulator treatment are not as high, for example, heat killed conidia infection resulted in a fold increase of 32 of IFNλ1 expression in CF corrected cells after 12 hours, but only a fold change of 5 in modulator treated CF cells. This suggests a partial rescue of the type I and III IFN response with modulator treatment after poly(I:C) stimulation and heat killed conidia infection, but not fixed hyphae infection.

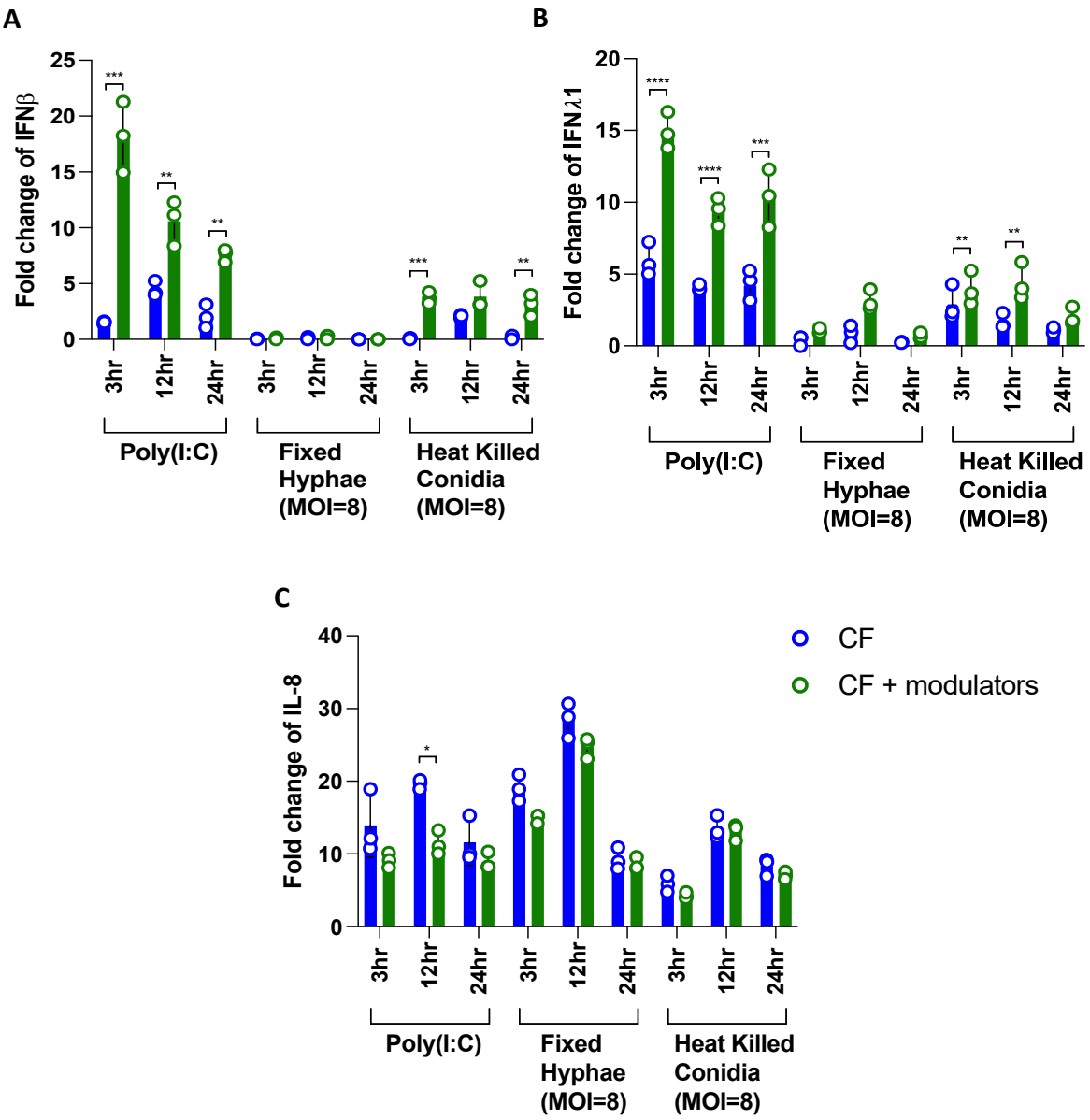

Figure 4.3.1: IFNβ and IFN**λ**1 expression by CF BECs after infection with *Af* fixed hyphae and heat killed conidia and combination CFTR modulator therapy. CF and CF corrected BECs were stimulated with poly(I:C) (10ug/ml) and infected with fixed *Af* hyphae (MOI=8) and heat killed *Af* conidia (MOI=8) for 3, 12 and 24 hours. 24 hours prior to infection the CF BECs were treated with 1ng/ml of modulator combination treatment at a 1:1:1 ratio. RNA was isolated from washed cells an RT-PCR was carried out to assess expression of (A) IFNβ, (B) IFNλ and (C) IL-8.

4.4 – Discussion

The main findings in this chapter were that modulator treatment influences the IFN response in the absence of *Af* infection, upregulating 7 ISGs, most notably IFNλ3. Alongside poly(I:C) stimulation, CFTR modulator treatment resulted in the upregulation of more than double the amount of ISGs expressed by the CF BECs (12 compared to 25) as well as increasing their expression. GSEA analysis confirmed this finding with significantly enriched IFNβ pathways and network analysis displays similar results with the upregulated ISGs more significantly expressed after modulator treatment when compared to poly(I:C) treatment alone. In the presence of *Af* infection there wasn't an increase in the number of ISGs expressed, however, multiple ISGs that were downregulated in the CF cells were then upregulated after modulator treatment and vice versa. For example, IFNλ3 was downregulated after fungal infection in CF cells but upregulated after fungal infected in the presence of modulator treatment and NLRC3 was upregulated in the absence but downregulated in the presence of modulators. Although there was no significance in the GSEA, the gene sets relating to the type I IFN response were trending towards significance after modulator treatment. Finally, the network analysis shows very clearly that there are no ISGs in the absence of modulator treatment but that there are 3 out of 5 genes that are ISGs in the presence of modulator treatment during fungal infection. These results were confirmed using RT-PCR to assess the expression of IFNβ and IFNλ1 which showed significantly increased IFNβ and IFNλ1 expression after heat killed conidia infection and poly(I:C) stimulation but not fixed hyphae infection.

The data showed that CFTR modulator treatment influences ISG expression both in the presence and absence of stimulation or *Af* infection. In the absence of stimulation or infection, CFTR modulator treatment stimulated upregulation of 6 ISGs including SHC4 which is involved

in signalling from PRRs to stimulate the inflammatory response and IL-24 which is involved in both the pro-inflammatory response and the regulation of it. IDO1 is involved in modulating the immune response, particularly regulating T-cell function, and immune tolerance, so priming towards the protective Th1 response and away from the Th2 response that results in sensitisation in the CF lung[359, 360]. Importantly, IFNλ3 was directly upregulated by the modulator treatment alone and is known for its potency among the type III IFNs, being 2-fold and 16-fold more potent that IFNλ1 and IFNλ2 respectively. IFNλ3 induces more anti-viral ISGs than IFNλ1 and IFNλ2, including genes such as IFNβ, TLR3, MYD88, and CXCL0. CFTR modulator also downregulated 4 ISGs, including PAMR1 which plays a role in the processing and stability of RNA during recognition and LMO2 which has a critical role in the differentiation of lymphocytes, specifically T-cells[361]. Interestingly, NLRC3 is also downregulated whose negative regulation of the type I and III IFN response has already been discussed (section 3.4).

When a poly(I:C) stimulus was applied to the CF cells alongside modulator treatment, there was a significant shift in ISG expression when compared to the poly(I:C) stimulation alone. There were 13 more ISGs significantly upregulated by a fold change >2 after modulator treatment compared to without, importantly IFNβ1 was upregulated by a fold change of 2.75 with poly(I:C) stimulation and modulator treatment but it was not upregulated with poly(I:C) stimulation alone. Other genes that were only upregulated in the presence of modulator treatment involve ISG15 which can directly inhibit viral replication, activate, and recruit T-cells and NK cells, and regulate autophagy in infected cells[362]. IFIT2 has similar functional abilities to ISG15 with an ability to directly reduce viral replication through binding viral mRNA and modulate the immune response to pathogens while also amplifying the antiviral state by enhancing IFN signalling and expression[363]. IL16 is also upregulated by a fold change of 2.02

and is a key chemoattractant targeting neutrophils, monocytes, DCs and, importantly, Th1 cells[364]. Th1 bias of the Th1/Th2 axis is a crucial factor during fungal clearance, ensuring fungal killing and reducing the risk of sensitivity[233, 239].

In the presence of *Af* heat killed conidia infection and modulator treatment, there was again a shift in ISG expression. IFNλ3 was significantly downregulated during infection without modulator treatment but significantly upregulated by a fold change of 5.15 after modulator treatment. IDO1 was downregulated by a fold change of 2.58 during infection alone, which would skew the Th1/Th2 ratio towards a sensitised Th2 bias, however, this gene was not significantly downregulated after modulator treatment[365]. Another important gene that was upregulated during infection alone and downregulated by a fold change of 4.38 after modulator treatment was NLRC3.

To my knowledge, one paper has been published on the effect of CFTR modulators on the type I IFN response. This paper by a group in Edinburgh was the first to show a CFTR-dependent dysregulation of the type I IFN response[41]. They first showed a dysregulation of the type I IFN response in human monocyte-derived macrophages (HMDMs) cultured ex vivo from CF patients after stimulation with LPS. When they compared this response to patients who had been receiving Kaftrio treatment for 6 months or more they saw no significant difference of the type I IFN response. However, when they cultured the HMDMs in the presence of Kaftrio, they observed significantly increased expression of key ISGs such as MX1, IFIT3, and IFI44L after 24 hours of LPS stimulation compared to those cultured in its absence. The work in this chapter focuses on in vitro epithelial cells rather than ex vivo culture of primary monocytes and includes data indicating an impact on the type III IFN response as well as the type I IFN response assessed in this paper. In addition, their paper reported a completely reversible

response, which differs from the partial rescue shown in this thesis. This is the first work to be completed on this response in bronchial epithelial cells, in the context of fungal infection and with the additional assessment of the type III IFN response.

To attempt to identify a target pathway effected by the CFTR combination therapy, pathways involved in the expression of the named ISGs whose expression was augmented by the treatment were assessed in literature. ISG15 induction has been reported after both type I and III IFN expression stimulated through TLR4/TRIF, cGAS/STING, and RIG-I/MAVs signalling resulting in IRF7 and IRF3 homodimer phosphorylation and subsequent IFN signalling[362]. DNA-damaging or genotoxic reagents can also induce a DNA-damage response and p53 induced ISG15 expression. IFNβ can induce expression of IDO1 through JAK1/TYK2 induced STAT1/2 signalling induced by activation of cGAS/STING, TLR4/TRAF6/IRF7, TLR4/TRIF/IRF3, and TLR3/7/8 signalling[359]. The IFNλ3 bias post modulator treatment both in the absence and presence of heat killed conidia suggests activation of PRRs that are subcellularly localised in favour of type III IFN activation, for example, peroxisomal MAVS or plasma membrane TLR4 signalling. Occhigrossi, et al., published evidence of a defect in the cGAS/STING/TBK1/IRF7 signalling in the production of type I IFN, in which both ISG15 and IFNβ expression can be affected[42]. Alongside the differential expression of NLRC3, known to target STING translocation, the cGAS/STING pathway is likely to be directly influenced by CFTR expression. However, it is likely there are several targets, this pathway could be an interesting topic of further investigation.

Several limitations to this work have been discussed in the previous chapter, including lack of live fungal infection, restrictions when using the STRING database for network analysis and removal of certain sets of genes during network filtering. Furthering this, it was out of the

scope of this project to confirm the effectiveness of the CFTR modulators using a calcium flux assay due to price and time constraints. Instead, CFTR modulator concentrations were confirmed using cell death and pro-inflammatory cytokine assays alongside previous literature and correction of chloride channel function was assumed. Effectiveness was confirmed with the vast differential gene expression and upregulation of CFTR expression observed post modulator treatment with RNA sequencing.

To continue the work presented in this chapter, specific RT-PCR confirmation experiments of the cGAS/STING signalling pathways could be completed to identify if there is a CFTR dependent defect in this pathway. Chloride channel functional assay would be completed to confirm restoration of chloride influx. Furthering this, nasal samples from patients with CF could be grown to ALI and infected with *Af* to observe if the same results are present in patient samples. This work has significant clinical impact as it allows confirmation of a CFTR-dependent defect in the type I and III IFN response and lays the foundation in determining the mechanism surrounding this, revealing possible therapeutic targets. This allows for the possibility of completely restoring the type I and III IFN response in CF patients who are receiving CFTR modulator treatment and reveals possible immunotherapeutic alternatives for patients with CF who do not or cannot receive modulator treatment.

Chapter 5: Effect of *Aspergillus fumigatus* infection on PBMCs isolated from healthy donors and patients with cystic fibrosis

Dendritic cells are known to be the most potent producers of type I and III IFN in the blood and recent literature describes the importance of monocytes and B cells in type I IFN release[366, 367]. Furthermore, advances showing a type I IFN defect in CF bone marrow derived macrophages (BMDMs) in mice and human CF PBMCs in response to *Pseudomonas aeruginosa* was identified and shown to be corrected by 2', 3' cGAMP treatment[42]. Therefore, to address aim 3 described in the introduction as the assessment of the type I and III IFN response to *Af* in PBMCs isolated from healthy donors and from patients with a CFTR mutation (section 1.4). It was hypothesised that there is a defect in the type I and type III IFN response in PBMCs isolated from patients with CF in response to *Af*.

5.1 – Patient information

Patients were recruited from the Royal Brompton and Harefield NHS Foundation Trust and Manchester University NHS Foundation Trust, Wythenshawe Hospital from two clinical studies, FREAL and TrIFIC, detailed in the methods (section 2.1.6). Table 5.1 shows the patient information for all samples used in this chapter. Patient information lacks details of all infections present across all patients or any previous infections the patient may have had.

Table 5.1: Details of patients recruited for the four patient groups from FREAL and TrIFIC.

Study Group	Study	Patient ID	Age	Sex	CFTR mutation	Underlying disease	Infection(s) present	Ethnicity
CF with fungal disease	FREAL	RB023	39	M	W126X/ V520F	CF	*Aspergillus fumigatus*	White British
		RB024	37	F	F508del/ F508del	CF	*Scedosporium*	White British

		RB027	33	M	F508del/ F508del	CF	*Rasamsonia*	White British
	TrIFIC	RBH007	51	M	R347P/ P67L	CF	*Aspergillus fumigatus*	White British
		RBH024	34	F	F508del/ L165S	CF	*Aspergillus fumigatus*	White British
CF without fungal disease	TrIFIC	RBH020	35	M	F508del/ R117H+7T	CF	*Pseudomonas aeruginosa*	White British
		RBH045	32	F	F508del/ C2052delA	CF	*Pseudomonas aeruginosa*	White British
		MFT024	22	M	F508del/ I507del	CF	*Pseudomonas aeruginosa*	White British
		MFT038	35	F	F508del/ F508del	CF	*Pseudomonas aeruginosa*	White British
		MFT086	25	M	F508del/ N1303K	CF	Normal flora	White other
Non-CF with fungal disease	FREAL	RB002	45	F	N/A	Asthma	*Aspergillus fumigatus*	White British
		RB003	62	M	N/A	ARDS	*Aspergillus fumigatus*	Asian
		RB009	61	M	N/A	Asthma	*Aspergillus fumigatus*	White British
		RB037	35	M	N/A	Nil	*Aspergillus fumigatus*	White British
		RB048	64	F	N/A	Nil	*Aspergillus fumigatus*	White British
Healthy donors	TrIFIC	HD01	42	M	N/A	N/A	N/A	Asian
		HD02	25	F	N/A	N/A	N/A	White British
		HD03	58	M	N/A	N/A	N/A	White British
		HD04	40	F	N/A	N/A	N/A	White British
		HD05	37	M	N/A	N/A	N/A	White British

5.2 – Optimisation of *Af* infection model in PBMCs isolated from healthy donors

To determine if the same defect is present after *Af* infection, a PBMC *Af* infection model using previously frozen PBMCs needed to be established. PBMCs from healthy donors were infected with an MOI of 2, 4 and 8 for 6 hours of both fixed hyphae and heat killed conidia. Reasons for these stimuli were described in chapter 1 (section 3.1). Heat killed conidia did not induce a type I or III IFN response to any MOIs used, however, fixed hyphae infection stimulated a dose dependent increase in both IFNβ and IFNλ1 expression. Due to poor RNA quality and quantity obtained from PBMCs infected at an MOI of 8, it was determined that, despite the significant increase in expression, this stimulus was too much for the cells. Therefore, it was decided that an MOI of 4 should be used moving forward.

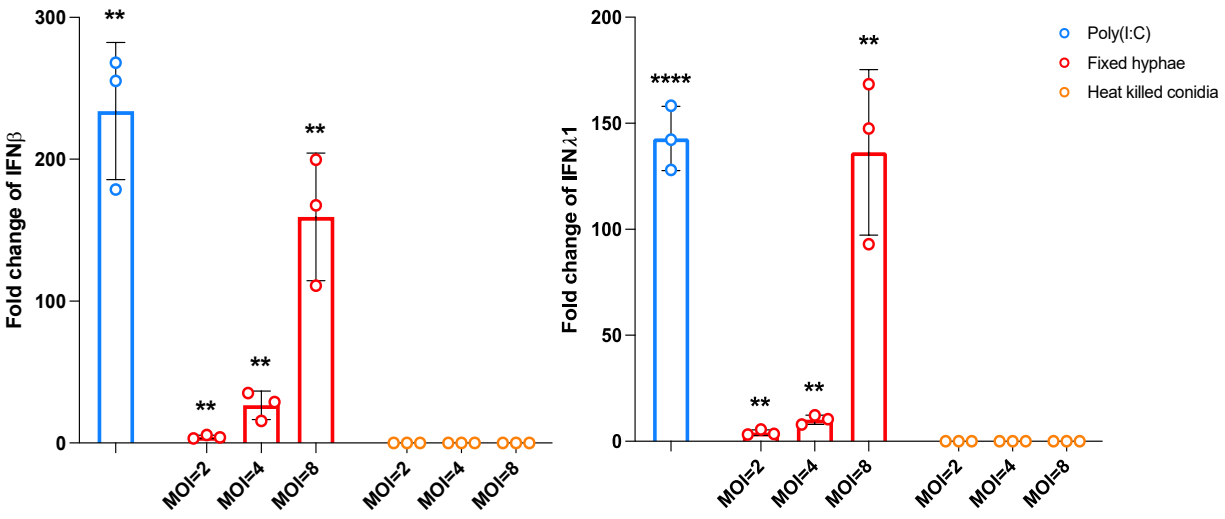

Figure 5.2.1: IFNβ and IFNλ1 expression by healthy PBMCs after fixed and heat killed *Af* infection. Healthy PBMCs were thawed and left in PBMC media with benzonase for 2 hours. The media was subsequently changed and stimulus of fixed hyphae, heat killed conidia (MOI=2, 4 and 8) or poly(I:C) (50ug/ml) was added for 6 hours. RT-PCR was used to assess (A) IFNβ expression and (B) IFNλ1 expression. All data was normalised to 18S RNA and fold change was calculated using the $\Delta\Delta C_T$ method. Data from three independent experiments and are mean ± SD, *p<0.05, **p<0.01, ***p<0.001, ****p<0.0001.

Once a MOI for infection was determined, a time point needed to be determined. Thawed, healthy PBMCs were infected with fixed hyphae at an MOI=4 for 6, 12 and 24 hours. Thawed PBMCs did not survive well past 12 hours, which was assessed by visualising the cells through a light microscope and collection of low concentrations of degraded RNA. Expression of IFNβ and IFNλ1 peaked at 12 hours after poly(I:C) stimulation, but there was minimal expression after fixed hyphae infection at this time point. From the data and the quality and quantity of RNA obtained post infection it was determined that 6 hours of infection with fixed hyphae at an MOI=4 was optimal.

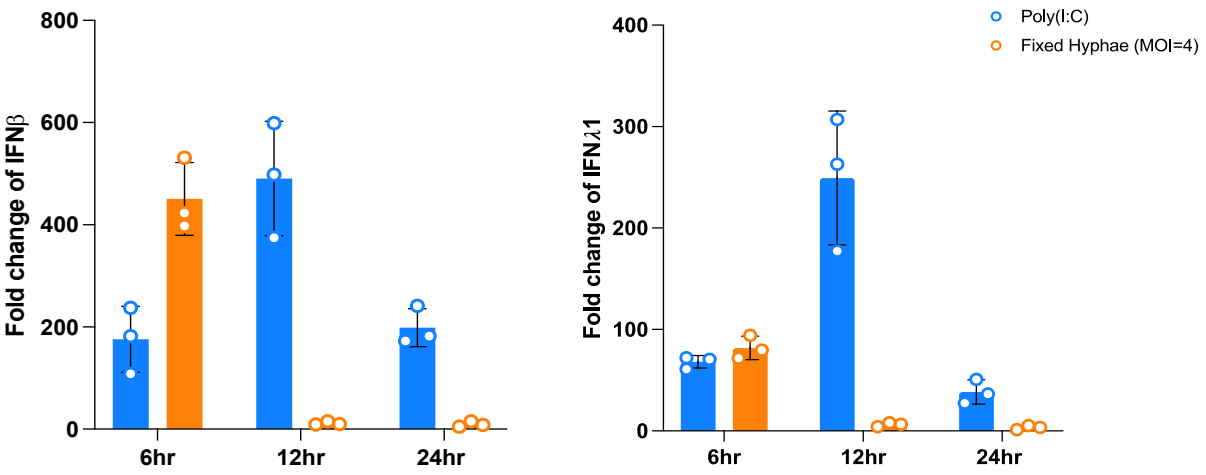

Figure 5.2.2: IFNβ and IFN**λ**1 expression by healthy PBMCs after fixed *Af* hyphae infection. Healthy PBMCs were thawed and left in PBMC media with benzonase for 2 hours. The media was subsequently changed and stimulus of fixed hyphae (MOI=4) or poly(I:C) (50ug/ml) was added for 6, 12, and 24 hours. RT-PCR was used to assess (A) IFNβ expression and (B) IFN**λ**1 expression. All data was normalised to 18S RNA and fold change was calculated using the $\Delta\Delta C_T$ method. Data from three independent experiments and are mean ± SD, *p<0.05, **p<0.01, ***p<0.001, ****p<0.0001.

5.3 – CF PBMCs do not display the same defect in IFNβ and IFN$\boldsymbol{\lambda}$1 expression after *Af* infection that is present in CF BECs

IFNβ, IFNλ1, TNFα expression and TNFα release from PBMCs stimulated with *Af* fixed hyphae (MOI=4) and poly(I:C) for 6 hours was studied in cells isolated from healthy donors, and patients using RT-PCR and ELISA. The patient groups were CF with fungal disease, CF without fungal disease, non-CF with fungal disease and healthy donors (n=5 across all groups). There was no significant difference in the IFNβ and IFNλ1 expression stimulated by both poly(I:C) and fixed hyphae between the groups (Fig5.3.1 A, B). This differs from the BEC data reported in chapter 3, suggesting a potential mucosal-specific defect. TNFα expression in CF patients with fungal infection was significantly higher when compared to the non-CF fungal infection patient group and healthy donors (Fig5.3.1 C). ELISA results showed significantly higher production of TNFα in the CF patients with and without fungal infection when compared to the non-CF fungal infection patient group (Fig5.3.1 D). This data correlates with published data showing the elevated inflammatory state in the CF lung detailed in the introduction. This work was performed in conjunction with Haina Zhang, an MSc student at Imperial College London.

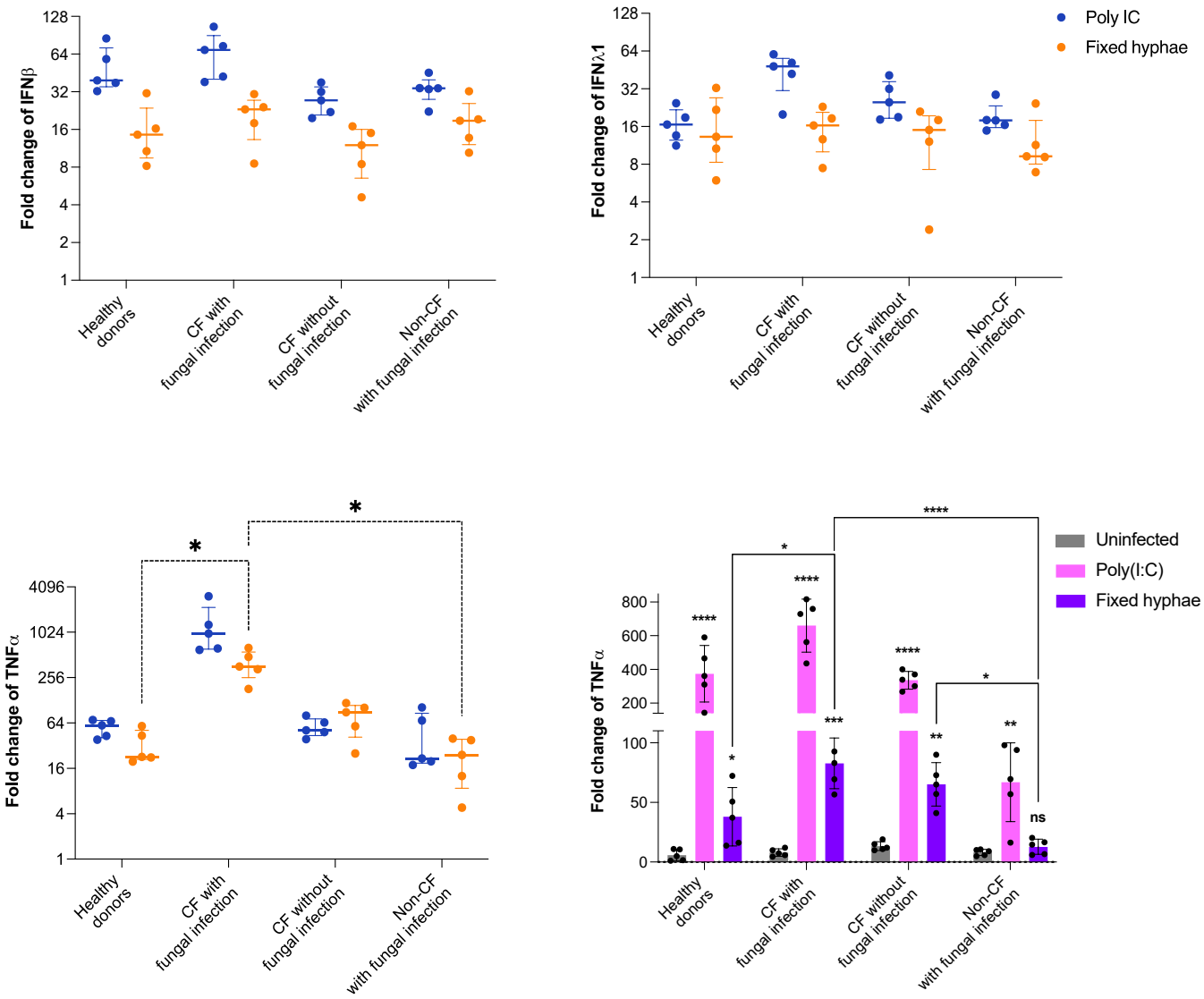

Figure 5.3.1: *Af* infection in PBMCs isolated from patient groups. PBMCs were isolated from stated patient groups and frozen for storage. When appropriate, PBMCs were thawed and placed in PBMC media with benzonase for 2 hours and subsequently challenged with *Af* fixed hyphae (MOI=4) or stimulated with 50ug/ml poly(I:C) for 6 hours before the supernatant was collected and RNA was isolated from washed cells. RT-PCR was used to assess (A) IFNβ expression, (B) IFNλ1 expression and (C) TNFα expression. D. TNFα production was assessed by ELISA using culture supernatant. Each patient group contains n=5. Data are mean ± SD of 2 technical repeats, *p<0.05, **p<0.01, ***p<0.001, ****p<0.0001.

5.4 – Discussion

The data in this chapter shows that healthy PBMCs produce IFNβ and IFNλ1 in response to fixed *Af* hyphae infection for 6 hours but do not respond to heat killed conidia. IFNβ was produced at higher concentrations than IFNλ1. When this expression was assessed in patient groups, there was no significant difference in the IFNβ or IFNλ1 expression between any group, indicating that the defect observed in the type I and III IFN response in CF bronchial epithelial cells is not present in CF PBMCs. TNFα expression was significantly higher in CF patients with fungal infection compared to non-CF fungal infection patients, indicating an elevated pro-inflammatory response in the CF patients. This finding was mirrored when assessing TNFα production by ELISA and revealed that even the CF patients without fungal infection produced significantly more TNFα than non-CF fungal infection and healthy donors alike.

Occhigrossi et al. recently reported a defect in the IFNβ production in CF PBMCs post *Pseudomonas aeruginosa* infection when compared to healthy, however, they used freshly isolated PBMCs which could explain the difference in expression levels they reported, alongside the different stimulus[42]. Several other studies highlight the importance for the type I and III IFN response to *Af* infection, using BAL from mouse models and human BECs but few studies directly assess this response in PBMCs isolated from healthy or CF patients, highlighting the novelty of this work[141, 163, 174].

Limitations of the work in this chapter was based around the lack of patient samples and the speed of recruitment. This project began in 2020, and due to the COVID-19 pandemic, coupled with the introduction of CFTR modulators, CF patients required fewer hospital admissions,

were shielding, and transitioned to at home or virtual care. Recruitment for our clinical studies were shadowed by COVID-19 studies during 2020, meaning we began recruitment a year later and with a much slower uptake than initially expected. This left little time for optimisation and completion of PBMC experiments and smaller patient groups than desired. Furthermore, it was required to be less selective regarding patient demographics and clinical status than initially planned, resulting in more variation of CFTR mutations and infections present. Detailed infection history and current infections/co-infections present in all patients was also unknown, making comparisons more difficult. If circumstances were different there would have been more effort allocated to recruiting more patients with *Af* infection who possess the F508del mutation to restrict as much variation. Due to the unpredictable nature of patient recruitment and the length of time required for the infection experiment, storage and, therefore, freezing of the PBMCs was necessary. Thawing of frozen PBMCs can have more of an effect on some cell types than others, for example, dendritic cells do not withstand freeze-thaws well, and with them being the largest producers of type I and III IFNs in PBMCs, this reduces a key cell population. Finally, due to time restraints, only the expression of IFNβ and IFNλ1 was assessed, leaving multiple type I and III IFNs expression levels unexplored. Therefore, increasing numbers of patients in the groups and amount of IFN targets measured, and development of a protocol using freshly isolated PBMCs would have been desirable and would be required to thoroughly investigate the type I and III IFN response in CF PBMCs.

Overall, the lack of difference of IFNβ and IFNλ1 expression across the patient groups suggests there could be a mucosal specific defect in the IFNβ and IFNλ1 response in CF cells in response to *Af* infection when compared to healthy cells, so rejecting the hypothesis stated at the start of the chapter. Clinically, this could highlight the importance of administration of a potential

type I or III IFN therapy to the mucosal surface, rather than vascularly, so targeting the location of the defect and the source of *Af* colonisation.

Chapter 6: Effect of exogenous type I and III interferons on healthy and cystic fibrosis neutrophil fungal control and cell survival

6.1 – Introduction

Neutrophils are the most abundant leukocyte in the human blood and are essential for both the control of pathogens and the restoration of homeostasis of the host environment. Neutrophils are key elements of the first line antifungal immune response and can eliminate fungus through phagocytosis, oxidative burst, and formation of NETs (described in Section 1.2.4.3)[368]. After recruitment to the site of infection, neutrophils uptake *Af* conidia for intracellular killing, release NADPH oxidase-mediated ROS which can induce an apoptosis-like programmed fungal death and induce NET production to prevent or slow down fungal growth[369]. A study conducted in 2018 by the Rivera lab revealed the importance of $CCR2^+$ monocytes and their crosstalk with neutrophils, involving type I and III IFNs, in the priming and fungicidal ability of neutrophils in the mouse lung[163]. Specifically, type I IFNs are required to successfully prime for the optimal production of type III IFNs by Ly6Chi monocytes, which then act directly on recruited neutrophils to promote fungicidal effector functions such as ROS production and their ability to restore homeostasis post infection.

As described in the introduction (Section 1.1.2) a neutrophilic inflammatory environment precedes colonisation and infection in CF. In addition, life span of neutrophil in CF respiratory samples is increased compared to non-CF samples, which in part is secondary to a reduction in apoptosis of CF neutrophils compared to healthy[52]. Neutrophils express CFTR both on their phagolysosome membranes and cell surface membranes and with defective CFTR there is

reduced phagolysosome acidification and reduced fungal killing. Consequently, despite the elevated number, increased survival, and increased ROS production of neutrophils in the CF airway, there is defective control or killing of pathogens and a reduction in the neutrophilic homeostatic ability, contributing to the overall hyperinflammatory state[53].

Therefore, it was hypothesised that type I and type III IFN may have a role in improving *Af* clearance and control of infection. To address this hypothesis this chapter aimed to:

1. Optimise a neutrophil *Af* infection assay using freshly isolated healthy and CF neutrophils.
2. Assess if the addition of type I and type III IFN improves control of *Af* infection through measuring:
    a. Fungal killing
    b. Cell cytotoxicity
    c. Mechanistic methods of fungal killing including NETosis and ROS production

6.2 – Optimisation of *Af* infection model in neutrophils isolated from healthy donors

To determine the effect of *Af* infection on the neutrophil innate immune response, neutrophils had to be isolated from healthy donors and patients with CF from the Royal Brompton and Harefield NHS Foundation Trust. Neutrophils were isolated using polymorphprep within 30 minutes of blood collection and the purity of the isolation was determined using flow cytometry. To accomplish this, cells were stained for surface markers CD3, CD19, CD14, CD56, CD123, CD11b, and CD66b. CD11b and CD66b are expressed by neutrophils but are not neutrophil specific, therefore, it was necessary to use a dump channel to gate out cells expressing the other mentioned markers which includes T-cells, B-cells, monocytes, NK cells, dendritic cells, eosinophils, and basophils. Cells were also stained with a Live/Dead stain to ensure cell viability. Initially, cells were gated by forward and side scatter, followed by gating out the doublets through forward scatter height and area (Fig6.2 A, B). Live cells were determined with the live-dead and all further cell percentages were calculated using the number of live cells (Fig6.2 C). The dump channel was used for to exclude CD11b and CD66b expression by the other immune cells mentioned (Fig6.2 D). Finally, the cells that were double positive for CD11b and CD66b were determined as neutrophils and the isolation was shown to have purity levels consistently above 94% (Fig6.2 E).

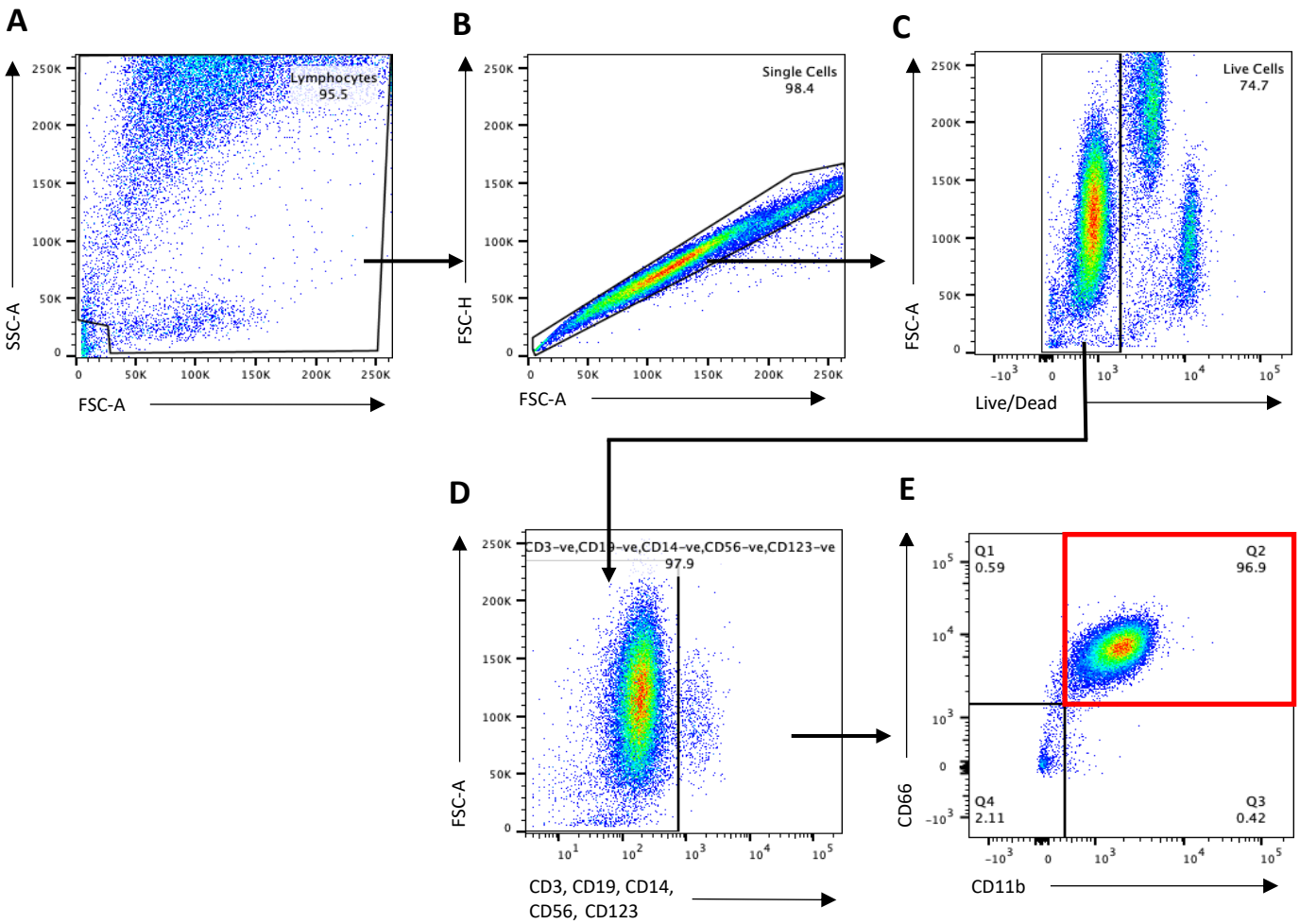

Figure 6.2: Representative flow cytometry gating strategy for isolation of neutrophils. All cells were first gated based on forward scatter area and side scatter area to determine the cells from the cell debris (A). Single cells were gated based on forward scatter area and forward scatter height to remove doublets (B). Live cells were selected for based on a positive control of cells stained with Live/Dead fixable aqua, dead cell stain kit (C). Cells were further gated on using a dump channel for CD3, CD19, CD14, CD16, CD56, and CD123 so gating out cell types such as B-cells, T-cells, NK cells, dendritic cells, monocytes, and macrophages (D). Finally, neutrophils were gated as double positive for CD11b and CD66 (E). From the original pool of all live cells gated in (C), 94% of cells were gated as neutrophils.

6.2.1 – Effect of exogenous IFNβ and IFNλ1 on fungal growth

Before proceeding to assess the effect of the exogenous IFNβ and IFNλ1 on neutrophil function, the impact of both cytokines on kinetics of CEA10 (Fig 6.2.1) and dsRed (Fig6.2.2) was examined. *Af* conidia of both fungal strains were imaged using wide field microscopy for 12 hours to assess conidial swelling and hyphal germination. Neither high or low concentration of IFNβ or IFNλ1 affected time from conidial swelling to hyphae germination. Both CEA10 and dsRed germinated at 5 hours on average and grew from an average of 4.3um and 4.9um at 0 hours to an average of 19.5um and 16.2um at 7 hours respectively (Fig6.2.1 and Fig6.2.2 respectively).

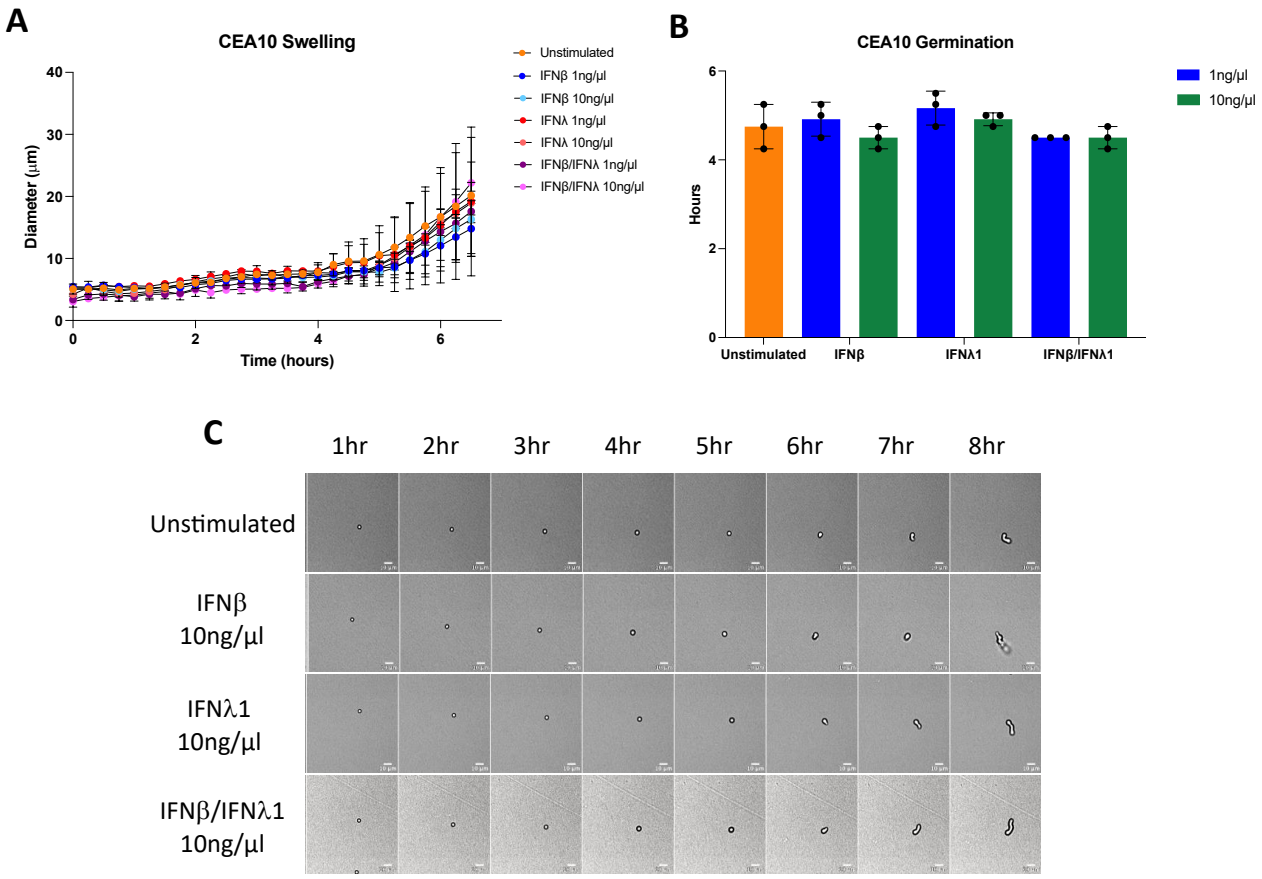

Figure 6.2.1: The effect of IFNβ and IFNλ1 on CEA10 growth and germination. CEA10 was grown in the presence and absence of IFNβ or IFNλ1 or both at 1ng/µl or 10ng/µl for 8 hours in clear RPMI. The diameter of CEA10 conidia under all conditions were measured to show fungal swelling (A) and the time at which the fungus germinated was plotted for comparison across all conditions (B). Representative images of CEA10 conidia swelling and germinating were taken every hour (C). All images and analysis were completed on ImageJ, Fiji. Statistical significance was tested with two-way ANOVA for swelling data and student's T-test for germination data. Data is from 3 experimental repeats (n=3). Error bars represent SD.

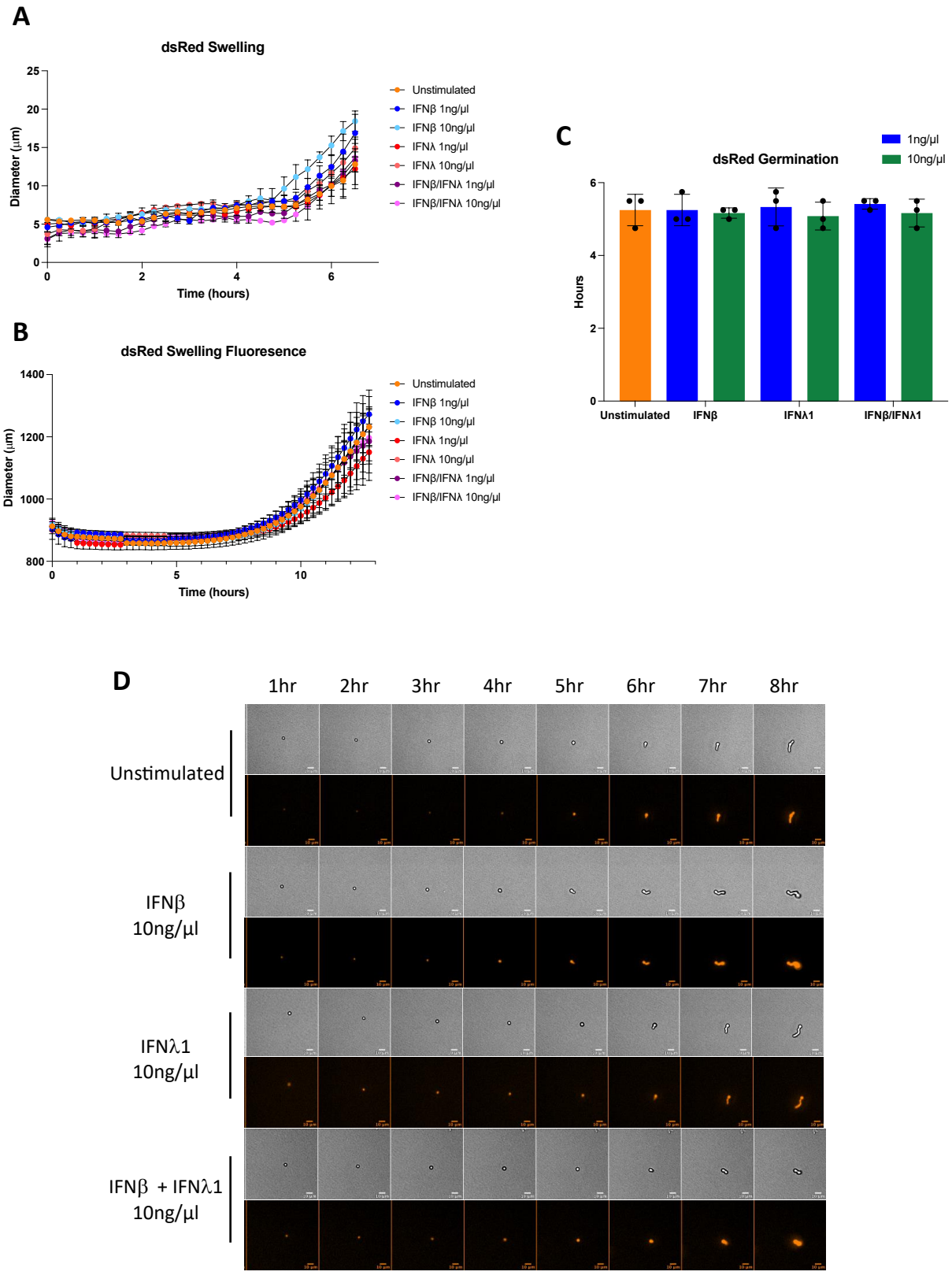

Figure 6.2.2: The effect of IFNβ and IFNλ1 on dsRed growth and germination. dsRed was grown in the presence and absence of IFNβ or IFNλ1 or both at 1ng/µl or 10ng/µl for 12 hours in clear RPMI. The diameter of dsRed conidia under all conditions were measured to show fungal swelling (A) and the

dsRed MFI was measured as another measure of fungal growth (B). The time at which the fungus germinated was plotted for comparison across all conditions (C). Representative images of CEA10 conidia swelling and germinating were taken every hour (D). All images and analysis were completed on ImageJ, Fiji. Statistical significance was tested with two-way ANOVA for swelling data and student's T-test for germination data. Data is from 3 experimental repeats (n=3). Error bars represent SD.

6.3 – Patient Information

Chapter 3 describes data showing a downregulated or delayed type I and III IFN response in CF BECs when compared to CF corrected BECs. As previously described (Section 1.2.4.3), this response is essential in regulating antifungal neutrophil responses, therefore with a downregulation already shown it was investigated if a treatment of exogenous type I and III IFN could have a direct effect on neutrophil antifungal response. In order to assess this, 5 healthy donors and 5 patients with CF were recruited from the Royal Brompton and Harefield NHS Foundation Trust under the TrIFIC clinical study, detailed in the methods (section 2.1.6).

Table 6.3: Details of patients recruited from TrIFIC.

Study Group	Study	Patient ID	Age	Sex	CFTR mutation	Underlying disease	Infection(s) present	Ethnicity
CF with fungal disease	TrIFIC	RBH062	46	M	F508del/ 3011_3019del	CF	*Aspergillus fumigatus*	White British
		RBH063	43	F	p.Arg74Gln/ p.Arg297Gln	CF	*Pseudomonas aeruginosa*	White British
		RBH064	20	F	F508del/ F508del	CF	*Staphylococcus aureus*	White British
		RBH065	32	F	F508del/ F508del	CF	N/A	White British
		RBH068	27	F	F508del/ F508del	CF	*Aspergillus fumigatus*	White British
Healthy donors	TrIFIC	HD01	42	M	N/A	N/A	N/A	Asian
		HD02	25	F	N/A	N/A	N/A	White British
		HD03	58	M	N/A	N/A	N/A	White British
		HD04	23	F	N/A	N/A	N/A	Asian
		HD05	27	M	N/A	N/A	N/A	Asian

6.4 – Effect of exogenous IFNβ and IFNλ1 on Neutrophil Function

6.4.1 – Effect of exogenous IFNβ and IFNλ1 on healthy neutrophil function

Once it was established that the exogenous IFNβ or IFNλ1 had no direct effect on fungal growth, their effect on healthy neutrophil antifungal response was investigated through assessing ROS production, NET production, cell survival and fungal killing. Fungal CFUs were carried out as a measurement of fungal killing and addition of IFNλ1 at both concentrations and both IFNβ and IFNλ1 together at 10ng/μl significantly reduced the number of CFUs after infection, so indicating increased fungal killing (Fig6.4.1 A). IFNβ alone had no significant impact on fungal CFUs. When cell cytotoxicity was observed as a measure for cell survival, exogenous IFNβ treatment alone had no significance, but cell cytotoxicity significantly increased with addition of exogenous IFNλ1 and both IFNβ and IFNλ1 together at both concentrations (Fig6.4.1 B).

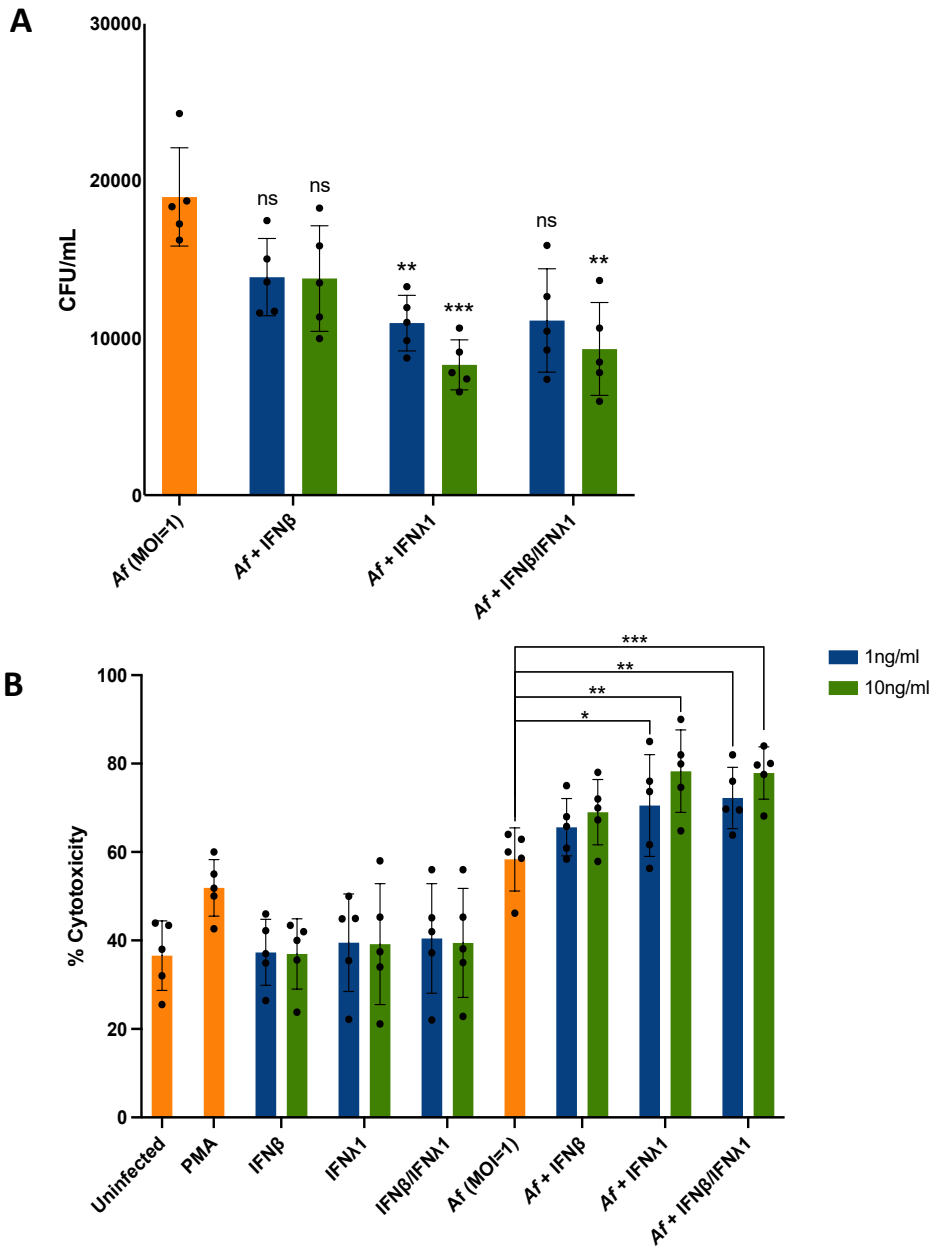

Figure 6.4.1: The effect of IFNβ and IFNλ1 on healthy neutrophil fungal killing and cell survival. Neutrophils were isolated from 5 healthy donors and treated with either IFNβ, IFNλ1 or both together at a concentration of 1ng/μl and 10ng/μl both in the presence and absence of *Af* infection at an MOI=0.5 or MOI=1 where stated. Cytotoxicity was assessed using an LDH assay on the supernatant after 3 hours of *Af* infection (E). CFUs were obtained from lysates of neutrophils after 3 hours of infection with the presence of exogenous IFN treatments (F). Statistical significance was tested with two-way ANOVA for ROS data and student's T-test for the rest of the data. Data is from 5 experimental repeats (n=5). Error bars represent SD. *p<0.05, **p<0.01, ***p<0.001, ****p<0.0001.

Uninfected neutrophils isolated from healthy donors had increased ROS production following addition of exogenous IFNβ and IFNλ1. ROS was significantly increased following PMA stimulation (positive control) and low dose IFNβ (1ng/μl) but there was no significant change for any other condition (Fig6.4.2 A). Addition of IFNβ and IFNλ1 in the setting of fungal infection did not lead to any significant changes in ROS compared to positive PMA control (Fig6.4.2 B). As expected, ROS was significantly raised after infection and stimulation in comparison to uninfected controls. NETosis levels were significantly increased with addition of IFNβ/IFNλ1 at both concentrations and IFNλ1 at 10ng/μl stimulated more NETs in the absence of fungal infection (Fig6.4.2 C). When NETosis levels were assessed after the addition of fungus, there was a much stronger response across all conditions (Fig6.4.2 D). Exogenous IFNβ at both concentrations during infection significantly reduced NET production when compared to just fungus alone, and IFNβ and IFNλ1 together at 10ng/μl significantly increased NET production compared to fungus alone.

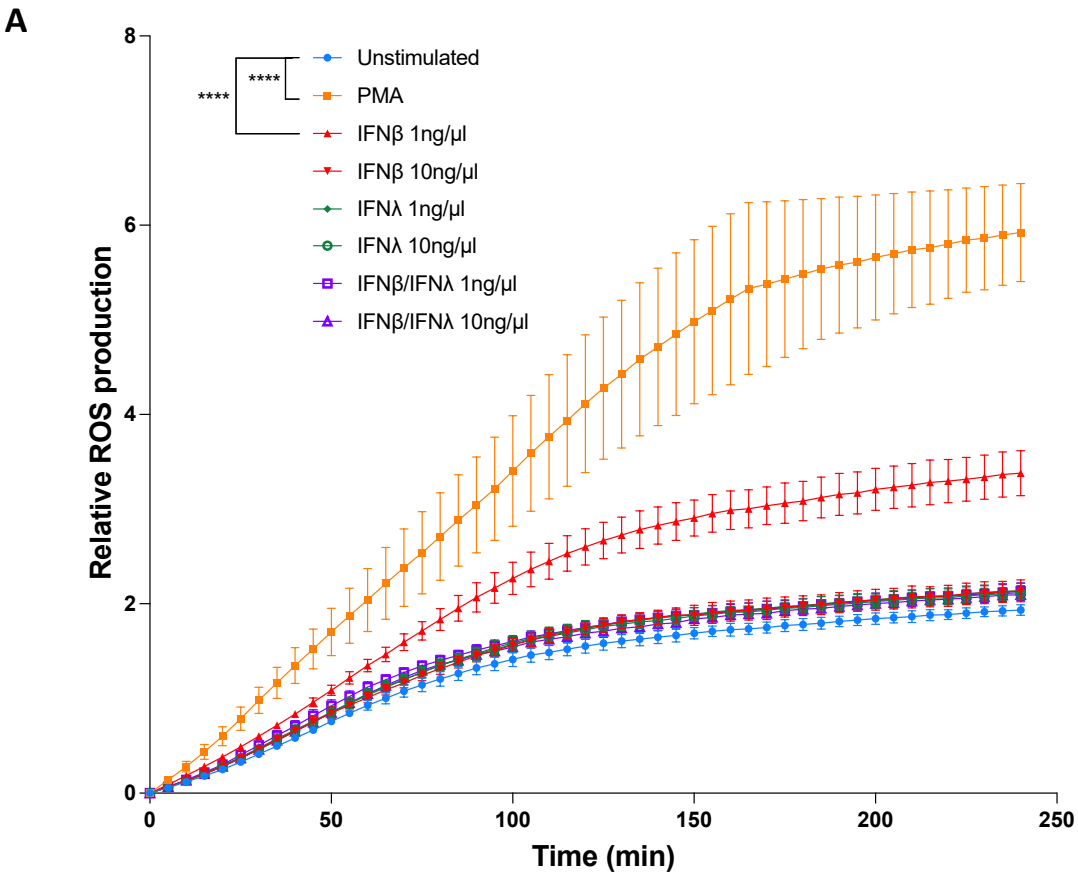
A
Relative ROS production
Time (min)
Unstimulated
PMA
IFNβ 1ng/µl
IFNβ 10ng/µl
IFNλ 1ng/µl
IFNλ 10ng/µl
IFNβ/IFNλ 1ng/µl
IFNβ/IFNλ 10ng/µl
****
****
0
2
4
6
8
0
50
100
150
200
250

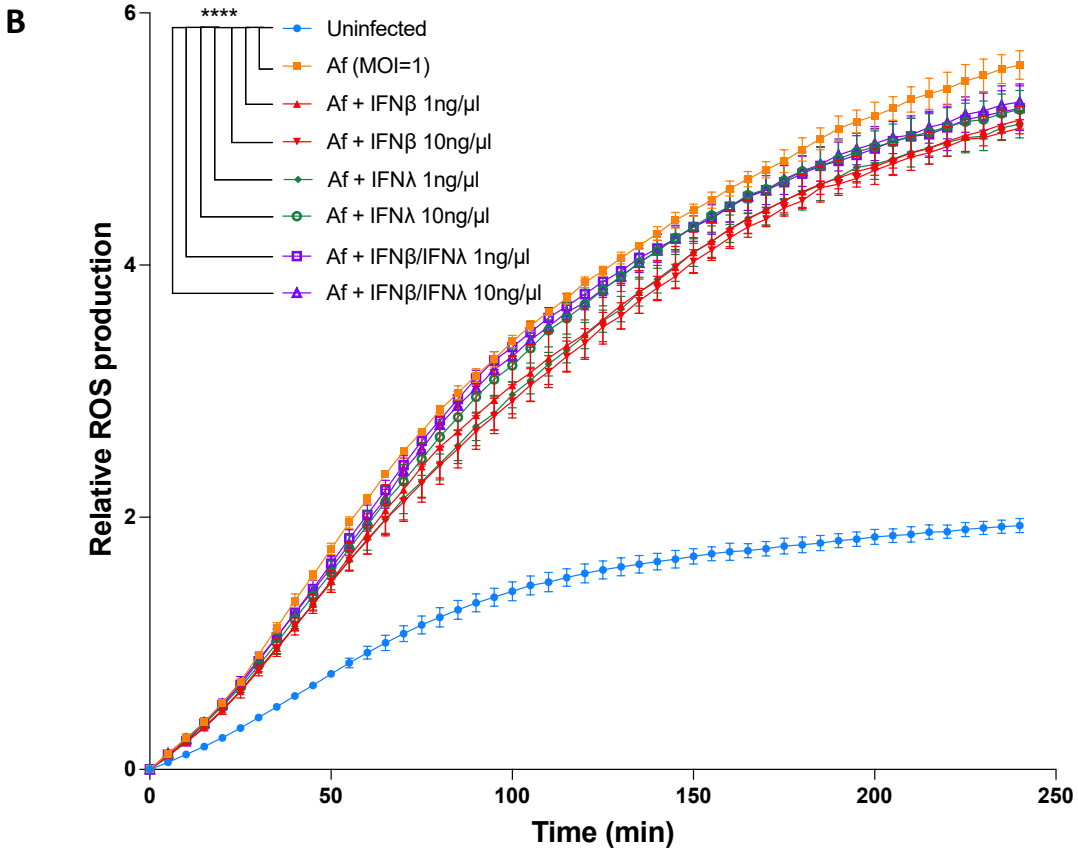
B
Relative ROS production
Time (min)
Uninfected
Af (MOI=1)
Af + IFNβ 1ng/µl
Af + IFNβ 10ng/µl
Af + IFNλ 1ng/µl
Af + IFNλ 10ng/µl
Af + IFNβ/IFNλ 1ng/µl
Af + IFNβ/IFNλ 10ng/µl
****
0
2
4
6
0
50
100
150
200
250

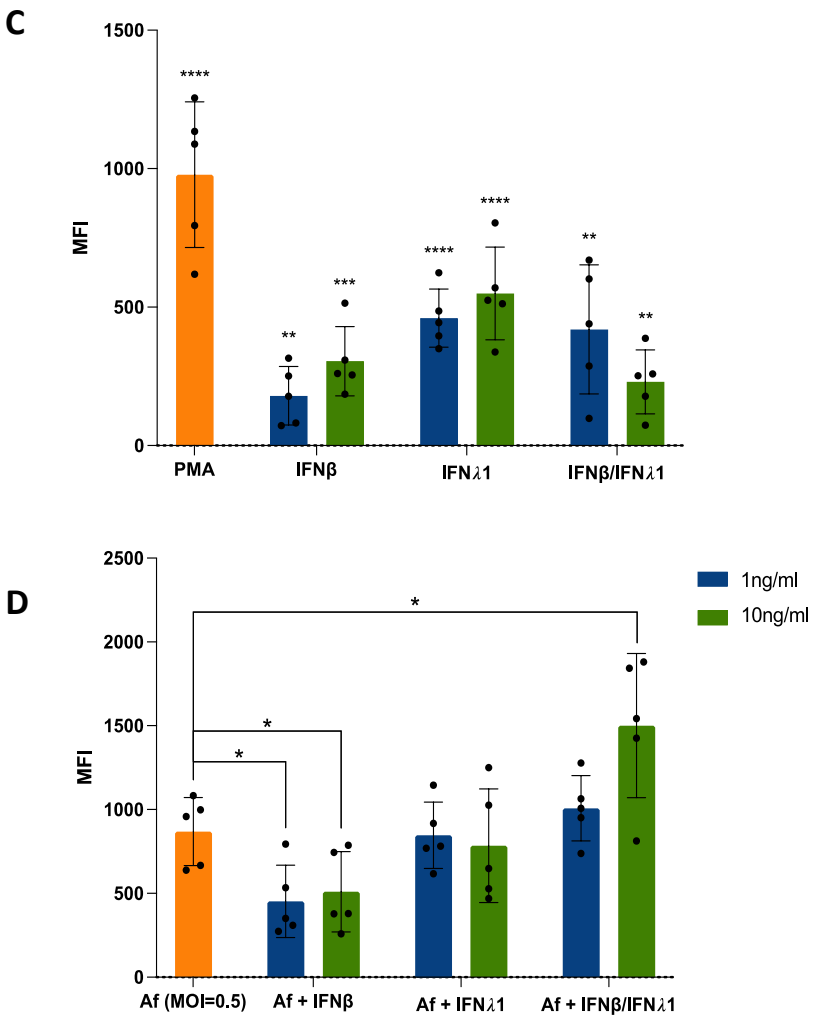

Figure 6.4.2: The effect of IFNβ and IFNλ1 on healthy neutrophil ROS and NET production. Neutrophils were isolated from 5 healthy donors and treated with either IFNβ, IFNλ1 or both together at a concentration of 1ng/μl and 10ng/μl both in the presence and absence of *Af* infection at an MOI=0.5 or MOI=1 where stated. ROS production was quantified using a Tecan plate reader over 4 hours (240 minutes) in the absence of fungal infection (A) and the addition of live swollen *Af* conidia at an MOI=1 (B). NETosis was measured after 3 hours of exogenous IFNβ, IFNλ1 or both together with and without live swollen *Af* infection (MOI=0.5) by staining with SYTOXGreen DNA stain and imaging using a Zeiss CD7 fluorescent microscope. MFI of the SYTOXGreen was calculated and background of cells alone was removed from images without fungus and data was presented as a measurement of extracellular NETs (C). Where *Af* infection was present, a second normalisation step was carried out to remove the fluorescence of the fungus, therefore MFI measurements of images with *Af* alone were also subtracted and data was presented as a measurement of extracellular NETs (D). Statistical significance was tested with two-way ANOVA for ROS data and student's T-test for the rest of the data. Data is from 5 experimental repeats (n=5). Error bars represent SD. *p<0.05, **p<0.01, ***p<0.001, ****p<0.0001.

6.4.2 – Effect of exogenous IFNβ and IFNλ1 on cystic fibrosis neutrophil function

After investigating the effects of exogenous IFN on healthy neutrophils revealed significant and interesting data, their effect on neutrophils isolated from patients with CF was next to be explored. When assessing fungal killing by measuring fungal CFU, IFNλ1 at 1ng/μl significantly reduced the number of CFU, so indicating increased fungal killing (Fig6.4.3 A). The exogenous IFN treatments had no impact of cell cytotoxicity across all conditions and concentrations (Fig6.4.3 B).

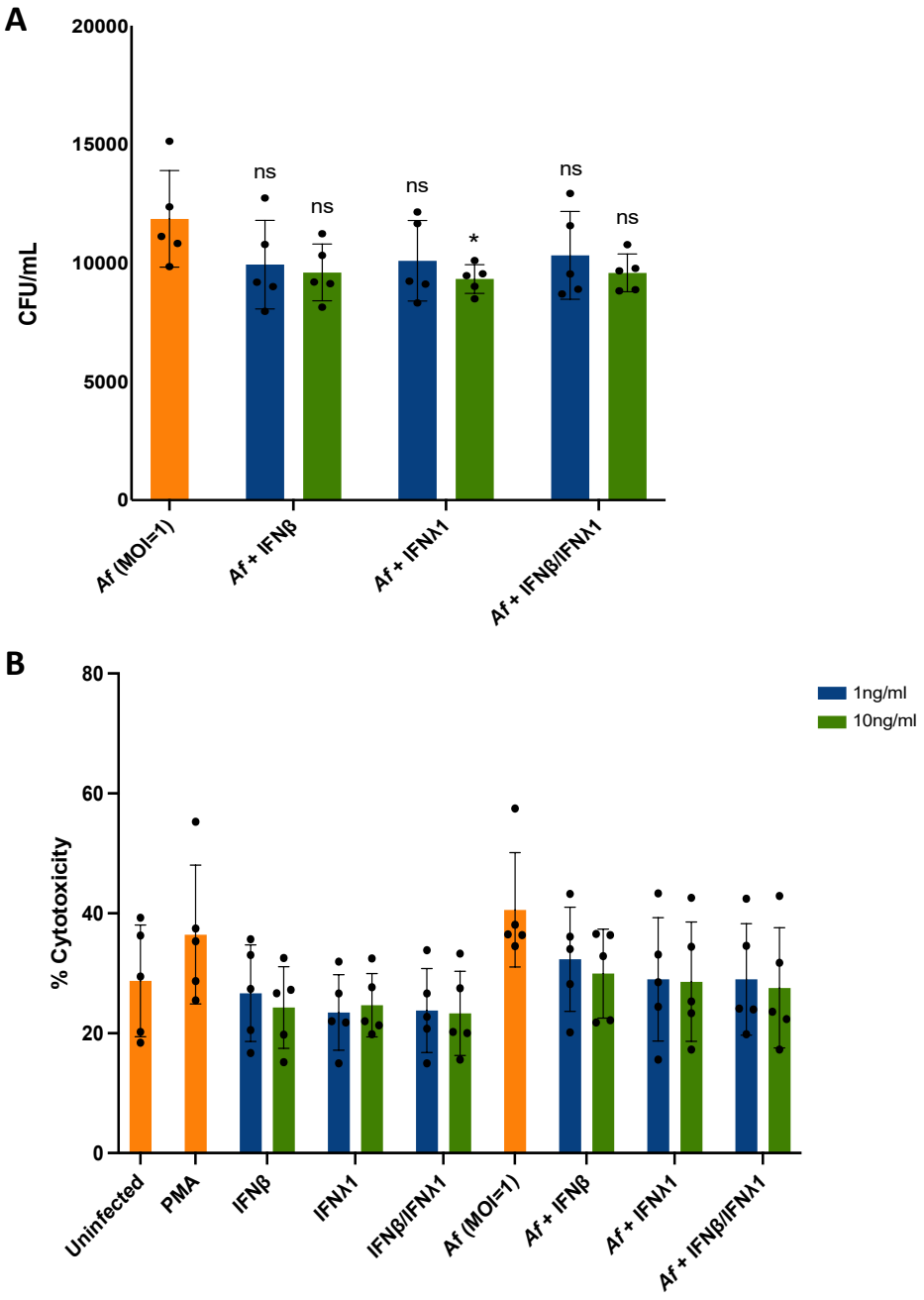

Figure 6.4.3: The effect of IFNβ and IFNλ1 on CF neutrophil fungal killing and cell survival. Neutrophils were isolated from 5 patients with CF and treated with either IFNβ, IFNλ1 or both together at a concentration of 1ng/μl and 10ng/μl both in the presence and absence of *Af* infection at an MOI=0.5 or MOI=1 where stated. CFUs were obtained from lysates of neutrophils after 3 hours of infection with the presence of exogenous IFN treatments (A). Cytotoxicity was assessed using an LDH assay on the supernatant after 3 hours of *Af* infection (B). Statistical significance was tested with two-way ANOVA for ROS data and student's T-test for the rest of the data. Data is from 5 experimental repeats (n=5). Error bars represent SD. *p<0.05, **p<0.01, ***p<0.001, ****p<0.0001.

There was no significant difference between the baseline ROS in CF patients compared to control donors, however, baseline NET production was higher in CF patients compared to health donors. Exogenous IFNβ and IFNλ1 at both 1ng/μl and 10ng/μl significantly increased ROS production in CF neutrophils, but not to the same extent as the PMA stimulated positive controls (Fig6.4.4 A). When the exogenous IFNs were added alongside fungal infection, there was a significant increase of ROS production when compared to uninfected across all conditions but IFNλ1 at both 1ng/μl and 10ng/μl significantly reduced ROS production when compared to *Af* infection alone (Fig6.4.4 B). Due to the baseline activation of CF neutrophils, there were NETs produced by unstimulated and uninfected neutrophils. Exogenous IFNβ at 1ng/μl significantly reduced NET production in CF neutrophils when added alone, but IFNβ at 10ng/μl significantly increased production of NETs (Fig6.4.4 C). IFNλ1 alone had no significant impact on NET production, but when added with IFNβ at 1ng/μl there was a significant increase. When the IFNs were added in addition to fungal infection, IFNβ had no significant effect at either concentration, but IFNλ1 at 10ng/μl and both IFNβ and IFNλ1 together at 1ng/μl and 10ng/μl concentrations significantly reduced NETosis when compared to *Af* infection alone (Fig6.4.4 D).

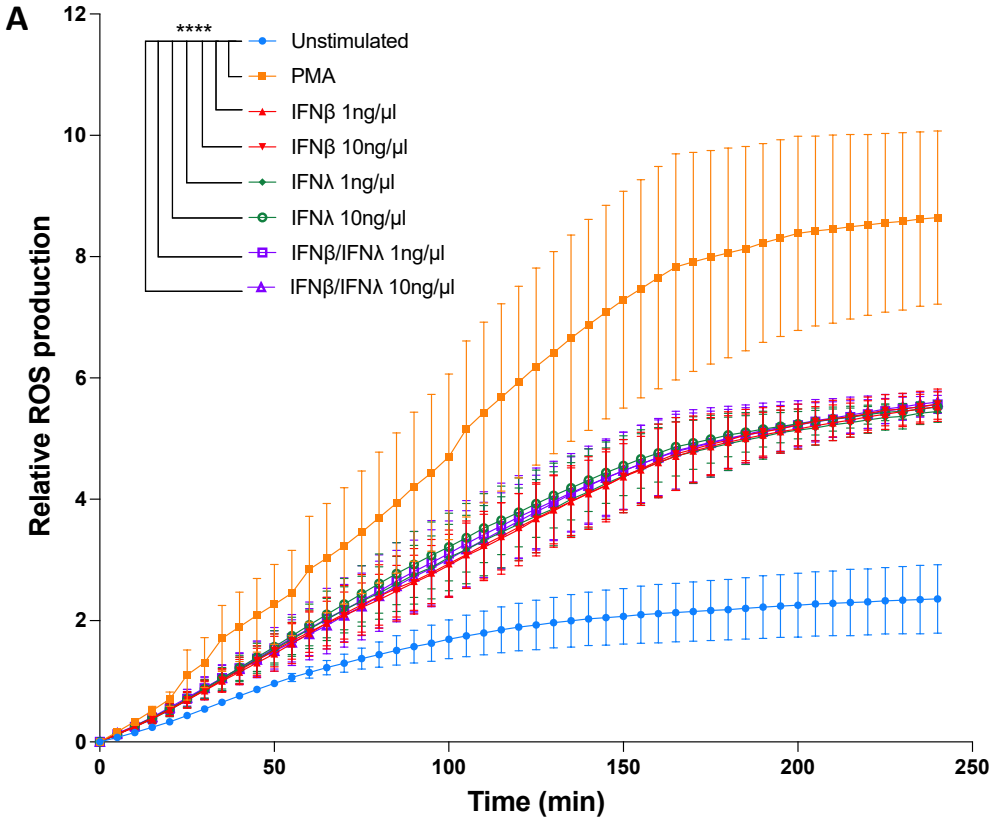
A
****
Unstimulated
PMA
IFNβ 1ng/μl
IFNβ 10ng/μl
IFNλ 1ng/μl
IFNλ 10ng/μl
IFNβ/IFNλ 1ng/μl
IFNβ/IFNλ 10ng/μl
Relative ROS production
Time (min)
0
2
4
6
8
10
12
0
50
100
150
200
250

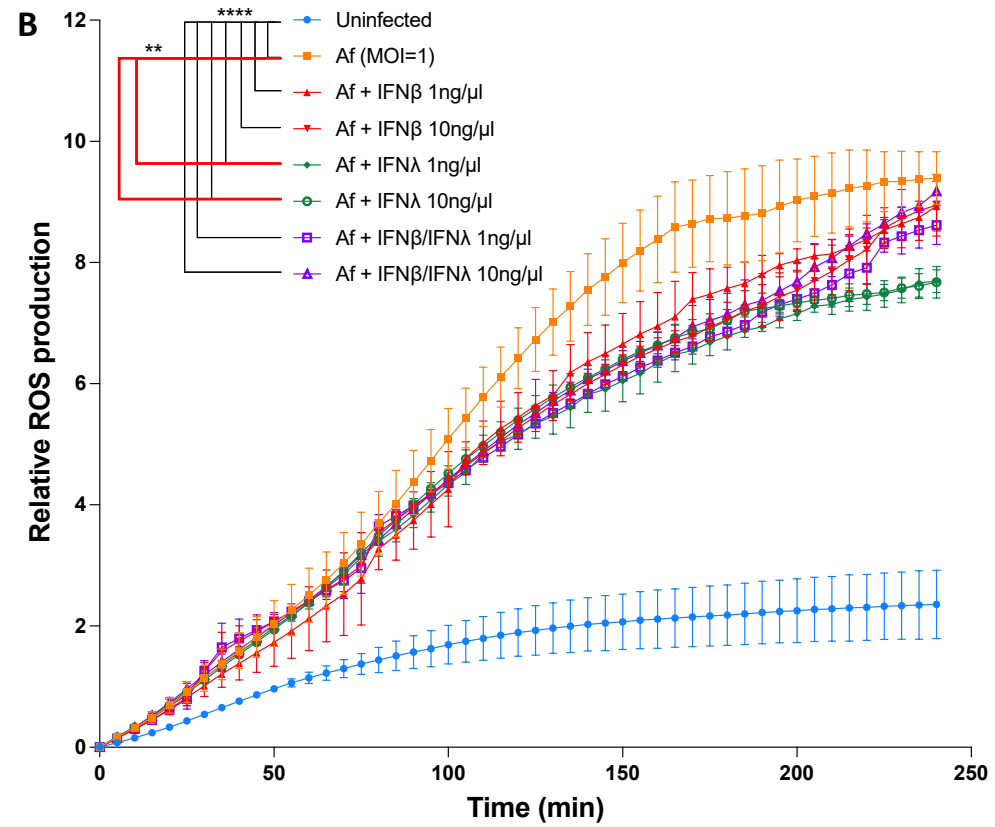
B
****
**
Uninfected
Af (MOI=1)
Af + IFNβ 1ng/μl
Af + IFNβ 10ng/μl
Af + IFNλ 1ng/μl
Af + IFNλ 10ng/μl
Af + IFNβ/IFNλ 1ng/μl
Af + IFNβ/IFNλ 10ng/μl
Relative ROS production
Time (min)
0
2
4
6
8
10
12
0
50
100
150
200
250

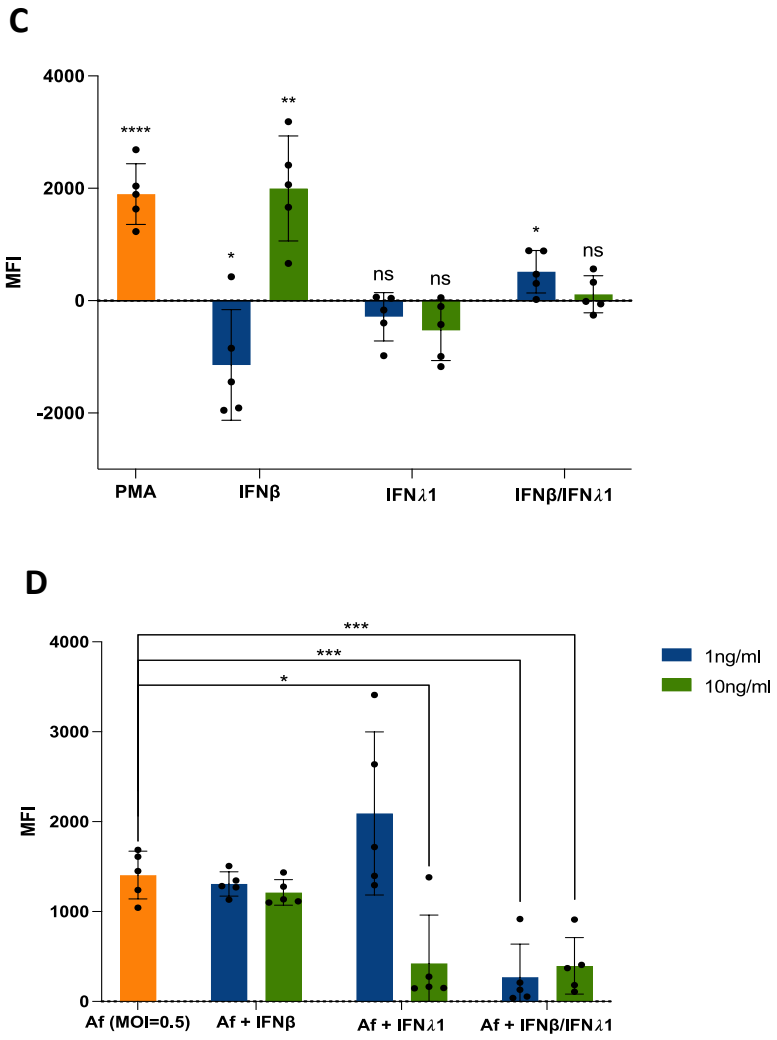

Figure 6.4.4: The effect of IFNβ and IFNλ1 on CF neutrophil ROS and NET production. Neutrophils were isolated from 5 patients with CF and treated with either IFNβ, IFNλ1 or both together at a concentration of 1ng/μl and 10ng/μl both in the presence and absence of *Af* infection at an MOI=0.5 or MOI=1 where stated. ROS production was quantified using a Tecan plate reader over 4 hours (240 minutes) in the absence of fungal infection (A) and the addition of live swollen *Af* conidia at an MOI=1 (B). NETosis was measured after 3 hours of exogenous IFNβ, IFNλ1 or both together with and without live swollen *Af* infection (MOI=0.5) by staining with SYTOXGreen DNA stain and imaging using a Zeiss CD7 fluorescent microscope. MFI of the SYTOXGreen was calculated and background of cells alone was removed from images without fungus and data was presented as a measurement of extracellular NETs (C). Where *Af* infection was present, a second normalisation step was carried out to remove the fluorescence of the fungus, therefore MFI measurements of images with *Af* alone were also subtracted and data was presented as a measurement of extracellular NETs (D). Statistical significance was tested with two-way ANOVA for ROS data and student's T-test for the rest of the data. Data is from 5 experimental repeats (n=5). Error bars represent SD. *p<0.05, **p<0.01, ***p<0.001, ****p<0.0001.

6.4.3 – CF neutrophils produce more ROS and NETs in response to *Af* compared to healthy neutrophils

The differing responses of CF and healthy neutrophils to *Af* infection was then assessed. CF neutrophils showed significantly less cytotoxicity than healthy neutrophils and their cytotoxicity seemed to be unaffected by the PMA and *Af* infection, unlike the healthy neutrophils (Fig6.4.5 B). The CF neutrophils had significantly fewer CFUs/ml after infection than healthy neutrophils, indicated increased fungal killing (Fig6.4.5 A).

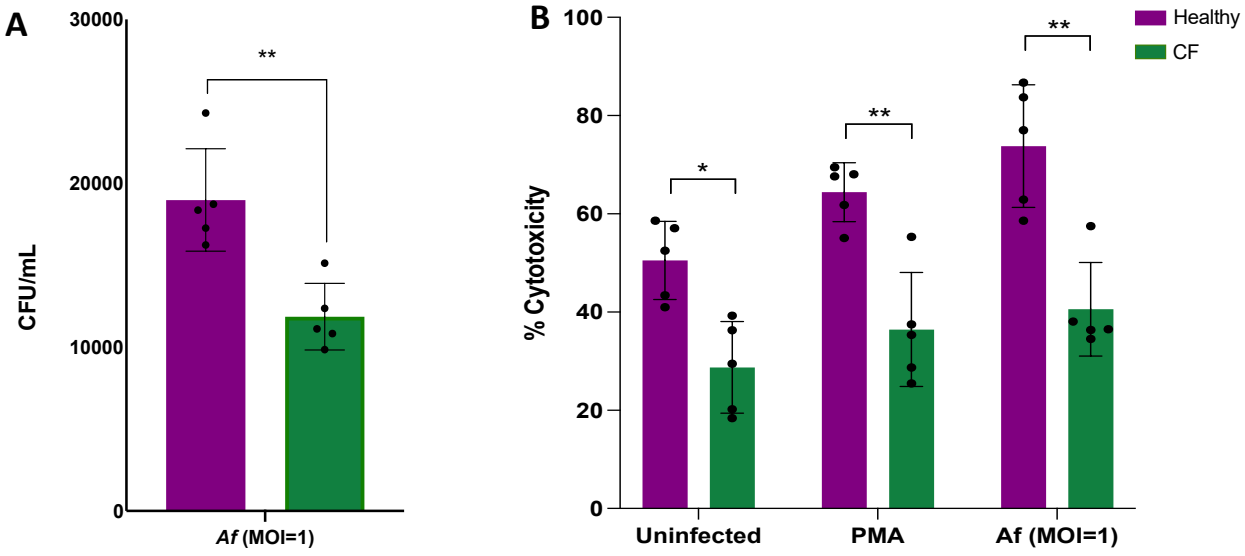

Figure 6.4.5: Comparison of CF and healthy neutrophil fungal killing and cell survival. Neutrophils were isolated from 5 healthy donors and 5 patients with CF and infected with *Af* at an MOI=0.5 or MOI=1 where stated and stimulated with PMA (20ng/μl) as a positive control. Cytotoxicity was assessed using an LDH assay on the supernatant after 3 hours of *Af* infection (C). CFUs were obtained from lysates of neutrophils after 3 hours of infection (D). Statistical significance was tested with two-way ANOVA for ROS data and student's T-test for the rest of the data. Data is from 5 experimental repeats (n=5). Error bars represent SD. *p<0.05, **p<0.01, ***p<0.001, ****p<0.0001.

CF neutrophils produced significantly more ROS after PMA stimulation and *Af* infection when compared to healthy neutrophils (Fig6.4.6 A). Despite the baseline NET production observed in the CF neutrophils, they continued to produce more NETs than healthy neutrophils after both PMA stimulation and *Af* infection (Fig6.4.6 B).

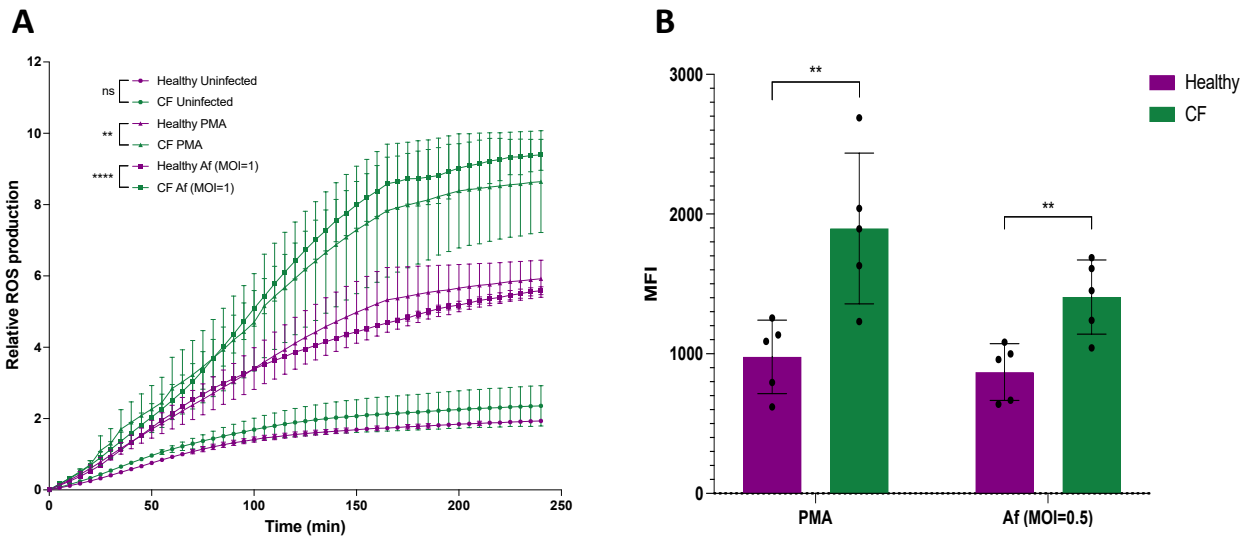

Figure 6.4.6: Comparison of CF and healthy neutrophil ROS and NET production. Neutrophils were isolated from 5 healthy donors and 5 patients with CF and infected with *Af* at an MOI=0.5 or MOI=1 where stated and stimulated with PMA (20ng/μl) as a positive control. ROS production was quantified using a Tecan plate reader over 4 hours (240 minutes) after the addition of live swollen *Af* conidia at an MOI=1 (A). NETosis was measured after 3 hours of infection with live swollen *Af* infection (MOI=0.5) by staining with SYTOXGreen DNA stain and imaging using a Zeiss CD7 fluorescent microscope. MFI of the SYTOXGreen was calculated and background of cells alone and a second normalisation step was carried out to remove the fluorescence of the fungus, therefore MFI measurements of images with *Af* alone were also subtracted and data was presented as a measurement of extracellular NETs (B). Statistical significance was tested with two-way ANOVA for ROS data and student's T-test for the rest of the data. Data is from 5 experimental repeats (n=5). Error bars represent SD. *p<0.05, **p<0.01, ***p<0.001, ****p<0.0001.

6.4.4 – Healthy neutrophils respond more to exogenous IFNβ treatment after *Af* infection compared to CF neutrophils

CF neutrophils showed significantly less cell cytotoxicity across all conditions, with and without fungus (Fig6.4.7 B). CFUs in the CF neutrophils were significantly lower in *Af* infection alone and after 1ng/μl of IFNβ, but not after 10ng/μl IFNβ as the CFU of the healthy neutrophils with the addition of 10ng/μl IFNβ has reduced to an average of 1050 CFUs/ml, similar to the 995 CFUs/ml in the CF neutrophils (Fig6.4.7 A).

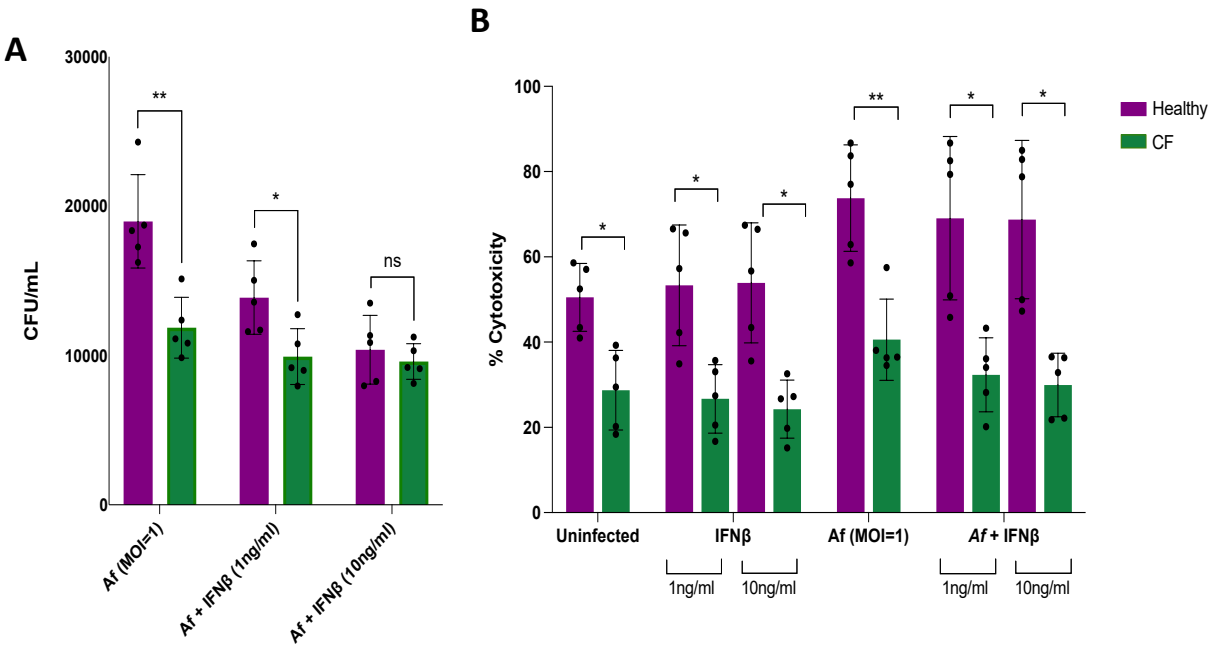

Figure 6.4.7: Comparison of the effects of IFNβ on *Af* infected healthy and CF neutrophil fungal killing and cell survival. Neutrophils were isolated from 5 healthy donors and 5 patients with CF and treated with IFNβ at a concentration of 1ng/μl and 10ng/μl both in the presence and absence of *Af* infection at an MOI=1. Cytotoxicity was assessed using an LDH assay on the supernatant after 3 hours of *Af* infection (A). CFUs were obtained from lysates of neutrophils after 3 hours of infection with the presence of exogenous IFN treatments (B). Statistical significance was tested with two-way ANOVA for ROS data and student's T-test for the rest of the data. Data is from 5 experimental repeats (n=5). Error bars represent SD. *p<0.05, **p<0.01, ***p<0.001, ****p<0.0001.

When comparing the effect of the exogenous IFNβ, despite healthy neutrophils producing significantly more ROS than their uninfected control after addition of 1ng/μl IFNβ, CF neutrophils produced significantly more ROS after 1 and 10ng/μl IFNβ, both in the presence and absence of *Af* infection (Fig6.4.8 A, B). 10ng/μl of IFNβ alone caused a significant increase of NET production in CF cells compared to neutrophils and when IFNβ was added with fungal infection, CF neutrophils also produced significantly more NETs than healthy cells (Fig6.4.8 C).

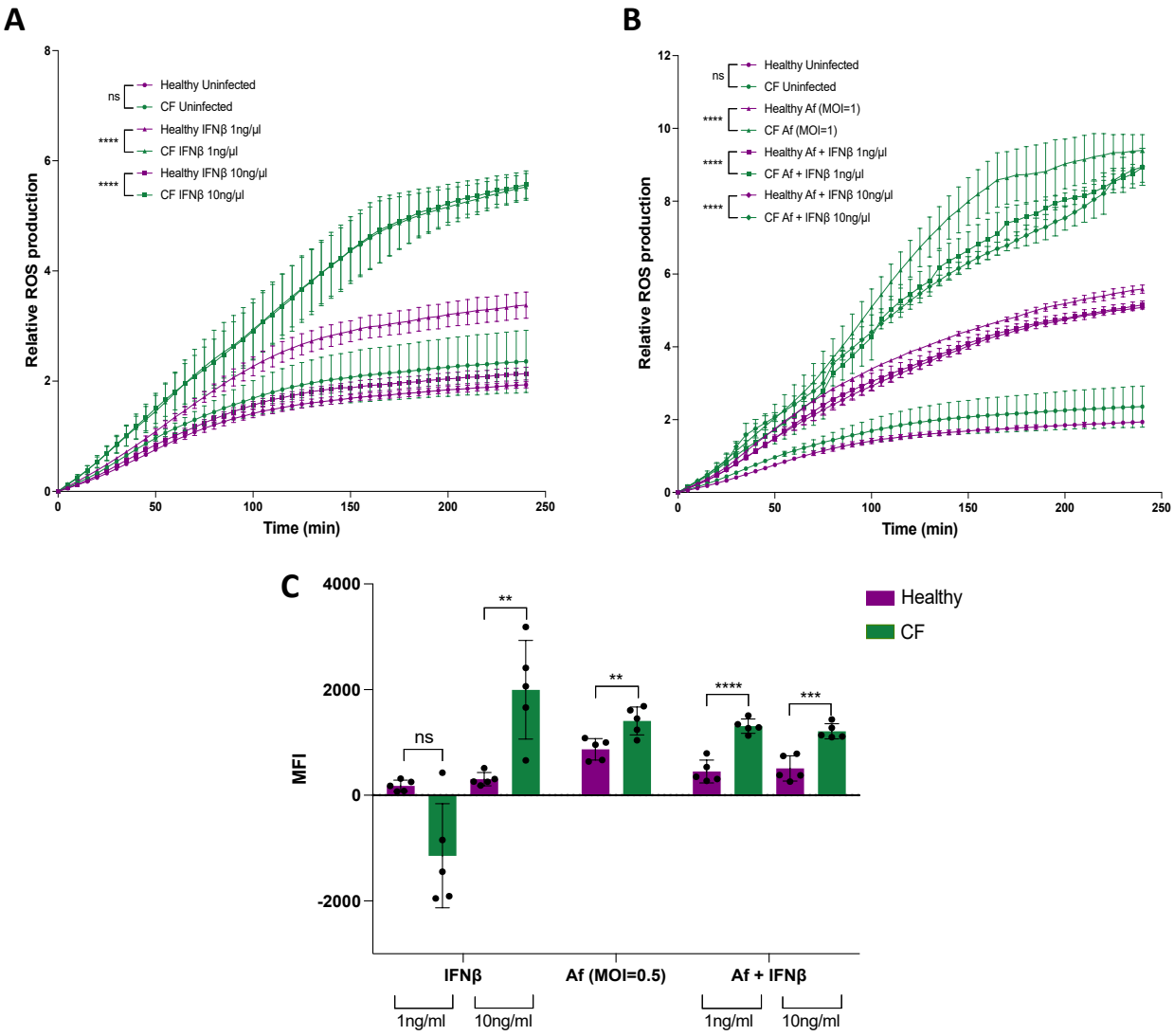

Figure 6.4.8: Comparison of the effects of IFNβ on *Af* infected healthy and CF neutrophil ROS and NET production. Neutrophils were isolated from 5 healthy donors and 5 patients with CF and treated with IFNβ at a concentration of 1ng/μl and 10ng/μl both in the presence and absence of *Af* infection at an

MOI=0.5 or MOI=1 where stated. ROS production was quantified using a Tecan plate reader over 4 hours (240 minutes) in the absence of fungal infection (A) and the addition of live swollen *Af* conidia at an MOI=1 (B). NETosis was measured after 3 hours of exogenous IFNβ with and without live swollen *Af* infection (MOI=0.5) by staining with SYTOXGreen DNA stain and imaging using a Zeiss CD7 fluorescent microscope. MFI of the SYTOXGreen was calculated and background of cells alone was removed from images without fungus and data was presented as a measurement of extracellular NETs. Where *Af* infection was present, a second normalisation step was carried out to remove the fluorescence of the fungus, therefore MFI measurements of images with *Af* alone were also subtracted and data was presented as a measurement of extracellular NETs (C). Statistical significance was tested with two-way ANOVA for ROS data and student's T-test for the rest of the data. Data is from 5 experimental repeats (n=5). Error bars represent SD. *p<0.05, **p<0.01, ***p<0.001, ****p<0.0001.

6.4.5 – Healthy neutrophils respond more to exogenous IFNλ1 treatment after *Af* infection compared to CF neutrophils

When assessing the differing effects of IFNλ1 in healthy and CF neutrophils with and without *Af* infection, it was clear that there was significantly less cell cytotoxicity in the CF neutrophils across all conditions compared to healthy (Fig6.4.9 B), but no significant difference in the CFU/ml in the CF or healthy neutrophils after IFNλ1 treatment at both 1 and 10ng/μl (Fig6.4.9 A).

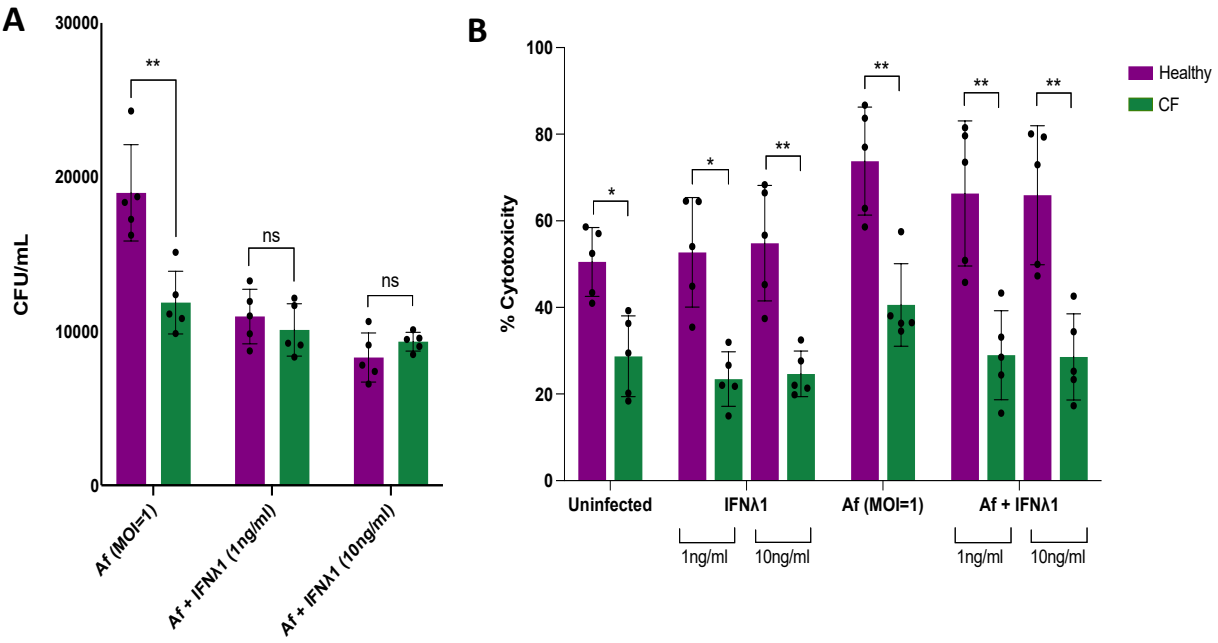

Figure 6.4.9 Comparison of the effects of IFNλ1 on *Af* infected healthy and CF neutrophil fungal killing and cell survival. Neutrophils were isolated from 5 healthy donors and 5 patients with CF and treated with IFNλ1 at a concentration of 1ng/μl and 10ng/μl both in the presence and absence of *Af* infection at an MOI=0.5 or MOI=1 where stated. CFUs were obtained from lysates of neutrophils after 3 hours of infection with the presence of exogenous IFN treatments (A). Cytotoxicity was assessed using an LDH assay on the supernatant after 3 hours of *Af* infection (B). Statistical significance was tested with two-way ANOVA for ROS data and student's T-test for the rest of the data. Data is from 5 experimental repeats (n=5). Error bars represent SD. *p<0.05, **p<0.01, ***p<0.001, ****p<0.0001.

IFNλ1 at 1 and 10ng/μl alone induced significantly more ROS in the CF neutrophils compared to healthy (Fig6.4.10 A). Despite the reduction in ROS production when IFNλ1 was added in the presence of *Af* infection in CF neutrophils, they still produced significantly more ROS than the healthy cells in the presence of *Af* and *Af* with IFNλ1 (Fig6.4.10 B). IFNλ1 at both concentrations lead to CF neutrophils producing significantly fewer NETs than healthy neutrophils in the absence of *Af* infection, but significantly more NETs were produced by the CF neutrophils with IFNλ1 at 1ng/μl in the presence of *Af* (Fig6.4.10 C).

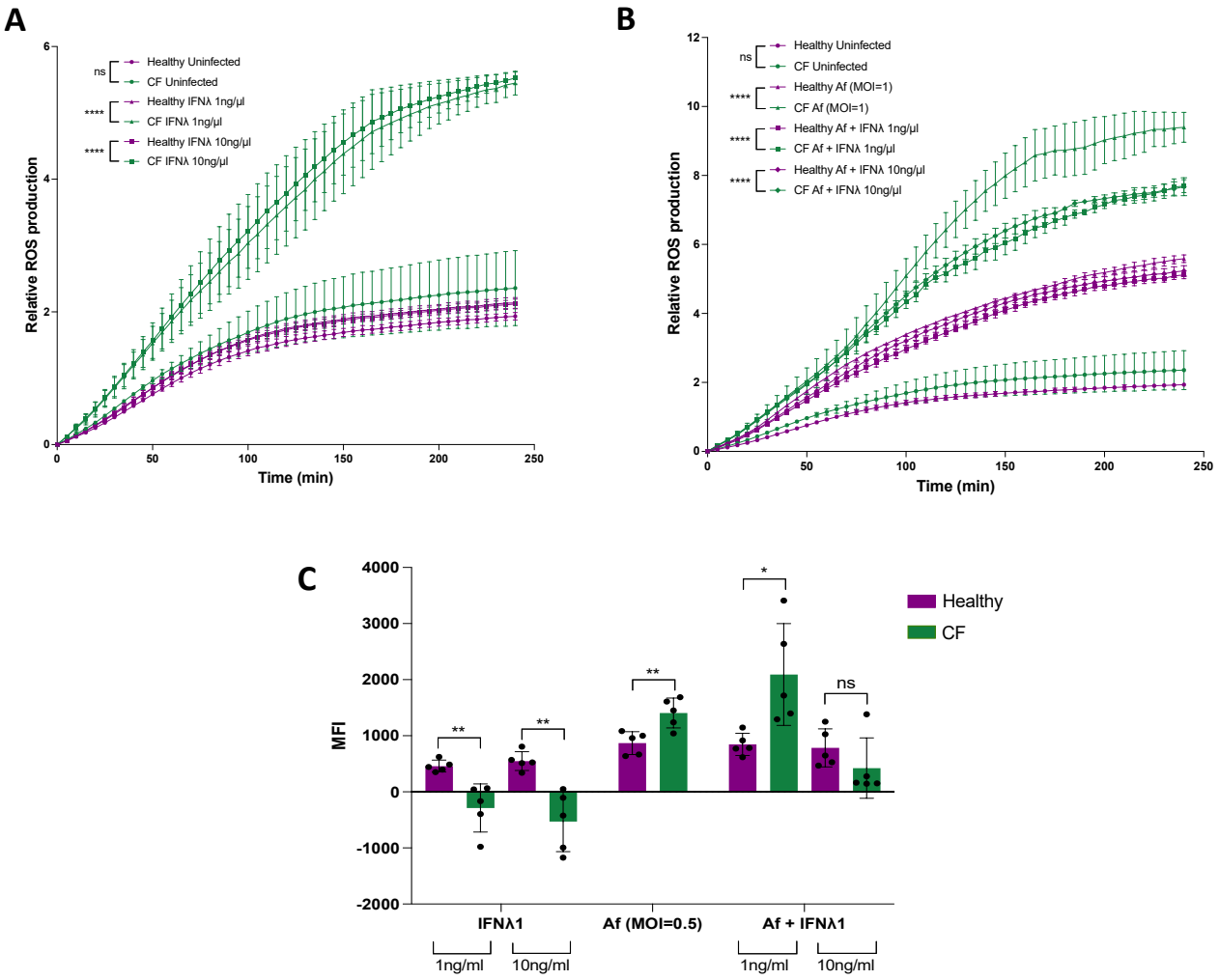

Figure 6.4.10: Comparison of the effects of IFNλ1 on *Af* infected healthy and CF neutrophil ROS and NET production. Neutrophils were isolated from 5 healthy donors and 5 patients with CF and treated with IFNλ1 at a concentration of 1ng/μl and 10ng/μl both in the presence and absence of *Af* infection at an

MOI=0.5 or MOI=1 where stated. ROS production was quantified using a Tecan plate reader over 4 hours (240 minutes) in the absence of fungal infection (A) and the addition of live swollen *Af* conidia at an MOI=1 (B). NETosis was measured after 3 hours of exogenous IFNλ1 with and without live swollen *Af* infection (MOI=0.5) by staining with SYTOXGreen DNA stain and imaging using a Zeiss CD7 fluorescent microscope. MFI of the SYTOXGreen was calculated and background of cells alone was removed from images without fungus and where *Af* infection was present, a second normalisation step was carried out to remove the fluorescence of the fungus, therefore MFI measurements of images with *Af* alone were also subtracted and data was presented as a measurement of extracellular NETs (C). Statistical significance was tested with two-way ANOVA for ROS data and student's T-test for the rest of the data. Data is from 5 experimental repeats (n=5). Error bars represent SD. *p<0.05, **p<0.01, ***p<0.001, ****p<0.0001.

6.4.6 – Healthy neutrophils respond more to both exogenous IFNβ and IFNλ1 treatment together after *Af* infection compared to CF neutrophils

When assessing the effects of treatment of both IFNβ and IFNλ1 together there was no significant difference between the CFUs/ml of the two types of cells treatment at both concentrations (Fig6.4.11 A). CF neutrophils showed lower cytotoxicity throughout all conditions than the healthy neutrophils (Fig6.4.11 B).

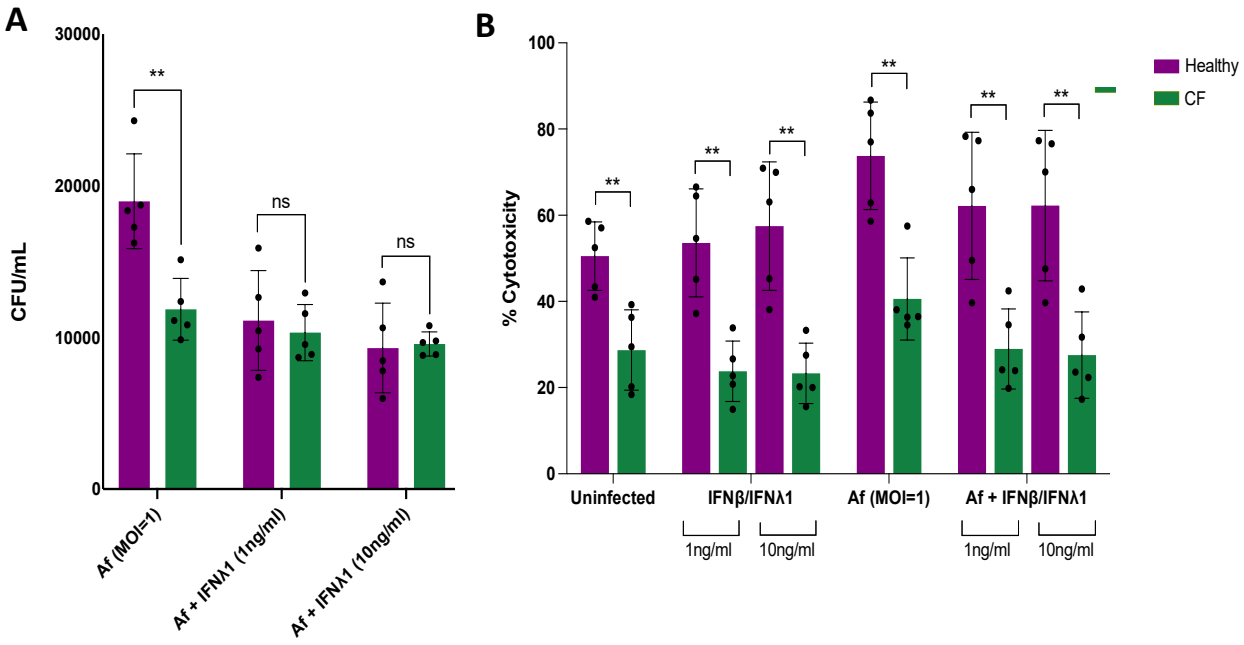

Figure 6.4.11: Comparison of the effects of both IFNβ and IFNλ1 on *Af* infected healthy and CF neutrophil ROS and NET production. Neutrophils were isolated from 5 healthy donors and 5 patients with CF and treated with IFNβ/IFNλ1 at a concentration of 1ng/μl and 10ng/μl both in the presence and absence of *Af* infection at an MOI=0.5 or MOI=1 where stated. CFUs were obtained from lysates of neutrophils after 3 hours of infection with the presence of exogenous IFN treatments (A). Cytotoxicity was assessed using an LDH assay on the supernatant after 3 hours of *Af* infection (B). Statistical significance was tested with two-way ANOVA for ROS data and student's T-test for the rest of the data. Data is from 5 experimental repeats (n=5). Error bars represent SD. *p<0.05, **p<0.01, ***p<0.001, ****p<0.0001.

Significantly more ROS was produced by the CF neutrophils after treatment at both concentrations both in the presence and absence of fungal infection (Fig6.4.12 A, B). CF neutrophils produced significantly fewer NETs after IFNβ and IFNλ1 treatment in the presence of fungal infection, but there were no significant differences in the NET production with IFNβ and IFNλ1 alone (Fig6.4.12 C).

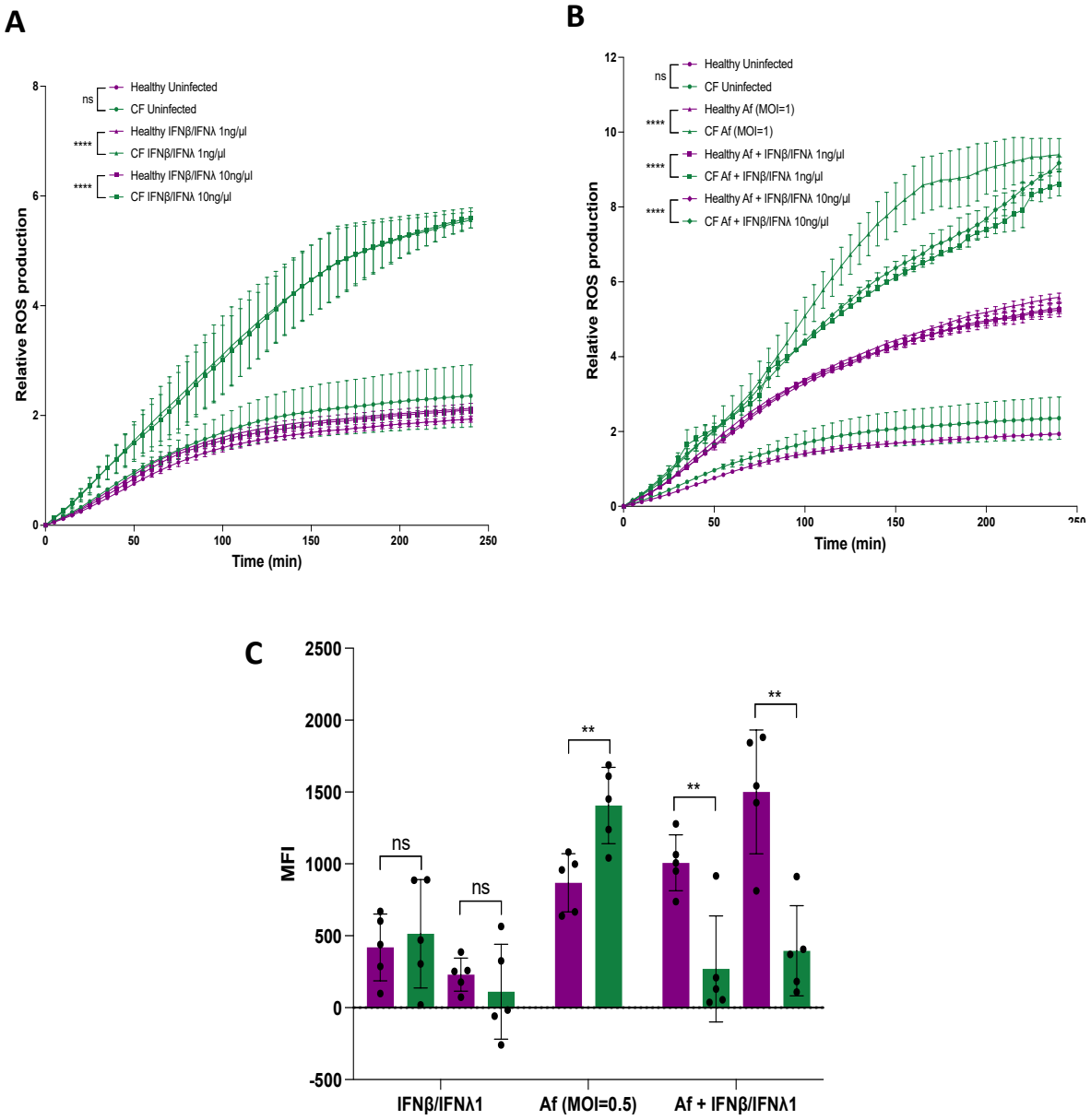

Figure 6.4.12: Comparison of the effects of IFNβ/IFNλ1 on *Af* infected healthy and CF neutrophil ROS and NET production. Neutrophils were isolated from 5 healthy donors and 5 patients with CF and treated with IFNβ/IFNλ1 at a concentration of 1ng/µl and 10ng/µl both in the presence and absence

of *Af* infection at an MOI=0.5 or MOI=1 where stated. ROS production was quantified using a Tecan plate reader over 4 hours (240 minutes) in the absence of fungal infection (A) and the addition of live swollen *Af* conidia at an MOI=1 (B). NETosis was measured after 3 hours of exogenous IFNβ/IFNλ1 with and without live swollen *Af* infection (MOI=0.5) by staining with SYTOXGreen DNA stain and imaging using a Zeiss CD7 fluorescent microscope. MFI of the SYTOXGreen was calculated and background of cells alone was removed from images without fungus and where *Af* infection was present, a second normalisation step was carried out to remove the fluorescence of the fungus, therefore MFI measurements of images with *Af* alone were also subtracted and data was presented as a measurement of extracellular NETs (C). Statistical significance was tested with two-way ANOVA for ROS data and student's T-test for the rest of the data. Data is from 5 experimental repeats (n=5). Error bars represent SD. *p<0.05, **p<0.01, ***p<0.001, ****p<0.0001.

6.5 – Discussion

The data in this chapter shows exogenous IFNβ and IFNλ1 treatments have no effect on the swelling or germination of CEA10 or dsRed *Af* alone. When neutrophils were isolated from healthy donors and infected with *Af*, IFNλ1 treatment at both high (10ng/μl) and low (1ng/μl) concentrations and IFNβ/IFNλ1 treatment at the higher concentration (10ng/μl) significantly decreased the number of CFUs collected after infection, signifying increased fungal killing. When observing cytotoxicity, there was significantly increased neutrophil cytotoxicity after IFNλ1 and IFNβ/IFNλ1 treatment at both concentrations when compared to fungal infection alone. Neutrophil killing involves several self-destructive mechanisms including NETosis, degranulation, and phagocytosis resulting in extensive oxidative burst which damages the cell. Therefore, the increase in cell cytotoxicity could be a direct consequence of increased neutrophil activation and fungal killing. To attempt to determine the mechanism of which fungal killing occurs, ROS and NET production where assessed. Low concentration IFNβ treatment (1ng/μl) alone increased ROS production in the neutrophils isolated from healthy donors, but no other IFNβ or IFNλ1 treatments had a significant affect. When the IFN treatment was coupled with *Af* infection, none of the treatments had any significant effect when compared to fungal infection alone. When observing NET production in the presence of IFN treatments alone, the healthy neutrophils produced significantly more NETs after all treatments, with IFNλ1 initiating the strongest NETosis response. In the presence of *Af* infection, IFNβ at both high and low concentrations significantly reduced NET production and IFNβ/IFNλ1 at 10ng/μl significantly increased NET production when compared to *Af* infection alone. When the same experiments were carried out in neutrophils isolated from patients with CF, only IFNλ1 treatment at high (10ng/μl) concentration significantly reduced the CFU

count after infection and there was no significant difference in cell cytotoxicity across all treatments and infections. All IFN treatments alone significantly increased ROS production, and interestingly, in the presence of fungal infection, IFNλ1 treatment at both high (10ng/μl) and low (1ng/μl) concentrations significantly reduced ROS production when compared to *Af* infection alone. There was baseline neutrophil activation in the cells isolated from patients with CF, resulting in NET production by the uninfected cells and accounting for the negative results observed in Fig6.4.4 C. Low concentration IFNβ treatment significantly reduced NETosis, while high concentration IFNβ treatment significantly increased it. IFNλ1 treatment didn't have a significant effect on NET production. IFNβ/IFNλ1 treatment significantly increased NET production at the lower concentration but had no effect at the higher concentration. In the presence of *Af* infection, high concentration IFNλ1 and both concentrations of IFNβ/IFNλ1 treatment significantly decreased NET production when compared to *Af* infection alone. Therefore, IFNβ has been shown to have a direct effect on antifungal neutrophil function in healthy neutrophils through reducing NET production but has no effect alone on fungal killing. IFNλ1 significantly improved fungal killing in healthy neutrophils and reduced neutrophil survival but had no significant effect on ROS or NET production in the presence of fungus. When IFNβ and IFNλ1 were used together, there was an increase in NET production at 10ng/μl which resulted in an increase of fungal killing. In CF neutrophils, however, significant improvement in fungal killing was only observed at 10ng/μl and this was coupled with an observation of reduced NETosis and ROS production.

When comparing the neutrophil responses of those isolated from healthy donors and from patients with CF, there was significantly more fungal killing and reduced cell cytotoxicity observed in CF neutrophils. As described in section 6.1, increased neutrophil life span is a

contributing factor to the neutrophilic inflammation observed in patients with CF. Increased fungal killing observed in the neutrophils isolated from patients with CF was an unexpected finding, however, this could be due to the CF neutrophils having already been exposed to and, therefore, primed towards an antifungal response whereas healthy neutrophils have not been exposed to *Af* before. Neutrophils isolated from patients with CF produced significantly less ROS and NETs compared to healthy without the presence of IFN treatments. Healthy neutrophils responded more readily to all IFN treatments compared to CF neutrophils.

Espinosa et al., published the first paper linking antifungal neutrophil response to type I and III IFN responses[163]. Their work used a mouse model to show that $CCR2^{+}$ monocytes are required to produce type I IFNs to prime for type III IFN release which are required for optimal antifungal neutrophil ROS production and neutrophil specific deletion of IFNLR1 and STAT1 increased mortality in mice due to invasive aspergillosis. Although they showed that human neutrophils also express IFNLR1, the rest of their work was in a mouse model and none of this has been linked to CF. Further work from this group shows dectin-1 is critical for the induction of the type I and III IFN response, however, all this work was carried out in mice[141]. Therefore, this is the first work showing IFNβ and IFNλ1 treatments can have a direct effect on human antifungal neutrophil responses and, importantly, increased fungal killing in both healthy and CF human neutrophils after IFNλ1 treatment.

There is limited understanding on whether NETosis is essential for pathogen protection or if it contributes more to a damaging inflammatory response. Excessive NETosis has been linked to many neutrophilic inflammatory pathologies such as systemic lupus erythematosus and sepsis[370, 371]. As described in the introduction (section 1.1.2), NETs consist of a meshwork of DNA, MPO, NE, lactoferrin-chelating proteins, and other pro-inflammatory molecules[372].

Therefore, they are a major source of inflammation as well as inducing coagulation through activating platelets[373]. This can result in inflammation driven tissue damage and severe vascular injury and thrombosis. Increased levels of DNA in sputum from CF patients further increases viscosity of the mucus and is associated with increased disease progression and lung function decline. It is now known that a significant amount of this DNA is sourced from NET production[60]. Despite their excess inflammatory properties, NETs have been shown to be able to trap and arrest fungal growth but have yet to be shown to kill fungus directly[369]. The data in this chapter suggests NETs are more involved in inflammation than killing as conditions resulting in reduction of NETs also resulted in improved fungal killing.

Limitations in this chapter include the number of patient samples used. As mentioned in the previous chapter, the COVID-19 pandemic limited recruitment time and frequency resulting in the smaller patient groups represented in this project. There is also variation in the CFTR mutations present in the CF patient samples, this was again a time specific issue that would have been avoided if possible. Furthermore, the ROS assay used measures the amount of hydroxl (OH), peroxides (O-O), and other ROS intermediates in the cell as one measurement, therefore, it was not possible to measure any differences between the composition of the ROS in the CF neutrophils compared to healthy neutrophils. Finally, due to the method used for NET production, it was not possible to look for mechanistic or timing differences between cell types and in different conditions as cells were fixed at 3 hours post infection for measurement. Further work would include larger patient groups and an assessment of neutrophil phagocytosis. As described in section 1.2.6, defective acidification of the phagolysosome through the lack of Cl^- ions reacting with H_2O_2 and MPO to form HOCl is another key contributor to reduced microbe clearance in CF patients.

This work may have clinical implications, if addition of IFNλ1 is confirmed to improve fungal clearance, while reducing the overactive NET and ROS production and the resulting sustained inflammation in CF airway, this would be an effective alternative to antifungal treatments. The importance of this is furthered by the emergence of antifungal resistance among CF patients.

Chapter 7: Discussion

The work in this thesis has demonstrated a novel downregulation of the epithelial type I and III IFN response in the presence of *Af* infection at the transcriptional level using analysis of the interferome and confirmatory RT-PCR in cells with a CFTR mutation. The data has shown that this defect is CFTR dependent as the CF corrected cell line used throughout the study as a control was only genetically corrected for the common CF-causing mutation it possessed, the *F508del* mutation. Furthermore, the disease phenotype was partially corrected through the use of CFTR modulator therapy. As the same defect was not observed in PBMCs isolated from patients with CF, this could suggest a mucosal-specific defect, however, restricted patient sampling and recently published conflicting data means further investigations are required to confirm this[41]. This work provides further understanding of the defect observed in the type I and III IFN response in cells with a CFTR mutation that has been established during both viral and bacterial infections but that has not been investigated in fungal infections previously[38-40]. With the statistics stating that up to 60% of CF patients worldwide provide positive *Af* cultures and work published in 2018 indicating the importance of both the type I and III IFN response in optimal anti-fungal neutrophil responses, the thesis investigates this link in a timely fashion[141, 163, 257]. The translational importance of the type I and III IFN defect was determined through exogenous IFNλ1 treatment of CF neutrophils resulting in increased antifungal killing without increasing inflammatory ROS or NET production. This provides an exciting prospective immunotherapy option to reduce fungal infection rates in patients with CF with the additional benefits of reducing the inflammatory milieu characteristic of the disease. Additionally, the recent clinical trials purposing pegylated interferon lambda for the

treatment of COVID-19 means there is an existing approved medication that can be repurposed to this effect[337].

CF is not the only respiratory disease that has been linked to a defect in the type I and III IFN response[374, 375]. Conflicting data has been published regarding this response in COPD patients, with some reporting IFNβ expression rates 40-65% lower in lower lung cells compared to healthy, while another showing an increased response compared to healthy[374, 376, 377]. The contradictory nature of these studies could be explained through differing sample types, such as sputum or cells, and the variation in numbers of patients sampled which range from 8 to 70. Similarly, severe asthmatics can present with impaired type I and III IFN response resulting in increased susceptibility to infection and a worsening of uncontrolled type 2 immunity, all increasing inflammation, and exacerbating symptoms[375, 378, 379]. Again, however, not all asthmatics have a deficient IFN response[378]. CF, COPD, and severe asthma are all conditions in which susceptibility to fungal infection is a main risk factor which contributes to disease progression and lung function decline[380, 381]. Therefore, translationally, an understanding of this defect and what it means for antifungal effector cells has the potential to improve morbidity and treatment across multiple lung conditions the importance of which is furthered with the rise an azole resistance observed in *Af* strains over the past few years[124, 126-128].

The introduction of CFTR modulators to CF care has posed questions surrounding the requirement of further investment into CF research and further treatments. Despite the evidence in this study that the modulators can alter and direct the disease phenotype towards a healthier one, it has been shown this is likely to be a partial rescue rather than a full restoration of the type I and III IFN response. Additionally, CFTR modulators do not work for

all CF-causing mutations leaving 10% of the CF population exempt and, of those that qualify, some cannot tolerate the medication due to side effects and drug-drug interactions[84, 382, 383]. Ultimately, CF is a lifelong disease which requires daily medication and treatments and there is little evidence of the long-term effects of CFTR modulator therapy, or what the treatment landscape of an aging CF population will look like. Sustained residual inflammation observed in patients with HIV is known to increase the risk of kidney, liver, and heart disease as well as quicken the development of metabolic and cognitive impairment[384]. Therefore, despite breakthrough research and medications, there is still an unmet medical need in the treatment of CF that needs to be addressed.

CF and CF corrected BECs were infected for 12 or 24 hours with *Af* heat killed conidia or fixed hyphae before RNA extraction for transcriptome profiling and bulk RNA sequencing. NLRC3 expression was increased in CF BECs both in the presence and absence of fungal infection and its expression was reduced by CFTR modulator treatment. Additionally, GSEA identified a downregulation in the TRAF6-mediated IRF7 activation pathway in CF cells. TRAF6 has been described as a functional partner of NLRC3 and it has been shown that NLRC3 can prevent TRAF6 autoubiquitination and, therefore, inhibit activation and down-stream signalling[352]. IRF7 binding sites are present on the genes encoding both type I and III IFNs so a reduction in IRF7 activation would reduce the expression of both type I and III IFNs[36, 385, 386]. Furthermore, NLRC3 modulates STING activity by directly associating and preventing translocation to the nucleus[355, 387]. It has also been shown that NLRC3 can interact with TBK1 to interfere with the interaction between TBK1 and STING, essential in the activation of IRF3 which, again, is involved in the expression of both type I and III IFNs[36, 353, 387]. Questions remain regarding how NLRC3 is directly affected by CFTR and should be investigated further, however, there has

been some evidence of other NLR family proteins being directly affected by CFTR[353]. Previously, elevated NLRP3 expression was decreased in patients with CF after three months of Trikafta therapy[388]. This downregulation correlated with reduced intracellular chloride concentrations and reduced P2X7R expression[256]. Additionally, K^+ efflux is a principal trigger for NLRP3 inflammasome activation and another study showed CFTR modulator treatment reduced Na^+ and K^+ transport dysregulation and, therefore, reduced the exaggerated inflammatory response observed[389, 390]. To confirm the increased expression of NLRC3 and the impact of this in cells with a CFTR mutation, confirmatory RT-PCR should be carried out along with ELISA to assess protein levels and *Af* infection experiments using NLRC3 KO cell lines. Additionally, NLRC3 expression should be assessed in PBMCs and immune cells such as neutrophils and the impact of increased expression should be investigated.

Neutrophils isolated from patients with CF were infected with live *Af* in the presence or absence of exogenous IFNβ or IFNλ1 treatment. Exogenous IFNλ1 treatment of CF neutrophils resulted in increased antifungal killing without increasing inflammatory ROS or NET production and IFNβ treatment had no significant effect on fungal killing, cell cytotoxicity or NET and ROS production in CF neutrophils. IFNβ and IFNλ1 treatment together reduced NET production but had no significant impact on ROS production or overall fungal killing. Reduction in NET production would have an overall anti-inflammatory effect as discussed in Section 6.5[49, 52]. ROS production also has inflammatory properties but is essential in microbial killing[171, 368]. This poses the question of how the IFNλ1 treatment in CF neutrophils resulted in an increase in fungal killing while also reducing ROS and NET production. As previously mentioned, Espinosa et al. reported the importance of type III IFN production to promote optimal antifungal ROS neutrophil responses, with less of an impact on cellular recruitment

and pro-inflammatory cytokine production[163, 195]. Although the mechanisms by which IFNλ controls this response are unknown, it is hypothesised to be STAT1-dependent and involve optimal NADPH enzyme expression in the phagosome[163]. The importance of neutrophilic ROS in fungal immunity is highlighted by the extreme susceptibility to fungal infection observed in patients with NADPH oxidase deficiencies such as in CGD[204, 391-393]. Neutrophils kill fungus through various mechanisms, of which only two have been investigated here. Nutritional starvation of small metals such as iron and zinc and neutrophil activated secretory granule release are other methods of fungal killing that should be investigated alongside IFN treatment to determine why the data has shown a decrease in CFU counts[368]. Phagocytosis of *Af* is impaired in patients with CF as described in the introduction (section 1.2.6), therefore, this could be a method of fungal killing that has been enhanced with IFNλ1 treatment and further work would need to be carried out to this effect.

The heat killed or fixed forms of *Af* were chosen as they elicited a type I and III IFN response in healthy BECs and live forms of fungus would not have been tolerated by the BEC culture. Future work should consider BEC/neutrophil co-cultures with low MOI live *Af* infection analysed in a time course manner to assess the differential responses throughout the fungal life cycle. It is also important to consider the complex nature of the lung epithelium and how this contributes to the disease phenotype. This has been recently considered in the context of fungal infection interactions and included how cell line work does not fully capture the relevant host epithelium-fungal interactions, for example, the lack of CFTR expressing ionocytes which regulate ion transport, fluid levels, and pH in the epithelium[394]. Submerged cell line culture doesn't allow assessment of the wider complexity; therefore, ALI culture of a CF primary cell line was used to begin to explore this. Although beneficial, further work with

the CF primary cell line ALI culture would restrict this analysis to just homozygous *F508del* mutation. To address this, nasal samples collected from patients with CF could be cultured to ALI and holistic approaches such as nasal ALI and immune cell co-cultures would allow *ex vivo* assessment of this response.

At the start of this thesis, it was hypothesised that there is a downregulated type I and type III IFN response during *Af* infection in cells with a CFTR mutation and that this defect results in reduced fungal clearance by CF neutrophils. The evidence presented accepts that there is a downregulated type I and III IFN response during *Af* infection in CF cells. The data further shows that exogenous IFNλ1 treatment does have a significant impact on fungal killing and therefore fungal clearance, but that IFNβ treatment does not. Therefore, despite both the type I and III IFN response being downregulated in cells with a CF-causing mutation, only the defect in the type III IFN response is having a direct impact on neutrophilic fungal killing ability.

7.1 – Concluding Remarks

In aggregate, this thesis presents for the first time a CFTR-dependent defect in the type I and III IFN response in epithelial cells, but not PBMCs, with a CFTR mutation in the presence of *Af* infection. This response was shown to be partially rescued by the administration of combination CFTR modulator treatment. There is evidence for the mechanisms underpinning this response as being directly related to an upregulation of NLRC3 expression and subsequent downregulation of STING mediated IRF3 and TRAF6-mediated IRF7 activation, although further investigation is required to understand the CFTR dependency of these genes and signalling pathways. Furthermore, exogenous IFNλ1 treatment of CF neutrophils resulted in more effective fungal killing without increasing inflammatory ROS or NET production. The data in this thesis increases understanding of fungal susceptibility in CF and paves the way for the potential of IFNλ1 immunotherapy in CF *Af* related disease to increase fungal killing while reducing the damaging inflammatory milieu that is characteristic of the progressive loss of lung function in CF.

References

1. Mehta G, Macek M, Jr., Mehta A, European Registry Working G. Cystic fibrosis across Europe: EuroCareCF analysis of demographic data from 35 countries. *J Cyst Fibros.* 2010; 9 Suppl 2: S5-S21.
2. Guo J, Garratt A, Hill A. Worldwide rates of diagnosis and effective treatment for cystic fibrosis. *J Cyst Fibros.* 2022; 21(3): 456-462.
3. Turcios NL. Cystic Fibrosis Lung Disease: An Overview. *Respir Care.* 2020; 65(2): 233-251.
4. Goetz DM, Savant AP. Review of CFTR modulators 2020. *Pediatr Pulmonol.* 2021; 56(12): 3595-3606.
5. ECFSPR 2021 Annual Data Report: Patient Registry 2021; https://www.ecfs.eu/sites/default/files/Annual%20Report_2021_09Jun2023.pdf.
6. Kerem B, Rommens JM, Buchanan JA, Markiewicz D, Cox TK, Chakravarti A, et al. Identification of the cystic fibrosis gene: genetic analysis. *Science.* 1989; 245(4922): 1073-1080.
7. Rommens JM, Iannuzzi MC, Kerem B, Drumm ML, Melmer G, Dean M, et al. Identification of the cystic fibrosis gene: chromosome walking and jumping. *Science.* 1989; 245(4922): 1059-1065.
8. Riordan JR, Rommens JM, Kerem B, Alon N, Rozmahel R, Grzelczak Z, et al. Identification of the cystic fibrosis gene: cloning and characterization of complementary DNA. *Science.* 1989; 245(4922): 1066-1073.
9. Poulsen JH, Fischer H, Illek B, Machen TE. Bicarbonate conductance and pH regulatory capability of cystic fibrosis transmembrane conductance regulator. *Proc Natl Acad Sci U S A.* 1994; 91(12): 5340-5344.
10. Bareil C, Bergougnoux A. CFTR gene variants, epidemiology and molecular pathology. *Arch Pediatr.* 2020; 27 Suppl 1: eS8-eS12.
11. Kerem BS, Zielenski J, Markiewicz D, Bozon D, Gazit E, Yahav J, et al. Identification of mutations in regions corresponding to the two putative nucleotide (ATP)-binding folds of the cystic fibrosis gene. *Proc Natl Acad Sci U S A.* 1990; 87(21): 8447-8451.
12. Welsh MJ, Smith AE. Molecular mechanisms of CFTR chloride channel dysfunction in cystic fibrosis. *Cell.* 1993; 73(7): 1251-1254.
13. Haardt M, Benharouga M, Lechardeur D, Kartner N, Lukacs GL. C-terminal truncations destabilize the cystic fibrosis transmembrane conductance regulator without impairing its biogenesis. A novel class of mutation. *J Biol Chem.* 1999; 274(31): 21873-21877.
14. Plasschaert LW, Zilionis R, Choo-Wing R, Savova V, Knehr J, Roma G, et al. A single-cell atlas of the airway epithelium reveals the CFTR-rich pulmonary ionocyte. *Nature.* 2018; 560(7718): 377-381.
15. Montoro DT, Haber AL, Biton M, Vinarsky V, Lin B, Birket SE, et al. A revised airway epithelial hierarchy includes CFTR-expressing ionocytes. *Nature.* 2018; 560(7718): 319-324.
16. Shah VS, Chivukula RR, Lin B, Waghray A, Rajagopal J. Cystic Fibrosis and the Cells of the Airway Epithelium: What Are Ionocytes and What Do They Do? *Annu Rev Pathol.* 2022; 17: 23-46.
17. Scudieri P, Musante I, Venturini A, Guidone D, Genovese M, Cresta F, et al. Ionocytes and CFTR Chloride Channel Expression in Normal and Cystic Fibrosis Nasal and Bronchial Epithelial Cells. *Cells.* 2020; 9(9).
18. Lei L, Traore S, Romano Ibarra GS, Karp PH, Rehman T, Meyerholz DK, et al. CFTR-rich ionocytes mediate chloride absorption across airway epithelia. *J Clin Invest.* 2023; 133(20).
19. Tirouvanziam R, de Bentzmann S, Hubeau C, Hinnrasky J, Jacquot J, Peault B, et al. Inflammation and infection in naive human cystic fibrosis airway grafts. *Am J Respir Cell Mol Biol.* 2000; 23(2): 121-127.
20. Hubeau C, Puchelle E, Gaillard D. Distinct pattern of immune cell population in the lung of human fetuses with cystic fibrosis. *J Allergy Clin Immunol.* 2001; 108(4): 524-529.
21. Petrocheilou A, Moudaki A, Kaditis AG. Inflammation and Infection in Cystic Fibrosis: Update for the Clinician. *Children (Basel).* 2022; 9(12).
22. Hartl D, Gaggar A, Bruscia E, Hector A, Marcos V, Jung A, et al. Innate immunity in cystic fibrosis lung disease. *J Cyst Fibros.* 2012; 11(5): 363-382.
23. Galli F, Battistoni A, Gambari R, Pompella A, Bragonzi A, Pilolli F, et al. Oxidative stress and antioxidant therapy in cystic fibrosis. *Biochim Biophys Acta.* 2012; 1822(5): 690-713.
24. Fruhwirth M, Ruedl C, Ellemunter H, Bock G, Wolf H. Flow-cytometric evaluation of oxidative burst in phagocytic cells of children with cystic fibrosis. *Int Arch Allergy Immunol.* 1998; 117(4): 270-275.
25. Gao Z, Su X. CFTR regulates acute inflammatory responses in macrophages. *QJM.* 2015; 108(12): 951-958.

26. Wang H, Cebotaru L, Lee HW, Yang Q, Pollard BS, Pollard HB, et al. CFTR Controls the Activity of NF-kappaB by Enhancing the Degradation of TRADD. *Cell Physiol Biochem.* 2016; 40(5): 1063-1078.
27. Mitri C, Xu Z, Bardin P, Corvol H, Touqui L, Tabary O. Novel Anti-Inflammatory Approaches for Cystic Fibrosis Lung Disease: Identification of Molecular Targets and Design of Innovative Therapies. *Front Pharmacol.* 2020; 11: 1096.
28. Pelullo M, Savi D, Quattrucci S, Cimino G, Pizzuti A, Screpanti I, et al. miR-125b/NRF2/HO-1 axis is involved in protection against oxidative stress of cystic fibrosis: A pilot study. *Exp Ther Med.* 2021; 21(6): 585.
29. Sass LA, Hair PS, Perkins AM, Shah TA, Krishna NK, Cunnion KM. Complement Effectors of Inflammation in Cystic Fibrosis Lung Fluid Correlate with Clinical Measures of Disease. *PLoS One.* 2015; 10(12): e0144723.
30. Trouve P, Ferec C, Genin E. The Interplay between the Unfolded Protein Response, Inflammation and Infection in Cystic Fibrosis. *Cells.* 2021; 10(11).
31. Zheng S, De BP, Choudhary S, Comhair SA, Goggans T, Slee R, et al. Impaired innate host defense causes susceptibility to respiratory virus infections in cystic fibrosis. *Immunity.* 2003; 18(5): 619-630.
32. Smith JJ, Travis SM, Greenberg EP, Welsh MJ. Cystic fibrosis airway epithelia fail to kill bacteria because of abnormal airway surface fluid. *Cell.* 1996; 85(2): 229-236.
33. Bonfield TL, Konstan MW, Berger M. Altered respiratory epithelial cell cytokine production in cystic fibrosis. *J Allergy Clin Immunol.* 1999; 104(1): 72-78.
34. Kotenko SV, Gallagher G, Baurin VV, Lewis-Antes A, Shen M, Shah NK, et al. IFN-lambdas mediate antiviral protection through a distinct class II cytokine receptor complex. *Nat Immunol.* 2003; 4(1): 69-77.
35. Schoggins JW. Recent advances in antiviral interferon-stimulated gene biology. *F1000Res.* 2018; 7: 309.
36. Wack A, Terczynska-Dyla E, Hartmann R. Guarding the frontiers: the biology of type III interferons. *Nat Immunol.* 2015; 16(8): 802-809.
37. Schreiber G. The molecular basis for differential type I interferon signaling. *J Biol Chem.* 2017; 292(18): 7285-7294.
38. Schogler A, Stokes AB, Casaulta C, Regamey N, Edwards MR, Johnston SL, et al. Interferon response of the cystic fibrosis bronchial epithelium to major and minor group rhinovirus infection. *J Cyst Fibros.* 2016; 15(3): 332-339.
39. Parker D, Cohen TS, Alhede M, Harfenist BS, Martin FJ, Prince A. Induction of type I interferon signaling by Pseudomonas aeruginosa is diminished in cystic fibrosis epithelial cells. *Am J Respir Cell Mol Biol.* 2012; 46(1): 6-13.
40. Chattoraj SS, Ganesan S, Faris A, Comstock A, Lee WM, Sajjan US. Pseudomonas aeruginosa suppresses interferon response to rhinovirus infection in cystic fibrosis but not in normal bronchial epithelial cells. *Infect Immun.* 2011; 79(10): 4131-4145.
41. Gillan JL, Chokshi M, Hardisty GR, Clohisey Hendry S, Prasca-Chamorro D, Robinson NJ, et al. CAGE sequencing reveals CFTR-dependent dysregulation of type I IFN signaling in activated cystic fibrosis macrophages. *Sci Adv.* 2023; 9(21): eadg5128.
42. Occhigrossi L, Rossin F, Villella VR, Esposito S, Abbate C, D'Eletto M, et al. The STING/TBK1/IRF3/IFN type I pathway is defective in cystic fibrosis. *Front Immunol.* 2023; 14: 1093212.
43. Tarique AA, Sly PD, Holt PG, Bosco A, Ware RS, Logan J, et al. CFTR-dependent defect in alternatively-activated macrophages in cystic fibrosis. *J Cyst Fibros.* 2017; 16(4): 475-482.
44. Li C, Wu Y, Riehle A, Ma J, Kamler M, Gulbins E, et al. Staphylococcus aureus Survives in Cystic Fibrosis Macrophages, Forming a Reservoir for Chronic Pneumonia. *Infect Immun.* 2017; 85(5).
45. Bruscia EM, Zhang PX, Ferreira E, Caputo C, Emerson JW, Tuck D, et al. Macrophages directly contribute to the exaggerated inflammatory response in cystic fibrosis transmembrane conductance regulator-/- mice. *Am J Respir Cell Mol Biol.* 2009; 40(3): 295-304.
46. Esther CR, Jr., Muhlebach MS, Ehre C, Hill DB, Wolfgang MC, Kesimer M, et al. Mucus accumulation in the lungs precedes structural changes and infection in children with cystic fibrosis. *Sci Transl Med.* 2019; 11(486).
47. Koller DY, Gotz M, Eichler I, Urbanek R. Eosinophilic activation in cystic fibrosis. *Thorax.* 1994; 49(5): 496-499.
48. Ye SC, Desai S, Karlsen E, Kwong E, Wilcox PG, Quon BS. Association between elevated peripheral blood eosinophil count and respiratory outcomes in adults with cystic fibrosis. *J Cyst Fibros.* 2022; 21(6): 1048-1052.

49. Conese M, Copreni E, Di Gioia S, De Rinaldis P, Fumarulo R. Neutrophil recruitment and airway epithelial cell involvement in chronic cystic fibrosis lung disease. *J Cyst Fibros.* 2003; 2(3): 129-135.
50. Dean TP, Dai Y, Shute JK, Church MK, Warner JO. Interleukin-8 concentrations are elevated in bronchoalveolar lavage, sputum, and sera of children with cystic fibrosis. *Pediatr Res.* 1993; 34(2): 159-161.
51. Borregaard N. Neutrophils, from marrow to microbes. *Immunity.* 2010; 33(5): 657-670.
52. Downey DG, Bell SC, Elborn JS. Neutrophils in cystic fibrosis. *Thorax.* 2009; 64(1): 81-88.
53. Hayes E, Pohl K, McElvaney NG, Reeves EP. The cystic fibrosis neutrophil: a specialized yet potentially defective cell. *Arch Immunol Ther Exp (Warsz).* 2011; 59(2): 97-112.
54. Pohl K, Hayes E, Keenan J, Henry M, Meleady P, Molloy K, et al. A neutrophil intrinsic impairment affecting Rab27a and degranulation in cystic fibrosis is corrected by CFTR potentiator therapy. *Blood.* 2014; 124(7): 999-1009.
55. Zhou Y, Song K, Painter RG, Aiken M, Reiser J, Stanton BA, et al. Cystic fibrosis transmembrane conductance regulator recruitment to phagosomes in neutrophils. *J Innate Immun.* 2013; 5(3): 219-230.
56. Hayes E, Murphy MP, Pohl K, Browne N, McQuillan K, Saw LE, et al. Altered Degranulation and pH of Neutrophil Phagosomes Impacts Antimicrobial Efficiency in Cystic Fibrosis. *Front Immunol.* 2020; 11: 600033.
57. Dickerhof N, Isles V, Pattemore P, Hampton MB, Kettle AJ. Exposure of Pseudomonas aeruginosa to bactericidal hypochlorous acid during neutrophil phagocytosis is compromised in cystic fibrosis. *J Biol Chem.* 2019; 294(36): 13502-13514.
58. Painter RG, Valentine VG, Lanson NA, Jr., Leidal K, Zhang Q, Lombard G, et al. CFTR Expression in human neutrophils and the phagolysosomal chlorination defect in cystic fibrosis. *Biochemistry.* 2006; 45(34): 10260-10269.
59. Cheng OZ, Palaniyar N. NET balancing: a problem in inflammatory lung diseases. *Front Immunol.* 2013; 4: 1.
60. Khan MA, Ali ZS, Sweezey N, Grasemann H, Palaniyar N. Progression of Cystic Fibrosis Lung Disease from Childhood to Adulthood: Neutrophils, Neutrophil Extracellular Trap (NET) Formation, and NET Degradation. *Genes (Basel).* 2019; 10(3).
61. Papayannopoulos V, Staab D, Zychlinsky A. Neutrophil elastase enhances sputum solubilization in cystic fibrosis patients receiving DNase therapy. *PLoS One.* 2011; 6(12): e28526.
62. Gray RD, Hardisty G, Regan KH, Smith M, Robb CT, Duffin R, et al. Delayed neutrophil apoptosis enhances NET formation in cystic fibrosis. *Thorax.* 2018; 73(2): 134-144.
63. Coakley RJ, Taggart C, McElvaney NG, O'Neill SJ. Cytosolic pH and the inflammatory microenvironment modulate cell death in human neutrophils after phagocytosis. *Blood.* 2002; 100(9): 3383-3391.
64. Voynow JA, Fischer BM, Zheng S. Proteases and cystic fibrosis. *Int J Biochem Cell Biol.* 2008; 40(6-7): 1238-1245.
65. McKelvey MC, Brown R, Ryan S, Mall MA, Weldon S, Taggart CC. Proteases, Mucus, and Mucosal Immunity in Chronic Lung Disease. *Int J Mol Sci.* 2021; 22(9).
66. Buhling F, Groneberg D, Welte T. Proteases and their role in chronic inflammatory lung diseases. *Curr Drug Targets.* 2006; 7(6): 751-759.
67. Brea D, Meurens F, Dubois AV, Gaillard J, Chevaleyre C, Jourdan ML, et al. The pig as a model for investigating the role of neutrophil serine proteases in human inflammatory lung diseases. *Biochem J.* 2012; 447(3): 363-370.
68. Twigg MS, Brockbank S, Lowry P, FitzGerald SP, Taggart C, Weldon S. The Role of Serine Proteases and Antiproteases in the Cystic Fibrosis Lung. *Mediators Inflamm.* 2015; 2015: 293053.
69. Birrer P. Proteases and antiproteases in cystic fibrosis: pathogenetic considerations and therapeutic strategies. *Respiration.* 1995; 62 Suppl 1: 25-28.
70. Cosgrove S, Chotirmall SH, Greene CM, McElvaney NG. Pulmonary proteases in the cystic fibrosis lung induce interleukin 8 expression from bronchial epithelial cells via a heme/meprin/epidermal growth factor receptor/Toll-like receptor pathway. *J Biol Chem.* 2011; 286(9): 7692-7704.
71. Muller U, Hentschel J, Janhsen WK, Hunniger K, Hipler UC, Sonnemann J, et al. Changes of Proteases, Antiproteases, and Pathogens in Cystic Fibrosis Patients' Upper and Lower Airways after IV-Antibiotic Therapy. *Mediators Inflamm.* 2015; 2015: 626530.
72. Thibodeau PH, Butterworth MB. Proteases, cystic fibrosis and the epithelial sodium channel (ENaC). *Cell Tissue Res.* 2013; 351(2): 309-323.
73. Paranjape SM, Mogayzel PJ, Jr. Cystic fibrosis. *Pediatr Rev.* 2014; 35(5): 194-205.

74. De Boeck K, Vermeulen F, Dupont L. The diagnosis of cystic fibrosis. *Presse Med.* 2017; 46(6 Pt 2): e97-e108.
75. Dickinson KM, Collaco JM. Cystic Fibrosis. *Pediatr Rev.* 2021; 42(2): 55-67.
76. Van Biervliet S, de Clercq C, Declercq D, Van Braeckel E, Van Daele S, De Baets F, et al. Gastro-intestinal manifestations in cystic fibrosis patients. *Acta Gastroenterol Belg.* 2016; 79(4): 481-486.
77. Galante G, Freeman AJ. Gastrointestinal, Pancreatic, and Hepatic Manifestations of Cystic Fibrosis in the Newborn. *Neoreviews.* 2019; 20(1): e12-e24.
78. Sathe MN, Freeman AJ. Gastrointestinal, Pancreatic, and Hepatobiliary Manifestations of Cystic Fibrosis. *Pediatr Clin North Am.* 2016; 63(4): 679-698.
79. Boyd JM, Mehta A, Murphy DJ. Fertility and pregnancy outcomes in men and women with cystic fibrosis in the United Kingdom. *Hum Reprod.* 2004; 19(10): 2238-2243.
80. Cohen-Cymberknoh M, Shoseyov D, Kerem E. Managing cystic fibrosis: strategies that increase life expectancy and improve quality of life. *Am J Respir Crit Care Med.* 2011; 183(11): 1463-1471.
81. Boyle MP, Sabadosa KA, Quinton HB, Marshall BC, Schechter MS. Key findings of the US Cystic Fibrosis Foundation's clinical practice benchmarking project. *BMJ Qual Saf.* 2014; 23 Suppl 1: i15-i22.
82. Lebecque P, Leonard A, De Boeck K, De Baets F, Malfroot A, Casimir G, et al. Early referral to cystic fibrosis specialist centre impacts on respiratory outcome. *J Cyst Fibros.* 2009; 8(1): 26-30.
83. Castellani C, Duff AJA, Bell SC, Heijerman HGM, Munck A, Ratjen F, et al. ECFS best practice guidelines: the 2018 revision. *J Cyst Fibros.* 2018; 17(2): 153-178.
84. Lopes-Pacheco M. CFTR Modulators: The Changing Face of Cystic Fibrosis in the Era of Precision Medicine. *Front Pharmacol.* 2019; 10: 1662.
85. De Boeck K, Amaral MD. Progress in therapies for cystic fibrosis. *Lancet Respir Med.* 2016; 4(8): 662-674.
86. Ramsey BW, Davies J, McElvaney NG, Tullis E, Bell SC, Drevinek P, et al. A CFTR potentiator in patients with cystic fibrosis and the G551D mutation. *N Engl J Med.* 2011; 365(18): 1663-1672.
87. Whiting P, Al M, Burgers L, Westwood M, Ryder S, Hoogendoorn M, et al. Ivacaftor for the treatment of patients with cystic fibrosis and the G551D mutation: a systematic review and cost-effectiveness analysis. *Health Technol Assess.* 2014; 18(18): 1-106.
88. Davies JC, Wainwright CE, Canny GJ, Chilvers MA, Howenstine MS, Munck A, et al. Efficacy and safety of ivacaftor in patients aged 6 to 11 years with cystic fibrosis with a G551D mutation. *Am J Respir Crit Care Med.* 2013; 187(11): 1219-1225.
89. Rowe SM, Heltshe SL, Gonska T, Donaldson SH, Borowitz D, Gelfond D, et al. Clinical mechanism of the cystic fibrosis transmembrane conductance regulator potentiator ivacaftor in G551D-mediated cystic fibrosis. *Am J Respir Crit Care Med.* 2014; 190(2): 175-184.
90. Wainwright CE, Elborn JS, Ramsey BW, Marigowda G, Huang X, Cipolli M, et al. Lumacaftor-Ivacaftor in Patients with Cystic Fibrosis Homozygous for Phe508del CFTR. *N Engl J Med.* 2015; 373(3): 220-231.
91. Middleton PG, Mall MA, Drevinek P, Lands LC, McKone EF, Polineni D, et al. Elexacaftor-Tezacaftor-Ivacaftor for Cystic Fibrosis with a Single Phe508del Allele. *N Engl J Med.* 2019; 381(19): 1809-1819.
92. Keating D, Marigowda G, Burr L, Daines C, Mall MA, McKone EF, et al. VX-445-Tezacaftor-Ivacaftor in Patients with Cystic Fibrosis and One or Two Phe508del Alleles. *N Engl J Med.* 2018; 379(17): 1612-1620.
93. De Boeck K. Cystic fibrosis in the year 2020: A disease with a new face. *Acta Paediatr.* 2020; 109(5): 893-899.
94. Rogers GB, Taylor SL, Hoffman LR, Burr LD. The impact of CFTR modulator therapies on CF airway microbiology. *J Cyst Fibros.* 2020; 19(3): 359-364.
95. Moliteo E, Sciacca M, Palmeri A, Papale M, Manti S, Parisi GF, et al. Cystic Fibrosis and Oxidative Stress: The Role of CFTR. *Molecules.* 2022; 27(16).
96. Veit G, Avramescu RG, Chiang AN, Houck SA, Cai Z, Peters KW, et al. From CFTR biology toward combinatorial pharmacotherapy: expanded classification of cystic fibrosis mutations. *Mol Biol Cell.* 2016; 27(3): 424-433.
97. Heijerman HGM, McKone EF, Downey DG, Van Braeckel E, Rowe SM, Tullis E, et al. Efficacy and safety of the elexacaftor plus tezacaftor plus ivacaftor combination regimen in people with cystic fibrosis homozygous for the F508del mutation: a double-blind, randomised, phase 3 trial. *Lancet.* 2019; 394(10212): 1940-1948.
98. Latge JP, Chamilos G. Aspergillus fumigatus and Aspergillosis in 2019. *Clin Microbiol Rev.* 2019; 33(1).
99. Kwon-Chung KJ, Sugui JA. Aspergillus fumigatus--what makes the species a ubiquitous human fungal pathogen? *PLoS Pathog.* 2013; 9(12): e1003743.

100. Mahieu LM, De Dooy JJ, Van Laer FA, Jansens H, Ieven MM. A prospective study on factors influencing aspergillus spore load in the air during renovation works in a neonatal intensive care unit. *J Hosp Infect.* 2000; 45(3): 191-197.
101. Abdel Hameed AA, Yasser IH, Khoder IM. Indoor air quality during renovation actions: a case study. *J Environ Monit.* 2004; 6(9): 740-744.
102. Wery N. Bioaerosols from composting facilities--a review. *Front Cell Infect Microbiol.* 2014; 4: 42.
103. Taha MP, Pollard SJ, Sarkar U, Longhurst P. Estimating fugitive bioaerosol releases from static compost windrows: feasibility of a portable wind tunnel approach. *Waste Manag.* 2005; 25(4): 445-450.
104. van de Veerdonk FL, Gresnigt MS, Romani L, Netea MG, Latge JP. Aspergillus fumigatus morphology and dynamic host interactions. *Nat Rev Microbiol.* 2017; 15(11): 661-674.
105. Rhodes JC. Aspergillus fumigatus: growth and virulence. *Med Mycol.* 2006; 44 Suppl 1: S77-81.
106. Loussert C, Schmitt C, Prevost MC, Balloy V, Fadel E, Philippe B, et al. In vivo biofilm composition of Aspergillus fumigatus. *Cell Microbiol.* 2010; 12(3): 405-410.
107. O'Gorman CM, Fuller H, Dyer PS. Discovery of a sexual cycle in the opportunistic fungal pathogen Aspergillus fumigatus. *Nature.* 2009; 457(7228): 471-474.
108. Kosmidis C, Denning DW. The clinical spectrum of pulmonary aspergillosis. *Thorax.* 2015; 70(3): 270-277.
109. Patterson TF, Thompson GR, 3rd, Denning DW, Fishman JA, Hadley S, Herbrecht R, et al. Practice Guidelines for the Diagnosis and Management of Aspergillosis: 2016 Update by the Infectious Diseases Society of America. *Clin Infect Dis.* 2016; 63(4): e1-e60.
110. Agarwal R, Muthu V, Sehgal IS, Dhooria S, Prasad KT, Aggarwal AN. Allergic Bronchopulmonary Aspergillosis. *Clin Chest Med.* 2022; 43(1): 99-125.
111. Agarwal R, Sehgal IS, Dhooria S, Muthu V, Prasad KT, Bal A, et al. Allergic bronchopulmonary aspergillosis. *Indian J Med Res.* 2020; 151(6): 529-549.
112. Takazono T, Izumikawa K. Recent Advances in Diagnosing Chronic Pulmonary Aspergillosis. *Front Microbiol.* 2018; 9: 1810.
113. Agarwal R, Gupta D, Aggarwal AN, Saxena AK, Chakrabarti A, Jindal SK. Clinical significance of hyperattenuating mucoid impaction in allergic bronchopulmonary aspergillosis: an analysis of 155 patients. *Chest.* 2007; 132(4): 1183-1190.
114. Alastruey-Izquierdo A, Cadranel J, Flick H, Godet C, Hennequin C, Hoenigl M, et al. Treatment of Chronic Pulmonary Aspergillosis: Current Standards and Future Perspectives. *Respiration.* 2018; 96(2): 159-170.
115. Denning DW, Cadranel J, Beigelman-Aubry C, Ader F, Chakrabarti A, Blot S, et al. Chronic pulmonary aspergillosis: rationale and clinical guidelines for diagnosis and management. *Eur Respir J.* 2016; 47(1): 45-68.
116. Denning DW. Invasive aspergillosis. *Clin Infect Dis.* 1998; 26(4): 781-803; quiz 804-785.
117. Cadena J, Thompson GR, 3rd, Patterson TF. Invasive Aspergillosis: Current Strategies for Diagnosis and Management. *Infect Dis Clin North Am.* 2016; 30(1): 125-142.
118. Greene R. The radiological spectrum of pulmonary aspergillosis. *Med Mycol.* 2005; 43 Suppl 1: S147-154.
119. von Eiff M, Roos N, Schulten R, Hesse M, Zuhlsdorf M, van de Loo J. Pulmonary aspergillosis: early diagnosis improves survival. *Respiration.* 1995; 62(6): 341-347.
120. Baddley JW, Andes DR, Marr KA, Kontoyiannis DP, Alexander BD, Kauffman CA, et al. Factors associated with mortality in transplant patients with invasive aspergillosis. *Clin Infect Dis.* 2010; 50(12): 1559-1567.
121. Caillot D, Couaillier JF, Bernard A, Casasnovas O, Denning DW, Mannone L, et al. Increasing volume and changing characteristics of invasive pulmonary aspergillosis on sequential thoracic computed tomography scans in patients with neutropenia. *J Clin Oncol.* 2001; 19(1): 253-259.
122. Ledoux MP, Herbrecht R. Invasive Pulmonary Aspergillosis. *J Fungi (Basel).* 2023; 9(2).
123. Wiederhold NP. Emerging Fungal Infections: New Species, New Names, and Antifungal Resistance. *Clin Chem.* 2021; 68(1): 83-90.
124. Snelders E, Huis In 't Veld RA, Rijs AJ, Kema GH, Melchers WJ, Verweij PE. Possible environmental origin of resistance of Aspergillus fumigatus to medical triazoles. *Appl Environ Microbiol.* 2009; 75(12): 4053-4057.
125. Odds FC. Drug evaluation: BAL-8557--a novel broad-spectrum triazole antifungal. *Curr Opin Investig Drugs.* 2006; 7(8): 766-772.

126. Wiederhold NP, Verweij PE. Aspergillus fumigatus and pan-azole resistance: who should be concerned? *Curr Opin Infect Dis.* 2020; 33(4): 290-297.
127. Bueid A, Howard SJ, Moore CB, Richardson MD, Harrison E, Bowyer P, et al. Azole antifungal resistance in Aspergillus fumigatus: 2008 and 2009. *J Antimicrob Chemother.* 2010; 65(10): 2116-2118.
128. Verweij PE, Mellado E, Melchers WJ. Multiple-triazole-resistant aspergillosis. *N Engl J Med.* 2007; 356(14): 1481-1483.
129. Aimanianda V, Bayry J, Bozza S, Kniemeyer O, Perruccio K, Elluru SR, et al. Surface hydrophobin prevents immune recognition of airborne fungal spores. *Nature.* 2009; 460(7259): 1117-1121.
130. Carrion Sde J, Leal SM, Jr., Ghannoum MA, Aimanianda V, Latge JP, Pearlman E. The RodA hydrophobin on Aspergillus fumigatus spores masks dectin-1- and dectin-2-dependent responses and enhances fungal survival in vivo. *J Immunol.* 2013; 191(5): 2581-2588.
131. Gow NAR, Latge JP, Munro CA. The Fungal Cell Wall: Structure, Biosynthesis, and Function. *Microbiol Spectr.* 2017; 5(3).
132. Fontaine T, Simenel C, Dubreucq G, Adam O, Delepierre M, Lemoine J, et al. Molecular organization of the alkali-insoluble fraction of Aspergillus fumigatus cell wall. *J Biol Chem.* 2000; 275(36): 27594-27607.
133. Latge JP, Beauvais A. Functional duality of the cell wall. *Curr Opin Microbiol.* 2014; 20: 111-117.
134. Gresnigt MS, Netea MG, van de Veerdonk FL. Pattern recognition receptors and their role in invasive aspergillosis. *Ann N Y Acad Sci.* 2012; 1273: 60-67.
135. Geijtenbeek TB, Gringhuis SI. Signalling through C-type lectin receptors: shaping immune responses. *Nat Rev Immunol.* 2009; 9(7): 465-479.
136. Hardison SE, Brown GD. C-type lectin receptors orchestrate antifungal immunity. *Nat Immunol.* 2012; 13(9): 817-822.
137. Hohl TM, Van Epps HL, Rivera A, Morgan LA, Chen PL, Feldmesser M, et al. Aspergillus fumigatus triggers inflammatory responses by stage-specific beta-glucan display. *PLoS Pathog.* 2005; 1(3): e30.
138. Osorio F, Reis e Sousa C. Myeloid C-type lectin receptors in pathogen recognition and host defense. *Immunity.* 2011; 34(5): 651-664.
139. Strasser D, Neumann K, Bergmann H, Marakalala MJ, Guler R, Rojowska A, et al. Syk kinase-coupled C-type lectin receptors engage protein kinase C-delta to elicit Card9 adaptor-mediated innate immunity. *Immunity.* 2012; 36(1): 32-42.
140. del Fresno C, Soulat D, Roth S, Blazek K, Udalova I, Sancho D, et al. Interferon-beta production via Dectin-1-Syk-IRF5 signaling in dendritic cells is crucial for immunity to C. albicans. *Immunity.* 2013; 38(6): 1176-1186.
141. Dutta O, Espinosa V, Wang K, Avina S, Rivera A. Dectin-1 Promotes Type I and III Interferon Expression to Support Optimal Antifungal Immunity in the Lung. *Front Cell Infect Microbiol.* 2020; 10: 321.
142. Sainz J, Lupianez CB, Segura-Catena J, Vazquez L, Rios R, Oyonarte S, et al. Dectin-1 and DC-SIGN polymorphisms associated with invasive pulmonary Aspergillosis infection. *PLoS One.* 2012; 7(2): e32273.
143. Vendele I, Willment JA, Silva LM, Palma AS, Chai W, Liu Y, et al. Mannan detecting C-type lectin receptor probes recognise immune epitopes with diverse chemical, spatial and phylogenetic heterogeneity in fungal cell walls. *PLoS Pathog.* 2020; 16(1): e1007927.
144. Sato K, Yang XL, Yudate T, Chung JS, Wu J, Luby-Phelps K, et al. Dectin-2 is a pattern recognition receptor for fungi that couples with the Fc receptor gamma chain to induce innate immune responses. *J Biol Chem.* 2006; 281(50): 38854-38866.
145. Robinson MJ, Osorio F, Rosas M, Freitas RP, Schweighoffer E, Gross O, et al. Dectin-2 is a Syk-coupled pattern recognition receptor crucial for Th17 responses to fungal infection. *J Exp Med.* 2009; 206(9): 2037-2051.
146. Haider M, Dambuza IM, Asamaphan P, Stappers M, Reid D, Yamasaki S, et al. The pattern recognition receptors dectin-2, mincle, and FcRgamma impact the dynamics of phagocytosis of Candida, Saccharomyces, Malassezia, and Mucor species. *PLoS One.* 2019; 14(8): e0220867.
147. Ifrim DC, Bain JM, Reid DM, Oosting M, Verschueren I, Gow NA, et al. Role of Dectin-2 for host defense against systemic infection with Candida glabrata. *Infect Immun.* 2014; 82(3): 1064-1073.
148. Griffiths JS, White PL, Czubala MA, Simonazzi E, Bruno M, Thompson A, et al. A Human Dectin-2 Deficiency Associated With Invasive Aspergillosis. *J Infect Dis.* 2021; 224(7): 1219-1224.
149. Loures FV, Rohm M, Lee CK, Santos E, Wang JP, Specht CA, et al. Recognition of Aspergillus fumigatus hyphae by human plasmacytoid dendritic cells is mediated by dectin-2 and results in formation of extracellular traps. *PLoS Pathog.* 2015; 11(2): e1004643.

150. Stappers MHT, Nikolakopoulou C, Wiesner DL, Yuecel R, Klein BS, Willment JA, et al. Characterization of antifungal C-type lectin receptor expression on murine epithelial and endothelial cells in mucosal tissues. *Eur J Immunol.* 2021; 51(9): 2341-2344.
151. Brown GD. Innate antifungal immunity: the key role of phagocytes. *Annu Rev Immunol.* 2011; 29: 1-21.
152. Bellocchio S, Montagnoli C, Bozza S, Gaziano R, Rossi G, Mambula SS, et al. The contribution of the Toll-like/IL-1 receptor superfamily to innate and adaptive immunity to fungal pathogens in vivo. *J Immunol.* 2004; 172(5): 3059-3069.
153. Mambula SS, Sau K, Henneke P, Golenbock DT, Levitz SM. Toll-like receptor (TLR) signaling in response to Aspergillus fumigatus. *J Biol Chem.* 2002; 277(42): 39320-39326.
154. Wang JE, Warris A, Ellingsen EA, Jorgensen PF, Flo TH, Espevik T, et al. Involvement of CD14 and toll-like receptors in activation of human monocytes by Aspergillus fumigatus hyphae. *Infect Immun.* 2001; 69(4): 2402-2406.
155. Beisswenger C, Hess C, Bals R. Aspergillus fumigatus conidia induce interferon-beta signalling in respiratory epithelial cells. *Eur Respir J.* 2012; 39(2): 411-418.
156. Netea MG, Warris A, Van der Meer JW, Fenton MJ, Verver-Janssen TJ, Jacobs LE, et al. Aspergillus fumigatus evades immune recognition during germination through loss of toll-like receptor-4-mediated signal transduction. *J Infect Dis.* 2003; 188(2): 320-326.
157. Meier A, Kirschning CJ, Nikolaus T, Wagner H, Heesemann J, Ebel F. Toll-like receptor (TLR) 2 and TLR4 are essential for Aspergillus-induced activation of murine macrophages. *Cell Microbiol.* 2003; 5(8): 561-570.
158. Braedel S, Radsak M, Einsele H, Latge JP, Michan A, Loeffler J, et al. Aspergillus fumigatus antigens activate innate immune cells via toll-like receptors 2 and 4. *Br J Haematol.* 2004; 125(3): 392-399.
159. Underhill DM, Ozinsky A, Hajjar AM, Stevens A, Wilson CB, Bassetti M, et al. The Toll-like receptor 2 is recruited to macrophage phagosomes and discriminates between pathogens. *Nature.* 1999; 401(6755): 811-815.
160. Overton NL, Denning DW, Bowyer P, Simpson A. Genetic susceptibility to allergic bronchopulmonary aspergillosis in asthma: a genetic association study. *Allergy Asthma Clin Immunol.* 2016; 12: 47.
161. Balloy V, Si-Tahar M, Takeuchi O, Philippe B, Nahori MA, Tanguy M, et al. Involvement of toll-like receptor 2 in experimental invasive pulmonary aspergillosis. *Infect Immun.* 2005; 73(9): 5420-5425.
162. Kesh S, Mensah NY, Peterlongo P, Jaffe D, Hsu K, M VDB, et al. TLR1 and TLR6 polymorphisms are associated with susceptibility to invasive aspergillosis after allogeneic stem cell transplantation. *Ann N Y Acad Sci.* 2005; 1062: 95-103.
163. Espinosa V, Dutta O, McElrath C, Du P, Chang YJ, Cicciarelli B, et al. Type III interferon is a critical regulator of innate antifungal immunity. *Sci Immunol.* 2017; 2(16).
164. Carvalho A, De Luca A, Bozza S, Cunha C, D'Angelo C, Moretti S, et al. TLR3 essentially promotes protective class I-restricted memory CD8(+) T-cell responses to Aspergillus fumigatus in hematopoietic transplanted patients. *Blood.* 2012; 119(4): 967-977.
165. Li ZZ, Tao LL, Zhang J, Zhang HJ, Qu JM. Role of NOD2 in regulating the immune response to Aspergillus fumigatus. *Inflamm Res.* 2012; 61(6): 643-648.
166. Zhang Y, Wu J, Xin Z, Wu X. Aspergillus fumigatus triggers innate immune response via NOD1 signaling in human corneal epithelial cells. *Exp Eye Res.* 2014; 127: 170-178.
167. Zhang HJ, Qu JM, Shao CZ, Zhang J, He LX, Yuan ZH. Aspergillus fumigatus conidia upregulates NOD2 protein expression both in vitro and in vivo. *Acta Pharmacol Sin.* 2008; 29(10): 1202-1208.
168. Xu ZJ, Zhao GQ, Wang Q, Che CY, Jiang N, Hu LT, et al. Nucleotide oligomerization domain 2 contributes to the innate immune response in THCE cells stimulated by Aspergillus fumigatus conidia. *Int J Ophthalmol.* 2012; 5(4): 409-414.
169. Gresnigt MS, Cunha C, Jaeger M, Goncalves SM, Malireddi RKS, Ammerdorffer A, et al. Genetic deficiency of NOD2 confers resistance to invasive aspergillosis. *Nat Commun.* 2018; 9(1): 2636.
170. Gresnigt MS, Jaeger M, Subbarao Malireddi RK, Rasid O, Jouvion G, Fitting C, et al. The Absence of NOD1 Enhances Killing of Aspergillus fumigatus Through Modulation of Dectin-1 Expression. *Front Immunol.* 2017; 8: 1777.
171. Said-Sadier N, Padilla E, Langsley G, Ojcius DM. Aspergillus fumigatus stimulates the NLRP3 inflammasome through a pathway requiring ROS production and the Syk tyrosine kinase. *PLoS One.* 2010; 5(4): e10008.
172. Karki R, Man SM, Malireddi RKS, Gurung P, Vogel P, Lamkanfi M, et al. Concerted activation of the AIM2 and NLRP3 inflammasomes orchestrates host protection against Aspergillus infection. *Cell Host Microbe.* 2015; 17(3): 357-368.

173. Rehwinkel J, Gack MU. RIG-I-like receptors: their regulation and roles in RNA sensing. *Nat Rev Immunol.* 2020; 20(9): 537-551.
174. Wang X, Caffrey-Carr AK, Liu KW, Espinosa V, Croteau W, Dhingra S, et al. MDA5 Is an Essential Sensor of a Pathogen-Associated Molecular Pattern Associated with Vitality That Is Necessary for Host Resistance against Aspergillus fumigatus. *J Immunol.* 2020; 205(11): 3058-3070.
175. Childs KS, Randall RE, Goodbourn S. LGP2 plays a critical role in sensitizing mda-5 to activation by double-stranded RNA. *PLoS One.* 2013; 8(5): e64202.
176. Lazear HM, Lancaster A, Wilkins C, Suthar MS, Huang A, Vick SC, et al. IRF-3, IRF-5, and IRF-7 coordinately regulate the type I IFN response in myeloid dendritic cells downstream of MAVS signaling. *PLoS Pathog.* 2013; 9(1): e1003118.
177. Wang X, Cunha C, Grau MS, Robertson SJ, Lacerda JF, Campos A, Jr., et al. MAVS Expression in Alveolar Macrophages Is Essential for Host Resistance against Aspergillus fumigatus. *J Immunol.* 2022; 209(2): 346-353.
178. Madan T, Eggleton P, Kishore U, Strong P, Aggrawal SS, Sarma PU, et al. Binding of pulmonary surfactant proteins A and D to Aspergillus fumigatus conidia enhances phagocytosis and killing by human neutrophils and alveolar macrophages. *Infect Immun.* 1997; 65(8): 3171-3179.
179. van Asbeck EC, Hoepelman AI, Scharringa J, Herpers BL, Verhoef J. Mannose binding lectin plays a crucial role in innate immunity against yeast by enhanced complement activation and enhanced uptake of polymorphonuclear cells. *BMC Microbiol.* 2008; 8: 229.
180. Kaur S, Gupta VK, Thiel S, Sarma PU, Madan T. Protective role of mannan-binding lectin in a murine model of invasive pulmonary aspergillosis. *Clin Exp Immunol.* 2007; 148(2): 382-389.
181. Mantovani A, Garlanda C, Doni A, Bottazzi B. Pentraxins in innate immunity: from C-reactive protein to the long pentraxin PTX3. *J Clin Immunol.* 2008; 28(1): 1-13.
182. Salvatori G, Campo S. Current understanding of PTX3 protective activity on Aspergillus fumigatus infection. *Med Mycol.* 2012; 50(3): 225-233.
183. Moalli F, Doni A, Deban L, Zelante T, Zagarella S, Bottazzi B, et al. Role of complement and Fcgamma receptors in the protective activity of the long pentraxin PTX3 against Aspergillus fumigatus. *Blood.* 2010; 116(24): 5170-5180.
184. Garlanda C, Hirsch E, Bozza S, Salustri A, De Acetis M, Nota R, et al. Non-redundant role of the long pentraxin PTX3 in anti-fungal innate immune response. *Nature.* 2002; 420(6912): 182-186.
185. Marra E, Sousa VL, Gaziano R, Pacello ML, Arseni B, Aurisicchio L, et al. Efficacy of PTX3 and posaconazole combination in a rat model of invasive pulmonary aspergillosis. *Antimicrob Agents Chemother.* 2014; 58(10): 6284-6286.
186. Heung LJ, Wiesner DL, Wang K, Rivera A, Hohl TM. Immunity to fungi in the lung. *Semin Immunol.* 2023; 66: 101728.
187. Wiesner DL, Klein BS. Lung epithelium: barrier immunity to inhaled fungi and driver of fungal-associated allergic asthma. *Curr Opin Microbiol.* 2017; 40: 8-13.
188. Guo Y, Kasahara S, Jhingran A, Tosini NL, Zhai B, Aufiero MA, et al. During Aspergillus Infection, Monocyte-Derived DCs, Neutrophils, and Plasmacytoid DCs Enhance Innate Immune Defense through CXCR3-Dependent Crosstalk. *Cell Host Microbe.* 2020; 28(1): 104-116 e104.
189. Lionakis MS, Levitz SM. Host Control of Fungal Infections: Lessons from Basic Studies and Human Cohorts. *Annu Rev Immunol.* 2018; 36: 157-191.
190. Seif M, Kakoschke TK, Ebel F, Bellet MM, Trinks N, Renga G, et al. CAR T cells targeting Aspergillus fumigatus are effective at treating invasive pulmonary aspergillosis in preclinical models. *Sci Transl Med.* 2022; 14(664): eabh1209.
191. Cunha C, Aversa F, Lacerda JF, Busca A, Kurzai O, Grube M, et al. Genetic PTX3 deficiency and aspergillosis in stem-cell transplantation. *N Engl J Med.* 2014; 370(5): 421-432.
192. Caffrey AK, Lehmann MM, Zickovich JM, Espinosa V, Shepardson KM, Watschke CP, et al. IL-1alpha signaling is critical for leukocyte recruitment after pulmonary Aspergillus fumigatus challenge. *PLoS Pathog.* 2015; 11(1): e1004625.
193. Snarr BD, St-Pierre G, Ralph B, Lehoux M, Sato Y, Rancourt A, et al. Galectin-3 enhances neutrophil motility and extravasation into the airways during Aspergillus fumigatus infection. *PLoS Pathog.* 2020; 16(8): e1008741.
194. Caffrey-Carr AK, Hilmer KM, Kowalski CH, Shepardson KM, Temple RM, Cramer RA, et al. Host-Derived Leukotriene B(4) Is Critical for Resistance against Invasive Pulmonary Aspergillosis. *Front Immunol.* 2017; 8: 1984.

195. Espinosa V, Jhingran A, Dutta O, Kasahara S, Donnelly R, Du P, et al. Inflammatory monocytes orchestrate innate antifungal immunity in the lung. *PLoS Pathog.* 2014; 10(2): e1003940.
196. Espinosa V, Dutta O, Heung LJ, Wang K, Chang YJ, Soteropoulos P, et al. Cutting Edge: Neutrophils License the Maturation of Monocytes into Effective Antifungal Effectors. *J Immunol.* 2022; 209(10): 1827-1831.
197. Kasahara S, Jhingran A, Dhingra S, Salem A, Cramer RA, Hohl TM. Role of Granulocyte-Macrophage Colony-Stimulating Factor Signaling in Regulating Neutrophil Antifungal Activity and the Oxidative Burst During Respiratory Fungal Challenge. *J Infect Dis.* 2016; 213(8): 1289-1298.
198. Osherov N. Interaction of the pathogenic mold Aspergillus fumigatus with lung epithelial cells. *Front Microbiol.* 2012; 3: 346.
199. Bertuzzi M, Hayes GE, Icheoku UJ, van Rhijn N, Denning DW, Osherov N, et al. Anti-Aspergillus Activities of the Respiratory Epithelium in Health and Disease. *J Fungi (Basel).* 2018; 4(1).
200. Culibrk L, Croft CA, Toor A, Yang SJ, Singhera GK, Dorscheid DR, et al. Phagocytosis of Aspergillus fumigatus by Human Bronchial Epithelial Cells Is Mediated by the Arp2/3 Complex and WIPF2. *Front Cell Infect Microbiol.* 2019; 9: 16.
201. Romani L. Immunity to fungal infections. *Nat Rev Immunol.* 2011; 11(4): 275-288.
202. Fernandes J, Hamidi F, Leborgne R, Beau R, Castier Y, Mordant P, et al. Penetration of the Human Pulmonary Epithelium by Aspergillus fumigatus Hyphae. *J Infect Dis.* 2018; 218(8): 1306-1313.
203. Murphy J, Summer R, Wilson AA, Kotton DN, Fine A. The prolonged life-span of alveolar macrophages. *Am J Respir Cell Mol Biol.* 2008; 38(4): 380-385.
204. Philippe B, Ibrahim-Granet O, Prevost MC, Gougerot-Pocidalo MA, Sanchez Perez M, Van der Meeren A, et al. Killing of Aspergillus fumigatus by alveolar macrophages is mediated by reactive oxidant intermediates. *Infect Immun.* 2003; 71(6): 3034-3042.
205. Thammasit P, Sripetchwandee J, Nosanchuk JD, Chattipakorn SC, Chattipakorn N, Youngchim S. Cytokine and Chemokine Responses in Invasive Aspergillosis Following Hematopoietic Stem Cell Transplantation: Past Evidence for Future Therapy of Aspergillosis. *J Fungi (Basel).* 2021; 7(9).
206. Taramelli D, Malabarba MG, Sala G, Basilico N, Cocuzza G. Production of cytokines by alveolar and peritoneal macrophages stimulated by Aspergillus fumigatus conidia or hyphae. *J Med Vet Mycol.* 1996; 34(1): 49-56.
207. Espinosa V, Rivera A. First Line of Defense: Innate Cell-Mediated Control of Pulmonary Aspergillosis. *Front Microbiol.* 2016; 7: 272.
208. Bozza S, Gaziano R, Spreca A, Bacci A, Montagnoli C, di Francesco P, et al. Dendritic cells transport conidia and hyphae of Aspergillus fumigatus from the airways to the draining lymph nodes and initiate disparate Th responses to the fungus. *J Immunol.* 2002; 168(3): 1362-1371.
209. Swiecki M, Colonna M. The multifaceted biology of plasmacytoid dendritic cells. *Nat Rev Immunol.* 2015; 15(8): 471-485.
210. Maldonado S, Fitzgerald-Bocarsly P. Antifungal Activity of Plasmacytoid Dendritic Cells and the Impact of Chronic HIV Infection. *Front Immunol.* 2017; 8: 1705.
211. Ramirez-Ortiz ZG, Lee CK, Wang JP, Boon L, Specht CA, Levitz SM. A nonredundant role for plasmacytoid dendritic cells in host defense against the human fungal pathogen Aspergillus fumigatus. *Cell Host Microbe.* 2011; 9(5): 415-424.
212. Pini G, Faggi E, Donato R, Sacco C, Fanci R. Invasive pulmonary aspergillosis in neutropenic patients and the influence of hospital renovation. *Mycoses.* 2008; 51(2): 117-122.
213. Lionakis MS, Drummond RA, Hohl TM. Immune responses to human fungal pathogens and therapeutic prospects. *Nat Rev Immunol.* 2023: 1-20.
214. Bonnett CR, Cornish EJ, Harmsen AG, Burritt JB. Early neutrophil recruitment and aggregation in the murine lung inhibit germination of Aspergillus fumigatus Conidia. *Infect Immun.* 2006; 74(12): 6528-6539.
215. Mircescu MM, Lipuma L, van Rooijen N, Pamer EG, Hohl TM. Essential role for neutrophils but not alveolar macrophages at early time points following Aspergillus fumigatus infection. *J Infect Dis.* 2009; 200(4): 647-656.
216. Jhingran A, Kasahara S, Shepardson KM, Junecko BA, Heung LJ, Kumasaka DK, et al. Compartment-specific and sequential role of MyD88 and CARD9 in chemokine induction and innate defense during respiratory fungal infection. *PLoS Pathog.* 2015; 11(1): e1004589.
217. Tkalcevic J, Novelli M, Phylactides M, Iredale JP, Segal AW, Roes J. Impaired immunity and enhanced resistance to endotoxin in the absence of neutrophil elastase and cathepsin G. *Immunity.* 2000; 12(2): 201-210.

218. Leal SM, Jr., Roy S, Vareechon C, Carrion S, Clark H, Lopez-Berges MS, et al. Targeting iron acquisition blocks infection with the fungal pathogens Aspergillus fumigatus and Fusarium oxysporum. *PLoS Pathog.* 2013; 9(7): e1003436.
219. Zarember KA, Sugui JA, Chang YC, Kwon-Chung KJ, Gallin JI. Human polymorphonuclear leukocytes inhibit Aspergillus fumigatus conidial growth by lactoferrin-mediated iron depletion. *J Immunol.* 2007; 178(10): 6367-6373.
220. Gazendam RP, van Hamme JL, Tool AT, Hoogenboezem M, van den Berg JM, Prins JM, et al. Human Neutrophils Use Different Mechanisms To Kill Aspergillus fumigatus Conidia and Hyphae: Evidence from Phagocyte Defects. *J Immunol.* 2016; 196(3): 1272-1283.
221. Bianchi M, Hakkim A, Brinkmann V, Siler U, Seger RA, Zychlinsky A, et al. Restoration of NET formation by gene therapy in CGD controls aspergillosis. *Blood.* 2009; 114(13): 2619-2622.
222. Bruns S, Kniemeyer O, Hasenberg M, Aimanianda V, Nietzsche S, Thywissen A, et al. Production of extracellular traps against Aspergillus fumigatus in vitro and in infected lung tissue is dependent on invading neutrophils and influenced by hydrophobin RodA. *PLoS Pathog.* 2010; 6(4): e1000873.
223. McCormick A, Heesemann L, Wagener J, Marcos V, Hartl D, Loeffler J, et al. NETs formed by human neutrophils inhibit growth of the pathogenic mold Aspergillus fumigatus. *Microbes Infect.* 2010; 12(12-13): 928-936.
224. Branzk N, Lubojemska A, Hardison SE, Wang Q, Gutierrez MG, Brown GD, et al. Neutrophils sense microbe size and selectively release neutrophil extracellular traps in response to large pathogens. *Nat Immunol.* 2014; 15(11): 1017-1025.
225. Clark HL, Abbondante S, Minns MS, Greenberg EN, Sun Y, Pearlman E. Protein Deiminase 4 and CR3 Regulate Aspergillus fumigatus and beta-Glucan-Induced Neutrophil Extracellular Trap Formation, but Hyphal Killing Is Dependent Only on CR3. *Front Immunol.* 2018; 9: 1182.
226. Ravindran M, Khan MA, Palaniyar N. Neutrophil Extracellular Trap Formation: Physiology, Pathology, and Pharmacology. *Biomolecules.* 2019; 9(8).
227. Lilly LM, Scopel M, Nelson MP, Burg AR, Dunaway CW, Steele C. Eosinophil deficiency compromises lung defense against Aspergillus fumigatus. *Infect Immun.* 2014; 82(3): 1315-1325.
228. Rothenberg ME, Hogan SP. The eosinophil. *Annu Rev Immunol.* 2006; 24: 147-174.
229. Omokawa A, Ueki S, Kikuchi Y, Takeda M, Asano M, Sato K, et al. Mucus plugging in allergic bronchopulmonary aspergillosis: Implication of the eosinophil DNA traps. *Allergol Int.* 2018; 67(2): 280-282.
230. Guerra ES, Lee CK, Specht CA, Yadav B, Huang H, Akalin A, et al. Central Role of IL-23 and IL-17 Producing Eosinophils as Immunomodulatory Effector Cells in Acute Pulmonary Aspergillosis and Allergic Asthma. *PLoS Pathog.* 2017; 13(1): e1006175.
231. Morrison BE, Park SJ, Mooney JM, Mehrad B. Chemokine-mediated recruitment of NK cells is a critical host defense mechanism in invasive aspergillosis. *J Clin Invest.* 2003; 112(12): 1862-1870.
232. Cenci E, Mencacci A, Bacci A, Bistoni F, Kurup VP, Romani L. T cell vaccination in mice with invasive pulmonary aspergillosis. *J Immunol.* 2000; 165(1): 381-388.
233. Beck O, Topp MS, Koehl U, Roilides E, Simitsopoulou M, Hanisch M, et al. Generation of highly purified and functionally active human TH1 cells against Aspergillus fumigatus. *Blood.* 2006; 107(6): 2562-2569.
234. Dewi IMW, van de Veerdonk FL, Gresnigt MS. The Multifaceted Role of T-Helper Responses in Host Defense against Aspergillus fumigatus. *J Fungi (Basel).* 2017; 3(4).
235. Luckheeram RV, Zhou R, Verma AD, Xia B. CD4(+)T cells: differentiation and functions. *Clin Dev Immunol.* 2012; 2012: 925135.
236. Wang F, Zhang C, Jiang Y, Kou C, Kong Q, Long N, et al. Innate and adaptive immune response to chronic pulmonary infection of hyphae of Aspergillus fumigatus in a new murine model. *J Med Microbiol.* 2017; 66(10): 1400-1408.
237. Hohl TM, Rivera A, Lipuma L, Gallegos A, Shi C, Mack M, et al. Inflammatory monocytes facilitate adaptive CD4 T cell responses during respiratory fungal infection. *Cell Host Microbe.* 2009; 6(5): 470-481.
238. Bartemes KR, Iijima K, Kobayashi T, Kephart GM, McKenzie AN, Kita H. IL-33-responsive lineage- CD25+ CD44(hi) lymphoid cells mediate innate type 2 immunity and allergic inflammation in the lungs. *J Immunol.* 2012; 188(3): 1503-1513.
239. Becker KL, Gresnigt MS, Smeekens SP, Jacobs CW, Magis-Escurra C, Jaeger M, et al. Pattern recognition pathways leading to a Th2 cytokine bias in allergic bronchopulmonary aspergillosis patients. *Clin Exp Allergy.* 2015; 45(2): 423-437.

240. Jolink H, de Boer R, Hombrink P, Jonkers RE, van Dissel JT, Falkenburg JH, et al. Pulmonary immune responses against Aspergillus fumigatus are characterized by high frequencies of IL-17 producing T-cells. *J Infect.* 2017; 74(1): 81-88.
241. Rieber N, Hector A, Kuijpers T, Roos D, Hartl D. Current concepts of hyperinflammation in chronic granulomatous disease. *Clin Dev Immunol.* 2012; 2012: 252460.
242. Geng WR, He HY, Zhang Q, Tong ZH. Th17 cells are involved in mouse chronic obstructive pulmonary disease complicated with invasive pulmonary aspergillosis. *Chin Med J (Engl).* 2020; 134(5): 555-563.
243. Murdock BJ, Falkowski NR, Shreiner AB, Sadighi Akha AA, McDonald RA, White ES, et al. Interleukin-17 drives pulmonary eosinophilia following repeated exposure to Aspergillus fumigatus conidia. *Infect Immun.* 2012; 80(4): 1424-1436.
244. Montagnoli C, Bozza S, Bacci A, Gaziano R, Mosci P, Morschhauser J, et al. A role for antibodies in the generation of memory antifungal immunity. *Eur J Immunol.* 2003; 33(5): 1193-1204.
245. Schroeder HW, Jr., Cavacini L. Structure and function of immunoglobulins. *J Allergy Clin Immunol.* 2010; 125(2 Suppl 2): S41-52.
246. Chen K, Xu W, Wilson M, He B, Miller NW, Bengten E, et al. Immunoglobulin D enhances immune surveillance by activating antimicrobial, proinflammatory and B cell-stimulating programs in basophils. *Nat Immunol.* 2009; 10(8): 889-898.
247. Boita M, Heffler E, Pizzimenti S, Raie A, Saraci E, Omede P, et al. Regulation of B-cell-activating factor expression on the basophil membrane of allergic patients. *Int Arch Allergy Immunol.* 2015; 166(3): 208-212.
248. Church MK. Allergy, Histamine and Antihistamines. *Handb Exp Pharmacol.* 2017; 241: 321-331.
249. Simran Sokhi SC, Siobhan Carr, Sarah Clarke. *CF Trust Annual Data Report 2021*. 2022.
250. Di A, Brown ME, Deriy LV, Li C, Szeto FL, Chen Y, et al. CFTR regulates phagosome acidification in macrophages and alters bactericidal activity. *Nat Cell Biol.* 2006; 8(9): 933-944.
251. Bruscia EM, Zhang PX, Satoh A, Caputo C, Medzhitov R, Shenoy A, et al. Abnormal trafficking and degradation of TLR4 underlie the elevated inflammatory response in cystic fibrosis. *J Immunol.* 2011; 186(12): 6990-6998.
252. Leveque M, Le Trionnaire S, Del Porto P, Martin-Chouly C. The impact of impaired macrophage functions in cystic fibrosis disease progression. *J Cyst Fibros.* 2017; 16(4): 443-453.
253. Tiringer K, Treis A, Fucik P, Gona M, Gruber S, Renner S, et al. A Th17- and Th2-skewed cytokine profile in cystic fibrosis lungs represents a potential risk factor for Pseudomonas aeruginosa infection. *Am J Respir Crit Care Med.* 2013; 187(6): 621-629.
254. Tan HL, Regamey N, Brown S, Bush A, Lloyd CM, Davies JC. The Th17 pathway in cystic fibrosis lung disease. *Am J Respir Crit Care Med.* 2011; 184(2): 252-258.
255. Forrest OA, Dobosh B, Ingersoll SA, Rao S, Rojas A, Laval J, et al. Neutrophil-derived extracellular vesicles promote feed-forward inflammasome signaling in cystic fibrosis airways. *J Leukoc Biol.* 2022; 112(4): 707-716.
256. Cantin AM. Cystic Fibrosis Lung Disease and Immunometabolism. Targeting the NLRP3 Inflammasome. *Am J Respir Crit Care Med.* 2019; 200(11): 1335-1337.
257. Moss RB. Fungi in cystic fibrosis and non-cystic fibrosis bronchiectasis. *Semin Respir Crit Care Med.* 2015; 36(2): 207-216.
258. Alspach E, Lussier DM, Schreiber RD. Interferon gamma and Its Important Roles in Promoting and Inhibiting Spontaneous and Therapeutic Cancer Immunity. *Cold Spring Harb Perspect Biol.* 2019; 11(3).
259. Isaacs A, Lindenmann J. Virus interference. I. The interferon. *Proc R Soc Lond B Biol Sci.* 1957; 147(927): 258-267.
260. Isaacs A, Lindenmann J, Valentine RC. Virus interference. II. Some properties of interferon. *Proc R Soc Lond B Biol Sci.* 1957; 147(927): 268-273.
261. Sheppard P, Kindsvogel W, Xu W, Henderson K, Schlutsmeyer S, Whitmore TE, et al. IL-28, IL-29 and their class II cytokine receptor IL-28R. *Nat Immunol.* 2003; 4(1): 63-68.
262. Lazear HM, Nice TJ, Diamond MS. Interferon-lambda: Immune Functions at Barrier Surfaces and Beyond. *Immunity.* 2015; 43(1): 15-28.
263. Garcia-Sastre A. Ten Strategies of Interferon Evasion by Viruses. *Cell Host Microbe.* 2017; 22(2): 176-184.
264. Wells AI, Coyne CB. Type III Interferons in Antiviral Defenses at Barrier Surfaces. *Trends Immunol.* 2018; 39(10): 848-858.
265. van Boxel-Dezaire AH, Rani MR, Stark GR. Complex modulation of cell type-specific signaling in response to type I interferons. *Immunity.* 2006; 25(3): 361-372.

266. Wilson EB, Yamada DH, Elsaesser H, Herskovitz J, Deng J, Cheng G, et al. Blockade of chronic type I interferon signaling to control persistent LCMV infection. *Science.* 2013; 340(6129): 202-207.
267. Zav'Yalov VP, Zav'Yalova GA. Interferons alpha/beta and their receptors: place in the hierarchy of cytokines. *APMIS.* 1997; 105(3): 161-186.
268. Viscomi GC. Structure-activity of type I interferons. *Biotherapy.* 1997; 10(1): 59-86.
269. Mogensen KE, Lewerenz M, Reboul J, Lutfalla G, Uze G. The type I interferon receptor: structure, function, and evolution of a family business. *J Interferon Cytokine Res.* 1999; 19(10): 1069-1098.
270. Walter MR. The Role of Structure in the Biology of Interferon Signaling. *Front Immunol.* 2020; 11: 606489.
271. Andreakos E, Zanoni I, Galani IE. Lambda interferons come to light: dual function cytokines mediating antiviral immunity and damage control. *Curr Opin Immunol.* 2019; 56: 67-75.
272. Pulverer JE, Rand U, Lienenklaus S, Kugel D, Zietara N, Kochs G, et al. Temporal and spatial resolution of type I and III interferon responses in vivo. *J Virol.* 2010; 84(17): 8626-8638.
273. Gad HH, Hamming OJ, Hartmann R. The structure of human interferon lambda and what it has taught us. *J Interferon Cytokine Res.* 2010; 30(8): 565-571.
274. Odendall C, Voak AA, Kagan JC. Type III IFNs Are Commonly Induced by Bacteria-Sensing TLRs and Reinforce Epithelial Barriers during Infection. *J Immunol.* 2017; 199(9): 3270-3279.
275. Odendall C, Dixit E, Stavru F, Bierne H, Franz KM, Durbin AF, et al. Diverse intracellular pathogens activate type III interferon expression from peroxisomes. *Nat Immunol.* 2014; 15(8): 717-726.
276. Honda K, Yanai H, Negishi H, Asagiri M, Sato M, Mizutani T, et al. IRF-7 is the master regulator of type-I interferon-dependent immune responses. *Nature.* 2005; 434(7034): 772-777.
277. Paun A, Pitha PM. The IRF family, revisited. *Biochimie.* 2007; 89(6-7): 744-753.
278. Zhang X, Brann TW, Zhou M, Yang J, Oguariri RM, Lidie KB, et al. Cutting edge: Ku70 is a novel cytosolic DNA sensor that induces type III rather than type I IFN. *J Immunol.* 2011; 186(8): 4541-4545.
279. Honda K, Takaoka A, Taniguchi T. Type I interferon [corrected] gene induction by the interferon regulatory factor family of transcription factors. *Immunity.* 2006; 25(3): 349-360.
280. Zhou Z, Hamming OJ, Ank N, Paludan SR, Nielsen AL, Hartmann R. Type III interferon (IFN) induces a type I IFN-like response in a restricted subset of cells through signaling pathways involving both the Jak-STAT pathway and the mitogen-activated protein kinases. *J Virol.* 2007; 81(14): 7749-7758.
281. Platanias LC. Mechanisms of type-I- and type-II-interferon-mediated signalling. *Nat Rev Immunol.* 2005; 5(5): 375-386.
282. Stanifer ML, Guo C, Doldan P, Boulant S. Importance of Type I and III Interferons at Respiratory and Intestinal Barrier Surfaces. *Front Immunol.* 2020; 11: 608645.
283. Mahony R, Gargan S, Roberts KL, Bourke N, Keating SE, Bowie AG, et al. A novel anti-viral role for STAT3 in IFN-alpha signalling responses. *Cell Mol Life Sci.* 2017; 74(9): 1755-1764.
284. Majoros A, Platanitis E, Kernbauer-Holzl E, Rosebrock F, Muller M, Decker T. Canonical and Non-Canonical Aspects of JAK-STAT Signaling: Lessons from Interferons for Cytokine Responses. *Front Immunol.* 2017; 8: 29.
285. Lee SJ, Kim WJ, Moon SK. Role of the p38 MAPK signaling pathway in mediating interleukin-28A-induced migration of UMUC-3 cells. *Int J Mol Med.* 2012; 30(4): 945-952.
286. Shaw AE, Hughes J, Gu Q, Behdenna A, Singer JB, Dennis T, et al. Fundamental properties of the mammalian innate immune system revealed by multispecies comparison of type I interferon responses. *PLoS Biol.* 2017; 15(12): e2004086.
287. Caine EA, Scheaffer SM, Arora N, Zaitsev K, Artyomov MN, Coyne CB, et al. Interferon lambda protects the female reproductive tract against Zika virus infection. *Nat Commun.* 2019; 10(1): 280.
288. Duncan CJ, Mohamad SM, Young DF, Skelton AJ, Leahy TR, Munday DC, et al. Human IFNAR2 deficiency: Lessons for antiviral immunity. *Sci Transl Med.* 2015; 7(307): 307ra154.
289. Schneider WM, Chevillotte MD, Rice CM. Interferon-stimulated genes: a complex web of host defenses. *Annu Rev Immunol.* 2014; 32: 513-545.
290. Schoggins JW. Interferon-stimulated genes: roles in viral pathogenesis. *Curr Opin Virol.* 2014; 6: 40-46.
291. Gizzi AS, Grove TL, Arnold JJ, Jose J, Jangra RK, Garforth SJ, et al. Author Correction: A naturally occurring antiviral ribonucleotide encoded by the human genome. *Nature.* 2020; 583(7814): E15.
292. Daffis S, Szretter KJ, Schriewer J, Li J, Youn S, Errett J, et al. 2'-O methylation of the viral mRNA cap evades host restriction by IFIT family members. *Nature.* 2010; 468(7322): 452-456.
293. Haller O, Staeheli P, Schwemmle M, Kochs G. Mx GTPases: dynamin-like antiviral machines of innate immunity. *Trends Microbiol.* 2015; 23(3): 154-163.

294. Hornung V, Hartmann R, Ablasser A, Hopfner KP. OAS proteins and cGAS: unifying concepts in sensing and responding to cytosolic nucleic acids. *Nat Rev Immunol.* 2014; 14(8): 521-528.
295. Hyde JL, Gardner CL, Kimura T, White JP, Liu G, Trobaugh DW, et al. A viral RNA structural element alters host recognition of nonself RNA. *Science.* 2014; 343(6172): 783-787.
296. Pichlmair A, Lassnig C, Eberle CA, Gorna MW, Baumann CL, Burkard TR, et al. IFIT1 is an antiviral protein that recognizes 5'-triphosphate RNA. *Nat Immunol.* 2011; 12(7): 624-630.
297. Daniels BP, Holman DW, Cruz-Orengo L, Jujjavarapu H, Durrant DM, Klein RS. Viral pathogen-associated molecular patterns regulate blood-brain barrier integrity via competing innate cytokine signals. *mBio.* 2014; 5(5): e01476-01414.
298. Lazear HM, Daniels BP, Pinto AK, Huang AC, Vick SC, Doyle SE, et al. Interferon-lambda restricts West Nile virus neuroinvasion by tightening the blood-brain barrier. *Sci Transl Med.* 2015; 7(284): 284ra259.
299. Lazear HM, Schoggins JW, Diamond MS. Shared and Distinct Functions of Type I and Type III Interferons. *Immunity.* 2019; 50(4): 907-923.
300. Schoggins JW. Interferon-Stimulated Genes: What Do They All Do? *Annu Rev Virol.* 2019; 6(1): 567-584.
301. Broggi A, Tan Y, Granucci F, Zanoni I. IFN-lambda suppresses intestinal inflammation by non-translational regulation of neutrophil function. *Nat Immunol.* 2017; 18(10): 1084-1093.
302. Le Bon A, Thompson C, Kamphuis E, Durand V, Rossmann C, Kalinke U, et al. Cutting edge: enhancement of antibody responses through direct stimulation of B and T cells by type I IFN. *J Immunol.* 2006; 176(4): 2074-2078.
303. Crouse J, Kalinke U, Oxenius A. Regulation of antiviral T cell responses by type I interferons. *Nat Rev Immunol.* 2015; 15(4): 231-242.
304. Litinskiy MB, Nardelli B, Hilbert DM, He B, Schaffer A, Casali P, et al. DCs induce CD40-independent immunoglobulin class switching through BLyS and APRIL. *Nat Immunol.* 2002; 3(9): 822-829.
305. Le Bon A, Schiavoni G, D'Agostino G, Gresser I, Belardelli F, Tough DF. Type i interferons potently enhance humoral immunity and can promote isotype switching by stimulating dendritic cells in vivo. *Immunity.* 2001; 14(4): 461-470.
306. Jordan WJ, Eskdale J, Srinivas S, Pekarek V, Kelner D, Rodia M, et al. Human interferon lambda-1 (IFN-lambda1/IL-29) modulates the Th1/Th2 response. *Genes Immun.* 2007; 8(3): 254-261.
307. Le Bon A, Etchart N, Rossmann C, Ashton M, Hou S, Gewert D, et al. Cross-priming of CD8+ T cells stimulated by virus-induced type I interferon. *Nat Immunol.* 2003; 4(10): 1009-1015.
308. Dai J, Megjugorac NJ, Gallagher GE, Yu RY, Gallagher G. IFN-lambda1 (IL-29) inhibits GATA3 expression and suppresses Th2 responses in human naive and memory T cells. *Blood.* 2009; 113(23): 5829-5838.
309. Egli A, Santer DM, O'Shea D, Barakat K, Syedbasha M, Vollmer M, et al. IL-28B is a key regulator of B- and T-cell vaccine responses against influenza. *PLoS Pathog.* 2014; 10(12): e1004556.
310. Lin Q, Dong C, Cooper MD. Impairment of T and B cell development by treatment with a type I interferon. *J Exp Med.* 1998; 187(1): 79-87.
311. Larner AC, Chaudhuri A, Darnell JE, Jr. Transcriptional induction by interferon. New protein(s) determine the extent and length of the induction. *J Biol Chem.* 1986; 261(1): 453-459.
312. Taghavi SA, Eshraghian A. Successful interferon desensitization in a patient with chronic hepatitis C infection. *World J Gastroenterol.* 2009; 15(33): 4196-4198.
313. Hardy GA, Sieg SF, Rodriguez B, Jiang W, Asaad R, Lederman MM, et al. Desensitization to type I interferon in HIV-1 infection correlates with markers of immune activation and disease progression. *Blood.* 2009; 113(22): 5497-5505.
314. Ronnblom L, Leonard D. Interferon pathway in SLE: one key to unlocking the mystery of the disease. *Lupus Sci Med.* 2019; 6(1): e000270.
315. Ronnblom L. The type I interferon system in the etiopathogenesis of autoimmune diseases. *Ups J Med Sci.* 2011; 116(4): 227-237.
316. Liau NPD, Laktyushin A, Lucet IS, Murphy JM, Yao S, Whitlock E, et al. The molecular basis of JAK/STAT inhibition by SOCS1. *Nat Commun.* 2018; 9(1): 1558.
317. Malakhov MP, Malakhova OA, Kim KI, Ritchie KJ, Zhang DE. UBP43 (USP18) specifically removes ISG15 from conjugated proteins. *J Biol Chem.* 2002; 277(12): 9976-9981.
318. Meuwissen ME, Schot R, Buta S, Oudesluijs G, Tinschert S, Speer SD, et al. Human USP18 deficiency underlies type 1 interferonopathy leading to severe pseudo-TORCH syndrome. *J Exp Med.* 2016; 213(7): 1163-1174.

319. Karlowitz R, Stanifer ML, Roedig J, Andrieux G, Bojkova D, Bechtel M, et al. USP22 controls type III interferon signaling and SARS-CoV-2 infection through activation of STING. *Cell Death Dis.* 2022; 13(8): 684.
320. Basters A, Geurink PP, El Oualid F, Ketscher L, Casutt MS, Krause E, et al. Molecular characterization of ubiquitin-specific protease 18 reveals substrate specificity for interferon-stimulated gene 15. *FEBS J.* 2014; 281(7): 1918-1928.
321. Malakhova OA, Kim KI, Luo JK, Zou W, Kumar KG, Fuchs SY, et al. UBP43 is a novel regulator of interferon signaling independent of its ISG15 isopeptidase activity. *EMBO J.* 2006; 25(11): 2358-2367.
322. Muir AJ, Shiffman ML, Zaman A, Yoffe B, de la Torre A, Flamm S, et al. Phase 1b study of pegylated interferon lambda 1 with or without ribavirin in patients with chronic genotype 1 hepatitis C virus infection. *Hepatology.* 2010; 52(3): 822-832.
323. Muir AJ, Arora S, Everson G, Flisiak R, George J, Ghalib R, et al. A randomized phase 2b study of peginterferon lambda-1a for the treatment of chronic HCV infection. *J Hepatol.* 2014; 61(6): 1238-1246.
324. Bayas A, Gold R. Lessons from 10 years of interferon beta-1b (Betaferon/Betaseron) treatment. *J Neurol.* 2003; 250 Suppl 4: IV3-8.
325. Newsome SD, Kieseier BC, Arnold DL, Shang S, Liu S, Hung S, et al. Subgroup and sensitivity analyses of annualized relapse rate over 2 years in the ADVANCE trial of peginterferon beta-1a in patients with relapsing-remitting multiple sclerosis. *J Neurol.* 2016; 263(9): 1778-1787.
326. Khan UT, Tanasescu R, Constantinescu CS. PEGylated IFNbeta-1a in the treatment of multiple sclerosis. *Expert Opin Biol Ther.* 2015; 15(7): 1077-1084.
327. Kappos L, Wiendl H, Selmaj K, Arnold DL, Havrdova E, Boyko A, et al. Daclizumab HYP versus Interferon Beta-1a in Relapsing Multiple Sclerosis. *N Engl J Med.* 2015; 373(15): 1418-1428.
328. Hauser SL, Bar-Or A, Comi G, Giovannoni G, Hartung HP, Hemmer B, et al. Ocrelizumab versus Interferon Beta-1a in Relapsing Multiple Sclerosis. *N Engl J Med.* 2017; 376(3): 221-234.
329. Reichard O, Norkrans G, Fryden A, Braconier JH, Sonnerborg A, Weiland O. Randomised, double-blind, placebo-controlled trial of interferon alpha-2b with and without ribavirin for chronic hepatitis C. The Swedish Study Group. *Lancet.* 1998; 351(9096): 83-87.
330. Yao JC, Guthrie KA, Moran C, Strosberg JR, Kulke MH, Chan JA, et al. Phase III Prospective Randomized Comparison Trial of Depot Octreotide Plus Interferon Alfa-2b Versus Depot Octreotide Plus Bevacizumab in Patients With Advanced Carcinoid Tumors: SWOG S0518. *J Clin Oncol.* 2017; 35(15): 1695-1703.
331. Janssen HL, van Zonneveld M, Senturk H, Zeuzem S, Akarca US, Cakaloglu Y, et al. Pegylated interferon alfa-2b alone or in combination with lamivudine for HBeAg-positive chronic hepatitis B: a randomised trial. *Lancet.* 2005; 365(9454): 123-129.
332. McHutchison JG, Lawitz EJ, Shiffman ML, Muir AJ, Galler GW, McCone J, et al. Peginterferon alfa-2b or alfa-2a with ribavirin for treatment of hepatitis C infection. *N Engl J Med.* 2009; 361(6): 580-593.
333. Cascinelli N, Belli F, MacKie RM, Santinami M, Bufalino R, Morabito A. Effect of long-term adjuvant therapy with interferon alpha-2a in patients with regional node metastases from cutaneous melanoma: a randomised trial. *Lancet.* 2001; 358(9285): 866-869.
334. Sarasin-Filipowicz M, Oakeley EJ, Duong FH, Christen V, Terracciano L, Filipowicz W, et al. Interferon signaling and treatment outcome in chronic hepatitis C. *Proc Natl Acad Sci U S A.* 2008; 105(19): 7034-7039.
335. Li C, Luo, F., Liu, C., Xiong, N., Xu, Z., Zhang, W., Wang, Y., Liu, D., Yu, C., Zeng, J., Zhang, L., Duo, L., Liu, Y., Feng, M., Liu, R., Mei, J., Deng, S., Zeng Z., He, Y., Liu, H., Shi, Z., Duan, M., Kang, D., Liao, J., Li, W., Liu, L. Engineered interferon alpha effectively improves clinical outcomes of COVID-19 patients *Research Square.* 2020.
336. Jhuti D, Rawat A, Guo CM, Wilson LA, Mills EJ, Forrest JI. Interferon Treatments for SARS-CoV-2: Challenges and Opportunities. *Infect Dis Ther.* 2022; 11(3): 953-972.
337. Reis G, Moreira Silva EAS, Medeiros Silva DC, Thabane L, Campos VHS, Ferreira TS, et al. Early Treatment with Pegylated Interferon Lambda for Covid-19. *N Engl J Med.* 2023; 388(6): 518-528.
338. Andrews S. *A Quality Control Tool for High Throughput Sequence Data*. http://www.bioinformatics.babraham.ac.uk/projects/fastqc/.
339. Kim D, Langmead B, Salzberg SL. HISAT: a fast spliced aligner with low memory requirements. *Nat Methods.* 2015; 12(4): 357-360.
340. Howe KL, Achuthan P, Allen J, Allen J, Alvarez-Jarreta J, Amode MR, et al. Ensembl 2021. *Nucleic Acids Res.* 2021; 49(D1): D884-D891.

341. Li H, Handsaker B, Wysoker A, Fennell T, Ruan J, Homer N, et al. The Sequence Alignment/Map format and SAMtools. *Bioinformatics.* 2009; 25(16): 2078-2079.
342. Liao Y, Smyth GK, Shi W. featureCounts: an efficient general purpose program for assigning sequence reads to genomic features. *Bioinformatics.* 2014; 30(7): 923-930.
343. Blanco-Melo D, Nilsson-Payant BE, Liu WC, Uhl S, Hoagland D, Moller R, et al. Imbalanced Host Response to SARS-CoV-2 Drives Development of COVID-19. *Cell.* 2020; 181(5): 1036-1045 e1039.
344. Subramanian A, Tamayo P, Mootha VK, Mukherjee S, Ebert BL, Gillette MA, et al. Gene set enrichment analysis: a knowledge-based approach for interpreting genome-wide expression profiles. *Proc Natl Acad Sci U S A.* 2005; 102(43): 15545-15550.
345. Liberzon A, Birger C, Thorvaldsdottir H, Ghandi M, Mesirov JP, Tamayo P. The Molecular Signatures Database (MSigDB) hallmark gene set collection. *Cell Syst.* 2015; 1(6): 417-425.
346. Godec J, Tan Y, Liberzon A, Tamayo P, Bhattacharya S, Butte AJ, et al. Compendium of Immune Signatures Identifies Conserved and Species-Specific Biology in Response to Inflammation. *Immunity.* 2016; 44(1): 194-206.
347. Kohl M, Wiese S, Warscheid B. Cytoscape: software for visualization and analysis of biological networks. *Methods Mol Biol.* 2011; 696: 291-303.
348. Doncheva NT, Morris JH, Gorodkin J, Jensen LJ. Cytoscape StringApp: Network Analysis and Visualization of Proteomics Data. *J Proteome Res.* 2019; 18(2): 623-632.
349. Morris JH, Kuchinsky A, Ferrin TE, Pico AR. enhancedGraphics: a Cytoscape app for enhanced node graphics. *F1000Res.* 2014; 3: 147.
350. Cambier S, Gouwy M, Proost P. The chemokines CXCL8 and CXCL12: molecular and functional properties, role in disease and efforts towards pharmacological intervention. *Cell Mol Immunol.* 2023; 20(3): 217-251.
351. Conti BJ, Davis BK, Zhang J, O'Connor W, Jr., Williams KL, Ting JP. CATERPILLER 16.2 (CLR16.2), a novel NBD/LRR family member that negatively regulates T cell function. *J Biol Chem.* 2005; 280(18): 18375-18385.
352. Schneider M, Zimmermann AG, Roberts RA, Zhang L, Swanson KV, Wen H, et al. The innate immune sensor NLRC3 attenuates Toll-like receptor signaling via modification of the signaling adaptor TRAF6 and transcription factor NF-kappaB. *Nat Immunol.* 2012; 13(9): 823-831.
353. Mangan MS, Latz E. NLRC3 puts the brakes on STING. *Immunity.* 2014; 40(3): 305-306.
354. Sun D, Xu J, Zhang W, Song C, Gao C, He Y, et al. Negative regulator NLRC3: Its potential role and regulatory mechanism in immune response and immune-related diseases. *Front Immunol.* 2022; 13: 1012459.
355. Zhang L, Mo J, Swanson KV, Wen H, Petrucelli A, Gregory SM, et al. NLRC3, a member of the NLR family of proteins, is a negative regulator of innate immune signaling induced by the DNA sensor STING. *Immunity.* 2014; 40(3): 329-341.
356. King JA, Nichols AL, Bentley S, Carr SB, Davies JC. An Update on CFTR Modulators as New Therapies for Cystic Fibrosis. *Paediatr Drugs.* 2022; 24(4): 321-333.
357. Guimbellot JS, Baines A, Paynter A, Heltshe SL, VanDalfsen J, Jain M, et al. Long term clinical effectiveness of ivacaftor in people with the G551D CFTR mutation. *J Cyst Fibros.* 2021; 20(2): 213-219.
358. Guimbellot JS, Ryan KJ, Anderson JD, Liu Z, Kersh L, Esther CR, et al. Variable cellular ivacaftor concentrations in people with cystic fibrosis on modulator therapy. *J Cyst Fibros.* 2020; 19(5): 742-745.
359. Mbongue JC, Nicholas DA, Torrez TW, Kim NS, Firek AF, Langridge WH. The Role of Indoleamine 2, 3-Dioxygenase in Immune Suppression and Autoimmunity. *Vaccines (Basel).* 2015; 3(3): 703-729.
360. Huang X, Zhang F, Wang X, Liu K. The Role of Indoleamine 2, 3-Dioxygenase 1 in Regulating Tumor Microenvironment. *Cancers (Basel).* 2022; 14(11).
361. Hirano KI, Hosokawa H, Koizumi M, Endo Y, Yahata T, Ando K, et al. LMO2 is essential to maintain the ability of progenitors to differentiate into T-cell lineage in mice. *Elife.* 2021; 10.
362. Perng YC, Lenschow DJ. ISG15 in antiviral immunity and beyond. *Nat Rev Microbiol.* 2018; 16(7): 423-439.
363. Zhou X, Michal JJ, Zhang L, Ding B, Lunney JK, Liu B, et al. Interferon induced IFIT family genes in host antiviral defense. *Int J Biol Sci.* 2013; 9(2): 200-208.
364. Cruikshank WW, Kornfeld H, Center DM. Interleukin-16. *J Leukoc Biol.* 2000; 67(6): 757-766.
365. Merlo LMF, DuHadaway JB, Montgomery JD, Peng WD, Murray PJ, Prendergast GC, et al. Differential Roles of IDO1 and IDO2 in T and B Cell Inflammatory Immune Responses. *Front Immunol.* 2020; 11: 1861.

366. Akkaya M, Akkaya B, Miozzo P, Rawat M, Pena M, Sheehan PW, et al. B Cells Produce Type 1 IFNs in Response to the TLR9 Agonist CpG-A Conjugated to Cationic Lipids. *J Immunol.* 2017; 199(3): 931-940.
367. Congy-Jolivet N, Cenac C, Dellacasagrande J, Puissant-Lubrano B, Apoil PA, Guedj K, et al. Monocytes are the main source of STING-mediated IFN-alpha production. *EBioMedicine.* 2022; 80: 104047.
368. Desai JV, Lionakis MS. The role of neutrophils in host defense against invasive fungal infections. *Curr Clin Microbiol Rep.* 2018; 5(3): 181-189.
369. Zhong H, Lu RY, Wang Y. Neutrophil extracellular traps in fungal infections: A seesaw battle in hosts. *Front Immunol.* 2022; 13: 977493.
370. Clark SR, Ma AC, Tavener SA, McDonald B, Goodarzi Z, Kelly MM, et al. Platelet TLR4 activates neutrophil extracellular traps to ensnare bacteria in septic blood. *Nat Med.* 2007; 13(4): 463-469.
371. Hakkim A, Furnrohr BG, Amann K, Laube B, Abed UA, Brinkmann V, et al. Impairment of neutrophil extracellular trap degradation is associated with lupus nephritis. *Proc Natl Acad Sci U S A.* 2010; 107(21): 9813-9818.
372. Knight JS, Kaplan MJ. Lupus neutrophils: 'NET' gain in understanding lupus pathogenesis. *Curr Opin Rheumatol.* 2012; 24(5): 441-450.
373. Fuchs TA, Brill A, Duerschmied D, Schatzberg D, Monestier M, Myers DD, Jr., et al. Extracellular DNA traps promote thrombosis. *Proc Natl Acad Sci U S A.* 2010; 107(36): 15880-15885.
374. Garcia-Valero J, Olloquequi J, Montes JF, Rodriguez E, Martin-Satue M, Texido L, et al. Deficient pulmonary IFN-beta expression in COPD patients. *PLoS One.* 2019; 14(6): e0217803.
375. Bergauer A, Sopel N, Kross B, Vuorinen T, Xepapadaki P, Weiss ST, et al. IFN-alpha/IFN-lambda responses to respiratory viruses in paediatric asthma. *Eur Respir J.* 2017; 49(3).
376. Schneider D, Ganesan S, Comstock AT, Meldrum CA, Mahidhara R, Goldsmith AM, et al. Increased cytokine response of rhinovirus-infected airway epithelial cells in chronic obstructive pulmonary disease. *Am J Respir Crit Care Med.* 2010; 182(3): 332-340.
377. Guo-Parke H, Linden D, Weldon S, Kidney JC, Taggart CC. Deciphering Respiratory-Virus-Associated Interferon Signaling in COPD Airway Epithelium. *Medicina (Kaunas).* 2022; 58(1).
378. Rich HE, Antos D, Melton NR, Alcorn JF, Manni ML. Insights Into Type I and III Interferons in Asthma and Exacerbations. *Front Immunol.* 2020; 11: 574027.
379. Koch S, Finotto S. Role of Interferon-lambda in Allergic Asthma. *J Innate Immun.* 2015; 7(3): 224-230.
380. Agarwal R, Muthu V, Sehgal IS. Relationship between Aspergillus and asthma. *Allergol Int.* 2023; 72(4): 507-520.
381. Tiew PY, Narayana JK, Quek MSL, Ang YY, Ko FWS, Poh ME, et al. Sensitisation to recombinant Aspergillus fumigatus allergens and clinical outcomes in COPD. *Eur Respir J.* 2023; 61(1).
382. Regard L, Martin C, Burnet E, Da Silva J, Burgel PR. CFTR Modulators in People with Cystic Fibrosis: Real-World Evidence in France. *Cells.* 2022; 11(11).
383. van der Meer R, Wilms EB, Heijerman HGM. CFTR Modulators: Does One Dose Fit All? *J Pers Med.* 2021; 11(6).
384. Ghosn J, Taiwo B, Seedat S, Autran B, Katlama C. Hiv. *Lancet.* 2018; 392(10148): 685-697.
385. Kotenko SV. IFN-lambdas. *Curr Opin Immunol.* 2011; 23(5): 583-590.
386. Onoguchi K, Yoneyama M, Takemura A, Akira S, Taniguchi T, Namiki H, et al. Viral infections activate types I and III interferon genes through a common mechanism. *J Biol Chem.* 2007; 282(10): 7576-7581.
387. Liu X, Wang C. The emerging roles of the STING adaptor protein in immunity and diseases. *Immunology.* 2016; 147(3): 285-291.
388. Gabillard-Lefort C, Casey M, Glasgow AMA, Boland F, Kerr O, Marron E, et al. Trikafta Rescues CFTR and Lowers Monocyte P2X7R-induced Inflammasome Activation in Cystic Fibrosis. *Am J Respir Crit Care Med.* 2022; 205(7): 783-794.
389. Lara-Reyna S, Holbrook J, Jarosz-Griffiths HH, Peckham D, McDermott MF. Dysregulated signalling pathways in innate immune cells with cystic fibrosis mutations. *Cell Mol Life Sci.* 2020; 77(22): 4485-4503.
390. Scambler T, Jarosz-Griffiths HH, Lara-Reyna S, Pathak S, Wong C, Holbrook J, et al. ENaC-mediated sodium influx exacerbates NLRP3-dependent inflammation in cystic fibrosis. *Elife.* 2019; 8.
391. Pollock JD, Williams DA, Gifford MA, Li LL, Du X, Fisherman J, et al. Mouse model of X-linked chronic granulomatous disease, an inherited defect in phagocyte superoxide production. *Nat Genet.* 1995; 9(2): 202-209.
392. Ahlin A, Elinder G, Palmblad J. Dose-dependent enhancements by interferon-gamma on functional responses of neutrophils from chronic granulomatous disease patients. *Blood.* 1997; 89(9): 3396-3401.

393. Falcone EL, Holland SM. Invasive fungal infection in chronic granulomatous disease: insights into pathogenesis and management. *Curr Opin Infect Dis.* 2012; 25(6): 658-669.
394. Crossen AJ, Ward RA, Reedy JL, Surve MV, Klein BS, Rajagopal J, et al. Human Airway Epithelium Responses to Invasive Fungal Infections: A Critical Partner in Innate Immunity. *J Fungi (Basel).* 2022; 9(1).